Cytoprotective effects of epoxyeicosatrienoic acids in pancreatic beta cells

Daniel Grimes

for the degree of

DOCTOR OF PHILOSOPHY

Keele University

March 2020

Acknowledgment

My greatest appreciation goes to my supervisor Dr David Watson for his mentorship and guidance during my research and in the development of this manuscript. I would also like to thank all of the Life Sciences staff and colleagues at Keele University and family and friends for your support throughout my studies.

Abstract

Pro-inflammatory cytokines and glucolipotoxicity are known mediators of beta cell death and dysfunction in the pathogenesis of type 1 and type 2 diabetes mellitus (DM). In contrast to the pro-apoptotic effects of long-chain saturated fatty acids in beta cells, mono- and poly- unsaturated species, including arachidonic acid (AA), are well-tolerated and can attenuate the effects of cytoxocity. AA-drived eicosanoids are well-studied in context to beta cell biology, with established contributions of cyclooxygenase (COX) and lipoxygenase (LOX) products in cytotoxicity studies, though comparatively less is known about the role of cytochrome P450-derived epoxyeicostrienoic acids (EETs) in this context, despite reported anti-inflammatory activity in other models. Therefore the aim of this thesis was to investigate the cytoprotective actions of EETs and their corresponding diol products of soluble epoxide hydrolase metabolism; dihydroxyeicosatrienoic acids (DHETs) in the rat pancreatic beta cell line BRIN-BD11. Preliminary investigations confirmed the cytotoxicity exerted by pro-inflammatory cytokines and palmtiate in reducing cell viability and increasing apoptosis. These effects were attenuated by co-incubation of 8(9)-EET, 11(12)-EET and 14(15)-EET isomers, a novel observation in a beta cell model. In contrast, DHETs failed to ameliorate palmitate toxicity however, 8(9)-DHET remarkably produced comparable effects to that of EETs against cytokine toxicity. These effects were associated with a reduction in cytokine-induced NF-κB activation and, in the case of EETs, decreased nitrite production. Futhermore, in these models EET effects were PPARγ-independent, with a wider range of PPAR and GPR antagonists failing to identify a single high affinity receptor site mediating EET actions against palmitate toxicity. Similarly, whilst alterations in gene expression of enzymes involved in palmitate oxidation and triglyceride synthesis were observed in repsonse to EET treatments, with a modest increase

in intracellular lipid droplets, pharmacological inhibition of these pathways suggests these are not required in mediating EET actions. This was further supported by the attentuation of toxicity exerted with the poorly metabolisable palmitate analogue, 2-Bromopalmitate, by EETs. Therefore, whilst mechanisms of actions remain poorly defined, this thesis provides the first direct evidence for the cytoprotective actions of EETs and DHETs in a beta cell model, establishing a foundation for future work to explore the manipulation of endogenous EETs in pancreatic beta cells and to further define their mode of action in models of type 1 and 2 DM.

Table of Contents

List of Figures

Chapter One

Chapter 3

Chapter Five

Chapter Six

List of Tables

List of Acronyms

2-BP	2-Bromopalmitate
7-AAD	7-Aminoactinomycin D
AA	Arachidonic acid
ACC	Acetyl-CoA-carboxylase
ACS4	Acyl-CoA-synthetase 4
ALA	Alpha linoleic acid
AP1	Activating protein 1
APAF-1	Apoptotic peptidase activating factor 1
APC	Antigen presenting cell
ATF	Activating transcription factor
BSA	Bovine serum albumin
CCK	Cholecystokinin A receptor
CHOP	C/EBP homologous protein
COX	Cyclooxygenase
CPT1	Carnitine palmitoyl transferase-1
CTLA-4	Cytotoxic T-lymphocyte-associated protein 4

CYP450	Cytochrome P450
DAG	Diacylglycerol
DAMP	Damage-associated molecular patterns
DGAT	Diacylglycerol acyl-transferase
DHA	Docosahexaenoic acid
DHET	Dihydroxyeicosatrienoic acid
DM	Diabetes mellitus
DMSO	Dimethyl sulphoxide
Ech1	Enoyl-CoA hydratase 1
EET	Epoxyeicosatrienoic acid
EGFR	Extracellular growth factor receptor
eIF2α	Eukaryotic initiation factor 2 alpha
ELovl6	Elongation of very long chain fatty acid protein 6
EPA	Eicosapentaenoic acid
ER	Endoplasmic reticulum
ERK	Extracellular signal-regulated kinases
ERAD	ER-associated degradation
FABP	Fatty acid binding protein

FADD	Fas-associated death domain
FAS	Fatty acid synthase
FasL	Fas ligand
FBS	Foetal bovine serum
FFA	Free fatty acid
FFAR	Free fatty acid receptor
GAD	Glutamate decarboxylase
GADD153	Growth arrest and DNA damage 153
GAS	gamma-activated sequence
GFP	Green fluorescent protein
GLP-1	Glucagon-like peptide-1
GOI	Gene of Interest
GPCR/GPR	G-protein coupled receptor/G-protein receptor
GSIS	Glucose stimulated insulin secretion
HETE	Hydroxyeicosatetraenoic acid
HLA	Human leukocyte antigen
HSP	Heat shock protein
HUVEC	Human umbilical vein endothelial cells

IA-2	Islet antigen 2
ICAM	Intercellular adhesion molecule
IFN-γ	Interferon gamma
IKK	IκB kinase
IL-1β	Interleukin 1 beta
IL1R	Interleukin 1 receptor
ILI-1	Insulin gene enhancer protein-1
iNOS	Inducible nitric oxide synthase
IP_3	Inositol 1,4,5-trisphosphate
IRAK	Interleukin receptor associated kinase
IRE-1	Inositol-requiring protein-1
IRF	Interferon regulatory factor
IRS-1	Insulin receptor substrate 1
Jak	Janus kinase
JNK	c-jun NH_2 terminal kinase
LADA	Latent autoimmune diabetes of adulthood
LCFA	Long-chain fatty acids
LOX	Lipoxygenase

LPS	Lipopolysaccharide
LXR	Liver X receptor
MAPK	Mitogen-activated protein kinase
MCFA	Medium-chain fatty acids
MIDD	Maternally inherited diabetes and deafness
MIP-1α	Macrophage inflammatory protein 1 alpha
MnSOD	Manganese superoxide dismutase
MODY	Maturity-onset diabetes of the young
MSK-1	Mitogen- and stress-activated protein kinase-1
NF-κB	Nuclear factor kappa-light-chain-enhancer of activated B cells
NO	Nitric oxide
PLD-1	Phospholipase D1
Pdx-1	Pancreatic and duodenal homeobox 1
PERK	Protein kinase RNA-like endoplasmic reticulum kinase
PG	Prostaglandins
PGHS	Prostaglandin H_2 synthase
PI3K	Phosphoinositide-3-kinase
PLA_2	Phospholipase A_2

PLC	Phospholipase C
PLN	Pancreatic lymph nodes
PKB	Protein kinase B
PPARα	Peroxisome proliferator-activated receptor alpha
PPARβ/δ	Peroxisome proliferator-activated receptor delta
PPARγ	Peroxisome proliferator-activated receptor gamma
PS	Phosphatidylserine
PTPN22	Protein tyrosine phosphatase, non-receptor 22
ROS	Reactive oxygen species
RXR	Retinoid X receptor
SCD	Stearoyl-CoA-desaturase
SCFA	Short-chain fatty acids
sEH	Soluble epoxide hydrolase
SERCA	Sarco endoplasmic reticulum calcium ATPase
SREBP1-c	Sterol response element binding protein 1-c
STAT1	Signal transducer and activator of transcription 1
STZ	Streptozotocin
TAG	Triacylglycerides

TLR	Toll-like receptor
TNF-α	Tumour necrosis factor alpha
TNFR	Tumour necrosis factor receptor
TRADD	TNF receptor-associated death domain protein
TRAF	TNF-receptor-associated factor
TX	Thromboxane
UPR	Unfolded protein response
VLCFA	Very long-chain fatty acid
Xbp-1	X-box binding protein 1
ZnT8	Zinc transporter 8

Chapter One

General Introduction

1 Introduction

With a concerning rise in the prevalence of diabetes mellitus (DM), the World Health Organisation has emphasised the forthcoming of a diabetes burden, with an estimated 552 million confirmed cases by 2030 by the International Diabetes Federation (IDF) (Alam *et al.,* 2014). The increasing rate of diagnosis of DM currently stands at 400 people per day in the UK, with estimated figures by 2025 to raise above a total four million cases. The spectrum of DM can be broadly classified as type 1 DM or type 2 DM. Type 1 DM (insulin dependent) represents an extreme of autoimmune destruction of the pancreatic beta cells and type 2 DM (typically non-insulin dependent) an extreme of metabolic dysfunction (Groop *et al.,* 2014; American Diabetes Association, 2007) leading to the loss in effective regulation of plasma glucose homeostasis.

Healthy individuals maintain glucose levels between 4.5-5mM, utilising glucose and/or fatty acids and ketones as a primary source of metabolic fuel in the 'starve-feed' cycle (Bano *et al.,* 2013;). The mechanisms leading to the development of type 1 or type 2 DM may be diverse; however, patients from both cohorts may display characteristics of a type 1 DM phenotype with impaired secretion or type 2 DM phenotype with metabolic syndrome and a degree of insulin resistance (Groop *et al.,* 2014). Patients with type 1 DM progressively display a decrease in insulin production, consequential to declining functional beta cell mass, whilst type 2 DM patients display an increase in insulin resistance in peripheral tissues, typically with an eventual decline in insulin secretion and reduction in beta cell mass. Although most newly diagnosed DM cases fall into one of these two main classifications, other distinct sub-types of DM include: Latent Autoimmune Diabetes in Adults (LADA), Maturity-Onset-Diabetes of the Young (MODY), neonatal diabetes, maternally inherited diabetes and deafness (MIDD) and

secondary diabetes; as a complication of either pancreas/endocrine related diseases (American Diabetes Association, 2007; Groop *et al.,* 2014).

1.1 Type 1 Diabetes Mellitus

Type 1 DM was first described in 1902 by the German pathologist Schmidt in a case of a boy presenting with characteristic signs of an inflammatory infiltration in the islets of Langerhans, which was later termed 'insulitis' by a Swiss pathologist; Von Meyenburg (In't Veld, 2011). The first link between the foci of small-cell infiltration, insulitis and type 1 DM was reported in 1928 by Stansfield and Warren whilst studying two patients; a six year-old girl (deceased two months after onset of type 1 DM in a diabetic coma) and an eleven year-old girl (deceased four weeks after initial symptoms) (In't Veld, 2011). Warren subsequently contradicted these initial findings of insulitis in both patients in a later study of ten children, with only 10% displaying characteristics of insulitis (type 1 DM). From the inconclusive data provided by Schmidt and Warren, LeCompte revisited the findings in 1958 with four cases of children involving acute onset and short duration of the disease (type 1 DM), proposing four possible explanations for the presence of cellular infiltration: 1) A direct invasion of the islets by an infectious agent, 2) A manifestation of functional overstimulation or strain, 3) A reaction to damage by some unknown non-bacterial agent and 4) an antigen-antibody reaction (LeCompte 1958).

The year 1965 witnessed a landmark study by pathologist Willy Gepts, who obtained tissue samples from young, recent onset type 1 DM cases. Out of the 22 diabetic patients under the age of 40, 68% showed the presence of a characteristic inflammatory lesion in the

islets, with a reduced beta cell mass by approximately 10% compared to non-diabetic controls. The use of anti-insulin sera further confirmed these observations showing the presence of lymphocytic infiltrates, thought to point to an autoimmune aetiology of the disease (Gepts, 1965). A follow-up study in 1978 found additional arguments in favour of an autoimmune process, observing that inflammation seemed to specifically target beta cell-containing islets, whilst islets whose beta cells had been depleted were devoid of lymphocytic infiltration (Gepts, 1978). Foulis *et al*., (1986) later confirmed these observations, with detectable insulitis present in 47/60 (78%) cases of young patients with recent onset diabetes (<1 year). These two landmark studies account for almost half of all cases with insulitis that have been published over the last century, owing to the limited availability of pancreatic donor specimens of recent onset type 1 DM patients (In't Veld, 2011) and continue to contribute to our understanding of the orchestration of the immune reponse in DM pathogenesis (Willcox *et al.,* 2010).

In 1985, Bottazzo *et al.*, observed the nature of a lymphocytic infiltrate in the islets of Langerhans from the pancreas of a 12 year old girl. This study reported that insulitis was present in 24% of the islets and immunophenotyping of the infiltrate revealed a large T-lymphocyte population, with $CD8^+$ cytotoxic/suppressor cells being most abundant (Bottazzo et al, 1985). This was later supported by a study showing that at all stages of insulitis, CD8+ T cells were predominant in the islet infiltrate, increasing in number with decreasing insulin-positive area, but disappearing when insulin-positivity was completely lost (In't Veld *et al.,* 2007). $CD20^+$ B-lymphocytes are the second most prominent cell type, whilst macrophages were present at relatively lower levels but become the most prominent infiltrating cell type in insulin-deficient islets (Willcox *et al.,* 2010).

1.1.1 Insulitis

The limited availbility of human pancreatic tissue sections from cadaveric donors with recent onset type 1 DM has been supported with studies in BB rat and NOD mice models, which develop spontaneous type 1 DM, to better understand the pathogenesis of type 1 DM, establishing pancreatic beta cells as the target for mononuclear cells in an autoimmune attack. During insulitis, a loss of functional beta cell mass occurs over a period of time (a protracted 'pre-diabetic' stage) resulting in a reduction of around 70-80% at the time of diagnosis (Cnop *et al.,* 2005; Yoon and Jun, 2005). The direct contact of activated macrophages and T-cells, and the exposure to soluble mediators secreted by these cells; cytokines, nitric oxide (NO) and oxygen free radicals, is believed to be the main cause of beta cell death *in vivo* (Pirot *et al.,* 2008).

Autoantibodies can be detected several months or years before the appearance of clinical symptoms of type 1 DM and are used as markers in identifying patients at risk of developing the condition (Jahromi *et al.,* 2007). The most common auto-antibodies detected in pre-diabetic patients are directed against the beta cell antigens glutamic acid decarboxylase (GAD65), tyrosine phosphatase-like protein (islet auto-antigen 2) (IA-2) and insulin (Pirot *et al.,* 2008). Around 90% of newly diagnosed type 1 DM patients have one or more auto-antibodies present and in combination with auto-antibodies against the zinc transporter ZnT8, this figure rises to 98% (Wenzlau *et al.,* 2007). Through linkage analysis, the human leukocyte antigen (HLA) region found on chromosome 6p21.3 is suggested to be the strongest genetic determinant for type 1 DM; with 50% of all known genetic risks being associated with this region (Groop *et al.,* 2014) however, more than 85% of cases show an absence of an affected first-degree relative. Those with inherited links to a first-degree relative have a 5% lifetime

risk of developing type 1 DM compared to 0.3% for the remaining population (Gan *et al.,* 2012), suggesting the requirement of an environmental trigger in the initiation of type 1 DM.

In the 1970's an association between specific HLA-loci (HLA-B alleles) and type 1 DM onset was first recognised, with further alleles including DR, DQB1 and A1 shown to predispose individuals to type 1 DM development (Gan *et al.,* 2012). A study involving >1000 patients with type 1 DM showed that ~95% express either the HLA-DR3 and/or DR4 allele, of which 40% were heterozygous for HLA-DR3 and DR4 in comparison to 3% of the general population, with DR4 then DR3 homozygosity and DR4/DRX having the next highest genetic risk genotypes (Gan *et al.,* 2012). Although specific HLA types indicate susceptibility to type 1 DM development; HLA-DR2, HLA-DR5 and HLA-DQB1 may confer protective roles, with HLA-DQB1 giving a 1 in 15,000 chance of developing the condition (Gan *et al.,* 2012). Other documented loci that have been shown to cause a predisposition in individuals are the insulin locus, cytotoxic T-lymphocytes antigen 4 (CTLA4) and phosphatase non-receptor type 22 (PTPN22); PTPN22 and CTLA4 are both negative regulators of lymphatic activity (Pirot *et al.,* 2008). Insulin may be present at low levels within the thymus and may lead to inefficient elimination of self-reactive T-cells with PTPN22 de-phosphorylating components of the T-cell receptor cascade, thus inhibiting antigen-specific T-cell activation (Todd *et al.,* 2007) and CTLA4, a T-lymphocyte receptor, can cause inhibition of T-lymphocyte activation (Kim *et al.,* 2005).

An external environmental trigger is believed to be necessary in order to meet the threshold in which the pool of self-reactive naïve T-cells are activated, leading to the initiation of insulitis, typically (though not exclusively) in patients with a genetic predisposition. The several suspected environmental triggers include; viral infection, dietary factors during

infancy (particualry cow's milk formula), vaccination, toxins and physiological beta cell turnover occuring in newborns (Pirot *et al.,* 2008). Whilst evidence points to the role of viral infection (Richardson *et al.,* 2009; Wilcox *et al.,* 2011), possibly attributed to the so-called 'hygiene hypothesis' and its hypothesised link to the increase in auto-immune diseases, as a potential 'trigger' for the development of type 1 DM, studies are yet to demonstrate a direct causal relationship between viral candidates and diabetogenesis *in vivo*.

In early insulitis, T-cell recruitment to the pancreatic islets may be potentiated by production of chemokines; initiating the recruitment, activation and co-stimulation of the immune system. Activation of antigen presenting cells (APC), such as resident dendritic cells and macrophages, further orchastrate the release of chemokines and pro-inflammatory cytokines, such as interleukin 1-beta (IL-1β) tumour necrosis factor alpha (TNF-α) and interferon gamma (IFN-γ), into the islet milieu (Lenzen *et al.,* 2001; Pirot *et al.,* 2008). NOD mice deficient in macrophage inflammatory protein-1α (MIP-1α), a known recruiter of proinflammatory cells, resulted in a reduction of insulitis and protection against diabetes (Cameron *et al.* 2000). Willcox *et al.,* (2010) highlighted the importance of therapeutic interventions, if early diagnosis of pateints with recent-onset type 1 DM during early insulitis is achievable, identifying makers of proliferation (Ki67) in human pancreas sections from deceased patients with recent-onset type 1 DM, suggesting beta cell proliferation, which may restore functional cell mass if immunotherapy/other intervention becomes possible. In support of this, Sherry *et al.,* (2006) observed similar findings, showing beta cell replication in NOD mice during progression to overt diabetes, effects that appeared to be stimulated in response to insulitus. Whilst beta cell proliferation rates declined following anti-CD3 mAb treatment (which binds to the CD3 T-cell co-receptor), it was suggested that recovery of

exisiting beta cells is possible following regranulation (Sherry *et al.,* 2006). However, regain in functional capacity was not sustained, with cell loss by apoptosis observed in the follow-up period; this may suggest an early apoptotic-priming signal during early insultis and may account for the limited results with anti-CD3 mAb treatment in phase 3 clinical trials (Simmons *et al.,* 2011), emphasising the need for continued development of our understanding of the mechanisms of beta cell apoptosis and further strategies aimed to prevent this.

Further coordination of islet insulitis is carried out by resident dendritic cells and macrophages migrating to the pancreatic lymph nodes (PLNs) and recruitment of T-helper cells ($CD4^+$ T-lymphocytes), with Pearly-Yafe *et al.,* (2007) demonstrating that the removal of pancreatic lymph nodes 3 weeks from birth protects NOD mice against developing insulitis. Naïve Th_0 $CD4^+$ T-cells are activated by presentation of beta cell antigens to their MCH class II receptors by antigen presenting cells, allowing differentiation into Th1 cells, which enhance the cytotoxic immune response achieved by the release of IL-12 (Pearly-Yafe *et al.,* 2007). These Th1 $CD4^+$ T-cells further secrete cytokines such as IL-2 and IFN-γ, allowing further antigen presenting cells to promote the release of IL-1β and TNF-α, leading to increased levels of NO production within beta cells and pancreatic ductal cells (Pirot *et al.,* 2008). This set of events continues to promote migration of $CD8^+$ T-cells and production of chemokines and cytokines, further aggravating an attack on beta cells (Cardozo *et al.,* 2003). The presence of $CD8^+$ cytotoxic T-cells, macrophages ($CD68^+$), $CD20^+$ and $CD138^+$ cells in human pancreatic tissue sections have been identified from 29 patients (mean age 11.7 years) with recent-onset type 1 diabetes (Willcox *et al.,* 2009) showing similar findings compared to rodent models. The predomidant $CD8^+$ cytotoxic T-cells during insulitis and macrophages contribute to the secretion of cytokines (Willcox *et al.,* 2009), with cytotoxic $CD8^+$ T-cells also activating the

extrinsic pathway of apoptosis through the Fas/FasL and perforin-granzyme B pathways, resulting in the activation of a caspase cascade and the inititation of beta cell apoptosis. Cytokines IL-1β, IFN-γ and TNF-α released from APCs bind to their cell surface receptors on beta cells, activating the transcription factors signal transducer and activator of transcription 1 (STAT-1) and nuclear factor kappa B (NF-κB) leading to subsequent alterations in multiple regulatory gene networks, caspase activation and cell death (Pirot et *al.,* 2008).

1.1.2 Mechanisms of Beta Cell Death in Type 1 DM

Clinical symptoms of type 1 DM appear when the functional beta cell mass has been depleted by 70-80%. It has been well established that the main mechanisms involved in beta cell apoptosis occur via the activation of the extrinsic pathway, triggered by ligands such as Fas and tumour necrosis factor receptor (TNFR), and the intrinsic pathway (known as the mitochondrial or Bcl-2-regulated pathway) (Thomas and Biden, 2009). Although initiation of these pathways differ, the two converge in activating common downstream cysteine-aspartate proteases (caspases), cleaving intracellular proteins resulting in beta cell death (Yin, 2000; McKenzie *et al.,* 2008; Grunnet *et al.,* 2009). The four main mechanisms believed to be involved in mediating beta cell death are ligation of Fas Ligand (FasL) with Fas receptors between $CD8^+$ T-cells and beta cells, the release of lytic granules and pro-apoptotic proteases by activated $CD8^+$ T-lymphocytes (particularly perforin and granzyme), secretion of pro-inflammatory cytokines IL-1β, IFN-γ and TNF-α via infiltrating immune cells and increase in the concentration of NO and reactive oxygen species (ROS) released by infiltrating dendritic cells and macrophages, and from cytokine-stimulated beta cells and pancreatic ductal cells (Yoon and Jun, 2005).

1.1.3 Fas ligand and Perforin:Granzyme Pathways

Fas (CD95) is part of the TNF-α receptor superfamily and is activated by the binding of FasL present on the surface of infiltrating $CD8^+$ T-cells in pancreatic islets, leading to beta cell apoptosis (Kawasaki *et al.,* 2004). The ligation of FasL with cell surface Fas receptors leads to the recruitment of the Fas-associated death domain (FADD) to the receptor, leading to mitochondrial pore formation and release of cytochrome c, as well as directly stimulating the auto-cleavage of pro-caspase-8. Acivated caspase-8 cleaves the effector pro-caspase-3 and also activates the intrinsic mitochondrial death pathway via cleavage of the BH3 protein Bid (Eizirik and Mandrup-Poulsen, 2001). BH3-only proteins such as Bad and tBid (activated by caspase-8), regulate the pro-survival Bcl-2 family, which regulates the pro-apoptotic members Bax and Bak and ultimately cyctochrome c release from the mitochondria via permiabilization of the membrane (Thomas and Biden, 2009; Wang and Youle, 2009). The release of cytochrome c into the cytosol from the mitochondria (in part occuring downstream of FasL/FasR ligation) interacts with apoptotic protease-activating factor 1 (APAF-1) and pro-caspase-9 to form the apoptosome, a large protein complex that also contains dATP (Li *et al.,* 1997). The formation of the apoptosome allows processing of pro-caspase-9, which can then proteolytically cleave pro-caspase-3. Now in its active form, caspase-3 targets a number of intracellular substrates for degradation in a highly organised ATP-dependent manner, ultimately leading to cellular termination (Taylor *et al.,* 2008).

The importance of Fas/FasL in models of type 1 DM as a contributor to beta cell apoptosis are well established in rodent models, as Fas-deficient NOD mice failed to develop diabetes, despite the infiltration of lymphocytes (Suarez-Pinzon *et al.,* 2000; Petrovsky *et al.,* 2002). Stimulation of beta cells with IL-1β and IFN-γ upregulates Fas expression (Kawasaki *et*

al., 2004), with Augstein *et al.,* (2004) observing an increase in Fas expression in NIT-1 mouse beta cells following treatment with IL-1β and IFN-γ for 24 hours from 1.4 to 29.7% Fas-positive cells; a treatment that was associated with an increase in caspase-3-like activity by 2.1-fold. Under these conditions, the addition of FasL for 3 hours augmented cytokine effects, resulting in a further a 1.8-fold increase in the caspase-3-like activity (Augstein *et al.,* 2004). Pro-inflammatory cytokines have been shown to lead to an increased expression of the inducible form of nitric oxide synthase (iNOS) in beta cells, resulting in an increase in NO production. Interestingly, iNOS inhibition still results in an increase in Fas expression via cytokine-induced beta cell damage in NIT-1 beta cells and intact mouse islets (Zumsteg *et al.,* 2000). Similarly iNOS knockout mice (iNOS -/-) failed to increase nitrite production after cytokine treatment, though the lack of cytokine-induced iNOS activity still witnessed a 3-fold increase in Fas expression, suggesting this occurs in a NO-independent manner, with NF-κB activation (downstream of cytokine signalling) likely playing a crucial role in Fas promoter regulation (Liu *et al.,* 2000).

$CD8^+$ T-cells also release the cytotoxic enzymes perforin and granzyme B as a result of TCR recognition of self-antigens presentated on the surface of beta cells by MHC-I molecules, with transgenic NOD mice lacking MHC class 1 not developing invasive intra-islet insulitis (De Jersey *et al.,* 2007; Pearly-Yafe *et al.,* 2007). Perforin and granzyme B are released into the extracellular milieu during insulitis, where perforin initiates pore formation across the cell membrane in a Ca^{2+}-dependent mechanism (Pirot *et al.,* 2008), allowing the serine protease granzyme B to enter the cell, inducing apoptosis (Estella *et al.,* 2006). Granzyme B-mediated apoptosis occurs only in the prescence of perforin and is associated with activation of caspases and cleavage of Bid, leading to the aforementioned mitochondrial distruption and activiation

of the intrinsic apoptosis pathway via cytochrome c release (Estella *et al.,* 2006). Mice deficient in Bid were protected from apoptosis after exposure to perforin/ granzyme B by resisting cytochrome c release, suggesting a direct link for granzyme B and Bid in apoptosis induction, bypassing the activation of caspase 8 (Barry *et al.,* 2000*).*

A study by Kreuwel *et al.,* (1999) investigated the relative contribution of Fas/FasL and perforin:granzyme B pathways in diabetes development in a $CD8^+$ adoptive transfer model using clone-4 TCR deficient mice. It was shown that blocking the perforin:granzyme pathway required a 30-fold increase in $CD8^+$ T-cells for diabetes to develop, in contrast to little effect in Fas/FasL deficient models, suggesting an important contribution (though not essential) of the perforin:granzyme pathways in diabetes development. Studies using NOD mice lacking perforin showed a reduced rate in the development of spontaneous diabetes from 77% in $perforin^{+/+}$ controls compared to 16% in perforin-deficient mice, but concluded chronic inflammation of the islets, which led to beta cell loss regardless of perforin, due to a secondary effector mechanism (Kägi *et al.,* 1997).

1.1.4 Activation of Pro-Inflammatory Cytokines: IL-1β, IFN-γ and TNF-α

Whilst the contribution of $CD8^+$ T cells to the autoimmune attack against pancreatic beta cells represents a form of direct cell:cell killing through the ligation of T-cell receptors with beta cell presented antigens, cytokines as soluble effectors of the immune response are also well-established contributors to beta cell loss (Cnop *et al.,* 2005; Willcox *et al.,* 2010). Much evidence points to an overall pro-apoptotic effect of cytokines by the activation of

intracellular signalling pathways culminating in beta cell demise. The following sections delineate the signalling pathways mediating the response to individual cytokines and the importance of cytokine synergy in beta cell death.

The release of IL-1β from $CD8^+$ T cells activates of the IL-1β receptor (IL-1R) on the beta cell surface inducing the formation of a multi-protein complex structure, which includes IL-1R accessory protein (IL-IRAcP), toll interacting protein (Tollip), myeloid differentiation primary 88 (MyD88), interleukin-1 receptor-associated kinase (IRAK-1) and interleukin-4 receptor-associated kinase (IRAK-4), with IRAK-4 phosphorylating IRAK-1, resulting in further activation and subsequent release of this protein from the IL-1R complex (Eizirik and Mandrup-Poulsen, 2001). IRAK-1 is now able to interact with the TNF-receptor-associated factor-6 (TRAF-6), enabling its phosphorylation and activation (Eizirik and Mandrup-Poulsen, 2001). In its activated form, TRAF-6 interplays between activating NF-κB and/or the mitogen activated protein kinase (MAPK) pathway (Eizirik and Mandrup-Poulsen, 2001). The phosphorylation of IκB kinase (IKK) by TRAF-6 leads to its activation and the phosphorylation of the inhibitory IκB subunit, leading to its dissociation from NF-κB and activation of the transcription factor.

Once activated, NF-κB translocates to the nucleus and regulates transcription of several target genes, including the up-regulation of Fas, C-Myc and CD40, which promotes beta cell apoptosis. NF-κB also promotes the up-regulation of iNOS, promoting the production of high levels of NO which contributes directly to the activation of pro-apoptotic signalling pathways and the expression of pro-apoptotic genes including TRAF-2, activating transcription factor 4 (ATF-4), C/EBP homologous protein (CHOP)/growth arrest and DNA damage-inducible gene 153 (GADD153), and spliced x-box binding protein 1 (XBP-1), as part of an adaptive endoplasmic reticulum (ER) stress response (Eizirik and Mandrup-Poulsen, 2001; Cardozo *et*

al., 2005). Other genes altered by NF-κB activation include the down-regulation of pancreatic and duodenal homeobox 1 (Pdx-1), insulin gene enhancer protein-1 (Isl-1), cholecystokinin A receptor (CCK-A receptor) and phospholipase D1 (PLD-1), leading to decreased beta cell proliferation and reduced beta cell function. Pro-apoptotic activity following modifications in expression of NF-κB target genes is associated with an increase in Bid and its cleavage to activated tBid, increasing the activation and expression of pro-apoptotic Bak and Bax, leading to activation of the mitochondrial pathway of apoptosis initiation via the release of cytochrome c (Cnop *et al.,* 2005).

A study by Heimberg *et al.,* (2001) showed that expression of IκB((SA)2), an inhibitor of NF-κB, inhibited cytokine-stimulated nuclear translocation and DNA-binding of NF-κB. Inhibition of NF-κB meant that increased expression of several downstream target genes of the pathway were prevented, namely iNOS, Fas and manganese superoxide dismutase (MnSOD), resulting in an increase in beta cell survival. Hohmeier *et al.,* (1998) showed that stable overexpression of MnSOD in INS-1 cells ameliorated the cytotoxic effects of IL-1β by a reduction in NO levels, correlating with reduced nitrosative and oxidative stress, with inhibition of iNOS producing similar findings; this may support an important role for peroxynitrite in beta cell death, produced in the equimolar reaction between NO and superoxide. In support of this, Azevedo-Martins *et al.,* (2003) showed in RINm5F cells that over-expression of MnSOD protected against cytokine toxicity, effects associated with reduced NF-κB and iNOS expression and that anti-sense MnSOD resulted in a 3-fold higher activation of NF-κB and 2-fold higher activation of iNOS compared to control, again emphasising the important role of toxic free radical species and the enzymes responsible for controlling their levels in beta cell death (Azevedo-Martins *et al.,* 2003; Lortz and Tiedge, 2003;

Gurgul *et al.,* 2004). Interestingly MnSOD overexpression in combination with hydrogen-peroxide inactivating-catalase provided greater protection against H_2O_2 and menadione in RINm5F cells than catalase expression alone (Lortz and Tiedge, 2003), supporting sensitivity of beta cells to cytokine stimulated, NF-κB-dependent, oxidative/nitrosative stress.

MAPK cascades play a crucial role in apoptosis signalling, resulting in phosphorylation and activation of p38 MAPK and c-jun NH_2 terminal kinase (JNK) (Saldeen *et al.,* 2001). IL-1β, but not IFN-γ, was shown to induce phosphorylation of p38 MAPK, JNK and mitogen- and stress-activated protein kinase-1 (MSK-1) in RINm5F cells (Saldeen *et al.,* 2001). With p38 MAPK known to activate downstream of Protein Kinase C δ (PKCδ) in some models (Chen *et al.,* 1999), which is directly activated by caspase-3, inhibition of PKCδ, but not PKCα, by over-expression of a kinase-dead (KD) mutant reduced iNOS expression, attenuated NO production and protected against cytokine-induced apoptosis in INS-1 beta cells, effects similarly observed with a PKCδ inhibitor (Carpenter *et al.* 2001; Carpenter *et al.* 2002). Interestingly, NF-κB activation was achieved independently of PKCδ in this model (Carpenter *et al.* 2002), despite others reporting that PKCδ stimulates NF-κB activity via the IκB kinase (Lallena *et al.,* 1999).

When TNF-α binds to the TNF receptor 1 (TNF-R1) this leads to the trimerization and recruitment of the adaptor protein TNF receptor-associated death domain protein (TRADD) (Eizirik and Mandrup-Poulsen, 2001). Once the TRADD complex is formed it allows the recruitment of the TRAF-2 and serine/ threonine kinase Rip. TRAF-2 also activates the NF-κB and MAPK pathways by similar mechanisms to IL-1β, suggesting an important syngergy between distinct cytokine species in beta cell death (Eizirik and Mandrup-Poulsen, 2001). Together, Rip and TRAF-2 can induce activation of the IKK complex, activating both IKKα and

IKKβ isoforms unlike IL-1β (Ortis *et al.,* 2012), and acitvates the MAPK pathway by interaction between the MAP2Ks: Ask-1 and MEKK-1 (Eizirik and Mandrup-Poulsen. 2001). In rat insulinoma cells, TNF-α preferentially phosphorylates and activates JNK and p38 MAPK similar to IL-1β, leading to activation of NF-κB (Saldeen *et al.,* 2001; Ortis *et al.,* 2008). Interestingly, TNF-α showed a similar level of activation of NF-κB and its subsequent downstream targets, however compared to IL-1β, TNF-α stimulated this at a lower rate, which lead to a delayed translocation of NF-κB to the nucleus compared to in response to IL-1β (Ortis *et al.,* 2008).

IFN-γ binding to its receptor results in receptor oligomerization, recruiting janus kinase (Jak) -1 and Jak2, both part of the Janus kinase family (Eizirik and Mandrup-Poulsen, 2001). Jak1 and 2 are then activated by transphosphorylation allowing the recruitment of the transcription factor STAT-1 and its subsequent phosphorylation. STAT-1 then migrates to the nucleus after homodimerizing and can regulate, similar to NF-κB, the expression of numerous cytokine-response genes containing a γ-activated sequence (GAS) in the promotor region, including Fas, caspases and iNOS (Battle and Frank, 2002). Further to this, STAT-1 is able to promote an increase in activated caspase-3 by increasing interferon regulatory factor (IRF-1) activity, which increases initiator caspase-1 levels, affecting caspase-3 activation (Cnop *et al.,* 2005). A study using IRF-1 deficient mice exposed to IL-1β (5 U/ml) and IFN-γ (1000 U/ml) showed a 30-50% reduction in iNOS mRNA expression and nitrite production, compared to the wild type (Pavlovic *et al.,* 1999), suggesting an important role of IRF-1 in elevating iNOS levels under co-stimulatory conditions with IL-1β.

1.1.5 Synergism of Cytokines

Although individual cytokines have an effect on beta cells, the idea that IL-1β, IFN-γ and TNF-α work in synergy, in alteration of multiple regulatory gene networks, promoting increased levels of apoptosis is more likely to be pathophysiologically relevant in the development of type 1 DM. Investigations into whether cytokine induced beta cell death is associated with changes in the expression of the surface receptors intercellular adhesion molecule (ICAM)-1 and activation of Fas/FasL in islets from diabetes-prone and congenic diabetes-resistant BB rats showed that IL-1β alone or in combination with IFN-γ and TNF-α decreased islet insulin content, suppressed glucose stimulated insulin secretion and enhanced the production of nitric oxide and DNA fragmentation (Wachlin *et al.,* 2003). This study also showed that only when islets were treated with a combination of cytokines, was there damage to the cell membranes, however independent of diabetes susceptibility, IL-1β was able to increase the amount of ICAM-1 expressed at the cell surface, and adding IFN-γ and TNF-α witnessed no further increase. The findings showed that IL-1β is the main stimuli for ICAM-1 expression, promoting further recruitment of immune cells *in vivo,* but also that a combination of all three cytokines induced maximum expression of Fas on the beta cell surface, independent of diabetes susceptibility (Walchin *et al.,* 2003).

Studies in human islets also revealed differences in susceptibility to individual cytokines alone and in combination, such that rat beta cells have been shown to be sensitive to apoptosis induced by IL-1β treatment alone (Ankarcrona *et al.,* 1994), whereas in mouse and human beta cells a combination of cytokines is necessary for significant beta cell loss (Cnop *et al.,* 2005). In combination with IL-1β, IFN-γ induced NO and CHOP expression in rodent and human beta cells as part of a cytokine-induced ER stress response (Cardozo *et al.,*

2005). Whilst only IL-1β alone (but not IFN-γ) was capable of inducing an ER stress response but not apoptosis, the combination of both cytokines markedly enhanced ER stress induction and apoptosis, effects in part associated with elevated iNOS expression and a reduction in ER chaperone expression (Cardozo *et al.,* 2005; Pirot *et al.,* 2006). Figure 1.1 summarises cytokine synergistic effects in the initiation in beta cell apoptosis and the role of the Fas/FasL and perforin/granzyme B pathways.

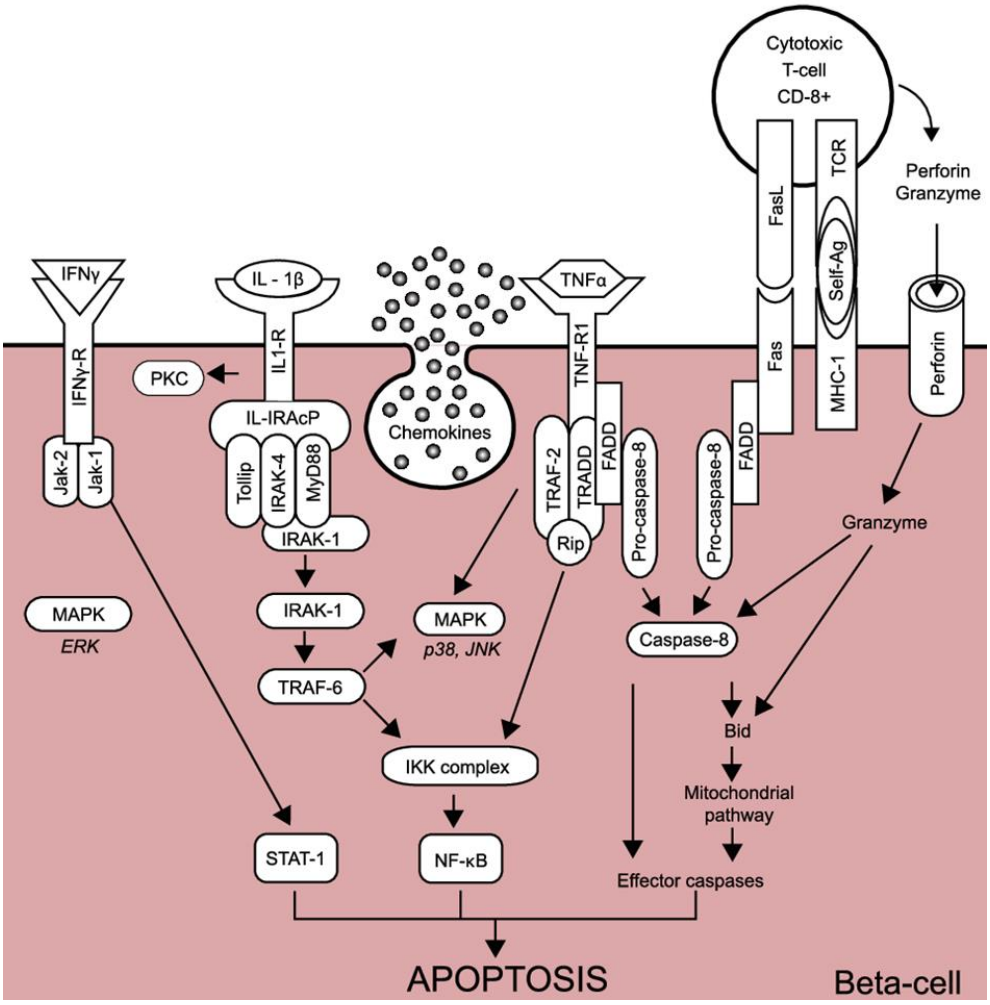

Figure 1.1 Pathways of beta cell apoptosis in type 1 DM. Synergistic activation of cytokine signalling pathways changes in STAT1 and NF-κB responsive target genes including iNOS leading to increased beta cell apoptosis, reduced defense capacity and altered beta cell function. Mechanisms of direct cell:cell killing by the actions of CD^{8+} cytotoxic T-cells include ligation of FasL with beta cell Fas receptors initiating caspase cascade and Bid cleavage activating the intrinsic mitochondria apoptotic pathway synergising with cytokine activity and pro-apoptotit perforin:granzyme B in the initiation of the caspase cascade culminating in beta cell apoptis (adapted from Tomita, 2017).

1.1.6 Endoplasmic and Oxidative Stress in Type 1 DM

The formation of NO and the interplay between different pools of 'reactive species' as a result of their high chemical reactivity, including the formation of peroxynitrite from the reaction between NO and superoxide, directly contributes to the activation of pro-apoptotic signalling pathways, including the activation of ER stress, disrupting ER calcium homeostasis and ER to mitochondrial calcium signalling, further promoting the release of pro-apoptotic cytochrome c. It is well known that NO production contributes directly to cytokine-induced beta cell death and dysfunction, first reported by Southern *et al.,* (1990), with subsequent studies confirming a role for NO, though not essential, in cytokine-induced apoptosis and ER stress (Oyadomari *et al.,* 2001; Cardozo *et al.,* 2005; Brovkovych *et al.,* 2011). Oyadomari *et al.,* (2001) showed that S-nitroso-N-acetyl-D, L-penicillamine (SNAP), an NO donor, increased cytosolic [Ca^{2+}], and agents depleting ER Ca^{2+} induced pro-apoptotic CHOP expression downstream of ER stress. This suggests that NO depletes ER Ca^{2+} since overexpression of calreticulin showed an increase in ER Ca^{2+} levels, protecting cells against NO-mediated apoptosis. Islets from CHOP knockout mice displayed increased resistance to NO, suggesting that NO depletes ER Ca^{2+} stores, leading to ER stress, resulting in beta cell apoptosis (Oyadomari *et al.,* 2001). Subsequently, Cardozo *et al.,* (2005) demonstrated that these effects were mediated by inhibition of an ER Ca^{2+} ATPase in response to pro-inflammatory cytokines in rodent beta cells, an effect that was blocked using an iNOS inhibitor, confirming the role of NO in mediating an ER stress response in beta cells. The complex interplay between reactive nitrogen and oxygen species, including the formation of peroxynitrite is also an acknowledged contributor to cytokine toxicity. Whilst some have suggested that human islets display reduced sensitivity to the deleterious effects of NO (Flodstrom *et al.,* 1997), others have

reported that these islets, and clonal beta cells are highly sensitive to peroxynitrite (DeLaney *et al.,* 1997). More recently, Broniowska *et al.,* (2013) found that addition of the NADPH oxidase activator phorbol 12-myristate 13-acetate in rat islets and insulinoma cells failed to stimulate peroxynitrite generation in response to cytokines; proposing that NO is the likely mediator of the toxic effects of the reactive nitrogen species component of cytokine-induced loss in viability and that beta cells do not produce peroxynitrite as a response. Furthermore when forced to produce superoxide using phorbol 12-myristate 13-acetate , the scavenging of nitric oxide by superoxide protected beta cells from nitric oxide-mediated toxicity (Broniowska *et al.,* 2013).

Disruption of ER homeostasis impairs ER folding capacity and results in the accumulation of misfolded proteins within the ER lumen, initiating the activation of an adaptive response called the unfolded protein response (UPR) (Ron and Walter, 2007). Transduction of the UPR by the activation of three transmembrane ER proteins; protein kinase RNA-like endoplasmic reticulum kinase (PERK), inositol-requiring protein-1 (IRE-1) and activating transcription factor 6 (ATF-6) following dissociation of the chaperone BiP from their ER luminal domains. These serve to mitigate ER stress and restore ER homeostasis by 1) increasing ER protein folding capacity via increased expression of ER resident chaperones and protein foldases, 2) controlling general protein translation to reduce demands on ER folding capacity, 3) up-regulation of ER-associated degradation (ERAD) genes, reducing the load of unfolded proteins by their unbiquitiniation, export from the ER and proteosomal degradation and 4) if these mechanisms fail to restore ER homeostasis, pro-apoptotic signals via the expression of pro-apoptotic CHOP (GADD153), JNK activation and initiation of the caspase

cascade, including the activation of mitochondrial-associated pathways (Ron and Walter, 2007).

Characteristic ER stress induction by cytokines is achieved by phosphorylation of eukaryotic initiation factor 2α (eIF2α) by PERK, necessary for increased ATF-4 levels and subsequent up-regulation of pro-apoptotic CHOP in prolonged ER stress, as well as activation of alternative mRNA splicing of XBP-1 by IRE1 (Pirot *et al.,* 2006; Pirot *et al.,* 2007). Of note, the ATF-6 branch of the UPR seems to be diminished following cytokine-induced ER stress, since Cardozo *et al.* (2005) demonstarted impaired ATF-6 signalling using an UPRE luciferase construct under the control of an ATF-6 target sequence, associated with reduced XBP-1 and lack of BiP induction; a key ER resident chaperone. Reduced BiP expression in response to IFN-γ may indicate a role of this cytokine in imparing a pro-adaptive UPR reponse against IL-1β-induced ER stress (Pirot *et al.,* 2006). Whilst Akerfeldt *et al.,* (2008) reported that induction of ER stress is dispensible for cytokine-induced ER stress, with the chemical chaperone phenylbutyrate (PBA) failing to attenutate cytokine toxicity, others have reported that the chemical chaperone TUDCA can confer protection in both human and islet models (Brozzi *et al.,* 2015). Targetting CHOP through siRNA produced similar results, suggesting an important contribution of ER stress in cytokine toxicity this, and observations that ER stress markers can be detected in pancreas sections of type 1 patients, continues to maintain interest in the understanding of this pathway leading to the pathogenesis of type 1 DM (Marhfour *et al.,* 2012; Brozzi *et al.,* 2015).

1.2 Type 2 Diabetes Mellitus

In contrast to the autoimmune destruction of pancreatic beta cells that is characteristic of type 1 DM, mechanisms responsible for beta cell death and dysfunction in type 2 DM are associated with chronic glucolipotoxicity resulting from high-fat diets and peripheral hyperglycaemia linked to insulin resistance in adipose and skeletal muscle. Overtime, persistent hyperglycaemia forms the basis of a 'pre-diabetic' state and eventually a diagnosis of type 2 DM (Donath *et al.,* 2013). This can in part be associated with a direct glucotoxic effect, as seen in isolated rodent islets exposed to high glucose concentrations of 16.7 or 33mM for 3-6 days resulting in detectable levels of significant beta cell apoptosis (Piro *et al.,* 2002; McKenzie *et al.,* 2010).

1.2.1 Type 1-Like Cytokine-Induced Beta Cell Apoptosis in Type 2 DM

Rather than two distinct subtypes, a diabetes 'spectrum' proposes that there may be characteristic traits of type 1 DM development evident in the pathogenesis of type 2 DM. The response to elevated circulating glucose and free fatty acids (FFAs) has been suggested to activate an innate inflammatory response in two proposed mechanisms; FFA-triggered inflammation by toll-like receptor (TLR)-dependent or TLR-independent pathways and cellular stress (Donath *et al.,* 2013). TLRs are important in recognising damage-associated molecular patterns (DAMP) in the development of type 2, with particular interest in the roles of TLR2 and TLR4. In rodent islets it has been demonstrated that saturated fatty acids, such as

palmitate (C16:0), can activate an inflammatory response mediated by signalling through the TLR4/MyD88 pathway, resulting in the recruitment of monocytes and macrophages, with enhanced chemokine secretion (Eguchi *et al.,* 2012). Interest has also focused on the importance of the NLRP3 inflammasome as a contributor to an inflammatory response in islets in models of type 2 DM and its activation by cellular stress as a result of high glucose and FFAs (Dixit, 2013), linked to the initiation of the intrinsic pathway of beta cell apoptosis (Wali *et al.,* 2013). Activated NLRP3 can also result in cell death via caspase activated-pyroptosis, an intermediate step between necrosis and apoptosis, including cytoplasmic swelling and DNA fragmentation (Wali et al., 2013; Man *et al.,* 2017).

Activation of the NLRP3-inflammasome also leads to the release of IL-1β into the islet milieu, leading to beta cell dysfunction via downstream effects of cytokine activation on intracellular mechanisms, previously discussed (Wali *et al.,* 2013). Physiologically, elevated ROS as seen in type 1 DM (consequential to the effects of pro-inflammatory cytokines on inducing oxidative stress) and type 2 DM (from increased glucose and FFA metabolism), can result in activation of the anti-oxidant enzyme thioredoxin by dissociation of its interacting protein TXNIP. The activation of an ER stress response has been shown to result in TXNIP up-regulation, which directly activates the inflammasome and enhances oxidative stress (Lerner *et al.,* 2012). Mouse islets treated with 33mM glucose have been observed to secrete IL-1β in a TXNIP-dependent manner (Zhou *et al.,* 2010) and so the idea that IL-1β is secreted by islets in a type 2 DM model suggests an overlap between cytokine-induced beta cell apoptosis in type 1 DM and type 2 DM. Another possible link is that palmitate can induce NLRP3 inflammasome activation in immune cells, such as resident macrophages in islets, with few studies directly addressing the link between FFAs and NLRP3-inflammasome activation (Wen

et al., 2011; Wali *et al.,* 2013). Interestingly, lipopolysaccharide (LPS)-primed bone marrow-derived macrophages (BMDMs), bone marrow-derived cells (BMDCs) and peritoneal macrophages treated with palmitate displayed increased expression of the NLRP3-inflammasome and IL-1β production. That macrophages lacking NLRP3 showed no production of IL-1β in this model (Wen *et al.,* 2011), further supports the importance of a type 2 DM innate inflammatory response with some similarity to type 1 DM.

1.3 Free Fatty Acid-Induced Beta Cell Apoptosis

Fatty acids are categorized dependent on carbon length; fatty acids less than 6 carbons are termed short-chain fatty acids (SCFA), between 6-12 carbons are termed medium-chain fatty acids (MCFA) and more than 12 carbons are termed long-chain fatty acids (LCFA). These are further classified into saturated or mono/poly- unsaturated depending on the presence and number of double bonds (Poudyal *et al.,* 2013). Rising levels of obesity in the population are of a major concern and is one of the primary contributors to the development of type 2 DM. Such hyperlipidemia leads to an increase in the levels of circulating non-esterified FFAs contributing to a reduction in beta cell mass via lipotoxicity, as wells as to the progression of insulin resistance in peripheral tissues (adipose, skeletal muscle). In *in vitro* models of type 2 DM, saturated fatty acids, particularly palmitate (the most abundant fatty acid in human plasma and the major fatty acid synthesized *de novo* in the liver) and stearate (C18:0), are well established inducers of beta cell apoptosis, with effects in part mediated via induction of an ER stress response (Cunha *et al.,* 2008; Diakogiannaki *et al.*, 2008). However, the extent of

toxicity is dependent on chain length, with medium-chain fatty acids such as Laurate (C12:0) showing reduced toxicity compared to long-chain fatty acids (Newsholme *et al.,* 2007).

Whilst elevated saturated fatty acids contribute to beta cell death and dysfunction, physiological beta cell function is enhanced by low levels of FFAs via augmentation of glucose-stimulated insulin secretion (GSIS) and depleting beta cells of intra-islet FFAs results in a reduction in GSIS (Stein *et al.,* 1996). Additionally, although long-chain saturated fatty acids induce beta cell apoptosis in high concentrations, mono- and poly-unsaturated species such as palmitoleate (C16:1), oleate (C18:1) or arachidonic acid (C20:4) are well tolerated and can attenuate the cytotoxicity observed in response to saturated fatty acids (Welters *et al.,* 2004; Diakogiannaki *et al.,* 2007; Keane *et al.,* 2011). Mechanisms resposible for these effects may include partioning of toxic FFA species into neutral lipids via triglyceride synthesis, with observations that the esterification of FFAs into triacylglycerides (TAG) in the ER appears to be the unlikely activator of an ER stress response by ER lipid overload, suggesting that TAG synthesis may be a protective mechanism againts elevated FFAs (Cuhna *et al.,* 2008).

1.3.1 Palmitate Metabolism

When free fatty acids enter the beta cell they are activated by acyl-CoA synthetase, which results in them either being oxidised (via entry to the mitochondria, mediated by carnitine palmitoyl transferase-1, CPT-1), serving as an important energy source in cells by β-oxidation, or re-esterified for storage as TAG (Prentki *et al.,* 2002). Importantly non-metabolisable methyl-ester derivatives of fatty acids are non-toxic to beta cells, failing to induce ER stress, suggesting the availability of palmitate to be metabolised is key in

metabolically activating triggers of ER stress and lipotoxicity (Cuhna *et al.,* 2008). High levels of long-chain fatty acids and very long-chain fatty acids can also result in β-oxidation in peroxisomes producing hydrogen peroxide as a byproduct (Elsner *et al.,* 2011; Plötz *et al.,* 2016). Given that pancreatic beta cells have been shown to lack the hydrogen peroxide inactivating enzyme catalase, this therefore represents an important source of FFA-induced oxidative stress (Lenzen *et al.,* 1996; Tiedge *et al.,* 1997; Elsner *et al.,* 2011), with overexpression of catalase protecting against palmitate toxicity in RINm5F cells (Elsner *et al.,* 2011).

In states of fasting FFAs serve as an important energy source, undergoing β-oxidation in the mitochondria, whereas in well-fed states, increased glucose metabolism generates ATP and cytosolic malonyl-CoA via acetyl-CoA-carboxylase (ACC) (Roduit *et al.,* 2004). Excess malonyl-CoA prevents β-oxidation via inhibition of CPT-1, which stops transportation of acyl-CoA into the mitochondria, thereby allowing an accumulation of cytosolic long-chain fatty acids. Under pathological conditions of hyperglycaemia and hyperlipidaemia, dysregulation of these processes by glucolipotoxicity further increases cytosolic accumulation of FFAs, contributing to cytotoxicity. In support of this, over-expression of CPT-1 protected against glucolipotoxicity in INS-1 cells (Sol *et al.,* 2008) and inhibition of CPT-1 in the same cell line by etomoxir augmented palmitate-induced cell death and its knockdown increased palmitate-induced CHOP levels, whilst reducing eIF2α and phosphorylated-JNK, suggesting alterations in palmitate-induced ER stress signals under conditions affecting β-oxidation (Choi *et al.,* 2011). Glucose concentrations exceeding 20mM have also been shown to potentiate palmitate-induced cell death in INS-1 cells and dispersed human beta cells, but not MIN6 cells or intact islets, reflecting a contribution of glucolipotoxicity in alterations in lipid handling in beta cells

(El-Assaad *et al.,* 2003; Sargsyan and Bergsten 2011). Differences between these models may relate to a higher expression level of ACC in INS-1 cells, thereby contributing to increased levels of malonyl-CoA in response to high glucose levels. Additionally, MIN6 cells display a higher expression level of stearoyl-CoA-desaturase 1 (SCD-1) (Lai *et al.,* 2008; Sargsyan and Bergsten, 2011), potentially reflecting differences in lipid handling in terms of fatty acid β-oxidation and TAG synthesis.

The contribution of TAG formation in beta cell models of lipotoxicity remains unclear and indeed whether or not this represents a mechanism contributing to the cytoprotective actions of unsaturated species. In regards of studies concerning this, non-metabolisable methyl-ester derivatives of FFA species and the poorly metabolisable palmitate analogue 2-Bromopalmitate (2-BP), which can be thioesterified to Coenzyme-A, but is unable to undergo further metabolism, have been employed. Cnop *et al.,* (2001) demonstrated that increased TAG formation correlated with higher cell viability in primary rat beta cells exposed to FFAs and observed toxicity of 2-BP, supporting that mitochondrial oxidation is not necessary for palmitate toxicity. This species is also incapable of being incorportated into triglycerides and may suppress palmitate-TAG formation through sequestring CoA and reducing available substrates for TAG synthesis (Diakogiannaki *et al.,* 2007). Listenberger *et al.,* (2003) showed that the unsaturated FFA oleate protected against palmitate toxicity in CHO cells by increasing its incorporation into neutral lipids and others have also reported a similar increase in TAG formation in co-incubation with the unsaturated fatty acid palmitoleate in BRIN-BD11 cells however, observations that methyl-palmitoleate failed to increase TAG, despite protecting against palmitate toxicity, suggests TAG formation is dispensible to the cytoprotective actions of unsaturated FFAs (Diakogiannaki *et al.,* 2007). Perilipin is a protein associated with

intracellular lipid stores, protecting lipid droplets from the action of hormone sensitive lipase, which is observed to be expressed in pancreatic beta cells and its over-expression in INS-1 cells was associated with increased TAG formation and protection against palmitate toxicity (Borg *et al.,* 2009). However, this view has again been challenged, with astudy showing that shRNA targeting perilipin did not alter the cytoprotective effects of oleate in RINm5F and INS-1 cells (Plotz *et al.,* 2006), despite demonstrating that a range of mono- and poly-unsaturated fatty acids increased total lipid droplet content.

The enzyme diacylglycerol acyl-transferase (DGAT) controls the last acylation step in TAG formation and over-expression of DGAT-1 in beta cells has been shown to increase palmitate incorporation into triglycerides 2-fold, with data also suggesting that glucose is required for palmitate to increase triglyceride mass, presumably by increasing glycerol availability form enhanced glycolytic flux (Briaud *et al.,* 2001 Kelpe *et al.,* 2002). In one study in MIN6 cells treated with palmitate and stearate, DGAT-1 and DGAT-2 expression were both increased up to 3-fold compared to controls (Thorn and Bergsten, 2010). In contrast, this study also showed that DGAT-1 expression was unchanged in the presence of the unsaturated fatty acid oleate, despite which unsaturated species were preferentially incorporated into TAG. The idea that unsaturated fatty acids preferentially favour TAG formation is reported in other beta cell models (Moffitt *et al.,* 2005; Diakogiannaki *et al.*, 2007) and hepatocytes (Leamy *et al.,* 2016). In support of this, Montell *et al.,* (2001) demonstrated that unsaturated fatty acids are preferentially channelled to TAG synthesis in muscle cells, with saturated fatty acids diverted towards diacylglycerol (DAG) formation and activation of PKC. Of note, PKCδ activation has been reported to be necessary for FFA-induced beta cell apoptosis, with PKCδ knockout mouse islets protected from palmitate-induced mitochondrial dysfunction (Eitel *et al.,* 2003; Hennige

et al., 2009). However, this view has been challenged in BRIN-BD11 cells, with down-regulation of PKCδ failing to attenuate palmitate toxicity in contrast to the use of the PKCδ inhibitor rottlerin, with data suggesting a potential role for other rottlerin-sensitive kinases in promoting beta cell death (Welters *et al.,* 2004b). Whilst limited incorporation of palmitate into TAG, despite the reported increase in DGAT expression, may seem counter-intuitive, the formation of tripalmitin (with three palmitate chains esterified to glycerol) has been shown to lead to ER stress induction and apoptosis in INS-1 cells (Moffitt *et al.,* 2005). Therefore, the presence of unsaturated species, in combination with palmitate, may increase TAG synthesis from alterations in total cellular lipid content.

Saturated FFAs can be directly converted into unsaturated species, including the conversion of palmitate to palmitoleate, by the enzyme SCD (Green and Olson, 2011). SCD is expressed as one of four isoforms with SCD-1 and -2 being the two major isoforms expressed in mouse beta cells and expression of SCD-1 being up-regulated in the presence of palmitate or stearate but decreased in the presence of their unsaturated counterparts (Thorn and Bergsten, 2010). In support of the preferential incorporation of unsaturated species into TAG, in CHO cells, over-expression of SCD-1 was sufficient in protecting against palmitate-induced toxicity, associated with a 5-fold increase in TAG (Listenberger *et al.,* 2003). However, whilst in palmitate-resistant MIN6 cells, SCD-1 function was found to be necessary in protecting against lipo-apoptosis, this was not associated with increased TAG formation (Busch *et al.,* 2005).

Peroxisome proliferator-activated receptor (PPAR) α agonists have also been associated with increased rates of β-oxidation and peroxisomal activity, with noticeable increases in SCD expression (Hellemans *et al.,* 2007). It has been shown that agonists of PPARα

and Liver X Receptors (LXR), nuclear oxysterol receptors with established roles in cholesterol and lipid metabolism, provide long-term protection against palmitate in rodent and human beta cells through increased SCD (Gerin *et al.,* 2005; Hellemans *et al.,* 2009). LXR-β is also required for expression of the cholesterol transporters ABCA1 and ABCG1 and, in pancreatic islets, lipid droplets may result from the accumulation of cholesterol esters (Gerin *et al.,* 2005), further supported by observations that SCD-dependent, palmitate-resistant MIN6 cells displayed increased intracellular cholesterol ester accumulation rather than TAG (Busch *et al.,* 2005).

As well as being desaturated, fatty acids can also be targeted for chain extension, achieved in multiples of two carbon units (from acetyl-CoA), by members of the elongation of very long chain fatty acids (Elovl) gene family, which encode for the elongase enzyme family (Jakobsson *et al.,* 2006). Fatty acid elongases can be divided into two distinct groups: 1) Elovl1, 3 and 6, suggested to be involved in the elongation of saturated and monounsaturated very long chain fatty acids (VLCFA) or 2) Elovl2, 4 and 5 which are elongases of polyunsaturated fatty acids (PUFAs) (Jakobsson *et al.,* 2006). Elovl-6 has been shown to be highly expressed in MIN6 cells and mouse islets, with comparable expression to that seen in brain and liver (Tang *et al.,* 2014), with Elovl3 and Elovl7 shown to be increased in MIN6 cells in response to palmitate (Thorn and Bergsten, 2010). Of note, Elovl6$^{-/-}$ mouse islets showed a decrease in several fatty acid metabolism-related genes including the transcription factors sterol response element binding protein (SREBP) -1c and Pdx-1, as well as fatty acid synthase (FAS) and SCD-1 (Tang *et al.,* 2014). However, Elovl6$^{-/-}$ islets from mice fed a high-fat diet showed lower C18:0/C16:0 ratios, though also displayed an increase in SCD-1 consistent with elevated ratios of C18:1 to C18:0 fatty acids, suggested to be protective against lipotoxicity in this model (Tang

et al., 2014). In support of this, knockdown of Elovl6 in INS-1 cells partially attenuated palmitate-induced ER stress and caspase-9 cleavage (Green and Olson, 2011). The major pathways of palmitate metabolism in beta cells and the role of ROS in the contribution to palmitate-induced apoptosis are summarised in figure 1.2.

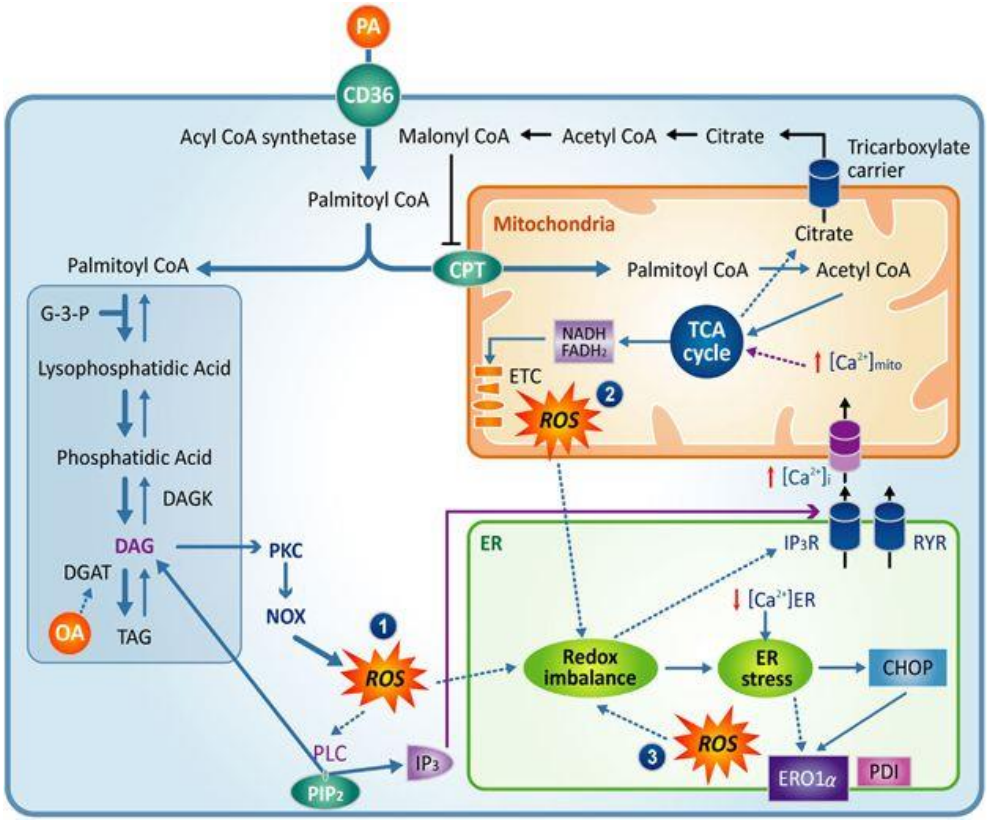

Figure 1.2 Major pathways of palmitate metabolism and ROS production in beta cells. (1) Preferential shuttling of cellular palmitoyl CoA into DAG formation leads to increase PKC activation and ROS production via NOX enzymes. These effects may, in part, be attenuated in the presence of unsaturated species such as oleate (OA) via increased TAG formation. (2) Entry of palmitoyl CoA into the mitochondria via the action of CPT1 which may increase ROS production via increased β-oxidation and superoxide release from the electron transport chain. (3) Elevated intracellular ROS directly contributes to a redox imbalance in the ER, including as a consequence of dysregulated ER calcium homeostasis promoting an ER stress response (section 1.3.3). Inhibitory action of malonyl CoA at CPT1, potentiated under hyperglycaemic conditions may increase palmitate metabolism in other pathways including DAG formation contributing to extra-mitochondrial ROS (Ly *et al.,* 2017).

1.3.2 Ceramide Synthesis

Alongside the production of TAG, palmitate can also be metabolised to ceramide, which has been implicated in beta cell death in models of type 1 and 2 DM. The two primary pathways for the production of ceramide are by palmitate and serine condensation (*de novo*

pathway) and re-acylation of sphingosine (salvage pathway). In models of type 1 DM, ceramide plays a role in apoptosis following exposure to cytokines, contributing to ER stress induction and mitochondrial release of cytochrome c (Lang *et al.,* 2011). In context to type 2 DM, ceramide production occurs in response to high levels of saturated fatty acids, which induce the *de novo* sphingolipid biosynthetic pathway, leading in an increase in ceramide accumulation, which also contributes to insulin resistance in peripheral tissues (Bikman and Summers, 2011). By increasing ceramide production, palmitate contributes to the development of insulin resistance by decreasing glucose uptake via inhibition of protein kinase B (PKB)/Akt, with prolonged exposure further shown to inhibit the insulin receptor substrate-1 (IRS1) in a protein kinase R-dependent manner (Hassan *et al.,* 2016). Furthermore, ablation of ceramide production by inhibition of ceramide synthase restores whole body energy expenditure and improves liver β-oxidation, resulting in improved glucose homeostasis (Turpin *et al.,* 2014).

Chronic exposure of beta cells to palmitate augments ceramide synthesis, leading to increased ER stress and apoptosis, attenuated by inhibition of ceramide synthetase, highlighting its importance for pharmacological inhibition to promote beta cell survival (Boslem *et al.,* 2011). Similar effects of palmitate exposure on ceramide production and positive results from inhibition of ceramide synthesis have also been shown in human islets to reduce FFA toxicity (Lupi *et al.,* 2002). Toxicity of ceramide has been linked to activation of ceramide-activated protein kinases, which may promote activation of MAPK pathways and JNK, leading to NF-κB activation and iNOS induction (Shimabukuro *et al.,* 1998a; Mathias *et al.,* 1998; Listenberger *et al.,* 2001). However, despite a known link between palmitate and ceramide production and that signalling pathways downstream of ceramide are known to

produce NO, numerous studies have shown no increase in NO production in beta cell line models in resposne to FFAs, however, these effects have been reported in some models, including islets, suggesting differences in the response to FFA toxicity between models and species (Cnop *et al.,* 2001; Busch *et al.,* 2005). In more recent studies using MIN6 cells, both Boslem *et al.,* (2011) and Watson *et al.,* (2011) inhibited *de novo* ceramide synthesis using serine palmitoyl transferase inhibitors (SPT) and showed it had no effect on GSIS with Thorn and Bergsten (2010) similarly showing that palmitate-induced ER stress was not accounted for by ceramide *de novo* synthesis. Rather palmitate initiated stronger expression changes in SCD-1, DGAT-1 and -2 and FAS, supporting ceramide-independent mechanisms of palmitate toxicity (Listenberger *et al.,* 2001).

1.3.4 Endoplasmic Reticulum (ER) Stress in Type 2 DM

Impaired insulin sensitivity and reduced secretion, together with a decline in functional beta cell mass in the development of type 2 DM occurs as individuals fail to compensate for the demand in insulin output, together with the effects of glucolipotoxicity on beta cell viability, which are associated with the activation of an ER stress response (Eizirik *et al.,* 2008; Cnop *et al.,* 2011). Under a high glucose load, beta cells may increase proinsulin synthesis by up to 10-fold to achieve regulation of glucose homeostasis, whilst maintaining normal beta cell function (Eizirik and Cnop, 2010). ER stress is highly regulated and normal ER function is associated with storage of Ca^{2+} three to four orders of magnitude higher than cytosolic Ca^{2+}, providing an oxidative folding environment for secretory and transmembrane proteins and synthesis of sterols and lipids, with uptake into the ER regulated by sarco(endo)plasmic reticulum Ca^{2+} ATPase proteins (SERCA) and Ca^{2+} release regulated by inositol 1,4,5-

trisphosphate (InsP(3)) and ryanodine receptors (Berridge, 2002). Alterations in ER Ca^{2+} homeostasis can lead to the induction of ER stress, as reported for the effects of cytokine-induced NO-dependent ER stress, associated with SERCA inhibition (Cardozo *et al.,* 2005). Recognition of unfolded proteins is achieved by the hydrophobic effect and the inability to shield hydrophobic regions of proteins during folding. Prevention of random folding and protection of hydrophobic regions is achieved by three distinct molecular chaperone families; heat shock protein (HSP) 70 (HSP70), HSP90 and lectin chaperones, which create a discreet folding space allowing correct conformational folded states to be obtained.

Under mild conditions of ER stress beta cells may recover following UPR induction. mediating translation inhibition and degradation of mis-folded ER proteins in a pro-adaptive ER stress response. However, chronic exposue to glucose and FFAs, can provide an unrecoverable burden on beta cells with increasing demands on ER folding capacity, as well as direct cytotoxic factors, initiating a pro-apoptotic ER stress response from sustained activation of the IRE1 and PERK pathways, leading to beta cell death (Eizirik *et al.,* 2008). The UPR can be divided into several phases to regulate different responses; 1) contribution to maintenance of homeostasis in normal (unstressed) cells, 2) co-ordinating the adaptive response in stressed cells and 3) induction of apoptosis after failing to resolve ER stress (Eizirik *et al.,* 2008). In addition to general translational inhibition, reducing ER protein folding demand, mis-folded proteins are marked for degradation by stimulation of ERAD, mediated via export and protesomal degradation (Mehnert *et al.,* 2010). Second to this, additional processes such as autophagy are activated to maintin cellular function (Kruse *et al.,* 2006), a process typically stimulated in response to starvation or other forms of nutrient deprivation, decreasing substrates for cellular energy generation (Kadowaki *et al.,* 2006). Autophagy also

serves to recycle excess or damaged intracellular organelles and under normal conditions is less active, acting more as a housekeeping mechanism, but plays a crucial role under stressed conditions, including following initiation of ER stress (Kaushik *et al.,* 2010). Autophagy has previously been associated with protein and organelle turnover; however, evidence has also linked autophagy to having other functions in response to certain types of metabolic stress induced by carbohydrate and lipid derangements (Kaushik *et al.,* 2010). Martino *et al.,* (2012) has shown that autophagy is activated in INS-1 cells and isolated rat and human islets in response to palmitate, whilst others have suggested that this process is not necessary for palmitate-induced beta cell loss and that treatment of INS-1 cells with 3-methyladenine, an inhibitor of autophagy, showed only a modest beneficial response under these conditions (Choi *et al.,* 2008).

The three main processes involved in the initiation of the UPR are the activation of IRE1, PERK and ATF6, in response to dissocation of the ER chaperone BiP from their luminal domain, as previously outlined (section 1.1.6) and are well-established mechanisms associated with palmitate toxicity, with unsaturated species partially protecting against palmitate-induced ER stress (Cunha *et al.,* 2008; Diakogiannaki *et al.,* 2008). High levels of IRE1α are found within the pancreas and, in response to ER stress, activated IRE1α cleaves the unspliced form of XBP-1 mRNA via its RNase domain, excising a 26 base-pair intron, forming spliced (XBP1s) mRNA, with noticeable levels of XBP1s detected in INS-1 cells treated with palmitate after 12 hours, compared to oleate (Tsuchiya *et al.,* 2018; Cuhna *et al.,* 2008). Increased XBP1s leads to the up-regulation of genes encoding the ER-associated degradation proteins, glycosylation enzymes, lipid synthesis enzymes, ER chaperones and secretory

proteins to remodel cellular output and restore cellular physiology (Ron and Walter, 2007; Tsuchiya *et al.,* 2018).

Alongside IRE1α, PERK becomes activated in response to ER stress via the dissociation of BiP, linked with high-molecular-mass complexes of activated PERK and IRE1α, with repression of the two signalling pathways achieved by overexpression of the BiP chaperone (Bertolotti *et al.,* 2000). The now active PERK results in phosphorylation of eIF2α by to prevent further protein overload within the ER, aiming to reduce ER stress by inhibiting translation initiation (Novoa *et al.,* 2001; Wortham and Pround, 2015). Activated PERK and eIF2α further induces translation of ATF4, with mRNA and protein levels of ATF4 induced 8-fold after 24 hours treatment of beta cells with palmitate, in comparison to only a 2-fold induction by the mono-unsaturated species oleate (Harding *et al.,* 2003; Cuhna *et al.,* 2008). ATF4 also increases expression of genes involved in ER protein folding, ERAD, amino acid biosynthesis and transport, antioxidant stress response, ATF3 and CHOP (Cnop *et al.,* 2017). CHOP expression, in part, is largely accounted for by the PERK-eIF2α-ATF4 pathway, with pro-apoptotic signalling downstream of palmitate-induced ER stress evident by increased CHOP expression; mRNA levels peaking at an 8-fold increase after 12 hours treatment and a 4-fold increase in CHOP protein detected after only 6 hours in INS-1 cells (Cunha *et al.,* 2008). Similar observations have also been reported in MIN6 cells treated with palmitate (Laybutt *et al.,* 2007) and CHOP deletion in mice results in an increased expression of UPR- and oxidative stress- related genes, including SOD and glutathione peroxidase, reducing levels of oxidative damage (as assessed by measurement of protein oxidation and lipid peroxidation) and beta cell apoptosis (Song *et al.,* 2008).

The increases in PERK phosphorylation and XBP-1 splicing, as well as downstream expression of the UPR target genes BiP, ATF4 and pro-apoptotic CHOP, support that fatty acids, such as palmitate induce beta cell apoptosis in part via ER stress (Laybutt *et al.,* 2007). Mechanisms by which CHOP up-regulation can induce apoptosis may be via initiation of the intrinsic apoptosis pathway, with CHOP shown to lead to a decreased expression of anti-apoptotic Bcl-2, which results in a reduction in cellular glutathione and perturbation of cellular redox control (McCullough *et al.,* 2001) and CHOP up-regulation can induce expression of PUMA (Cazanave *et al.,* 2010), leading to mitochondrial Bax translocation, cytochrome c release and caspase cleavage (Gurzov *et al.,* 2010). Examination of the integrated role of CHOP and the transcription factor activating protein-1 (AP-1) in mediating PUMA induction by palmitate showed that knockdown of CHOP by shRNA attenuated palmitate-induced apoptosis in Huh-7 cells (Cazanave *et al.,* 2010), a response associated with a reduction in PUMA mRNA and protein levels as well as Bax activation. Bax and Bak deficient mice have been shown to be resistant to ER stress-mediated apoptosis, as well as from over-expression of Bcl-2 which is able to block CHOP-induced apoptosis (Wei *et al.,* 2001).

ATF6 is released from the membrane under conditions of ER stress, where it translocates to the Golgi and is cleaved by site-1 and -2 proteases, which also process sterol response element binding proteins in response to cholesterol. Cleaved ATF6 translocates to the nucleus and activates ER stress-inducible promoters, of which Grp78/BiP is most characterised, as well as genes encoding other ER chaperone proteins and protein folding enzymes (Hong *et al.,* 2004). ATF6 also directly upregulates XBP-1 mRNA, working in synergism with IRE1α-mediated XBP-1 splicing (Lee *et al.,* 2002). However, whilst several branches of the UPR signaling pathway are present and up-regulated in beta cells in response to palmitate

(including activation of IRE1α, PERK, eIF2α phosphorylation, ATF-4, XBP-1s and CHOP), some have shown limited activation of ATF6 in INS-1 cells, suggesting impaired activation of this pathway under these conditions (Cardozo *et al.,* 2005). Conversely others have reported increased ATF6 activation in response to palmitate in MIN6 cells (Laybutt *et al.,* 2007), possibly reflective of species/cell type differences in the ER stress response. However, over-expression of BiP (as one of the main targets of ATF6 signaling), failed to attenuate palmitate toxicity in INS-1 cells (Lai *et al.,* 2008), suggesting lipotoxicity may occur independently to ER stress induction, though this does not preclude a potential contribution of other ATF6 targets to the differences observed between INS-1 and MIN6 cell line models.

Prolonged exposure to ER stress ultimately results in beta cell apoptosis, however under acute ER stress, mechanisms to counteract the UPR and translational repression upon restoration of homeostasis are mediated through growth arrest and DNA damage inducible 34 (GADD34). This interacts with protein phosphatase 1c (PP1c), leading to the dephosphorylation of eIF2α, lifting the inhibition on general protein translation as a part of a pro-adaptive ER stress response, with mutated PP1c failing to dephosphorylate eIF2α and blocking attenuation of CHOP by GADD34 (Novoa *et al.,* 2001). Whilst this serves as a mechanism to counteract UPR signalling under acute conditions, in response to prolonged ER stress, this may serve to allow increased expression of pro-apoptotic proteins. In a screen of molecules able to alter cellular ER stress signalling in PC-12 cells, salubrinal was indentified as an inhibitor of eIF2α dephosphorylation and protected against ER stress induced by thapsigargin (SERCA inhibitor) or tunicamycin (ER glycosylation inhibitior) (Boyce *et al.,* 2005). Under these conditions it is likely that cells were able to maintain a level of ER chaperone protein expression, whilst decreasing overall protein load in the ER, leading to a pro-adaptive

response. In contrast, salubrinal augmented palmitate-induced ER stress and apoptosis in beta cells and induced apoptosis when used alone (Cnop *et al.,* 2007), such differences when applied to beta cell models is likely indicative of an enhanced vulnerability to any perturbation in the delicate balance of pro-adaptive and pro-apoptotic ER stress signalling, given the secretory capacity of these cells. Nonetheless, the cytoprotective effects of unsaturated FFAs in models of palmitate toxicty have been associated with a reduction in ER stress markers, with palmitoleate also protecting against tunicamycin-induced ER stress in BRIN-BD11 cells (Diakogiannaki *et al.,* 2008). Of note, this study also reported protection against salubrinal toxicity, suggesting that monounsataurated species may exert their effects by acting at an early step in the initiation of ER stress.

1.3.3 Free Fatty Acid Receptors

Alongside direct intracellular changes in lipid handling/metabolism, fatty acids also exert their effects through extracellular receptor activation. Several free fatty acid receptors have been identified, which are of interest because of their effects on promoting insulin secretion. One such FFA receptor, FFAR1, G-protein coupled receptor 40 (GPR40), is expressed on the cell surface in both human and rat beta cells and has been identified as a potential target for FFAs, with high mRNA expression in the pancreas (Briscoe *et al.,* 2003; Itoh and Hinuma, 2005; Suckrow *et al.,* 2014). In *in vitro* models of type 2 DM, treatment with saturated fatty acids results in decreased FFAR1 expression, with the effect reversed in the prescence of unsaturated fatty acids, protecting against lipotoxicity (Tuo *et al.,* 2012). Evidence suggests that FFA-GPR40 activation in rat pancreatic beta cells increases intracellular calcium levels and insulin secretion via receptor activation of phospholipase C (PLC), a

membrane bound enzyme, in the prescence of oleate, with the PLC inhibitor U-73122 attenuating these effects and reducing PLC-directed formation of DAG and inositol-1,4,5-trisphosphate (IP3) (Fujiwara *et al.,* 2005; Thore *et al.,* 2005). GPR40 signalling has also been implicated in the activation of signal-regulated protein kinases 1 and 2 (ERK1/2), in mediating protection against palmitate-induced beta cell death, in part, via increased phosphorylation of ERK 1/2 in response to a GPR40 agonist (Wagner *et al.,* 2013; Panse *et al.,* 2015). Of note, some have suggested a role of GPR40 in mediating the cytoprotective actions of monounsaturated FFAs against lipotoxicity, with siRNA targeting GPR40 in NIT-1 partially preventing the decrease in apoptosis in co-incubation with oleate (Zhang *et al.,* 2007). However, though this study firstly confirmed successful GPR40 silencing with three different siRNAs, studies on the effects of this on apoptosis induction were only carried out with one of silencing constructs (Zhang *et al.,* 2007) and these observations are not consistent with the view that saturated FFAs are also ligands for GPR40 whereas methyl-esters of monounsaturates are not, and yet mediate a similar protective action (Morgan and Dhayal, 2009).

GPR120 also functions as a receptor for saturated and unsaturated long-chain fatty acids and has been shown to play a crucial role in several physiological homeostatic mechanisms, with modest levels of GPR120 found in pancreatic islets (Suckrow *et al.,* 2014). In humans, an increase in GPR120 expression has been associated with an increase in obesity and, compared to lean controls, GPR120-deficient mice fed a high-fat diet developed fatty liver, glucose intolerance and obesity (Ichimura *et al.,* 2012). Activation of GPR120 stimulates the secretion of the incretin hormone glucagon-like peptide-1 (GLP-1) and exhibits anti-diabetic effects as shown with agonists in obese mice (Tanaka *et al.,* 2008; Oh *et al.,* 2014).

Similar to GPR40, GPR120 can induce activation of ERK 1/2, phosphoinositide-3-kinase (PI3K) and the serine/threonine protein kinase Akt (Hara *et al.,* 2009), which is suggested to be the main mechanism for protection against serum deprivation by FFAs in intestinal epithelial cells, with over-expression of GPR120 cDNA reducing caspase-3 activation (Katsuma *et al.,* 2005). Binding of α-linolenic acid (ALA), a natural ligand for GPR120, provoked an increase in Ca^{2+} in HEK293 cells expressing rat GPR120 (rGPR120), which shares an 85 and 98% sequence homology to humans and mouse, respectively (Tanaka *et al.,* 2008). In context to beta cell biology, long-term administration of ALA increased beta cell proliferation in Sprague-Dawley rats via enhanced GLP-1 secretion, which has been shown to reverse lysosomal dysfunction, known to contribute to beta cell death via release of cathepsin D and impairing autphagic flux (Tanaka *et al.,* 2008; Nagasawa *et al.,* 2018; Zummo *et al.,* 2017).

A role for GPR119 is of interest in type 2 DM given its contribution in animal models to negatively influencing food intake, reducing visceral fat mass and lowering body weight. (Morgan and Dhayal, 2009). GPR119 binds ethanolamides and is predominately present in rodent pancreas and gastrointestinal tract, with speculation that GPR119 activation may be mediated in part through the lipid signalling agent oleoylethanolamide (OEA), which has been shown to act peripherally in reducing food intake and body weight gain in rat feeding models (Overton *et al.,* 2006). A direct role for GPR119 in beta cells remains controversial, with some beta cells reported not to express the receptor (reviewed in Morgan and Dhayal, 2009) and some showing that GPR119 agonists failed to protect against palmitate toxicity in BRIN-BD11 cells (Stone *et al.,* 2012). Activation of GPR119 has also been shown to improve glucose homeostasis via cAMP-mediated enchancement of GLP-1 release, improving glucose-dependent insulin release (Chu *et al.,* 2008), highlighting important differences between

direct physiological roles (if any) within beta cells in contrast to GPR119 activity possibly contributing to increasing the incretin effect on GSIS *in vivo*.

Other G-protein coupled receptors have been identified in relation to fatty acid binding and activation such as GPR41 and GPR43 (Brown *et al.,* 2003), however with GPR40, GPR119 and GPR120 known to directly bind fatty acids and their derivatives, with well-characterised signalling activities, these continue to be the main focus of the GPCRs in this context (Morgan and Dhayal, 2009).

1.4 Arachidonic Acid Metabolism

Arachidonic Acid (AA) is a polyunsaturated fatty acid (C20:4) bound to lipid membranes and/or other complex lipids and constitutes >30% of the glycerolipid fatty acid mass in rodent islets (Ramanadham *et al.,* 1993). AA can be esterified/released at the sn-2 position of the glycerol backbone of membrane phospholipids by phospholipase A_2 (PLA_2), recognising the sn-2 acyl bond of the phospholipids, resulting in their hydrolysis and the release of AA (Imig, 2000; Luo and Wang, 2011). AA release is known to positively contribute to GSIS as part of normal cellular function, with inhibition of its release from the phospholipid membrane negatively affecting insulin secretion (Ramanadham *et al.,* 2004). Further, inhibition or knockdown of $iPLA_2\beta$ expression, a calcium-dependent PLA_2 enzyme, in INS-1 cells is associated with a decrease in insulin secretion and transgenic over-expression of $iPLA_2\beta$ results in an enhanced GSIS response (Song *et al.,* 2005; Bao *et al.,* 2006). Several other PLA_2 family members have been shown to be involved in beta cell function such as cytosolic PLA_2 ($cPLA_2$), shown to enhance insulin exocytosis (Juhl *et al.,* 2003). Second to this, secretory PLA2 ($sPLA_2$) subtypes GX- and GV- $sPLA_2$ have differential actions, negatively regulating insulin

secretion by enhancing prostaglandin E_2 (PGE_2) production and serving to enhance GSIS, respectively (Shridas *et al.,* 2017).

AA and its metabolites have also been shown to be cytoprotective in models of lipo-apoptosis, with over-expression of $cPLA_2$ in MIN6 beta cells increasing endogenous AA release and protecting against loss in viability induced by palmitate (Papadimitriou *et al.,* 2007). Similar evidence is also reported in BRIN-BD11 cells, with data suggesting that this may by mediated by a reduction in NF-κB, iNOS and NADPH oxidase subunit levels and a reduction in NO and ROS levels, respectively (Keane *et al.,* 2011). Although this study supports the idea of an increase in iNOS expression and subsequent production of NO in beta cells in response to FFA treatment, others suggest the absence of an increase in iNOS expression and NO production, including in same beta cell line (Cnop *et al.,* 2001; Welters *et al.,* 2004a). Nonetheless, the contribution of oxidative stress to lipotoxicity in beta cells is well-established (Elsner *et al.,* 2001) and AA (or its metabolites) may contribute to the attenuation of this (Keane *et al.,* 2011). Potential mechanisms of AA action (or its metabolites) have also been explored, with some observations suggesting changes in the expression of genes involved in FFA metabolism, which may indicate AA actions in context to changes in lipid handling in these cells. Treatment of BRIN-BD11 cells with AA resulted in a down regulation of SCD-2 and ATP-binding cassette, sub-family G, member 1 (Abcg1), with concomitant up-regulation of enoyl-CoA-Hydratase (Ech1) and angiopoietin-like 4 (Angptl4); collectively suggesting a decrease in synthesis of fatty acids (SCD-2) and a decrease in cholesterol transport to high density lipoprotein (Abcg1) (Keane *et al.,* 2011). The increase in Ech1 would allow increased entry of unsaturated fatty acids into the pathway of β-oxidation and an increase in Angptl4 has a potential to increase cholesterol synthesis. Whether increased fatty acid β-oxidation under

these conditions directly contributes to cytoprotection is yet to be clearly demonstrated however, increased cholesterol synthesis may favour the formation of cholesterol esters, sequestering cytotoxic palmitate, rather than TAG formation, as suggested in earlier studies in MIN6 cells (Busch *et al.,* 2005).

Arachidonic acid released from the membrane can be metabolised by three major routes: cyclooxygenase (COX), lipoxygenase (LOX) and cytochrome P450 (CYP) pathways producing various eicosanoids, prostaglandins and leukotrienes. Whether or not AA requires metabolic conversion for its cytoprotective effects remains unclear, however in BRIN-BD11 cells the methyl ester of AA (as with monounsaturated species), which is a poor substrate for COX and LOX enzymes, similarly protected against palmitate toxicity. Additionally ETYA, a broad-spectrum inhibitor of all three pathways of AA metabolism, containing four alkyne groups, failed to attenuate AA action (Dhayal and Morgan, 2011); however, this analogue of AA has also been shown to active PPARs (Keller *et al.,* 1993; Kliewer *et al.,* 1995). Interestingly, AACOCF3 (a trifluoro-methyl-ketone derivative of AA) dose-dependently antagonised AA actions in BRIN-BD11 cells, suggesting that this derivative may be capable of binding to the same, as yet unidentified, binding site mediating AA activity (Dhayal and Morgan, 2011).

Although data suggests that bolus addition of exogenous AA mediates cytoprotective actions independent to AA metabolism, the contribution of COX and LOX metabolites of endogenous AA metabolism have been extensively studied in beta cell biology. The role(s) of CYP450-derived eicosanoids, the focus of this thesis, have received comparatively less attention in these models and so the following sections summarise some of the current understanding of COX and LOX pathways in beta cell (dys)function before considering the evidence for the roles of CYP450-eicosanoids in a variety of models (outlined in figure 1.3).

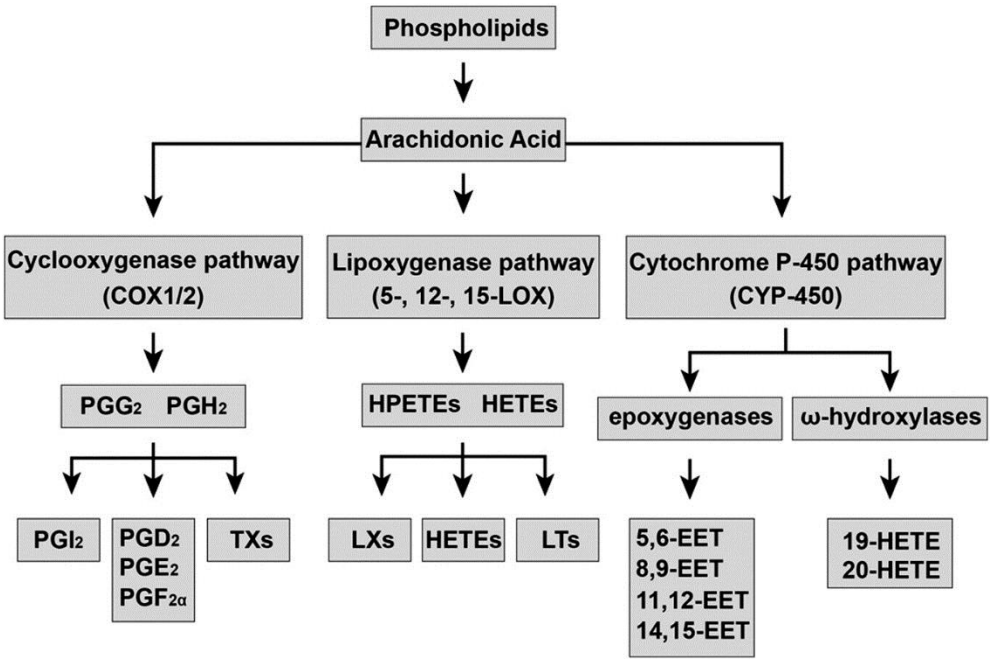

Figure 1.3 AA-derived eicosanoids of COX, LOX and CYP450 pathways. AA is a precursor for metabolism by COX, LOX and CYP450 enzymes following its release from membrane phospholipids by the action of phospholipase enzymes (Yuan *et al.,* 2014).

1.4.1 Cyclooxygenase (COX) Derived Eicosanoids

The major derivatives of AA from the COX pathway are prostaglandins (PGs) and thromboxane (TX), with AA released from the phospholipid pool by $cPLA_2$ able to undergo oxidative metabolism by COX -1 and -2 to produce the endoperoxide PGH_2 (Rouzer and

Marnett, 2011). PGH_2 is now a target for PG synthases, which produces a variety of active prostaglandins, PGE_2, PGD_2, $PGF_{2\alpha}$, prostacyclin (PGI_2) and thromboxane A_2 (TxA_2) (Hao and Breyer, 2007). PGE_2 has been identified in rat islets and has been reported to be the predominant product via the COX pathway in beta cells, responsible for the modulation of beta cell function (Tran *et al.,* 2002), with COX-2 expression predominating over COX-1 in beta cells, supporting that PGE_2 is most abundant COX product (Roberston, 1998). Actions of PGs are mediated through their binding to DP, EPs; EP_1, EP_2, EP_3 and EP_4, IP, FP and TP receptors (Roberston, 1998; Hao and Breyer, 2007) and in models of type 1 DM, it is known that IL-1β can activate COX-2 and EP_3 expression via the NF-κB pathway, resulting in a decrease in GSIS, with the COX-2 inhibitor SC58236 promoting GSIS whereas SC58560, a COX-1 inhibitor, failed to inhibit PGE_2 production (Tran *et al.,* 1999; Tran *et al.,* 2002). Further to this, the EP receptor promoter contains an NF-κB binding site, with studies showing that inhibition of NF-κB decreases EP_3 receptor expression (Arakawa *et al.,* 1996; Tran *et al.,* 2002). Persaud *et al.,* (2007) showed that COX-2 inhibition enhanced basal insulin secretion in human islets and in mouse models transgenic over-expression of COX-2 and PGE synthase increased PGE_2, which resulted in deleterious effects on beta cell mass (Oshima *et al.,* 2006), with earlier observations also showing that COX-2 inhibitors prevented hyperglycaemia in a streptozotocin (STZ) mouse model (Tabatabaie *et al.,* 2000). A 2.5-fold increase in pancreatic PGE_2 levels was observed in transgenic mice over-expressing COX-2 and PGE synthase-1, associated with decreased beta cell number (Oshima et al., 2006), however sections of the pancreas when examined showed no reduction in beta cell mass suggesting that PGE_2 itself may not contribute directly to beta cell apoptosis and its effects may instead be related to effects on beta cell proliferation *in vivo* (Oshima et al., 2006; Luo and Wang, 2010). In BRIN-BD11 cells, inhibition of COX-1 decreased D-glucose and L-alanine-stimulated insulin secretion (Keane *et*

al., 2011), suggesting that under these conditions whereby AA will preferentially be metabolised by COX-2, these metabolites also directly impair secretion. Further follow-up experiments with an inhibitor of COX-2 in combination with exogenously administered AA significantly enhanced insulin secretion, supporting evidence that COX-2 metabolites have a negative effect on insulin secretion.

In type 1 DM cytokine-induced beta cell apoptosis is associated with an increase in NO production, which has been shown to activate COX-1 and COX-2 isoforms, resulting in an increase in PGE_2 (Salvemini *et al.,* 1993). Furthermore, the COX-2 promoter contains NF-κB, AP-1 and cAMP-response element binding protein consensus sequences and in models of db/db mice it has been suggested that cytokines in synergy cause beta cell death due to the induction of COX-2 and iNOS, enhancing oxidative stress (McDaniel *et al.,* 1996). Earlier work by Rabinovitch *et al.,* (1990) demonstrated that non-selective COX inhibitors could protect rat islets and INS-1 cells against the deleterious effects of pro-inflammatory cytokines, thus arguing for a pro-apoptotic role of AA-derived eicosanoids, including PGE_2, with maximal effects on the prevention of beta cell death observed under conditions of COX and LOX inhibition. In another study, treatment of rat islets with IL-1β (1U/mL) for 40 hours resulted in a 7-fold increase in both PGE_2 and nitrite production (Heitmeier *et al.,* 2004). However, under conditions of COX-2 inhibition using SC58236, although formation of PGE_2 was prevented, IL-1β-induced increases in nitrite levels and beta cell dysfunction was unaffected, suggesting cell death was independent to COX-2 activity. Further studies investigating the effects of COX inhibitors in models of islet transplantation have since failed to demonstrate any long-term beneficial effects (Gysemans *et al.,* 2003). The earlier findings of Rabinovitch *et al.,* (1990) therefore contradicts others (Heitmeier *et al.,* 2004; Papdimitriou *et al.,* 2007); these later

studies used more selective COX-2 inhibitors (SC58236 and Celecoxib) than the non-specific inhibitors used in earlier studies and argue that whilst cytokines lead to increased expression of the inducible COX-2, that this does not directly contribute to cell dysfunction. A protective role of PGE_2 has also been reported (Papdimitriou *et al.,* 2007), and it is suggested that PGE_2 can exert autocrine and paracrine effects at cell surface prostaglandin EP receptors leading to cAMP generation, increased expression of the anti-apoptotic protein Bcl-2, and activation of the PI3K/PKB pathway and JNK activation (Heitmeier *et al.,* 2004; Papdimitriou *et al.,* 2007).

1.4.2 Lipoxygenase (LOX) Derived Eicosanoids

The major products of the LOX pathway of AA metabolism are hydroxyeicosatetranoic acids (HETEs), particularly; 12(S)-HETE, 12(R)-HETE and 15(S)-HETE, and leukotrienes (LTs); LTA_4, LTB_4, LTC_4, LTD_4 and LTE_4 (Persaud *et al.,* 2007; Luo and Wang, 2011). In total, there have been six identified LOX isoforms in humans and seven isoforms have been reported in mice (Dobrian *et al.,* 2019), with the lipoxygenases classified according to the positional insertion of a hydroperoxy group as 5-LOX, 8-LOX, 12-LOX and 15-LOX; 5-LOX and 12-LOX isoforms have been detected in human and rodent islets (Persaud *et al.,* 2007; Mochizuki and Kwon, 2008). Several substrates have been proposed as a target for 12-LOX, including: AA, dihomo-γ-linoleic acid, docosahexaenoic acid (DHA), and eicosapentaenoic acid (EPA) (Ikei *et al.,* 2012), with 12-LOX expression identified in beta cells (Bleich *et al.,* 1998; Kawajiri *et al.,* 2000), and to a higher extent than alpha cells, as well as 5-LOX. However, lower levels of 5-LOX products have been identified in rodent pancreatic islets (Morgan and Laychock, 1988; Shannon *et al.,* 1992; Chen *et al.,* 2005). Although products of 5-LOX have been identified, cross-production of 5-LOX products could be attributed to other pathways of AA metabolism, as Bleich *et al.,* (1998)

observed that 12-LOX is specifically expressed in pancreatic beta cell lines and primary cells from Zucker fatty rats; however 5-LOX or 15-LOX were not. AA-derived HETEs, involves the insertion of a hydroperoxide group producing hydroperoxyeicosatetranoic acids (HPETEs), which are subsequently reduced by glutathione peroxidase to form a more stable product; hydroxyeicosatetranoic acid; in the case of 12-LOX activity with AA, a hydroperoxide group is introduced at position 12 (12-HPETE), which is then reduced to 12-HETE (Haeggström *et al.,* 2011). Cross-production of other LOX metabolites can also occur, albeit with a lower specificity since 12-LOX can produce both 12-HETE and 15-HETE but at a ratio of 6:1; the role of 12-HETE has been extensively studied in models of rodent diabetes (Haeggström *et al.,* 2011) and unlike 5-LOX, which can produce both HETEs and leukotrienes, the predominant product of 12-LOX is 12-HETE.

In models of type 1 DM, cytokine-induced beta cell apoptosis is associated with activation of 12-LOX and its subsequent translocation from the cytosol to the cell membrane (Ma *et al.,* 2010) and has been identified to be up-regulated in islets and beta cells (Bleich *et al.,* 1995). Deletion of 12-LOX also protects against STZ-induced DM in mice (Bleich *et al.,* 1999), and in rat islets, treatment with IL-1β enhanced the production of 12-HETE via NO-dependent mechanisms. Similarly, in a later study in human islets and mouse β-TC3 cells, treatment with IL-1β, IFN-γ and TNF-α increased 12-LOX activation, however it was suggested that the total protein levels of 12-LOX were not increased, but that increased expression/activity of iNOS can induce post-translational modification of 12-LOX enzymes, resulting in their activation (Chen *et al.,* 2005). Evidence that cytokine-induced 12-LOX activation contributes to reduced insulin secretion and beta cell death was further demonstrated by treatment with the 12-LOX inhibitor baicalein, resulting in an inhibition of

12(S)-HETE production in mouse beta cells and human islets. This was associated with increased insulin secretion and attenuation of cytokine-induced JNK and p38 activation and apoptosis (Chen *et al.,* 2005). With others reporting similar findings that p38 phosphorylation is increased when 12-LOX is overexpressed (Reddy *et al.,* 2002), this suggests a contribution of 12-LOX and its products in cytokine-induced beta cell dysfunction.

1.4.3 Cytochrome P450-Derived Eicosanoids

Whilst much attention has focussed on the contribution of COX and LOX metabolites of AA to beta cell death and dysfunction in DM models, comparatively less attention has been given to the contribution of metabolites of the CYP 450 pathway. Four epoxyeicosatrienoic acid (EET) isomers of AA can be produced by the action of distinct CYP450 enzymes, depending on which of the double bonds undergoes epoxidation, with two possible enantiomers for each (figure 1.4)

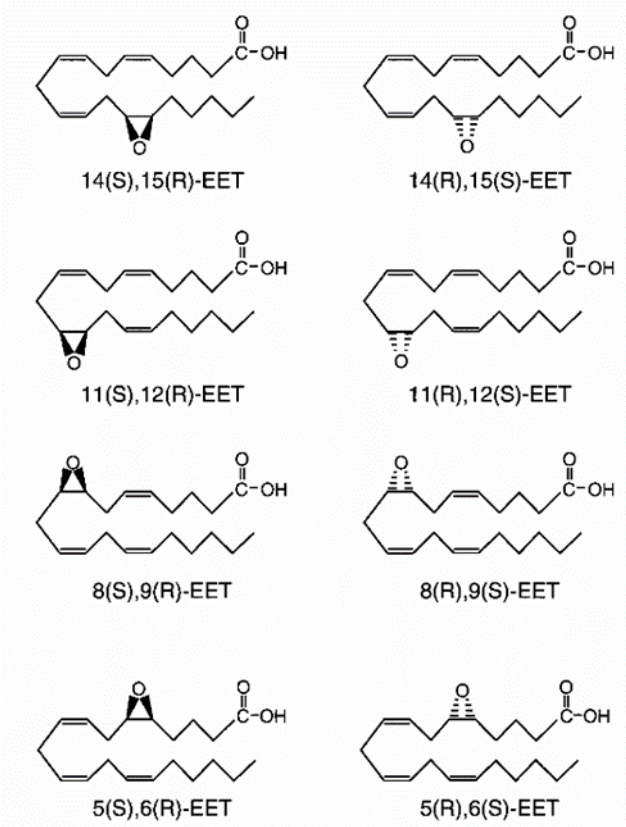

Figure 1.4 Structure of each EET regioisomer. Position of epoxide groups are shown identifying different structural characteristics of each EET (Zeldin, 2001).

Different members of the CYP450 family (share 40% sequence homology) and subfamily (share 55% sequence homology) have different catalytic efficiencies in metabolising AA into EETs. CYP1A, CYP2B, CYP2C, CYP2D, CYP2G, CYP2J, CYP2N and CYP4A are known to contribute to EET production (Zeldin, 2001) and evidence suggests that the major CYP epoxygenases for the formation of EETs from AA in islets are the CYP 2C and CYP 2J isoforms (Imig and Hammock, 2009). The CYP isoform CYP 2C8 has been shown to produce 14(15)-EET and 11(12)-EET at a ratio of 1.3:1.0 yet does not produce detectable amounts of 8(9)-EET, whereas CYP 2C9, which has a >80% sequence identity to CYP 2C8, can produce the same EETs at a ratio of 2.4:1.0:0.5, respectively.

EETs produced by CYP450 epoxygenases are reported to have potent anti-inflammatory properties and in transgenic mice, over-expression of the CYP 2J2 isoform protects against ischemia/reperfusion injury (Seubert *et al.,* 2004). Similarly Wang *et al.,* (2014) showed that CYP 2J2-derived EETs suppress ER stress using an *in vivo* model of heart failure in mice over-expressing CYP 2J2, an effect that was associated with restored SERCA2a expression and increased expression of catalase and MnSOD. Although the protective effects of EETs against ER stress induced by pro-inflammatory cytokines in *in vitro* models of type 1 DM have not been studied, it is tempting to speculate that elevation of EETs either through exogenous administration or from over-expression of CYP 2J2 or 2C11 (the rat homolog of human 2C8) may reduce ER stress in these models. Particularly since cytokine-induced ER, stress is associated with reduced expression of SERCA2a in an NO-dependent manner in beta cells (Cardozo *et al.,* 2005). Similarly, EETs have also been shown to exert anti-inflammatory effects through the inhibition of NF-κB by acting upstream of its activation by IKK (Node et al., 1999), suggesting the possibility that targeting EETs may impair cytokine-induced beta cell death through an inhibitory effect on NF-κB activation, acting upstream of the transcription factors' effects on global gene expression changes, contributing to beta cell apoptosis. In endothelial cells, inhibition of NF-κB was achieved by treatment with 11(12)-EET, and 8(9)-EET with 11(12)-EET and 14(15)-EET inhibiting endothelial apoptosis through activation of the PI3K/Akt pathway, subsequently inhibiting ERK1/2 dephosphorylation (Spiecker and Liao, 2005). Other mechanisms have also been implicated with EET action, such as 11(12)-EET being shown to stimulate angiogenesis through activation of EphB4-coupled PI3K/Akt pathways (Webber *et al.,* 2008), as well as activating sphingosine kinase-1 mediating cell proliferation and angiogenesis (Yan *et al.,* 2008). Studies in cardiomyocytes have also reported similar findings through the activation of the pro-survival PI3K/Akt pathway, and have shown

activation of the myocardial K_{ATP} channels by decreasing their sensitivity to ATP (Wang *et al.,* 2006). Relevant to the aetiology of type 2 DM, over-expression of CYP 2J2 in mice models of obesity-induced insulin resistance recovered insulin sensitivity via effects on an endothelial NOS isoform (Xu *et al.,* 2011) and Bettaieb *et al.,* (2013) suggest that EETs may protect liver cells against high fat diet-induced ER stress and metabolic dysfunction. Whilst more recent studies have demonstrated that CYP 2J2 overexpression restores glucose tolerance and improves hepatic insulin resistance in db/db mice, a model for dyslipidaemia (Li *et al.,* 2015), no studies have directly assessed a potential cytoprotective activity of EETs in pancreatic beta cells under lipotoxic conditions.

EETs are further metabolised by soluble epoxide hydrolase (sEH) into corresponding vicinal diols, dihydroxyeicosatrienoic acids (DHETs), metabolites with considerably reduced biological activity than EETs (Imig and Hammock, 2009). A study by Zeldin *et al.,* (1993) has shown that rates of hydration by cytosolic soluble epoxide hydrolase favours 14(15)-EET producing 4.5 μmol of product/mg of protein/min in comparison to 11(12)-EETs and 8(9)-EETs showing only 1.6 and 1.5, respectively. Inhibitors of sEH are suggested to exert beneficial properties in the treatment of cardiovascular disease, owing to increased levels of biologically active EETs. Further to this, inhibition of sEH lowers blood pressure in various animal models however, little is known about the involvement of sEH and blood glucose control in DM models. Studies have shown that in STZ-induced diabetes in mice, sEH knock-out or pharmacological inhibition improves glucose tolerance and increases plasma insulin concentrations, likely as a result of increased GSIS and preserved beta cell mass possibly owing to the anti-inflammatory properties of EETs (Luo *et al.,* 2010; Chen *et al.,* 2013). This suggests that beta cells express appreciable levels of sEH, with Luo *et al.,* (2010) reporting that mouse

islets express sEH at 0.93ng/μg protein and confirmed sEH expression in NIT-1 clonal beta cells by Western blotting. That sEH inhibitors protect liver and adipose cells of mice fed high-fat diets against ER stress (Bettaieb *et al.,* 2013) and improve functional beta cell mass in STZ-induced DM models suggests that this approach may protect clonal beta cells against physiological inducers of beta cell death in models of type 1 (pro-inflammatory cytokines) and type 2 (lipotoxicity) DM.

The fate of EETs is not solely by sEH metabolism and they can also be metabolised by acyl transferases, resulting in their incorporation into cellular EET-phospholipids. Glutathione S-transferases are also able to utilize EETs and form glutathione conjugates and EETs can be further oxidised by prostaglandin G/H synthase (PGHSs) and P450s resulting in the formation of epoxyprostaglandins, diepoxides, THF-diols and epoxy-alcohols. Additionally, intracellular fatty acid binding protein (FABP) can bind EETs and DHETs and control their metabolism, activity and targeting (Zeldin, 2001). EETs and DHETs are also able to feed into mitochondrial and peroxisomal β-oxidation pathways, forming shortened-chained fatty acids, including 7(8)-dihydroxy-hexadeadienoic acid 7(8)-DHHD, which is reported to display comparable effects on vascular function as 11(12)-EET/DHET (Fang *et al.,* 1996). Additional β-oxidation products also include shortened-chain epoxide derivatives, the levels of which may be enhanced in models investigating effects of sEH inhibition (Fang *et al.,* 2001; Fang *et al.,* 2004)

It has been proposed that EET mechanisms of action may involve binding to cell surface receptors and activation of intracellular mechanisms, binding to intracellular lipid binding proteins, or by their incorporation into cellular phospholipids (Spector and Norris, 2007). Extensive data has suggested that an extracellular mechanism, in part, may be one of their modes of action, with data suggesting a selective EET receptor of the G-protein coupled

receptor family, with activation of an intracellular signal transduction pathway associated with increased intracellular cAMP (Yang *et al.,* 2008). A radiolabelled 14(15)-EET analogue has been shown to bind at the plasma membrane in U937 cells, increasing cAMP, an effect that was competitively inhibited by 14(15)-EET and 14(15)-EEZE (a reported EET antagonist). Although the molecular identity of any such receptor remains elusive, a recent study screening EET action at 105 known GPCRs failed to identify a single high-affinity receptor, instead demonstrating activity at a number of low-affinity prostaglandin (PG) receptors (including $PTGER_2$, $PTGER_4$, PTGFR, PTGDR and $PTGER_3$IV), concluding that EETs may signal through multiple GPCRs (Liu *et al.,* 2017). Whilst the role of PGE_2 in insulin secretion (which signals through $PTGER_2$, $PTGER_4$ and $PTGER_3$IV) remains unclear, activation of these receptors (and PTGDR by PGD) leads to increased cAMP, supporting a possible role in EET-Gαs signalling (Wong *et al.,* 2000; Yang *et al.,* 2008).

Other proposed mechanisms are that EETs bind to receptors for other lipid-soluble agonists that also function to activate intracellular signalling pathways and that EETs have characteristics of long-chain fatty acids and can undergo similar metabolic processing. Several studies have shown the involvement of an intracellular mechanism through incorporation into phospholipids and binding to cytoplasmic FABPs and PPARγ (Widstrom *et al.,* 2003; Spector *et al.,* 2004; Liu *et al.,* 2005). In particular, PPARγ activation has become a well-established target for EETs in a number of non-beta cell models, mediating anti-inflammatory activity, which in part has been attributed to reduced NF-κB activation (Liu *et al.,* 2005). Of note, PPARγ is the target of the thiazolidinedione (TZD) class of insulin sensitizers used in the treatment of type 2 DM, which mediate their action via association with the PPARγ ligand binding domain, facilitating heterodimerisation with the retinoid X receptor (RXR) and increasing the

expression of lipogenic genes, improving dyslipidaemia. Although the significance of PPARγ expression and/or activity in beta cells remains unclear, TZDs have been reported to protect beta cells from both cytokine and palmitate toxicity (Saitoh *et al.,* 2008; Hong *et al.,* 2018), which may indicate EETs could display similar activity in these models. However, others have demonstrated lack of efficacy of TZDs in this context, with an inhibitory action of over-expression of PPARγ on insulin secretion (Cnop *et al.,* 2002; Nakamich *et al.,* 2003).

Incorporation of EETs into membrane phospholipids has also been shown at the sn-2 position of the glycerol backbone; however, it is uncertain whether this represents an important mode of action of EETs, with studies showing that release of EETs from phospholipids can be achieved without stimulation necessary for PLA_2 activation (Spector *et al.,* 2004). It has been suggested that incorporation of EETs into phospholipids may occur to control alterations in properties of the cell membrane, temporarily allowing functional changes to protein domains (Spector *et al.,* 2004). Coronary endothelial cells treated with *N,N'*-dicyclohexyurea (DCU), a selective inhibitor of sEH, increased cellular levels of 14(15)-EET and its conversion into phospholipids (Fang *et al.,* 2001). Functionally, incorporation of EETs into phospholipids may serve to decrease the concentration of unesterified EETs, representing an important mechanism for controlling EET actions through sequestration into the phospholipid pool. EET-containing phospholipids are also the precursors for the production of 2-epoxyeicosatrienoylglycerols (2-EG), containing 11(12)-EET or 14(15)-EET, likely mediated via phospholipase C hydrolysis and diacylglycerol lipase cleavage of the sn-1 fatty acid (Chen *et al.,* 2008). These products have been suggested to display endocannabinoid-like activity, similar to the endogenous AA-derived anandamide (arachidonylethanolamide), with 2-14(15)-EG shown to activate epidermal growth factor

receptors via ligand release upon binding to cannabinoid receptors CB1 and CB2 (Chen *et al.,* 2008). Interestingly, these effects are not known to mediate free EET action, with no activity at cannabinoid receptors reported (Chen *et al.,* 2008) and given that CB receptors signal through $G_{i/o}$-coupled mechanisms, inhibiting adenylate cyclase and decreasing cAMP, the significance of the 2-EG products for mediating EET action *in vivo* and *in vitro* remains unclear, especially since any extracellular receptor activity of EETs has been attributed to Gαs coupled receptors and increased cAMP (Wong *et al.,* 2000; Yang *et al.,* 2008). Both CB1 and CB2 receptors have been shown to be expressed in RINm5F cells and in BRIN-BD11 cells and anandamide, an endogenous CB receptor ligand, has been shown to protect against palmitate toxicity however, in this model effects were blocked by inhibition of fatty acid amide hydrolase (FAAH), suggesting these effects were mediated by conversion of anandamide to arachidonic acid rather than its direct receptor binding (Stone *et al.,* 2012).

Earlier work in rat islets reported that EETs have beneficial effects on promoting insulin and glucagon release (Falck *et al.,* 1983) however, later data in INS-1 cells contradicted these observations suggesting that free-EETs have an inhibitory action on insulin secretion (Klett *et al.,* 2013). In this model, expression of acyl-CoA-synthase-4 (Acsl4) was reported to control the ratio between membrane-esterified and free EETs, suggesting that this may be a mechanism of sequestering EETs into phospholipids, which promoted GSIS. However, the scarcity of additional data on potential mechanisms of direct EET action between the publication of these two studies highlight the need for further studies in this area, as acknowledged in earlier (Luo and Wang, 2011) and more recent (Xu *et al.,* 2016) reviews on the role of eicosanoids in beta cell function. A further link between EETs and beneficial effects on islet function was reported by Luo *et al.,* (2010), whereby a possible EET contribution was

assessed through pharmacological inhibition of sEH or its knock-down, which restored normoglycaemia and increased plasma insulin levels in STZ-induced diabetes in mice, associated with increased beta cell mass. Together with data showing islet expression of CYP 2C11 in rodent models (Chen *et al.,* 2013), this suggests that EETs could also protect beta cells against pathophysiologically relevant inducers of beta cell death in models of type 1 (pro-inflammatory cytokines) and type 2 (lipotoxicity) DM.

1.5 Aims

Studies over the last three decades have firmly established pro-inflammatory cytokines, hyperglycaemia and dyslipidaemia as direct contributors to loss of functional beta cell mass by apoptosis in the pathogenesis of type 1 and type 2 DM. Similarly, in models of type 2 DM the cytoprotective effects of mono- and poly-unsaturated FFAs are also well-documented, including that of AA. Whilst mechanisms of AA action in this context continue to be defined, the contribution of the COX and LOX pathways and the products produced from the endogenous metabolism of AA have been widely studied in beta cell biology. However, evidence for the potential functional role(s) of CYP450-derived EETs and their less active vicinal diols (DHETs) in *in vitro* models of type 1 and 2 DM is lacking, therefore the specific aims of this thesis are to:

- confirm the cytotoxic effects of pro-inflammatory cytokines and the saturated FFA palmitate in BRIN-BD11 cells, establishing appropriate *in vitro* models for further investigations, as well as confirming existing knowledge on the protective effects of AA in this context.
- investigate the cytoprotective effects of EETs and DHETs in models of lipotoxicity and explore potential mechanisms of action through pharmacological modulation of known potential targets of eicosanoids and FFA signalling.
- determine whether EET action is associated with changes in lipid handling in BRIN-BD11 cells and the contribution of known pathways of FFA metabolism through pharmacological inhibitor studies.

- investigate the cytoprotective effects of EETs and DHETs against pro-inflammatory cytokine toxicity and whether any effects of EET action are associated with changes in cytokine signalling, particularly activation of NF-κB.
- investigate whether manipulation of endogenous EET levels through over-expression of the rat CYP 2C11 epoxygenase or pharmacological inhibition of sEH can recapitulate effects of exogenously applied EETs.

Chapter Two

Methods

2 Methods

2.1 Cell Culture

The rat pancreatic beta cell line, BRIN-BD11 (a gift from Professor Noel Morgan, University of Exeter), was used in this study. Derived by electrofusion of RINm5F cells with New England Deaconess Hospital (NEDH) rat pancreatic islets (McClenaghan *et al.,* 1996), BRIN-BD11 cells are glucose-responsive, insulin secreting cells commonly used in *in vitro* studies of cytotoxicity in models of type 1 (pro-inflammatory cytokine toxicity) and type 2 (lipotoxicity) DM. BRIN-BD11 cells were routinely cultured in 75cm^2 tissue culture flasks at 37^{o}C in a humidified atmosphere of 5% CO_2: 95% air in RPMI-1640 medium supplemented with 10% foetal bovine serum (FBS), 2mM L-glutamine, 100U/mL penicillin and 100µg/mL streptomycin (complete medium). Cells were used between passages 23-38, with stock cultures (~1x10^6 cells/mL) stored at -196^{o}C in liquid nitrogen in complete media supplemented with 40% FBS and 10% dimethyl sulphoxide (DMSO).

A BassAire P5HB culture hood was used for all cell culture work, with laminar flow maintained at 100 Pascals and surfaces cleaned with 70% industrial methylated spirit (IMS). All materials were sterile and culture reagents pre-warmed to 37^{o}C before use. Cells were passaged at ~80% confluency, with spent medium removed from 75cm^2 tissue culture flasks and discarded into Virkon (1% w/v). Following this, excess phosphate buffer saline (PBS, pH 7.4) was washed over the cells to remove residual medium and cells were then trypsinized using 0.25% Trypsin: EDTA for 3 minutes at 37^{o}C at 5% CO_2. Confirmation of trypsinisation was observed under an inverted microscope, with cells washed over and suspended in 10mL fresh RPMI-1640 complete medium to inactivate residual trypsin. Cells were then centrifuged at

1200xG for 6 minutes, with spent medium discarded in Virkon and cells re-suspended in 10mL fresh RPMI-1640 medium and used to seed new flasks, or sub-cultured (section 2.1.1) for further studies.

2.1.1 Sub-cultures

Cells were sub-cultured into 96-well (15,000 cells/well in 200µL), 24-well (50,000 cells/well in 500µL) and 6-well (200,000 cells/well in 2mL) plates, or 25cm^2 tissue flasks (1 million cells/flask in 5mL) dependent on assay protocol (see relevant sections). Following preparation of cell suspension (as described in section 2.1), a 10µL sample of the cell suspension was mixed with 10µL of 0.4% Trypan blue and cell number determined using a haemocytometer with coverslip, counting the number of unstained viable cells in each of the four corner 4x4 grids. Total viable cell number was then determined according to equation 1 and cell suspensions diluted to the appropriate density for seeding. Cells were then incubated for 24 hours prior to treatment in complete medium, unless otherwise stated.

Eq. 1 $$Cells\ per\ mL = Average\ cell\ count\ \times 2 \times 10^4$$

2.2 Preparation of Fatty Acid-Albumin Complexes

Stock solutions of FFAs were prepared as follows; sodium palmitate (C16:0) (Sigma Aldrich), a long-chain saturated fatty acid, was dissolved in 50% ethanol (EtOH) (v/v) at 70^{o}C to a concentration of 50mM. Similarly, Oleate (C18:1) (Sigma Aldrich), a mono-unsaturated fatty acid, was dissolved in filter-sterilised water to 50mM. Arachidonic Acid (C20:4) (Sigma

Aldrich), a poly-unsaturated fatty acid, and 2-bromopalmitate (Sigma Aldrich), an analogue of palmitic acid, were prepared in 90% ethanol (v/v) to a concentration of 90mM.

Fatty acid-free Bovine Serum Albumin (BSA) (Sigma Aldrich) was prepared in deionised water and filter-sterilised using a 0.22µm filter in preparation for complexing with fatty acids. Within pathological conditions the ratio of free fatty acids (FFAs) to albumin can rise as high as 6:1 and whilst cellular models of beta cell lipotoxicity employ a range of FFA:BSA treatment ratios, Oliveira *et al.* (2015) report a ratio of 3.3:1 to be optimum, as using a ratio greater than 5:1 could exceed FFA solubility, especially with long-chain fatty acids, introducing artefacts in cultures and enhanced detergent-like effects of FFAs on cell membranes, whilst lower ratios will limit FFA delivery. Therefore, all FFAs used in this thesis were complexed to BSA at a final ratio of 3.3:1 using 5mM FFA: 10% BSA, unless otherwise stated, followed by incubation for 1 hour at 37^{o}C. Once formed, complexes were aliquoted, stored at -20^{o}C and used within one month.

Epoxyeicosatrienoic acids (EETs) (Caymen Chemical): (±)5(6)-, (±)8(9)-, (±)11(12)- and (±)14(15)- and dihydroxyeicosatrienoic acids (DHETs) (Caymen Chemical): (±)8(9)-, (±)11(12)- and (±)14(15)- were supplied at 100µg/mL (0.32mM) in 100% ethanol. To concentrate the fatty acids (thus avoiding higher residual ethanol concentrations in cell treatment), a stream of nitrogen gas at <10L/min was used to evaporate the ethanol and all EET/DHET isomers were reconstituted in 100% ethanol, purged under nitrogen, to a stock concentration of 3.2mM and prepared in BSA at a final concentration of 100µM: 0.2% BSA (maintaining a molar ratio 3.3:1). An analogue of (±)14(15)-EET with the addition of a methyl sulphonamide group: (±)14(15)-EET-SI (Caymen Chemical) was supplied at 100µg/mL (0.32mM) in 100% methyl acetate. Following the procedure of evaporation under nitrogen for EETs and DHETs, (±)14(15)-EET-SI

was reconstituted to a stock concentration of 3.2mM in ethanol and similarly prepared in BSA to a final concentration of 100µM: 0.2% BSA (molar ratio 3.3:1).

2.3 Cell Treatment

Treatment with the pro-inflammatory cytokines, IL-1β (100U/mL), IFN-γ (20U/mL) and TNF-α (500U/mL) (PeproTech EC), was used as a model of cytokine toxicity in type 1 DM, with preliminary dose response data establishing optimum conditions in this model (see Chapter 3). To mimic lipotoxicity induced by long-chain saturated FFAs, cells were treated with palmitate:BSA complexes to a final concentration of 250µM palmitate (unless otherwise stated), with AA used in co-incubation in both models at concentrations up to 80µM. Cytoprotective effects of EETs and their derivatives were routinely studied at a final concentration of 10µM (unless otherwise stated). Control cultures were treated with corresponding concentrations of EtOH (or other vehicle) and BSA (see relevant chapters).

Further investigations utilised a range of pharmacological inhibitors/antagonist to explore potential mechanisms of EET/DHET and AA action, as summarised in Table 2.1 (see relevant chapters). The concentrations indicated were based on preliminary dose response data (screened using the MTT assay (section 2.4.1)) under control and/or palmitate-treated conditions, to ensure appropriate low toxicity profiles and limiting any enhancement of toxicity in response to palmitate treatment. Stock concentrations of all agents were prepared in appropriate solvents (water, EtOH or DMSO) according to supplier specifications, with control cultures in viability studies treated with the appropriate vehicle.

Table 2.1 Pharmacological inhibitors/antagonists used in the study of EET action.

Compound	Target	Concentration used (μM)
DC260126 *(Tocris)*	GPR40	1.25, 2.5
AH7614 *(Tocris)*	GPR120	1.25, 2.5
GW6471 *(Tocris)*	PPARα	1.25, 2, 2.5
GSK3787 *(Tocris)*	PPARβ/δ	1.25, 2, 2.5
T0070907 *(Tocris)*	PPARγ	1.25, 2, 2.5
HX531 *(Tocris)*	RXR	1.25, 2.5
Etomoxir *(Tocris)*	CPT1	50
Xanthohumol *(Tocris)*	DGAT	5
A939572 *(Tocris)*	SCD-1	2
t-AUCB *(Cayman Chemical)*	sEH	10
TPPU *(Cayman Chemical)*	sEH	10
OBBA *(Tocris)*	$cPLA_2$	1.25, 2.5

2.4 Cell Viability Assays

2.4.1 MTT Assay

The MTT (3-[4, 5-dimethylthiazol-2-yl]-2, 5 diphenyltetrazolium bromide) (Sigma Aldrich) assay was used to determine cell viability following the procedure outlined by Mossman, (1983), with some modifications. The MTT assay largely reflects mitochondrial activity whereby viable cells with active mitochondria reduce the tetrazolium salt to a blue-purple formazan product, which can then be solubilised in DMSO (Mossman, 1983). Initially thought to be catalysed by enzymes of the respiratory chain (notably succinate-tetrazolium reductase), the conversion of MTT to formazan has since been shown to also occur outside the mitochondria (Berna and Dobrucki, 2002). Nonetheless, this is regarded as being relative to the number of viable (respiring) cells and therefore the absorbance of solubilised formazan measured at 540nm is proportional to, and a quantitative measure of, cell viability. A 5mg/mL

MTT stock solution was prepared in PBS (pH 7.4) and diluted in complete RPMI-1640 medium to a final assay concentration of 0.5mg/mL. Following treatment with test agents, spent media was removed from the wells of a 96-well plate and cells were treated with 100µL/well dilute MTT solution, followed by incubation for 4 hours at 37^{o}C with 5% CO_2. Following incubation, the MTT:media solution was replaced with 100µL/well DMSO and plates gently agitated on a rocking platform. Absorbance was measured at 540nm using a BioTek EL800 plate reader, with data expressed as mean percentage cell viability +/-SEM, as compared to vehicle-treated control (see relevant chapters), with absorbance values corrected using a cell-free blank.

2.4.2 Neutral Red Assay

The Neutral red (Sigma Aldrich) assay was used to determine cell viability following the procedure outlined by Repetto *et al.,* (2008), with some modifications. The neutral red assay provides a quantitative measure of viable cells in culture by assessing the cells' ability to incorporate the supravital dye neutral red within lysosomes, with absorbance of solubilised neutral red deposits being proportional to cell viability (Repetto *et al.,* 2008). A 0.33% (w/v) neutral red stock in PBS (pH 7.4) was diluted in complete RPMI-1640 medium to a final assay concentration of 0.03% and used at 100µL/well, following treatment of 96-well plates with test agents and removal of treatment media. Plates were then incubated for 2 hours at 37^{o}C with 5% CO_2 and following this, cells were washed in PBS and neutral red deposits dissolved in 100µL 50% ethanol: 1% acetic acid (v/v), with plates gently agitated on a rocking platform. Absorbance was measured at 540nm using a BioTek EL800 plate reader, with data expressed as mean percentage cell viability +/-SEM, as compared to vehicle-treated control (see relevant chapters), with absorbance values corrected using a cell-free blank.

2.4.3 Trypan Blue Vital Dye Exclusion

Trypan blue (Sigma Aldrich) is a diazo dye that has widely been used to identify viable and non-viable cells. The negatively charged dye is not retained in viable cells, with preserved membrane integrity and actively exclude the dye, but is retained in dead/dying cells with membrane damage (Tran *et al.,* 2011). This technique remains a commonly used, reliable method for the determination of cell viability, as a measurement of altered plasma membrane integrity, a method complementary to assays associated with the measurement of other indicators of cell death, such as the MTT and neutral red assays.

This assay was used to determine viable and non-viable cells from 24-well plates, unless otherwise stated, following treatment with test agents. Cells were harvested for counting by removal of spent media (containing detached cells) into correspondingly labelled tubes and the remaining cell monolayer washed in PBS (pH 7.4) (1X volume), with any cells detaching in the PBS wash solution being combined with the corresponding well media. Remaining attached cells were trypsinized at 37^{o}C with 5% CO_2 in 0.25% Trypsin: EDTA (1X volume) and following detachment, the corresponding spent media/ PBS was used to inactive residual trypsin, with each well washed using the mix to collect the total cell population, which was then centrifuged at 1200xG for 6 minutes. The pelleted cells were then concentrated by resuspension in 200µL and the cell suspension diluted 1:2 with Trypan blue (0.4%) and examined by a haemocytometer, with cells retaining the dye considered non-viable. Total and viable cell numbers were determined as described in section 2.1.1, using triplicate wells per treatment condition.

2.4.4 Assessing Apoptosis by Flow Cytometry

Apoptosis is a mechanism to arrest cell growth and activate regulatory pathways of cell death. In this thesis, two complementary flow cytometry apoptosis assays were used to measure apoptosis induction in treated cells; i) the MUSE™ Annexin V & Dead Cell Assay and ii) MUSE™ MultiCaspase assay.

During apoptosis, intracellular signalling events result in characteristic changes such as phosphatidylserine (PS), which is usually localised internally on the plasma membrane of healthy cells, being externalised to the cell surface (Muse protocol a, 2016). Annexin V is a calcium-dependent phospholipid binding protein that has a high affinity for PS. Along with Annexin V, a dead cell marker 7-amino-actinomycin D (7-AAD) is incorporated into the assay reagent and can identify damage to cell membranes, whereby it is omitted from viable cells that retain membrane integrity. Flow cytometry analysis using the MUSE™ analyser scores cells after incubation with the assay reagent according to the following populations; non-apoptotic cells: Annexin V (-) and 7-AAD (-), early apoptotic cells: Annexin V (+) and 7-AAD (-) late stage apoptotic and dead cells: Annexin V (+) and 7-ADD (+) and mostly nuclear debris: Annexin V (-) and 7-ADD (+).

Following the manufacturer's protocol; cells were harvested as described in section 2.4.3, re-suspended to a concentration of $1x10^5$ to $1x10^7$cells/mL and diluted 1:2 in Annexin V & Dead Cell Reagent to a final concentration of $1x10^4$ to $5x10^5$cells/mL. Samples were protected from light, incubated at room temperature for 20 minutes and measured using the Muse™ Cell Flow Cytometry Analyser, with data expressed as mean percentage total apoptosis using triplicate samples per treatment condition from three independent replicates.

Further to PS externalisation, pro-apoptotic signals associated with activation of caspases were also assayed by flow cytometry using the Muse™ MultiCaspase kit, to determine total activate caspases (caspase-1, 3, 4, 5, 6, 7, 8 and 9) in treated cells. This assay simultaneously determines total count and percentage of cells with caspase activity by utilising a derived VAD-peptide in combination with a dead cell dye (Muse protocol b, 2016). Using Flourescent-Labelled Inhibitor of Caspases (FLICA) the VAD-peptide binds to activated caspases resulting in a fluorescence signal proportional to the number of active caspases in cells. Similar to the Annexin V assay, the dead cell dye (7-AAD) determines membrane structural integrity and cell death by increasing fluorescence intensity, compared to viable cells that actively excludes the dye (Muse protocol b, 2016). The MUSE™ analyser scores cells after incubation with the reagent according to the following populations: Live cells: Caspase (-) and 7-AAD (-), Caspase (+) cells exhibiting pan caspase activity: Caspase (+) and 7-AAD (-), Late stage of Caspase activity cells: Caspase (+) and 7-AAD (+) and Necrotic cells: Caspase (-) and 7-AAD (+).

Following manufacturer's protocol: cells were harvested as described in section 2.4.3 and re-suspended in 1X Caspase Buffer. MultiCaspase Reagent working solution was added to each corresponding tube and incubated for 30 minutes at 37^{o}C with 5% CO_2. Following this, the samples were diluted 1:4 with Caspase 7-AAD working solution to a final concentration of $1x10^5$ to $1x10^6$cells/mL and incubated at room temperature for 5 minutes, protected from light and measured using the Muse™ Cell Flow Cytometry Analyser, with data expressed as mean percentage total caspase activity using triplicate samples per treatment condition from three independent replicates.

2.4.6 Griess Assay

The Griess assay was used to determine nitrite levels in cell supernatants as an indirect assessment of iNOS activity following cytokine treatment. Nitrite present within the culture media reacts with the amino group of sulphanilamide under acidic conditions forming a diazonium cation, which couples with N-Naphylethylenediame (NEDA) to form a corresponding azo dye, which can be measured at 540nm (Tsikas, 2007).

Sodium nitrite ($NaNO_2$) standards were produced across the range 0-100µM, these were then dispensed (100µL/ well) in duplicate onto a 96-well plate. Alongside this, culture media from cytokine-treated 96-well plates was also transferred to a fresh 96-well plate. To all wells (standards and samples), 50µL Griess solution A (1% Sulphanilamide (w/v) in 5% ortho-phosphoric acid (v/v)) was added, immediately followed by 50µL Griess solution B (0.1% NEDA (w/v)). Absorbance was measured at 540nm using a BioTek EL800 plate reader and nitrite levels in cytokine-treated supernatants determined (µM) relative to the standard calibration graph plotted (calibration data was collected each time the assay was carried out, with a representative plot shown in Appendix A, figure A.1).

2.5 Quantification of Intracellular Lipid Droplets

A Lipid Droplet Fluorescence Assay Kit (Caymen Chemical) was used to quantify intracellular lipid droplets using the lipophilic lysochrome Nile Red, which strongly fluoresces in the hydrophobic environment of intracellular neutral lipids. Following manufacturer protocol, cells were treated in 24-well plates with palmitate (250µM), alone or in combination with EETs (10µM), for 24 hours and then harvested as described in section 2.4.3. Treatment

with 250µM oleate was used a positive control, as referenced in the manufacturer protocol. Cell samples were re-suspended in Assay Buffer before being centrifuged at 1200xG for 5 minutes, after which the cell supernatant was aspirated and cells re-suspended in Fixative Solution. After incubation for 10 minutes at room temperature, samples were centrifuged for a further 5 minutes at 1200xG, and the supernatant aspirated. Assay Buffer was added to wash the samples, which were again centrifuged at 1200xG for 5 minutes before the addition of Nile Red Staining Solution. Samples were then incubated at room temperature for 15 minutes, protected from light, before proceeding to aspirate the staining solution. Samples were then washed again and further centrifuged at 1200xG for 5 minutes and the supernatant discarded. Samples were re-suspended in Assay Buffer before fluorescence intensity was measured by FITC (ex/em 485/535) using a Guava® easyCyte™ Flow cytometer. Results were analysed using FLOWJO V10 software by conversion of the histogram plot into a cumulative distribution function plot and mean fluorescence corrected against control, expressed as fold change +/- SEM.

2.6 Plasmid Preparation

The plasmid vectors used in this study were obtained commercially. The pNL3.2.NF-κB-RE[NlucP/NF-κB-RE/Hygro] reporter vector was purchased from Promega, supplied at 20µg and reconstituted at 100ng/µL in deionised water (section 2.7.2). pCMV6-Cyp2c11 (untagged ORF)-Rat cytochrome P450, subfamily IIC (mephenytoin 4-hydroxylase) (Cyp2c11) and pCMV6-Entry mammalian vector with C-terminal Myc-DDK tag (empty vector) were purchased from OriGene, supplied at 10µg and reconstituted at 100ng/µL in deionised water

(section 2.7.3). Prior to transfection in BRIN-BD11 cells, transfection ready plasmids were prepared according to the following sections.

2.6.1 Preparation of Luria-Bertani (LB) agar plates and liquid medium

Lennox LB with agar (Sigma Aldrich) was supplied as a powder and reconstituted to 35g/L in deionised water. After reconstitution, the LB solution was autoclaved at 121^{o}C, cooled slightly before making additions of antibiotic (either 50µg/mL ampicillin or kanamycin, depending on the resistance gene encoded by the plasmid; see Appendix B) and poured into sterile petri dishes and allowed to solidify.

LB Broth (Lennox) (Sigma Aldrich) was supplied as a powder and reconstituted to 20g/L in deionised water. After reconstitution, the LB solution was autoclaved at 121^{o}C, cooled slightly before making additions of antibiotics (as stated above).

2.6.2 Transformation of Chemically Competent Cells

Alpha-Select Chemically Competent Bronze-Efficiency *E.coli* Cells (Bioline) were supplied transformation ready. All aseptic techniques were performed in a Triple Red J Bio Microbiology Fume Culture Hood. Following manufacturer protocol; cells were thawed on ice and 50µL cell samples aliquoted into sterile pre-chilled microcentrifuge tubes. A sufficient amount of vector (2-5µL at 100ng/µL) was added to the cell suspension, gently mixed and incubated on ice for 30 minutes. Samples were heat shocked at 42^{o}C for 30 seconds and immediately returned to ice for 2 minutes. The transformation reaction was diluted 1:20 with

SOC medium, mixed thoroughly and placed in a shaking incubator at 37°C, medium speed (~250rpm) for 60 minutes to allow recovering of the cells post-transformation and facilitate expression of antibiotic resistance genes prior to plating. Bacterial cultures were plated onto LB agar (+/- antibiotic, as indicated in 2.6.1 and dependent on the resistance gene encoded by the plasmid) using a lawn method and incubated for 24 hours at 37°C. Successful, antibiotic resistant, colonies were individually collected and transferred to 5mL LB liquid medium (+/- antibiotic) and further incubated for 24 hours at 37°C before being diluted 1:250 in LB liquid medium (+ antibiotic) to expand the cultures for plasmid purification.

2.6.3 Zyppy™ Plasmid Miniprep Kit

The Zyppy™ plasmid miniprep kit (Zymo Research) was used to prepare sample plasmids for sequencing before further colony expansion and Maxiprep purification. Following manufacturer protocol; bacterial cultures were grown in LB liquid medium (+/- antibiotic) as described in section 2.6.2 and samples of the initial 5mL culture were centrifuged at 13,000xG at room temperature. Bacterial cultures were lysed using 7X Lysis Buffer before adding Neutralisation Buffer and samples centrifuged for 4 minutes. The supernatant was transferred into provided Zymo-Spin IIN Column with Collection Tube and centrifuged for a further 15 seconds. Following this, the flow-through was discarded and Endo-Wash Buffer added to the column to remove residual endotoxins and centrifuged again for 30 seconds. After this, Zyppy™ Wash Buffer was added to the column and further centrifuged for 1 minute before plasmid DNA was eluted by the addition of 30µL Zyppy™ Elution Buffer direct to the column matrix and centrifuging. Isolated plasmid DNA was then quantified using a Thermo Scientific Nanodrop™ 1000 spectrophotometer, with samples then diluted to 10µg/µL and sent for

sequencing (MWG Eurofins) using pre-supplied forward and reverse sequencing primers for the pCMV6 vector (Origene).

2.6.4 GeneJET Plasmid Maxiprep Kit

GeneJET Plasmid Maxiprep Kit (Thermo Scientific™) was used for high yield transfection-ready (endo-free) plasmid isolation from 250mL LB liquid cultures, prepared as described in section 2.6.2. Following manufacturer protocol; bacterial cultures were grown in 250mL LB liquid medium (+ antibiotic) and plasmid DNA harvested using GeneJET Plasmid Maxi Prep protocol using a low speed centrifugation method (up to 5,000xG). Bacterial cultures were centrifuged at 5,000xG for 10 minutes at room temperature, with cell supernatant discarded and pellets re-suspended in Resuspension Solution and mixed before adding a 1X volume of Lysis Solution; samples were then lysed (SDS/alkaline lysis) for 3 minutes at room temperature before adding Neutralization Solution to re-anneal plasmids. Following this, Endotoxin Binding Reagent was added to isolate endotoxins, preventing their subsequent binding to spin column matrix, allowing isolation of transfection-ready (endotoxin-free) plasmids. Samples were gently mixed by inverting, incubated at room temperature for 5 minutes and further centrifuged at 5,000xG for 40 minutes after the addition of a 1X volume (equal to neutralisation solution) of 96% ethanol to pellet cell debris and chromosomal DNA. The supernatants were decanted into fresh tubes, avoiding transferring or disturbing the white precipitate, samples were then transferred to a spin column and centrifuged (~20mL at a time until the entire sample volume was processed) for 3 minutes at 2,000xG in a swinging bucket rotor. Plasmid DNA bound to the column matrix was then washed twice using Wash Solution I (low concentration of chaotropic salts in

isopropanol to remove residual protein), followed by Wash Solution II (containing ethanol to remove salt prior to elution), centrifuging for 2 minutes at 3,000xG after each wash and discarding the flow-through. Finally, plasmid DNA was eluted in a fresh tube using 1mL Elution Buffer and incubating the samples at room temperature for 2 minutes before proceeding to centrifuge at 3,000xG for 5 minutes. Plasmid yield was quantified using a Thermo Scientific Nanodrop™ 1000 spectrophotometer, with an A260/A280 ratio of 1.8-1.9 indicating a high purity. Isolated plasmid DNA was then stored at -20^{o}C until use.

2.7 Plasmid Transfection

2.7.1 Lipofectamine® 2000 Transfection

Preliminary investigations using NanoJuice® Transfection Kit (Merck), Lipofectamine® 2000 Transfection Reagent (Invitrogen™) and Lipofectamine® 3000 Transfection Reagent (Invitrogen™) were trialled to determine the optimum method for plasmid transfection in BRIN-BD11 cells using the Green Fluorescence Protein (GFP)-expressing plasmid pmaxGFP (gift from Dr Mirna Maarabouni, Keele University). Both NanoJuice® and Lipofectamine®3000 failed to produce successful transfections (data not shown), in comparison to ~56% transfection efficiency using Lipofectamine® 2000. Having established an appropriate ratio of Lipofectamine® 2000: plasmid DNA (see Appendix A, figure A.2), cells were routinely transfected according to the following manufacturer protocol. BRIN-BD11 cells were cultured to 70-90% confluency prior to transfection. Lipofectamine® 2000 was diluted in Opti-MEM® (Gibco®) medium separate to Opti-MEM® (Gibco®) medium containing plasmid DNA. The dilute DNA and Lipofectamine® 2000 solutions were combined at a ratio of 1:1 and incubated

at room temperature for 5 minutes to allow transfection complexes to form before addition to cell cultures at the following final concentration ratios of lipofectamine® 2000:plasmid DNA; 96-well plates: 0.3µL: 0.1µg/ well, 24-well plates: 1.5µL: 0.5µg/ well and 6-well plates: 7.5µL: 2.5µg/ well. Cells were incubated at 37^{o}C with 5% CO_2 for 24 hours before being re-plated and/or treated for cell viability assays (see section 2.7.2 and 2.7.3).

2.7.2 NF-κB-NanoLuc® Reporter Vector Assay

A pNL3.2.NF-κB-RE[NlucP/NF-κB-RE/Hygro] reporter vector (Promega) expressing the NanoLuc® luciferase under the control of five copies of the NF-κB response element was used in combination with Nano-Glo® Luciferase Assay System to determine NF-κB activation following cytokine treatment in BRIN-BD11 cells. NanoLuc® luciferase is a small enzyme (19.1kDa) that reports luminescence in the presence of Nano-Glo® substrate using a novel coelenterazine analogue (furimazine) that produces a high intensity, glow-type, ATP-independent luminescence reaction (Promega technical manual, 2015). BRIN BD11 cells were seeded onto 96-well black plates and transfected with the pNL3.2.NF-κB-RE vector as described in section 2.7.1 for 24 hours before treatment with test agents (see Chapter 5) for a further 24 hours. Following treatment, plates were equilibrated to room temperature for 10 minutes before Nano-Glo® Luciferase Assay Reagent (equal to 1X culture volume) was added and gently mixed. Plates were incubated for 3 minutes before measuring luminescence using the Promega Glomax® Multi-Detection System (E9032). Data was expressed following manuscript calculation as fold induction of NF-κB, as compared to control (equation 2).

Eq 2. $$Fold\ Induction = \frac{Average\ relative\ light\ units\ of\ induced\ cells}{Average\ relative\ light\ units\ of\ control\ cells}$$

2.7.3 Cytochrome P450 2C11 (CYP 2C11) Stable Transfection

pCMV6-Cyp2c11 and pCMV6-Entry plasmids were prepared for transfection as described in section 2.6 (with the addition of kanamycin) and after confirmation of successful cloning by sequencing, BRIN-BD11 cells were seeded onto 6-well plates and transfected with either the pCMV6-Cyp2c11 vector or pCMV6-Entry vector as described in section 2.7.1. After 48 hours, cells were passaged and serially diluted across the range 1:125-1:2000 in fresh RPMI-1640 media containing Geneticin (G-418; Roche) at a concentration of 1µg/mL. Cells were incubated in the presence of G-418 for two weeks with media replaced every 2-3 days until formation of islands appeared. Following distinct island formation, several large, isolated colonies were collected individually by trypsin:EDTA detachment using a cloning ring, and further seeded into 24-well plates in the presence of G-418. Cells were continuously monitored for 2-3 weeks, with media changed every 2-3 days, and then further sub-cultured into 96-well plates at one cell/well by serial dilution. After this, cells were progressively cultured in G-418-containing media until the cultures were scaled to confluent 75cm^2 tissue culture flasks, yielding G418 resistant BRIN-BD11 cells stably expressing CYP 2C11. Four stable cell lines transfected with pCMV6-Cyp2c11 vector and two transfected with pCMV6-Entry were isolated, these were designated as C11-1, C11-2, C11-3 and C11-4, or pCMV6-EV1 and -EV2, with stable expression of CYP 2C11 confirmed by Western blotting (section 2.8).

2.8 Western Blotting

2.8.1 Preparation of BRIN-BD11 Cell Lysates

For specific details on the application of Western blotting and cell treatment conditions, see relevant chapters. Following treatment, total BRIN-BD11 cell samples were collected from culture plates or flasks and pelleted (750,000 cells), as described in section 2.4.3, and the resulting cell pellets washed twice in excess ice-cold PBS, centrifuging at 1200xG for 6 minutes. Following this, protease inhibitor (Sigma Aldrich) was diluted 1:10 in RIPA Buffer (Sigma Aldrich) and cells re-suspended in 30µL of RIPA/ protease inhibitor cocktail and incubated at 4^{o}C for 5 minutes before being centrifuged at 13000xG for 10 minutes to pellet cell debris. After centrifugation, 20µL of cell supernatant (corresponding to the lysate of 500,000 cells) was removed and diluted with 4X Laemmli Buffer (BIO-RAD) containing 10% β-mercaptoethanol, resulting in a loading sample of 500, 000 cells in 1X Laemmli, with samples heated to 95^{o}C for 4 minutes and briefly centrifuged.

2.8.2 SDS-PAGE

A Precision Plus Protein™ Dual Colour Standards (BIO-RAD) ladder was used to confirm migration of proteins, transfer quality of proteins and molecular weight confirmation for all western blot samples.

Samples were loaded into 10-well Mini-PROTEAN® TGX™ gels (BIO-RAD) at either 10 or 12% polyacrylamide (depending on target protein), in a BIO-RAD Mini-PROTEAN® Tetra System tank containing 1X Tris-Glycine-SDS running buffer (Fisher Scientific™) and separated

by electrophoresis using a Consort EV231 system at 150 Volts for 1 hour at room temperature until separated. Materials for an overnight Western blot transfer were prepared as follows: one PVDF Transfer membrane (0.45µm; Thermo Scientific™) was briefly soaked in 100% methanol for 20 seconds, this and two Whatman™ Chromatography grade 3mm filter papers, and two filter pads supplied with the BIO-RAD Mini-PROTEAN™ 3 Cell overnight transfer tank were then were pre-soaked for at least 20 minutes in 1X NuPAGE™ Transfer Buffer (Thermo Scientific™) before assembly.

After successful protein migration, the gel cassette was removed, the gel rinsed in transfer buffer to remove residual SDS and the gel placed onto the PVDF membrane and sandwiched between two filter papers and two filter pads. The membrane unit cassette was loaded into a BIO-RAD Mini-PROTEAN™ 3 Cell overnight transfer tank in 1X NuPAGE™ Transfer Buffer (Thermo Scientific™) with an ice pack and stirring bead and transferred using a Consort EV231 system at 30 Volts, 90mA for 16 hours at 4^{o}C.

2.8.3 Western Blot

After transfer of the samples to PVDF membranes, blots were processed for immuno-detection using the following protocol; all samples were incubated at room temperature unless otherwise stated. The membrane was removed from the overnight transfer unit and washed in excess 1X TBS (Fisher Scientific™) to remove residual transfer buffer. The membrane was incubated in 5% non-fat milk (w/v TBS) or 5% goat serum (v/v TBS) blocking solution for 1 hour and gently rocked at slow speed (~15rpm) using a Gyro-platform rocker. Following this, the membrane was washed three times in excess 1X TBS (Fisher Scientific™) to

remove residual blocking solution, before adding 1% blocking solution containing primary antibody, dependent on target protein (see relevant chapters), covered and incubated overnight at 4^{o}C with gentle rocking at slow speed. Following primary antibody incubation the membrane was washed in 1X TBS (Fisher Scientific™) or 1X TBS Tween®-20 Buffer (Thermo Scientific™) three times for 5 minutes whilst gently rocked at slow speed. After washing, the secondary antibody (HRP-conjugated polyclonal goat anti-mouse secondary (Dako, P0447) at 1:1000), was added in 5% blocking solution, covered and further incubated overnight at 4^{o}C with gentle rocking at slow speed. Following secondary antibody incubation, the membrane was washed five times for 5 minutes in 1X TBS (Fisher Scientific™) or 1X TBS Tween®-20 Buffer (Thermo Scientific™) before adding Clarity™ Western ECL Substrate (BIO-RAD) and incubating for 5 minutes protected from light. Once incubated, the membrane was imaged using a C-DiGit® Blot Scanner (*LI-COR®*), set at high-sensitivity for all Western blot samples. After the membrane was scanned, the membrane was then washed in excess 1X TBS (Fisher Scientific™) before the addition of Restore™ PLUS Western Blot Stripping Buffer (Thermo Scientific™) for 10 minutes and gently rocked at slow speed. The stripped membrane was then washed three times in excess 1X TBS (Fisher Scientific™) before being re-blocked in 5% blocking solution for 30 minutes. The membrane was then washed in excess 1X TBS (Fisher Scientific™) before the addition of a mouse monoclonal anti-β-Actin (Sigma Aldrich, A2228, clone AC-74) at 1:1000 dilution in 1% blocking solution. Following a 1 hour incubation, the membrane was again washed three times in 1X TBS (Fisher Scientific™) for 5 minutes before being incubated with the corresponding polyclonal goat anti-mouse secondary (Dako, P0447) at 1:1000 in 5% blocking solution for 2 hours. Following this, the membrane was washed five times in 1X TBS (Fisher Scientific™) before proceeding to incubate with Clarity™ Western ECL Substrate (BIO-RAD) for 5 minutes protected from light. Once incubated, the membrane was imaged using a

C-DiGit® Blot Scanner (*LI-COR®*). Results were analysed using the *LI-COR®* software supplied and expressed as relative ratio of protein of interest against β-Actin expression.

2.9 Real Time-Polymerase Chain Reaction (RT-PCR)

2.9.1 RNA Extraction and Purification

BRIN-BD11 cells were seeded in 24- or 6-well plates and, following treatment with 250µM palmitate, alone or in combination with EETs (10µM), cells were harvested for RNA extraction using Direct-zol™ RNA MiniPrep (Zymo Research). Following manufacturer's protocol, all centrifugation steps were performed at 13000xG for 30 seconds. To isolate RNA from the total cell population, spent media from treated wells was centrifuged at 12000xG for 6 minutes to pellet any detached cells. The remaining adhered cells were lysed directly in the culture plate using TRIzol® (Zymo Research), an acid-guanidinium-phenol based reagent that functions to solubilise biological compounds and denature proteins, in the process of cell lysis, whilst isolating RNA, DNA and protein, which was then transferred to the isolated pellet from the culture media. After lysing the cells in Trizol, an equal volume of ethanol (100% v/v) was added and the samples were transferred to a Zymo-Spin™ IIC Column with collection tube and centrifuged to bind nucleic acids to the silica-based column matrix, eliminating inaccuracies with phase separation and precipitation-based methods of RNA isolation. The column was then transferred to a new collection tube and RNA Wash buffer was added and samples centrifuged to remove residual protein before proceeding with DNase I treatment to remove genomic DNA contamination. DNase I (6U/µL) was diluted with DNA Digestion Buffer at a 1:16

ratio, before directly applying to the column matrix (80µL/column) and incubated at room temperature (20-30^{o}C) for 15 minutes.

The column was then washed twice to eliminate digested DNA, discarding the flow-through, using Direct-Zol™ RNA PreWash, followed by a final addition of RNA Wash Buffer to remove PreWash buffer salts and centrifuged. Sample tubes were then centrifuged (empty) for 2 minutes to ensure complete removal of residual wash buffers before columns were transferred to new collection tubes ready for sample elution in 30µL of DNase/RNase-Free Water, directly added to the column matrix before centrifugation. Samples were quantified using Thermo Scientific Nanodrop™ 1000 spectrophotometer, with a ratio of A260/A280 of 1.8-2.1 indicating a high purity RNA sample. Integrity of the eluted RNA was confirmed by preparation of 1µg RNA/sample in a 1X DNA loading buffer (Bioline) and separation on a 1% (w/v) agarose mini-gel in 1X tris-acetate-EDTA buffer (TAE) containing ethidium bromide for 20 minutes at 100V alongside a 1,000kBp DNA ladder (Biolone). Gels were visualised using a Syngene U:Genius 3 UV Transilluminator and RNA integrity/purity confirmed by a 2:1 ratio of the 28S and 18S rRNA bands, the absence of high molecular weight gDNA bands or band smearing (see Appendix A, figure A.3). Samples were then stored at -80^{o}C or used immediately for cDNA synthesis.

2.9.2 cDNA Synthesis by Reverse Transcription

High Capacity cDNA Reverse Transcription Kit (Applied Biosystems) was used to synthesise cDNA from RNA for RT-PCR. Following manufacturers protocol; all materials were kept on ice, including RNA samples (thawed on ice if stored at -80^{o}C) throughout. A 2X RT

master mix was prepared with the following components: 2X RT Buffer, dNTP Mix (4mM), 2X RT Random Primers, MultiScribe™ Reverse Transcriptase (50U/reaction), RNase Inhibitor (20U/reaction) and Nuclease-free H_2O to a total of 10µL per reaction. The 2X RT master mix was kept on ice whilst RNA samples were prepared to a final concentration of 1µg/10µL, which was then gently mixed with 10µL of the 2X RT master mix. Samples were loaded into an Eppendorf Mastercycler® nexus (thermal cycler) and conditions set to: Step 1 – 25°C for 10 minutes, Step 2 – 37°C for 120 minutes, Step 3 – 85°C for 5 minutes and Step 4 – hold at 4°C indefinitely. Samples were stored long-term at -20°C.

2.9.3 QuantiNova™ SYBR® Green PCR Kit

QuantiNova™ SYBR® Green PCR kit was used to determine gene expression in cDNA samples. SYBR® Green I dye binds to the minor groove of any double-stranded DNA with excitation producing a strong fluorescence with minimal background noise from unbound SYBR® Green I dye (Life Technologies Protocol, 2012). Following manufacturers protocol; a reaction master mix was prepared in a 1X SYBR Green PCR Master Mix containing; QN ROX Reference Dye for normalisation of fluorescence signal (low-ROX), Forward primer (as desired), Reverse primer (as desired), template cDNA was diluted into the reaction master mix to a final concentration of 10ng and reaction volume made up to 20µL in Nuclease-free H_2O. PCR amplification and real-time quantification of fluorescence was carried out using an AriaMx Real Time PCR System G8830A (Agilent Technologies) under the following cycling conditions; PCR initial heat activation for 2 minutes at 95°C, followed by 2-step cycling (denaturation for 5 seconds at 95°C and annealing/extension for 10 seconds at 60°C) over 40 cycles. Specificity of the amplification was then determined by melt curve analysis.

Efficiency for each target gene was determined using a standard curve of real-time PCR data across the range of 0.01, 0.1, 1 and 10ng. All primers had an efficiency between 90-110% and showed no visible primer-dimer formation, as determined by specificity of amplification from melt curve analysis, showing a single peak (see Appendix A, figure A.4 and table A.2).

All data was analysed using the AriaMx qPCR software to compare C_t values for the gene of interest (GOI) in treated samples with vehicle-treated controls, relative to the 18S rRNA gene as a normaliser (equation 3), deriving a value for $\Delta\Delta C_t$ (equation 4) with data expressed as fold change in expression (as compared to control; equation 5).

Eq. 3

$$\Delta C_{t\ sample} = C_{t\ GOI} - C_{t\ 18S\ rRNA}$$

$$\Delta C_{t\ control} = C_{t\ GOI} - C_{t\ 18S\ rRNA}$$

Eq. 4

$$\Delta\Delta C_t = \Delta C_{t\ sample} - \Delta C_{t\ control}$$

Eq. 5

$$Fold\ change = 2^{-\Delta\Delta Ct}$$

To confirm suitability of 18S rRNA as a normaliser relative to the GOIs, comparative efficiency plots were produced for each GOI by plotting the mean ΔC_t between the 18S rRNA gene and the GOI from the standard curve data against input amount of RNA (see Appendix A, table A.2). Whilst absolute comparison between ΔC_t values for any given input amount of RNA target should be identical, the slope of these comparative efficiency plots produced values <0.1, which is considered acceptable deviation when using the $\Delta\Delta C_t$ method for RT-PCR expression analysis, thereby confirming suitability of the 18S rRNA gene for normalisation in this study.

2.9.4 Primer Design

Primers were designed using Primer-BLAST (https://www.ncbi.nlm.nih.gov/tools/primer-blast/) provided by National Centre for Biotechnology Information (NCBI) and integrated DNA technologies, with primer specificity further confirmed using NCBI-BLAST.

Table 2.2 Primers used in the study of EET action

Target	Primers	Sequences (5' to 3')	Length of Product (bp)
18S	Forward	GCAATTATTCCCCATGAACG (20)	123
	Reverse	GGCCTCACTAAACCATCCAA (20)	
CPT1	Forward	CAGCTCGCACATTACAAGGA (20)	128
	Reverse	TGCACAAAGTTGCAGGACTC (20)	
Elovl6	Forward	ACACGTAGCGACTCCGAAGAT (21)	145
	Reverse	AGCGCAGAAAACAGGAAAGACT (22)	
Ech1	Forward	TGTGGTCTCTGGTGCAGGAAAG (22)	134
	Reverse	GGTATCGGCTGATGAGGTCTCG (22)	
DGAT1	Forward	TGCTCTTTTTCACCCAGCTT (20)	82
	Reverse	TTGAAGGGCTTCATGGAGTT (20)	

2.10 Statistical Analysis

All experiments were performed as three independent replicates, unless otherwise stated. Results expressed as mean +/- SEM. Data was tested for normality and level of significance was calculated by using one-way ANOVA followed by Tukey's test *post hoc* and where appropriate a two-way ANOVA followed by Bonferroni's *post hoc* (GraphPad Prism 7). A P value of less than 0.05 ($P<0.05$) was regarded as significant.

Chapter Three

Preliminary Investigations

3 Preliminary investigations into cytotoxic effects of cytokines and palmitate in BRIN-BD11 cells

3.1 Introduction

Broadly classified, DM is mainly characterised into type 1 DM and type 2 DM. Type 1 DM occurs as a result of an autoimmune attack on pancreatic beta cells within the islets of Langerhans, reducing functional cell mass by 70-80% by the time of diagnosis and is characterised by the infiltration of immune cells, mainly $CD4^+$ and $CD8^+$ T-cells and macrophages, in a process termed insulitis (Willcox *et al.,* 2009). Type 2 DM is often associated with chronic glucolipotoxicity, influenced by high-fat diets and increased insulin resistance in adipose and skeletal muscle, typically forming the foundation of a pre-diabetic hyperglycaemic state before progressing to overt type 2 DM (Donath *et al.,* 2013). Understanding the mechanisms responsible for targeted beta cell destruction in the development of type 1 DM and the sensitivity of beta cells to pro-inflammatory cytokines, oxidative and nitrosative stress, and the glucolipotoxic environment in the milieu of islet beta cells in the pathogenesis of both main forms of DM remains a major aim of diabetes research. The establishment of a range of *in vitro* pancreatic beta cell line models, as well as *ex vivo* islets and primary cells, and *in vivo* animal models continue to advance these aims.

3.1.1 *In vitro* models of type 1 DM

The main mechanisms believed to be involved in beta cell demise via apoptosis induction in type 1 DM include: 1) ligation of Fas Ligand (FasL) expressed by infiltrating $CD8^+$ with cell surface Fas Receptors, 2) the release of pore-forming perforins and the granzyme B serine protease, 3) secretion of pro-inflammatory cytokines; IL-1β, IFN-γ and TNF-α by infiltrating immune cells and 4) increase in NO and ROS (Yoon and Jun, 2005).

In models of type 1 DM, it is well-established that pro-inflammatory cytokines are the main soluble mediators involved in beta cell death. Treatment with these cytokines has been shown to increase apoptosis in a range of pancreatic beta cell lines and primary islets and is, in part, mediated by the alteration in expression of NF-κB and STAT1 target genes, downstream of cytokine receptor activation, including the upregulation of iNOS and subsequent NO production (Cnop *et al.,* 2005). The contribution of NO to beta cell dysfunction was first reported by Southern *et al.,* (1990) and has since been observed to mediate, in part, pro-apoptotic cytokine-induced cell death (Ankarcrona *et al.,* 1994; Eizirik *et al.,* 1996; Cardozo *et al.,* 2005); although both NO-dependent and NO-independent effects are known. In INS-1 cells subjected to IL-1β and IFN-γ, microarray analysis showed alteration in expression of 698 genes over 1, 2, 4, 8, 12 and 24 hours treatment, with several apoptosis-related genes altered within 2-4 hours, preceding increased iNOS expression (typically occurring within 6 hours of cytokine treatment). Alternatively, between treatment times of 8-24 hours, 46% of gene analyses were altered because of NO production and were classified as NO-dependent despite which, inhibition of NO production failed to attenuate cytokine toxicity (Kutlu *et al.,* 2003).

The extent of pro-inflammatory cytokine toxicity, and indeed the contribution of iNOS expression to cytokine-induced beta cell apoptosis, is variable between different model systems, as well as being influenced both by concentration (and type) of cytokines administered and treatment periods across a range of beta cell and islet models. In rat RINm5F cells, studies on the contribution of individual cytokines in mediating beta cell death showed that IL-1β and IFN-γ alone, but not TNF-α, increased beta cell death by activation of the intrinsic mitochondrial pathway (Holohan *et al*., 2007). Synergistic actions of IL-1β and IFN-γ were also demonstrated to be central to beta cell death, supporting previous studies carried out in RINm5F cells and isolated rat primary beta cells, and human beta cells (Rabinovitch and Suarez-Pinzon, 1998; Eizirik and Mandrup-Poulsen, 2001). Whilst earlier studies in the same cell line reported that IL-1β and TNF-α (but not IFN-γ) alone increased iNOS expression and induced apoptosis (Ankarcrona *et al.,* 1994; Cetkovi-Cvrlje and Eizirik, 1994), other studies in murine insulinoma cells showed TNF-α has synergistic effects with IFN-γ in causing beta cell death in the absence of IL-1β (Chang *et al.,* 2004). It is clear, therefore, that cytokine synergy, through costimulatory activation of numerous pro-apoptotic signalling pathways, is essential in beta cell death and more closely reflects the *in vivo* autoimmune attack on beta cells.

Cytokine-induced iNOS expression has been shown to be mediated by NF-κB activation, downstream of IL-1β binding to its receptor (Flodstrom *et al.,* 1996; Kutlu *et al.,* 2003), with consensus sequences for NF-κB identified in the iNOS promoter region (Xie *et al.,* 1994). Further synergistic contribution of IFN-γ activated pathways in mediating iNOS expression, such as IRF-1 and STAT1 are also well-established; with consensus sequences for IRF-1 also identified in the iNOS promoter region (Xie *et al.,* 1994) and IRF-$1^{-/-}$ mice have been shown to produce little or no NO, with iNOS mRNA barely detectable when treated with IFN-

γ (Kamijo *et al.,* 1994). This cross-talk between pathways indicates that IFN-γ may potentiate IL-1β mediated iNOS expression by enhancement of NF-κB action in this context. Whilst iNOS expression and NO production can be considered as a classical 'hallmark' of cytokine action in beta cells, the contribution of this radical as a mediator of beta cell death in type 1 DM remains unclear. Exogenous treatment of beta cells with chemical NO donors has been shown to induce cytotoxicity comparable to cytokine-stimulated endogenous NO production (Eizirik *et al.,* 1996) and the ER stress response in rodent beta models exposed to cytokines appears NO-dependent (Oyadomari *et al.,* 2001; Cardozo *et al., 2*005). However, iNOS inhibition may only partially rescue clonal cells and islets from cytokine toxicity (Kutlu *et al.,* 2003) and cytokine effects in human islet models are largely NO-independent (Eizirik *et al.,* 1994; Zhong *et al.,* 2018). Nonetheless, recent studies aimed at the development of novel and more potent/selective iNOS inhibitors and their effects on cytokine toxicity in rodent beta cell lines and islet models (Zhong *et al.,* 2018), as well as observations that improved siRNA delivery into human islets targeting iNOS induced a modest reduction in apoptosis in response to cytokine treatment (Li and Mahato 2007), continues to maintain interest in its role in models of type 1 DM.

3.1.2 *In vitro* models of type 2 DM

In contrast to the autoimmune attack on pancreatic beta cells in type 1 DM, type 2 DM is partly associated with glucolipotoxicity, with chronic elevation of long-chain fatty acids (particularly palmitate (C16:0)) alongside prevailing hyperglycaemia directly contributing to declining functional beta cell mass. Although mechanisms responsible for glucolipotoxicity-induced beta cell apoptosis are not fully understood, elevated glucose levels lead to increased

cytosolic malonyl-CoA, with a direct inhibitory action on CPT1 decreasing entry of long-chain fatty acyl-CoA groups into the mitochondria for oxidation.

Accumulation of cytosolic acyl-CoA, largely from cellular lipid overload, increases the rate of fatty acid metabolism in other pathways including *de novo* ceramide synthesis and peroxisomal β-oxidation. This latter pathway leads to increased production of H_2O_2, which, coupled to very low expression of the H_2O_2-detoxifying oxidoreductase enzyme, catalase in beta cells (Tiedge *et al.,* 1997), directly provides a mechanistic link between lipotoxicity, ROS generation and oxidative stress. In support of this Elsner *et al.,* (2011) showed that peroxisomal and cytosolic over-expression of catalase could protect RINm5F beta cells against palmitate toxicity, suggesting that this represents a major route of palmitate-induced ROS, in addition to the possible contribution of mitochondria-derived ROS from the release of superoxides in the respiratory chain, with enhanced palmitate oxidation. That over-expression of CPT1 has been shown to protect against lipotoxicity in INS-1 cells further supports extra-mitochondrial fatty acid metabolism as a main contributor to lipotoxicity (Sol *et al.,* 2008).

One well-established mechanism of lipotoxicity is the activation of ER stress and initiation of the UPR by palmitate overload in beta cells (Cnop *et al.,* 2008; Diakogiannaki *et al.,* 2008). In INS-1 cells, palmitate treatment has been shown to induce a marked elevation in the activation and/or increased expression of the three main branches of the UPR (Cuhna *et al.,* 2008), with similar effects also observed in MIN6 beta cells (Laybutt *et al.,* 2007), as well as human islets (Lai *et al.,* 2008). Similarly, the cytoprotective actions of mono- and poly-unsaturated fatty acids have also been associated with a reduction in palmitate-induced ER stress markers (Diakogiannaki *et al.*, 2008). However, over-expression of the ER resident chaperone BiP failed to attenuate palmitate toxicity in INS-1 cells, nor alter palmitate

sensitivity in MIN6 cells (Lai *et al.,* 2008), highlighting that whilst ER stress initiation may be a factor in lipotoxicity, it is not the sole mediator of beta cell apoptosis under these conditions.

Similar to the action of cytokines in mediating beta cell death in cellular models of type 1 DM, species and cell type-specific variation in the response of clonal cell lines and *ex vivo* islets to the lipotoxic action of palmitate are also noted in a number of studies. The phenomenon of glucolipotoxicity, whereby hyperglycaemia potentiates lipotoxicity (possibly via effects on decreased mitochondrial β-oxidation) has been reported in several studies utilising the rat beta cell line INS-1 (El-Assaad *et al.,* 2003; Sargsyan and Bergsten, 2011). In contrast however, Sargsyan and Bergsten., (2011) showed that whilst high glucose markedly enhanced palmitate-induced DNA fragmentation and caspase activation in INS-1 cells, such effects were not evident in MIN6 cells. Similarly, human islets also displayed reduced sensitivity to glucose-augmented lipotoxicity, suggesting important species/model system differences. However, El-Assaad *et al.,* (2003) reported comparable enhancement in dispersed human islets exposed to palmitate and 25mM glucose, as assessed by Hoechst and TUNEL staining, to that observed in INS-1 cells. Differences between these two models likely reflects additional protection afforded by the intact islet architecture; this may be attributable to higher antioxidant enzyme capacity facilitating ROS clearance in intact islets, given the likely contribution of peroxisomal H_2O_2 to lipotoxicity (Elsner *et al.,* 2011).

Differences between the rat INS-1 and mouse MIN6 cell line models may also reflect differential lipid handling between the two models, with palmitate oxidation rates less affected by high glucose in MIN6 compared to INS-1, effects associated with higher acetyl-CoA Carboxylase activity in INS-1 cells (Sargsyan and Bergsten, 2011). Similarly both human islets and MIN6 cells have been shown to express higher levels of SCD-1 compared to INS-1 cells (Lai

et al., 2008), which converts toxic saturated fatty acid species to the more well-tolerated monounsaturated species. Such differences in lipid handling may also explain variation in palmitate doses and/or exposure times in a range of studies in these cell lines used to model lipotoxicity, whereby concentrations of palmitate exceeding 400µM over longer incubation periods of 48 hours in MIN6 cells witness a comparable reduction in cell viability to that seen with 125-250µM over 24 hours in INS-1 cells when assessed by MTT reduction assays.

3.1.3 BRIN-BD11 cells a model for cytotoxicity studies

The BRIN-BD11 rat pancreatic beta cell line, used in the current study, was established in the mid-1990's, producing a more glucose-responsive cell line from parental RINm5F cells (which continue to also be extensively utilised despite poor secretory capacity), by electrofusion with NEDH rat islet beta cells (McClenaghan *et al.,* 1996). BRIN-BD11 cells in contrast, display an enhanced GSIS profile, owing to high expression of GLUT2 and a higher glucokinase:hexokinase ratio, facilitating enhanced glucose uptake, glucose oxidation and ATP production necessary for stimulus-secretion coupling; with similarly enhanced activity in responses to amino acids and hypoglycaemic agents (McClenaghan *et al.,* 1996; McClenaghan and Flatt 1999). These properties have been exploited in functional studies into the roles of novel insulinotropic peptides with potential clinical utility, with activity related to GLP-1 signalling and the GLP-1 mimetic exendin-4 (O'Harte *et al.,* 2016; Long *et al.,* 2018).

BRIN-BD11 cells have also been utilised as a model for the study of lipotoxicity and, to a lesser extent, pro-inflammatory cytokine toxicity. Establishing cytotoxic effects of palmitate in BRIN-BD11 cells treated with 250µM palmitate, studies have shown comparable effects to

that seen in INS-1 and primary rodent islets in the extent of cytotoxicity, as assessed utilising a range of cell viability assays including trypan blue vital dye exclusion staining, caspase activation and Annexin V/PS staining (Welters *et al.,* 2004; Dhayal *et al.,* 2008). Furthermore, this cell line has also been employed in studies investigating the cytoprotective actions of mono- and poly-unsaturated fatty acids against palmitate toxicity, defining important structural characteristics for cytoprotection in terms of chain length and number and configuration of double bonds (Dhayal and Morgan 2008; Dhayal *et al.,* 2008). Potential mechanisms of action have also been reported, both in terms of ameliorating palmitate-induced ER stress (Diakogiannaki *et al.,* 2008) and defining potential requirements for a fatty acid binding site(s) in as yet undefined receptor(s) (Dhayal and Morgan 2008). Mechanisms of cytoprotection afforded by AA, relevant to the current study, have also been explored in this cell line (Dhayal and Morgan 2008; Keane *et al.,* 2011), with these studies exploring the dependence of AA-derived COX and LOX metabolites and, whilst their contribution to the cytoprotective effects of AA is minimal (Dhayal and Morgan 2008), COX1 metabolites may positively contribute to augmentation of insulin secretion in co-incubation with AA and palmitate (Keane *et al.,* 2008).

In contrast to RINm5F, INS-1 and MIN6 clonal beta cells, comparatively fewer studies have fully established the actions of pro-inflammatory cytokines in the BRIN-BD11 cell line. Nonetheless beta cell dysfunction, loss in cell viability and induction of apoptosis have been reported, with this rat cell line shown to respond modestly to IL-1β used alone (Gao *et al.,* 2003), in agreement with the sensitivity of the parental RINm5F cells to this singular cytokine treatment (Ankarcrona *et al.,* 1994; Holohan *et al.,* 2008). Similarly, synergistic action of cytokines is also evident, with a combination of IL-1β and IFN-γ increasing cell death to ~40%

as assessed by vital dye staining (Welters *et al.,* 2004) and reducing cell viability as assessed by neutral red up-take (Hsu *et al.,* 2012). Furthermore, a combination of IL-1β, IFN-γ and TNF-α produced a 5-fold increase in apoptosis as assessed by flow cytometry (Cunningham *et al.,* 2005).

Of note, the contribution of iNOS and NO production in BRIN-BD11 cells to cytokine (and palmitate) toxicity remains unclear. Whilst numerous studies report an increase in nitrite levels in cytokine-treated BRIN-BD11 cells (Gao *et al.,* 2003; Welters *et al.,* 2004; Cunningham *et al.,* 2005; Hsu *et al.,* 2012), inhibition of iNOS activity by L-NAME failed to attenuate cytokine toxicity in one study, despite reducing cytokine-stimulated nitrite production (Hsu *et al.,* 2012), whereas Cunningham *et al.,* (2005) observed a 31% decrease in cytokine-induced apoptosis. Of note, in those studies reporting on the cytoprotective effects of palmitoleate (Welters *et al.,* 2004), alanine (Cunningham *et al.,* 2005), or novel plant extracts (Hsu *et al.,* 2012) against cytokine toxicity, all were suggested to occur by mechanisms independent to NO production and similarly in BRIN-BD11 cells, the iNOS inhibitor 1400W failed to attenuate a cytokine-induced decrease in insulin secretion, in contrast to effects in mouse islets in the same study (Michalska *et al.,* 2010). Collectively, this may suggest that BRIN-BD11 cells display a comparatively reduced sensitivity to cytokine-derived NO and nitrosative stress than some other beta cell line models, though studies in this regard are limited. Interestingly though, a dual inhibitor of iNOS and NADPH oxidase displayed a markedly enhanced protection against cytokine-induced apoptosis compared to iNOS inhibition alone, despite comparable reduction in nitrite levels (Cunningham *et al.,* 2005), suggesting a more important combination of NO and ROS together in mediating cell death under these conditions. Similar effects have been also been reported *in vivo*, whereby the dual iNOS inhibitor and peroxynitrite scavenger

guanidinoethyldisulphide decreased diabetes incidence in NOD mice and protected against cytokine toxicity in isolated islets (Suarez-Pinzon *et al.,* 2001).

In lipotoxicity models, although the contribution of ROS production is a well-established mediator of palmitate toxicity (Elsner *et al.,* 2011; Keane *et al.,* 2011), the role of NOS-derived NO remains unclear. However, the general consensus indicates NO-independency with most studies failing to detect an increase in palmitate-induced NO accumulation, including in BRIN-BD11 cells (Welters *et al.,* 2004; Cnop *et al.,* 2005). Interestingly though, Keane *et al.,* (2011) observed a significant increase in NO production in BRIN-BD11 cells treated with palmitate concentrations above 100µM, an effect attenuated by co-incubation with 100µM AA, in disagreement with other studies in these cells (Welters *et al.,* 2004).

3.2 Aims

The aim of this chapter is to establish a model system in BRIN-BD11 cells, characterising cell death in response to pro-inflammatory cytokines and the lipotoxic actions of palmitate, confirming validity of the model in context to previous studies and establishing appropriate conditions for further investigations. Specifically the aims are to:

- characterise the response of BRIN-BD11 cells to pro-inflammatory cytokines alone and in combination as a model of cytokine synergy and determine appropriate optimum conditions for further study.
- confirm the dose-dependent action of palmitate in BRIN-BD11 cells and determine appropriate optimum concentrations.
- investigate a dose-response relationship for the cytoprotective effects of the polyunsaturated FFA, arachidonic acid (AA).
- compare a range of assays for the measurement of cell viability and apoptosis for use in models of inflammatory cytokine and lipo- toxicity.

3.3 Methods

Cell viability was determined using MTT, neutral red and trypan blue vital dye exclusion assays, or apoptosis quantification by flow cytometry using the MUSE™ Annexin V and Dead Cell Assay (Chapter 2.4). As a model of cytokine-toxicity, BRIN-BD11 cells were treated with IL-1β (100U/mL), IFN-γ (20U/mL) and TNF-α (500U/mL), alone or in combination, with the Griess assay used for the quantification of nitrite in cell supernatants, as a measure of cytokine-induced iNOS expression. Additionally, cytokine-induced iNOS expression was determined by SDS-PAGE/Western blotting using cell lysates (500,000 cells) from cultures treated with the combination of all three cytokines for 6 or 24 hours. Lysates were separated on 10% resolving gels and, after transfer to PVDF, membranes were blocked in 5% goat serum (v/v TBS) and probed with a mouse monoclonal anti-iNOS (1:500 in TBS), subsequent steps were carried out as described (Chapter 2.8, using 1X TBS Tween®-20 Buffer for washing), with expression levels quantified relative to β-actin. For the study of palmitate-induced lipotoxicity, palmitate:BSA complexes were prepared at a ratio of 3.3:1, as described (Chapter 2.2) and diluted into 1% FBS-supplemented RPMI-1640 media to final concentrations ranging from 31.25µM-1000µM. Cytoprotective effects of AA in both models were also explored using AA:BSA complexes (molar ratio 3.3:1) at final concentrations ranging from 0.625µM-100µM in combination with palmitate or cytokines. In all treatments with fatty acids, control cultures were treated with 0.5% BSA (w/v) and 0.25% ethanol (v/v).

3.4 Results

To establish the effect of known cytotoxic mediators of pancreatic beta cell death and dysfunction in DM pathogenesis in BRIN-BD11, preliminary investigations into the effects of cytokines and the saturated fatty acid palmitate were established. Cytokines are well-known contributors to pancreatic beta cell dysfunction and loss in type 1 DM with evidence suggesting an overall pro-apoptotic effect by subjecting beta cells to cytokines activating intracellular pathways culminating in beta cell demise (Collier *et al.,* 2011)

Initial preliminary studies dosing a range of concentrations of IL-1β, IFN-γ and TNF-α (data not shown) established suitable concentration ranges to investigate cytokine synergy in the current model. BRIN-BD11 cells were then treated with concentrations of IL-1β (100U/mL), IFN-γ (20U/mL) and TNF-α (500U/mL), alone and in combination, for 24 and 48 hours, with cell viability initially assessed using the MTT assay (figure 3.1).

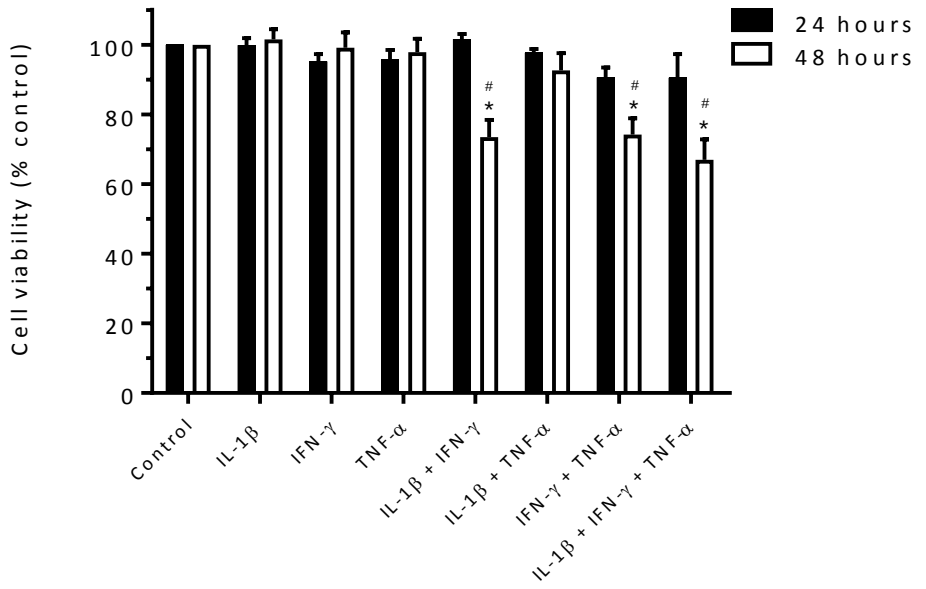

Figure 3.1. Cell viability in BRIN-BD11 cells exposed to cytokines assessed by MTT assay. Cells were treated with IL-1β (100U/mL), IFN-γ (20U/mL) and TNF-α (500U/mL), alone and in combination, for 24 and 48 hours. Cell viability was assessed by MTT assay, with values represented as mean (+/- SEM), n=3. *P<0.05 relative to time matched controls. #P<0.05 relative to corresponding treatment at 24 hours, as determined by two-way ANOVA and Bonferroni's post-test.

The cytotoxic effects of cytokines when treated in combination for 24 and 48 hours resulted in a decrease in cell viability when assayed by MTT. Treatment with IL-1β (100U/mL), IFN-γ (20U/mL) and TNF-α (500U/mL) alone for 24 and 48 hours showed no significant difference in cell viability (*P*>0.05). However, in combination, significant loss in cell viability was evident with IL-1β plus IFN-γ, IFN-γ plus TNF-α and all three cytokines together after 48 hours (*P*<0.05), supporting previous studies of synergism. However, treatment with the combination IL-1β plus TNF-α failed to increase cytotoxicity, suggesting the role of cytokine synergism was most potent following co-stimulatory activation of NF-κB and STAT1. The combination of IL-1β plus IFN-γ treatment after 24 hours resulted in no significant decrease in cell viability, however, after 48 hours, viability was significantly decreased to 73.5% (+/-5.0) (*P*<0.05). Analysis of IFN-γ plus TNF-α showed similar results to that of IL-1β plus IFN-γ with no significance at 24 hours but a significance at 48 hours 74.2% (+/-4.7) (*P*<0.05) and

treatment with IL-1β plus IFN-γ plus TNF-α for 48 hours witnessed maximal loss in cell viability, decreasing to 66.9% (+/-5.9).

To further confirm activation of known pathways mediating cytokine toxicity, BRIN-BD11 cells were also assayed for nitrite production as a hallmark of cytokine toxicity; this method can be used as an indirect analysis reflecting an increase in iNOS levels (figure 3.2).

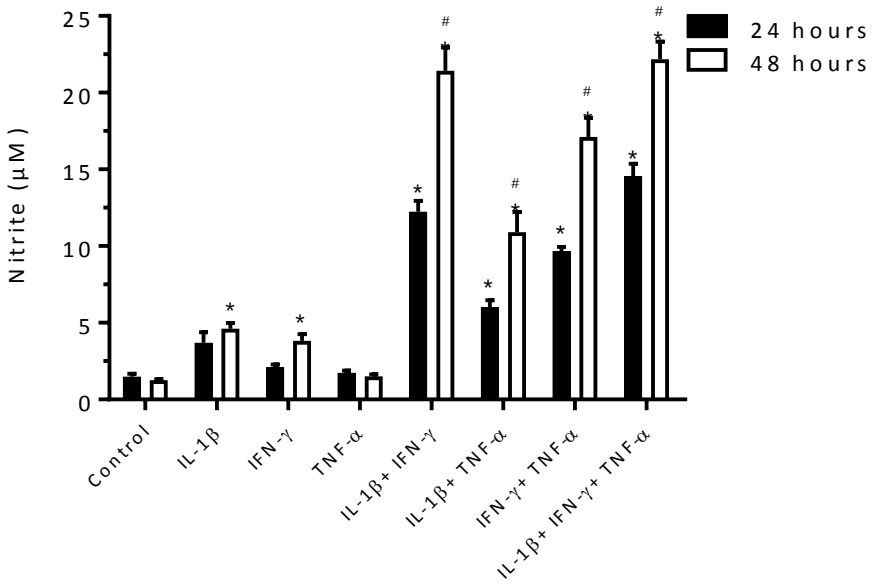

Figure 3.2. Nitrite production in BRIN-BD11 cells exposed to cytokines assessed by Griess assay. Cells were treated with IL-1β (100U/mL), IFN-γ (20U/mL) and TNF-α (500U/mL), alone and in combination, for 24 and 48 hours. Nitrite production was assessed by Griess reagent. Values are represented as mean (+/- SEM), n=4. *P<0.05 relative to time matched controls. #P<0.05 relative to corresponding treatment at 24 hours, as determined by two-way ANOVA and Bonferroni's post-test.

In general, an increase in nitrite production correlated with the decrease in cell viability (figure 3.1). All treatments after 24 and 48 hours showed a significant increase in nitrite production (*P*<0.05), except TNF-α alone, with the largest increase seen with the combination of all three cytokines after both 24 and 48 hours to 14.5µM (+/-0.8) and 22.2µM (+/-1.1), respectively, confirming cytokine synergism. Furthermore, confirmation that IL-1β and TNF-α acting through similar intracellular mechanisms, with IL-1β being the predominant activator of the NF-κB pathway, is shown by the combination treatment of IL-1β and TNF-α witnessing

the smallest increase in nitrite production of all cytokines in combination. Interestingly and in agreement with cell viability data (figure 3.1), treatment with IL-1β plus IFN-γ in combination produced similar results for 24 hours; 12.2µM (+/-0.7) and 48 hours; 21.4µM (+/-1.5) when compared to treatment with all three cytokines at both time points.

Given the lack of a significant effect of cytokine combinations on loss in cell viability over 24 hours and the modest decrease in viability at 48 hours, as assessed by the MTT assay, cell viability was further assessed under the same treatment conditions using the neutral red assay (figure 3.3).

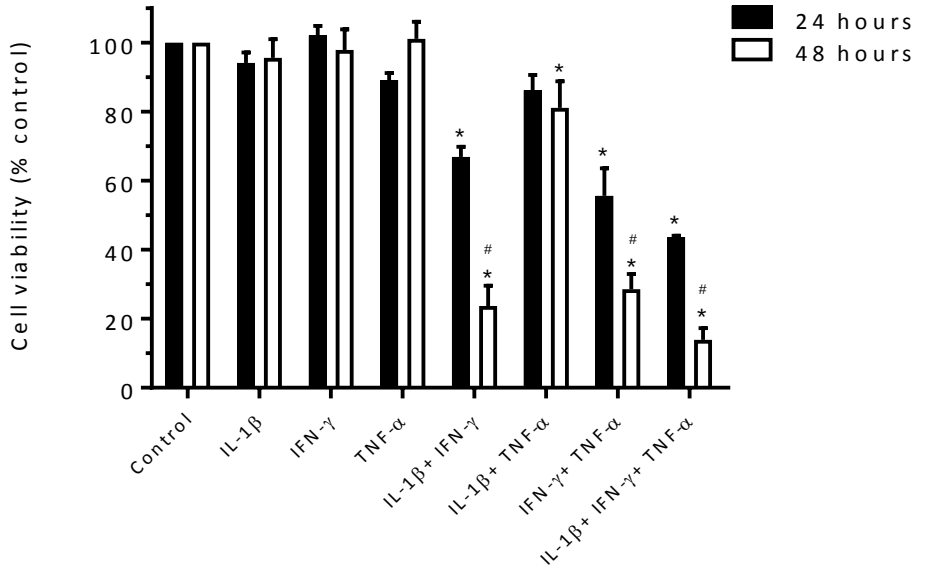

Figure 3.3. Cell viability in BRIN-BD11 cells exposed to cytokines assessed by neutral red assay. Cells were treated with IL-1β (100U/mL), IFN-γ (20U/mL) and TNF-α (500U/mL,) alone and in combination, for 24 and 48 hours. Cell viability was assessed by neutral red assay. Values are represented as mean (+/- SEM), n=3. *P<0.05 relative to time matched controls. #P<0.05 relative to corresponding treatment at 24 hours, as determined by two-way ANOVA and Bonferroni's post-test.

Treatment with IL-1β plus IFN-γ in combination resulted in a significant decrease in viability after 24 hours to 66.9% (+/-2.9) (P<0.05), in contrast to the MTT assay which showed no difference after 24 hours (P>0.05). At 48 hours cell viability continued to decrease to 23.7%

(+/-5.9) compared to control (P<0.05); an almost 80% reduction in cell viability compared to only 25% reduction when assayed by MTT. Treatment with IFN-γ plus TNF-α for 24 hours similarly showed a decrease to 55.7% (+/-8.0) when compared to control (P<0.05), again such a reduction in cell viability by 45% was not witnessed when assayed by MTT. Treatment with the combination of all three cytokines also showed a significant decrease in cell viability at both time points compared to control (P<0.05); at 24 hours there was a decrease in cell viability to 43.6% (+/-0.5), reducing to 13.9% (+/-3.4) at 48 hours. Comparing the data obtained between the two assays (figure 3.1 and 3.3), discrepancy in the results in terms of the extent of loss in cell viability could be accounted by differences in assay sensitivity in the current cell model, emphasising the need to use multiple methods, as reported by Fotakis and Timbrell, (2006).

To further confirm cytokine effects on BRIN-BD11 cell viability, total and viable cells were assayed manually using trypan blue vital dye exclusion, as an extension to the automated colorimetric MTT and neutral red assays. As IL-1β plus IFN-γ in combination showed the highest decrease in cell viability, this combination was used along with IL-1β and IFN-γ alone and the combination of all three cytokines (figure 3.4).

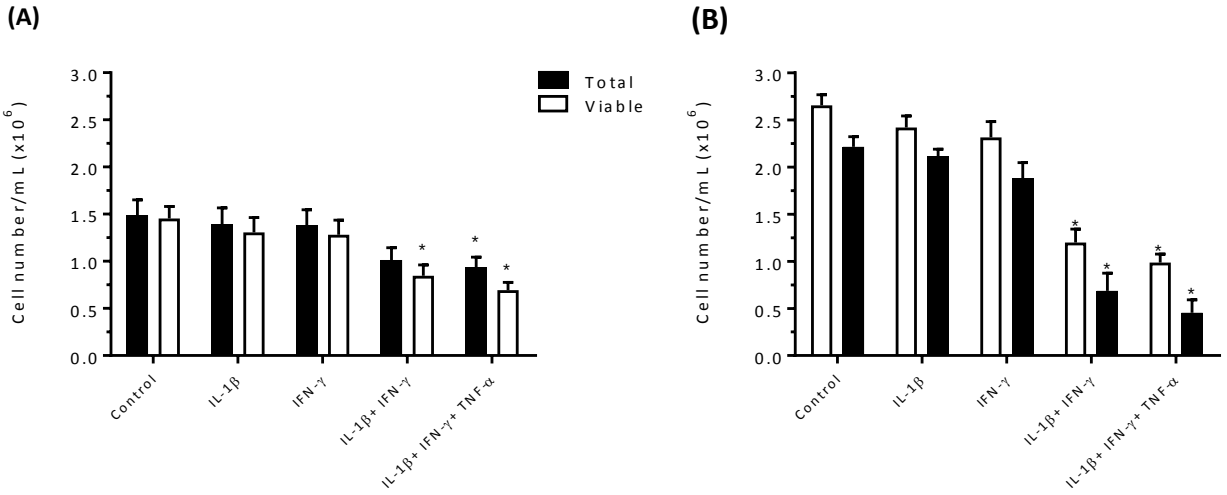

Figure 3.4. Total and viable cell number in BRIN-BD11 cells exposed to cytokines assessed by trypan blue vital dye exclusion. Cells were treated with IL-1β (100U/mL), IFN-γ (20U/mL) and TNF-α (500U/mL), alone and in combination, for (A) 24 hours and (B) 48 hours. Total and viable cell numbers were assessed by trypan blue vital dye exclusion. Values are represented as mean (+/- SEM), n=3. *P<0.05 relative to time matched controls as determined by two-way ANOVA and Bonferroni's post-test.

Treatment with IL-1β and IFN-γ alone for either 24 or 48 hours witnessed no significant decrease in either total or viable cell number compared to control (*P*>0.05) confirming results of previous assays. When treated with a combination of IL-1β plus IFN-γ viable cell number decreased from 1.45 x10^6 cells/mL (+/-0.13) to 0.85 x10^6 cells/mL (+/-0.11) (*P*<0.05) after 24 hours, with a decrease from 2.21 x10^6 cells/mL (+/-0.11) to 0.69 x10^6 cells/mL (+/-0.19) after 48 hours (P<0.05). Furthermore, the addition of TNF-α further decreased viable cell number to 0.69 x10^6 cells/mL (+/- 0.08)(*P*<0.05) after 24 hours and decreasing from 2.21 x10^6 cells/mL (+/-0.11) to 0.45 x10^6 cells/mL (+/-0.14) after 48 hours. These results therefore confirm findings from the neutral red data (figure 3.3), suggesting that the MTT assay (figure 3.1) under these conditions lacks sensitivity. Of note, as with previous assays, the inclusion of TNF-α leads to further decreases in viable cell number, though the effects are not significantly different to the combination of IL-1β plus IFN-γ, suggesting near maximal effects under these conditions.

Finally, to confirm the increase in nitrite production as a hallmark of iNOS expression, cells were treated with the combination of all three cytokines and assessed for iNOS expression by Western blotting after 6 and 24 hours (figure 3.5).

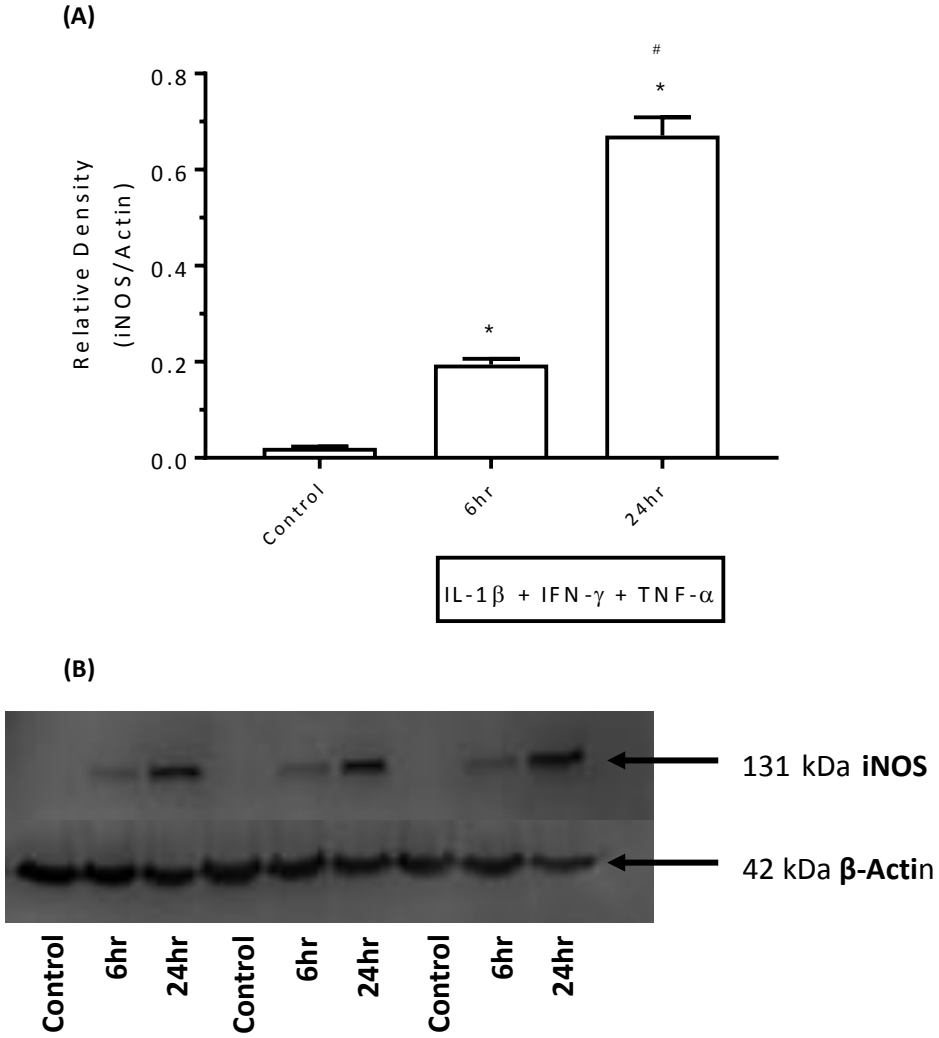

Figure 3.5. Relative density of iNOS/β-actin expression in BRIN-BD11 cells exposed to cytokines for 6 and 24 hours assessed by Western blotting. Cells were treated with IL-1β (100U/mL), IFN-γ (20U/mL) and TNF-α (500U/mL) for 6 and 24 hours and cells harvested for SDS-PAGE/Western blotting. Panel (A) represents relative density ratio of iNOS/β-actin Values are represented as mean (+/- SEM), n=3. *P<0.05 relative to control and #P<0.05 relative to 6 hour, as determined by one-way ANOVA and Tukey's post-test. Panel (B) represents the western blot from independent replicate lysates.

iNOS expression was significantly increased relative to control at after both 6 and 24 hour incubation, such that iNOS expression was increased 10-fold compared to control after

6 hours, with a further 3.5-fold significant increase from 6 to 24 hours (P<0.05). It is clear therefore that whilst iNOS expression is detectable after 6 hours, a further increase in expression is observed after 24 hours.

Following characterisation of cytokine-induced beta cell death as an *in vitro* models of type 1 DM, BRIN-BD11 cells were further investigated to establish their response to palmitate (C16:0), a long-chain saturated fatty acid thought to be a major contributor to lipotoxicity in type 2 DM. BRIN-BD11 cells were treated with increasing concentrations of palmitate from 31.25µM to 1000µM, resulting in a dose dependent effect on cell viability, as assessed by MTT assay (figure 3.6).

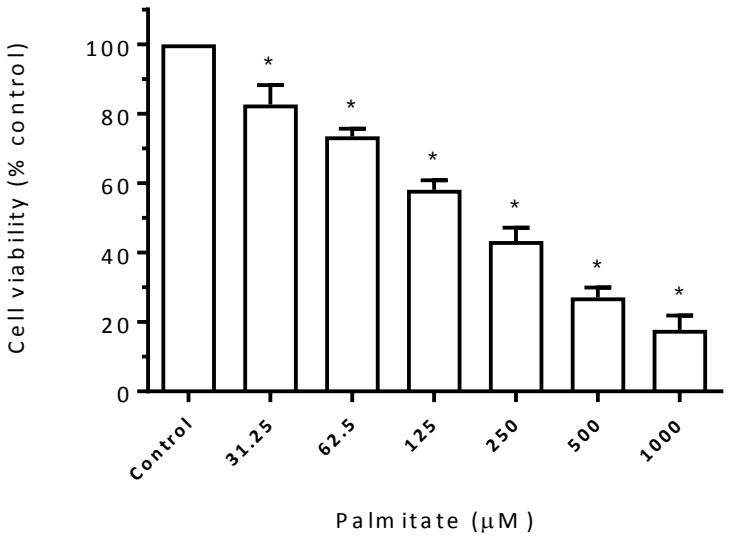

Figure 3.6. Cell viability in BRIN-BD11 cells exposed to palmitate assessed by MTT assay. Cells were treated with increasing concentrations of palmitate from 31.25µM to 1000µM for 24 hours and cell viability was assessed by MTT assay. Values are represented as mean (+/- SEM), n=3. *P<0.05 relative to control as determined by one-way ANOVA and Tukey's post-test.

All concentrations of palmitate resulted in a significant decrease in cell viability, from 31.25µM – 82.6% (+/-5.6) to 1000µM – 17.7% (+/-4.2) (P<0.05) compared to control. At a concentration of 250µM cell viability was reduced to 43.3% (+/-3.9), decreasing to 27.1% (+/-

2.9) with 500µM, yielding the largest decrease in cell viability between treatment groups of ~16%. Given the discrepancy between the MTT assay data and other assays obtained in the cytokine model, the neutral red assay was used to assess cell membrane integrity in response to the same palmitate dose range (figure 3.7)

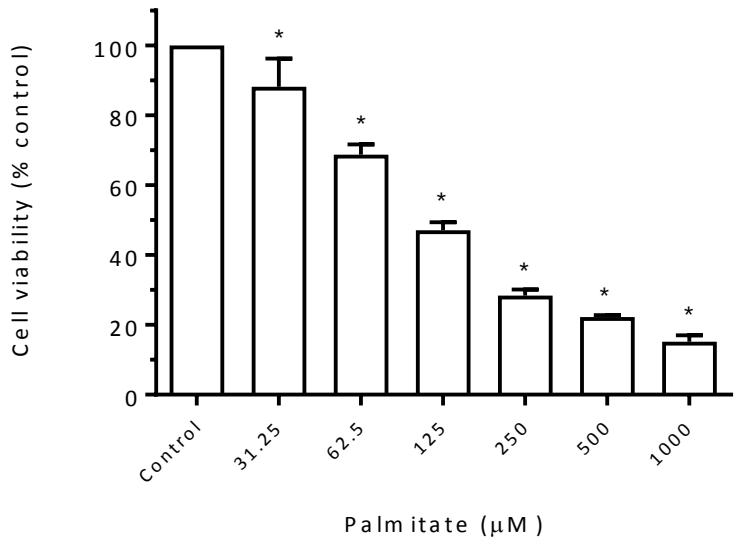

Figure 3.7. Cell viability in BRIN-BD11 cells exposed to palmitate assessed neutral red assay. Cells were treated with increasing concentrations of palmitate from 31.25µM to 1000µM for 24 hours and cell viability was assessed by neutral red assay. Values are represented as mean (+/- SEM), n=3. *P<0.05 relative to control as determined by one-way ANOVA and Tukey's post-test.

A similar dose-dependent response was observed across all concentrations of palmitate, confirming data from the MTT assay. Treatment with 250µM and 500µM palmitate witnessed a decrease in cell viability to 28.4% (+/-1.7) and 22.2% (+/-0.6), respectively, compared to control (P<0.05). However, unlike the data from the MTT assay, the highest decrease in cell viability between treatments was from 62.5µM to 125µM, and 125µM to 250µM, both witnessing ~20% loss in cell viability, again this may be reflective of a higher sensitivity of the neutral red assay. However, possibly owing to treatment of cells with palmitate requiring a reduction in serum composition of the media from 10% to 1% (to account for the levels of BSA in FBS, ensuring the palmitate:BSA complex ratio was maintained

at 3.3:1), this appeared to affect the ability of the cells to remain adhered to the wells following incubation in neutral red, causing potential loss of cells during the washing and solubilisation steps. As such, this may account for the apparent stunting of the dose response at concentrations exceeding 250µM, whereby cell viability decreased from 28.4% (+/-1.7) to 22.2% (+/-0.6) at 500µM, compared to ~2-fold decrease in the MTT assay across the same doubling of the palmitate concentration.

The lipotoxic response in BRIN-BD11 cells treated with palmitate was then further investigated across the range 62.5µM to 500µM and assessed for total and viable cell number by trypan blue vital dye exclusion (figure 3.8).

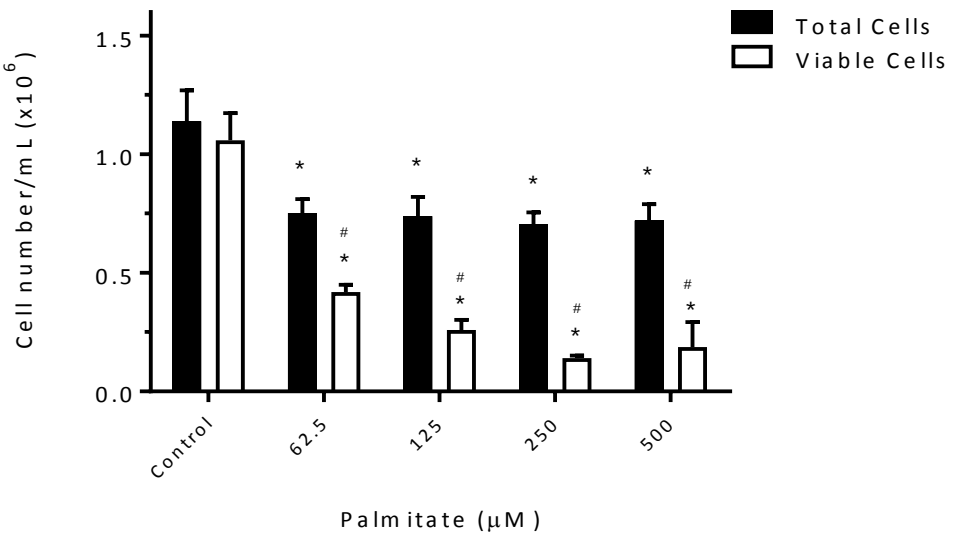

Figure 3.8. Total and viable cell number in BRIN-BD11 cells exposed to palmitate assessed by trypan blue vital dye exclusion. Cells were treated with increasing concentrations of palmitate from 62.5µM to 1000µM for 24 hours with total and viable cell numbers assessed by trypan blue vital dye exclusion. Values are represented as mean (+/- SEM), n=3. *P<0.05 relative to corresponding control. #P<0.05 relative to corresponding total cells as determined by two-way ANOVA and Bonferroni's post-test.

Increasing concentrations of palmitate resulted in a significant decrease in both total and viable cell number for all treatments compared to control (*P*<0.05). Treatment with 250µM observed the highest decrease in both total and viable cells, with viable cells reducing from 1.06 x10^6 cells/mL (+/- 0.11) in control to 0.140 x10^6 cells/mL (+/- 0.01) (*P*<0.05), ~9-fold

decrease, and overall supports data from the MTT and neutral red assays showing a dose-dependent decrease in cell viability in BRIN-BD11 cells treated with palmitate.

To confirm effect of palmitate treatment in BRIN-BD11 cells in terms of apoptosis induction, the percentage of Annexin V positive cells thereby displaying PS externalisation in response to 250μM palmitate was assessed by flow cytometry (figure 3.9). Additionally, any effect on the cells of the necessary reduction in FBS composition of the media from 10% to 1% was also compared.

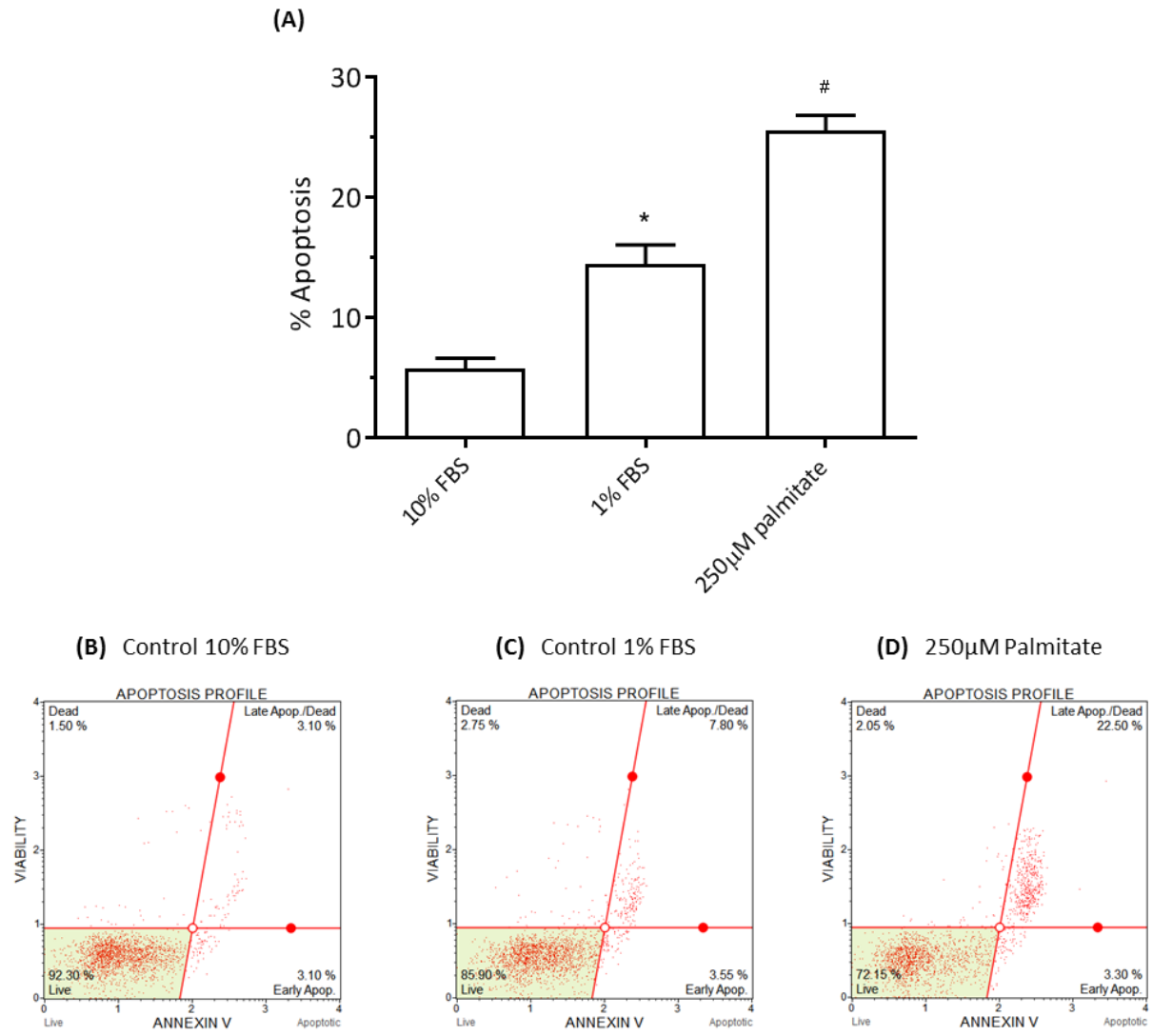

Figure 3.9. **Comparative analysis of BRIN-BD11 cells cultured in 10% and 1% FBS-supplemented media and palmitate assessed by Annexin V & Dead Cell assay.** Cells were treated for 24 hours +/- 250µM palmitate in 1% FBS-supplemented media, or 10% FBS-supplemented complete media and the total apoptosis profile (A) was assessed by flow cytometry using the Muse™ Annexin & Dead Cell kit. Panels (B) to (D) show representative apoptosis profiles of cells under each treatment condition. Values in panel (A) are represented as mean percentage apoptosis (+/- SEM), n=3. *P<0.05 relative to control. #P<0.05 relative to 1% FBS and determined by one-way ANOVA and Tukey's post-test.

The apoptosis profile for cells cultured in 10% and 1% FBS-supplemented media shows basal apoptosis rates for BRIN-BD11 cells of 5.7% (+/-0.9) and 14.5% (+/-1.6), respectively, suggesting a significant increase in response to serum reduction. However treatment with 250µM palmitate shows a further increase in total apoptosis from the 1% FBS-supplemented control from 14.5% (+/-1.6) to 25.6% (+/-1.3) (P<0.05). Comparison of panel (B) and (C) shows

a modest increase in late apoptosis/dead (upper right quadrant), from 3.1% to 7.8%, respectively, whereas comparison of panel (C) to (D) shows an increase in late apoptosis/ dead from 7.8% to 22.5%, ~3-fold increase. Between panels (B), (C) and (D), there is a clear increase in percentage late apoptosis/dead as seen in the upper right quadrant, which shows a clear increase in apoptosis induction due to the cytotoxic effects of palmitate compared to control.

To conclude, preliminary findings of palmitate treatment in BRIN-BD11 cells suggests that the data presented from MTT, neutral red, trypan blue vital dye exclusion and Annexin & Dead Cell assays supports evidence from others that BRIN-BD11 cells respond to palmitate in a dose-dependent manner (Welters *et al.,* 2004; Dhayal and Morgan 2008; Keane *et al.,* 2011). Due to the inherent difficulties of treatment of cells in media supplemented with 1% serum in processing of the neutral red assay, this assay was not used further in these models.

Whilst the current data (and others) support the lipotoxic action of palmitate in BRIN-BD11 cells, it has also established that mono- and poly- unsaturated species such as palmitoleate (C16:1) or oleate (C18:1) are well tolerated and can ameliorate the cytotoxic effects observed in response to saturated fatty acids (Welters *et al.,* 2004; Diakogiannaki *et al.,* 2007; Keane *et al.,* 2011). The main focus of this thesis is the cytoprotective effects of AA-derived eicosanoids (specifically EETs) against palmitate and cytokine toxicity (subsequent chapters). Therefore, the effects of AA in co-incubation with palmitate was first confirmed as part of these preliminary investigations by treating BRIN-BD11 cells with increasing concentrations of AA against fixed concentrations of 250µM and 500µM palmitate (figure 3.10).

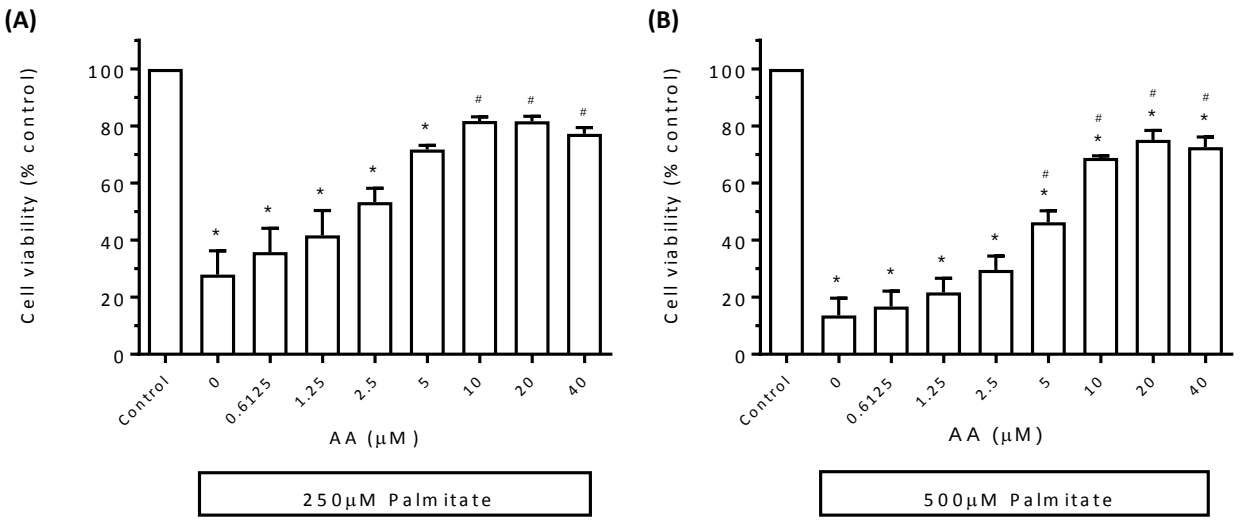

Figure 3.10. Cell viability in BRIN-BD11 cells exposed to palmitate against increasing concentrations of AA assessed by MTT assay. Cells were treated with increasing concentrations of AA (0.6125μM to 40μM) against a fixed dose of either 250μM (A) or 500μM (B) palmitate for 24 hours. Cell viability was assessed by MTT assay, with results represented as mean (+/- SEM), n=3. *P<0.05 relative to control and #P<0.05 relative to palmitate alone as determined by one-way ANOVA and Tukey's post-test.

Treatment with 250μM palmitate in combination with increasing concentrations of AA dose-dependently increased cell viability with respect to palmitate treatment alone, increasing from 27.9% (+/- 8.3) with 0.6125μM AA to 71.7% (+/- 1.5) with 5μM AA, though this remained significantly lower than control. Co-incubation with concentrations of AA at 10μM and above resulted in no significant difference between treatments and control (P>0.05), these were also the only concentrations of AA where significant protection against palmitate toxicity was observed (P<0.05 vs. palmitate alone), despite the trend in increased viability observed in co-incubation with 0.625-5μM AA. Similarly, a 2-fold increase in the concentration of palmitate to 500μM in co-incubation with the same range of AA concentrations, resulted in a dose-dependent increase in cell viability, however whilst concentrations of AA above 5μM significantly increased cell viability compared to palmitate treatment alone, all combined treatment groups resulted in a cell viability that remained significantly lower than untreated control (P<0.05). Whilst a clear dose-dependent effect of AA was observed, the highest

maximum effect of AA was achieved with a concentration of 10µM therefore, to further confirm these effects, cell viability was assessed using the MTT assay with a palmitate dose response against a fixed concentration of 10µM AA (figure 3.11).

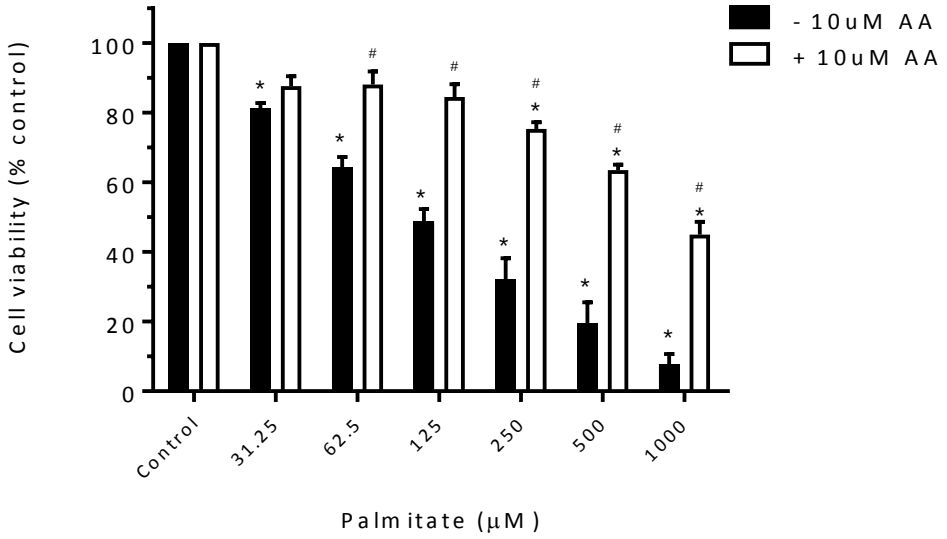

Figure 3.11. Cell viability in BRIN-BD11 cells exposed to increasing concentrations of palmitate +/- 10µM AA assessed by MTT assay. Cells were treated with increasing concentrations of palmitate (31.25µM to 1000µM) +/- 10µM AA for 24 hours. Cell viability was assessed by MTT assay with results expressed as mean cell viability (+/- SEM), n=3. *P<0.05 relative to corresponding control and #P<0.05 relative to corresponding palmitate treatment group as determined by two-way ANOVA and Bonferroni's post-test.

Treatment with 10µM AA in co-incubation with increasing concentrations of palmitate supports the previous data showing a dose-dependent decrease in cell viability in treatment with palmitate alone, with all concentrations significantly decreasing cell viability compared to control (*P*<0.05). Co-incubation with 10µM AA resulted in a significant increase in cell viability against all palmitate concentrations from 62.5µM to 1000µM compared to corresponding palmitate treatment alone (*P*<0.05). Interestingly, treatment with 10µM AA also significantly increased cell viability in co-incubation with 1000µM palmitate from 7.8% (+/-2.9) to 45.1% (+/-3.6) (*P*<0.05), though with all palmitate concentrations above 250µM in

co-incubation with 10µM AA cell viability remained significantly lower than untreated controls suggesting partial protection (*P*>0.05).

The data collected with the MTT assay in cells co-incubated with palmitate and AA showed that regardless of higher AA concentrations cell viability did not exceed ~80% therefore, and as with previous data, the trypan blue vital dye exclusion assay was used to assess total and viable numbers in cells treated with palmitate in co-incubation with 1µM, 5µM and 10µM AA (figure 3.12); this, and all subsequent data with palmitate was collected using a fixed concentration of 250µM.

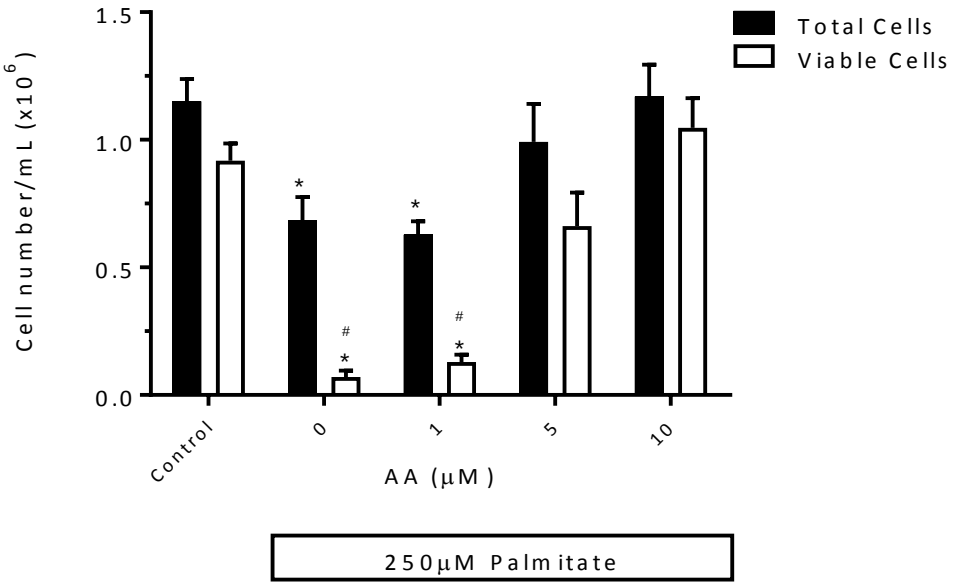

Figure 3.12. Total and viable cell number in BRIN-BD11 cells exposed to 250µM palmitate co-incubated with 1µM, 5µM and 10µM AA assessed by trypan blue vital dye exclusion. Cells were treated with 250µM palmitate co-incubated with either 1µM, 5µM or 10µM AA for 24 hours before total and viable cell numbers were determined using trypan blue vital dye exclusion assay. Values are represented as mean (+/- SEM), n=3. *P<0.05 relative to control. #P<0.05 relative to total cells as determined by two-way ANOVA and Bonferroni's post-test.

Treatment with 250µM palmitate significantly decreased both total and viable cells compared to control from 1.15 x10^6 cells/mL (+/-0.09) to 0.68 x10^6 cells/mL (+/-0.09), roughly

2-fold, and 0.92 x10^6 cells/mL (+/-0.07) to 0.07 x 10^6 cells/mL (+/-0.03) cells/mL, roughly 9-fold (*P*<0.05), respectively. Treatment with 250µM palmitate in the presence of 1µM AA produced a similar, significant decrease in total and viable cells compared to control, with 1µM AA failing to protect against palmitate toxicity (*P*>0.05). Increasing the concentration of AA from 1µM to 5µM resulted in a significant increase in viable cell number from 0.13 x10^6 cells/mL (+/- 0.03) to 0.66 x10^6 cells/mL (+/-0.13), respectively, an increase of ~5-fold (*P*<0.05). Similar observations were seen in increasing the concentration of AA from 5µM to 10µM with viable cells increasing from 0.66 x 10^6 cells/mL (+/-0.13) to 1.05 x10^6 cells/mL (+/-0.12) (*P*<0.05), a further increase of ~1.6-fold in viable cells.

Comparing total and viable cells treated with 250µM palmitate in the presence of 10µM AA respective to untreated controls, there is no significant difference (*P*>0.05). However, there is a modest increase in viable cell number from 0.92 x10^6 cells/mL (+/- 0.07) to 1.05 x10^6 cells/mL (+/- 0.12), in contrast to the maximum cell viability of ~80% observed in the MTT assay (potentially indicative of limitations of the MTT assay in this context) and perhaps suggesting a protective effect of AA against the effects of the lower serum levels in this model. To further confirm the protective effects of AA against palmitate toxicity, the Annexin V & Dead Cell assay was used to determine the percentage of cells undergoing apoptosis (figure 3.13).

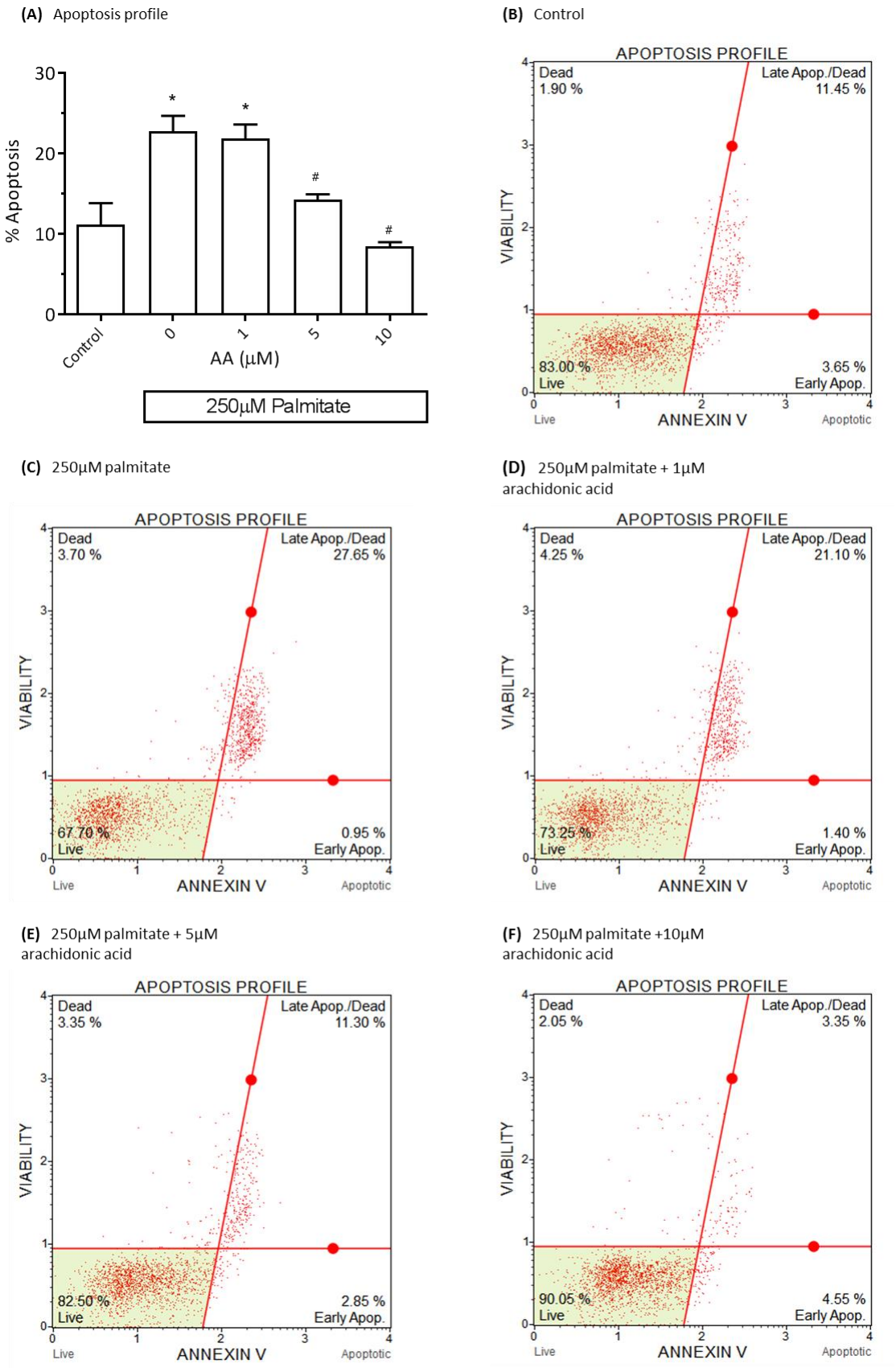

Figure 3.13. Comparative analysis of BRIN-BD11 cells exposed to 250μM palmitate co-incubated with 1μM, 5μM and 10μM AA assessed by Annexin V & Dead Cell assay. Cells were treated for 24 hours with 250μM palmitate in combination with increasing concentrations of AA (1μM, 5μM or 10μM) and the total apoptosis profile (A) was assessed by flow cytometry using the Muse™ Annexin V & Dead Cell kit. Panels (B) to (F) show representative apoptosis profiles of cells under each treatment condition. Values in panel A are represented as mean percentage apoptosis (+/- SEM), n=3. *P<0.05 relative to control. #P<0.05 relative to palmitate alone as determined by one-way ANOVA and Tukey's post-test.

Confirmation of the protective effects of AA are evident from the apoptosis profiles with 5µM and 10µM AA in the presence of 250µM palmitate producing a significant decrease in percentage apoptosis from 22.8% (+/-1.9) with 250µM palmitate alone to 14.3% (+/-0.7) and 8.4% (+/-0.6) (P<0.05), respectively; to values not significantly different from control (P>0.05). As with previous flow cytometry representative apoptosis profiles (figure 3.9), there is a clear population of apoptotic cells within the upper right quadrant showing basal levels of apoptosis (figure 3.13 panel: B, upper right quadrant). Increasing clusters of apoptotic cells were observed when treated with 250µM palmitate (panel: C, upper right quadrant) and reduced with increasing concentrations of AA (panels: D and E, upper right quadrant) to below basal levels when co-incubated with 10µM AA (panel: F, upper right quadrant). This corresponds with the modest increase in viable cell number under the same conditions (figure 3.12), suggesting that AA can compensate for the increase in basal apoptosis exerted by using media supplemented with 1% FBS in these models (figure 3.9). The final preliminary investigation into the protective effects of AA therefore determined the total and viable cell numbers in BRIN-BD11 cells treated under these conditions with 10µM AA alone, alongside co-incubation with 250µM palmitate (figure 3.14).

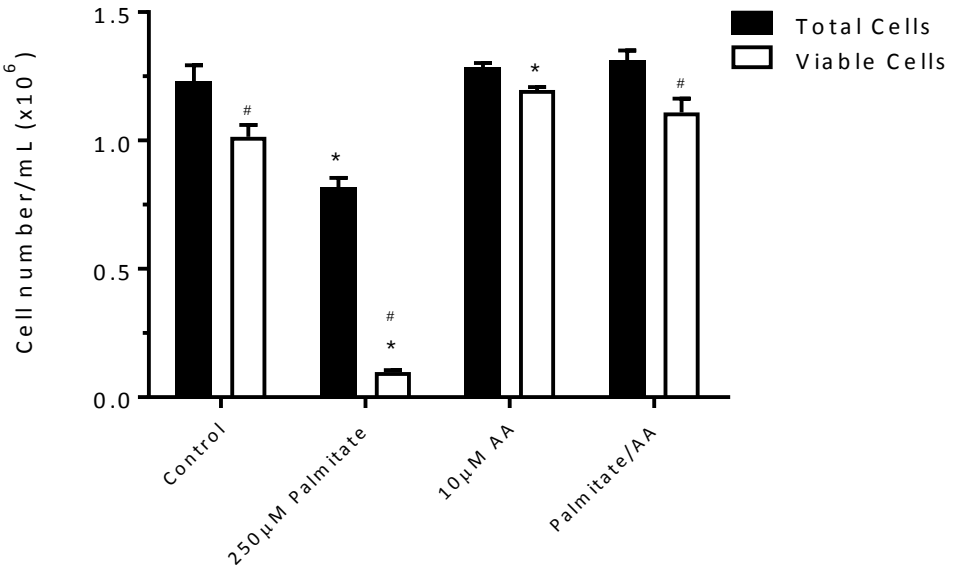

Figure 3.14. Total and viable cell number in BRIN-BD11 cells exposed to 250µM palmitate and 10µM AA alone and in co-incubation assessed by trypan blue vital dye exclusion. Cells were treated with 250µM palmitate and 10µM AA individually or in combination for 24 hours before total and viable cell numbers were assessed by trypan blue vital dye exclusion. Values are represented as mean (+/- SEM), n=3. *P<0.05 relative to corresponding control. #P<0.05 relative to total cells as determined by two-way ANOVA and Bonferroni's post-test.

Treatment with 10µM AA alone witnessed no increase in total cell number compared to control conditions (*P*>0.05) however, there was a significant increase in viable cell number from 1.01 x10^6 cells/mL (+/-0.05) to 1.20 x10^6 cells/mL (+/-0.01), ~1.2-fold increase (*P*<0.05), supporting the suggestion that AA can protect cells against lower serum levels under these conditions. Additionally this result also confirms, as previously seen, that AA protects against palmitate toxicity with no significant difference between the combined treatment group and the control, suggesting that AA completely ameliorates palmitate toxicity, with over a 10-fold increase in viable cell number.

Further to the protective effects of AA in an *in vitro* model of type 2 DM, protective effects of AA were then investigated in the type 1 DM model of cytokine toxicity in BRIN-BD11 cells. Preliminary investigations into any dose-dependent protective effects of AA against

cytokine-induced beta cell death was assessed by MTT assay against the combination of IL-1β (100U/mL) plus IFN-γ (20U/mL), or with the inclusion of TNF-α (500U/mL) for 24 and 48 hours, with nitrite levels also determined using Griess assay (figure 3.15 A-D). Additionally, effects of AA on the combination of all three cytokines, representing the most patho-physiologically relevant combination, were also assessed by trypan blue vital dye exclusion assay in combination with 80μM AA. Due to the additional contribution of BSA from media supplemented with 10% FBS, for the purpose of this data all treatments were in 1% FBS-supplemented media, in accordance with the previous model whereby AA is delivered to cells complexed to BSA, maintaining the molar ratio of 3.3:1.

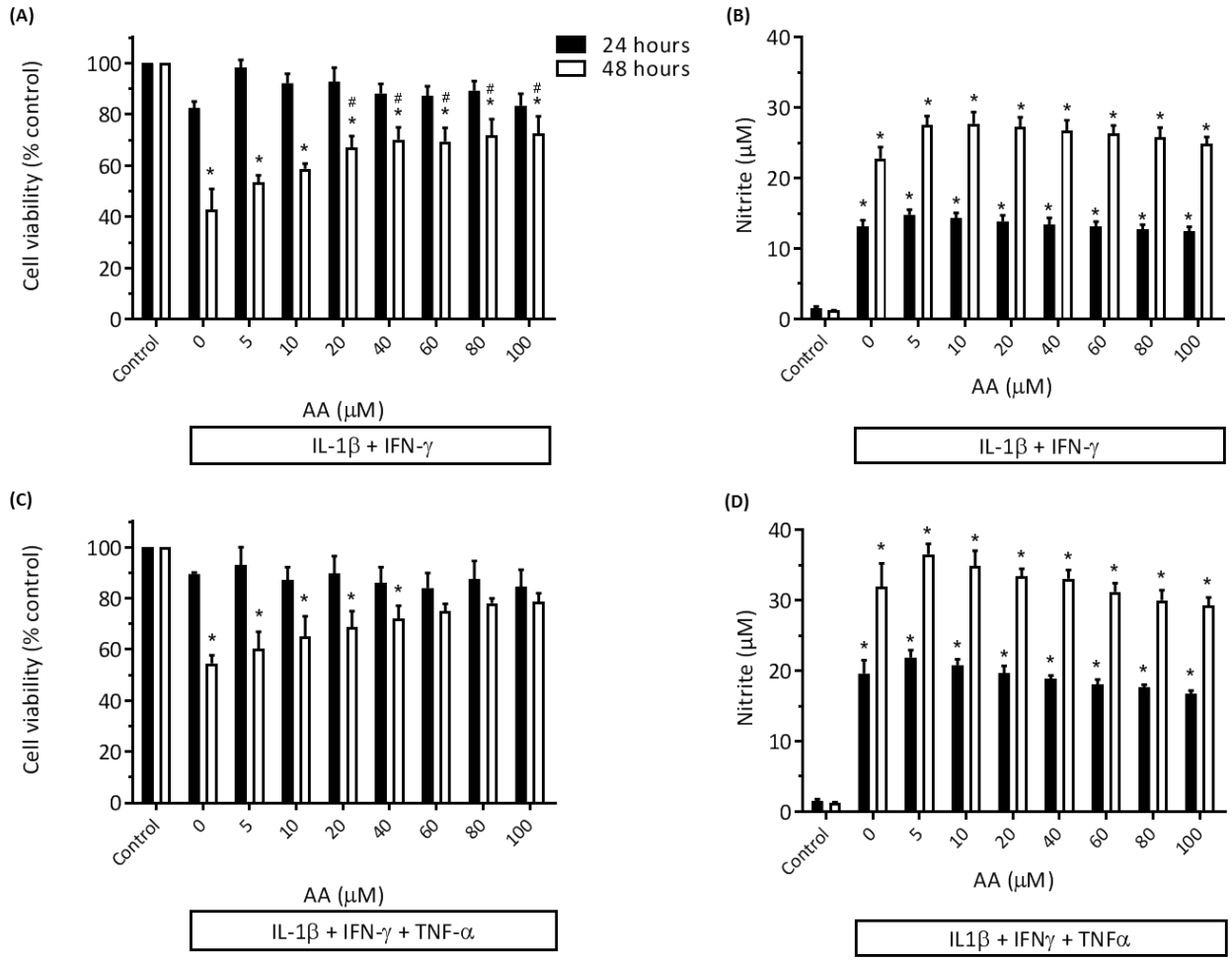

Figure 3.15 Effects of AA on cytokine-induced loss in cell viability and nitrite production assess by MTT and Griess assay. Cells were treated with a combination of IL-1β (100U/mL) and IFN-γ (20U/mL) with or without TNF-α (500U/mL) in co-incubation with AA at increasing concentrations for 24 or 48 hours. Cell viability was assessed by MTT assay (panels A and C), with nitrite levels quantified using Griess reagent (panels B and D). Values are represented as mean (+/- SEM), n=3. *P<0.05 relative to corresponding control. #P<0.05 relative to corresponding cytokines alone as determined by two-way ANOVA and Bonferroni's post-test.

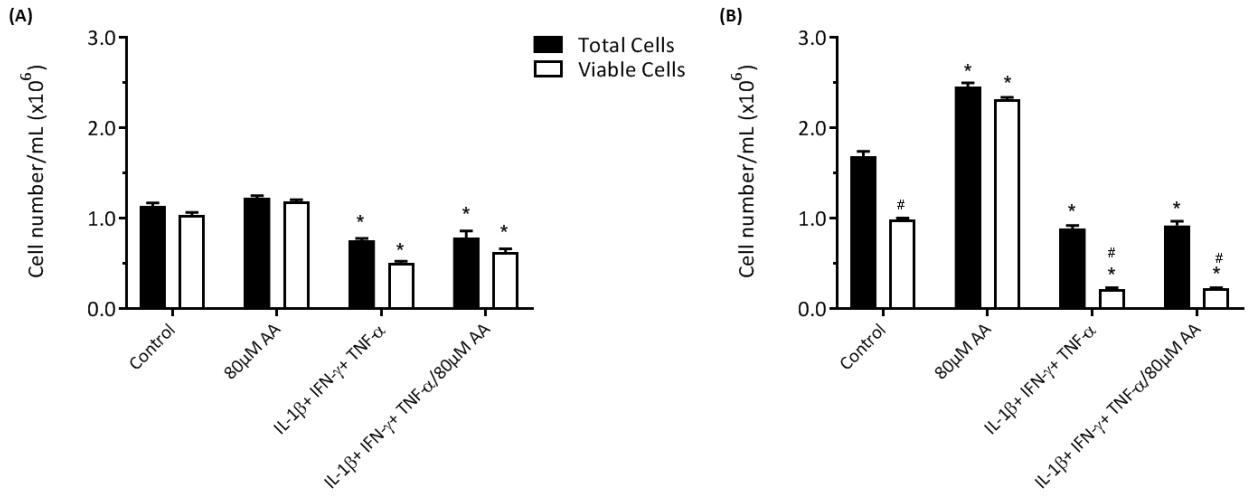

Figure 3.16 Effects of AA on cytokine-induced BRIN-BD11 cell death assessed by trypan blue vital dye exclusion. Cells were treated with cytokines in combination of IL-1β (100U/mL) and IFN-γ (20U/mL) and TNF-α (500U/mL) in co-incubation with 80μMAA 24 (A) or 48 (B) hours. Total and viable cell numbers were assessed by trypan blue vital dye exclusion. Values are represented as mean (+/- SEM), n=3. *P<0.05 relative to control. #P<0.05 relative to total cells as determined by two-way ANOVA and Bonferroni's post-test.

As with previous data, minimal loss in cell viability was observed in treatment with cytokines over 24 hours, as assessed by MTT assay, with a significant decrease observed after 48 hours. Increasing concentrations of AA in combination with IL-1β plus IFN-γ over 48 hours witnessed a significant increase in cell viability from 42.9% (+/8.1) with cytokines alone to 70.2% (+/-4.7) with 40μM AA (*P*<0.05). No increase in protection was observed upon increasing concentrations of AA further, suggesting that higher concentrations of AA may be needed to ameliorate cytokine-induced beta cell death, as compared to the effects seen at 10μM AA with palmitate. Though similar to the palmitate model, AA effects seem to plateau at 70-80% cell viability (figure 3.15), suggesting a limiting factor that prevents any further increase in the observed cell viability. In contrast, effects of AA on cell viability in treatment with combined IL-1β and IFN-γ were not mirrored by a decrease in nitrite accumulation, suggesting any effects are NO-independent. However, with inclusion of TNF-α, whilst producing comparable overall effects on loss in cell viability with combined IL-1β and IFN-γ,

AA failed to ameliorate the cytotoxic effects of all three cytokines, though an overall trend in increasing cell viability up to 70-80% was also noted (figure 3.15, panel: C), which again may reflect limitations of the MTT assay in this model. However, when total and viable cell numbers (figure 3.16) were determined by trypan blue vital dye exclusion, the combination of all three cytokines alone showed a significant decrease in cell populations compared to control ($P<0.05$), an effect not reversed in the presence of 80μM AA ($P>0.05$ compared to cytokine treatment alone).

The fact that 80μM AA failed to ameliorate cytokine-induced cytotoxicity likely reflects distinct modes of action dependent upon the nature of the apoptotic stimuli between the type 1 and type 2 models established. Interestingly, after 48 hours there was a significant increase in total and viable cell numbers with 80μM AA treatment alone compared to control ($P<0.05$), increasing from 1.69 $x10^6$ cells/mL (+/-0.06) and 0.98 $x10^6$ cells/mL (+/-0.02) to 2.46 $x10^6$ cells/mL (+/-0.04) and 2.31 $x10^6$ cells/mL (+/-0.03) ($P<0.05$), respectively. Again, this likely reflects protection against serum withdrawal under these culture conditions and/or a pro-proliferative effect of AA at this higher concentration. This therefore may explain the observed protective effect noted with IL-1β and IFN-γ in combination with 20μM AA and above, when assessed by MTT assay, suggesting an overall lack of effect of AA against cytokine toxicity in the current model.

3.5 Discussion

The aims of this chapter were to characterise the response of BRIN-BD11 cells to pro-inflammatory cytokines and the saturated fatty acid palmitate (C16:0), establishing model systems reflecting cytokine toxicity associated with the development of type 1 DM and lipotoxicity in the pathogenesis of type 2 DM. Additionally, this chapter also established the cytoprotective effects of AA in these models, in agreement with previous studies in this cell line (Keane *et al.,* 2011), as well as comparative differences in methods used to assess cell viability. BRIN-BD11 cells were selected for this study owing to their favourable growth characteristics, long-term stability in culture and expression of appropriate cell-type markers and characteristics of beta cell function (McClenaghan *et al.,* 1996).

Cell viability obtained following treatment of BRIN-BD11 cells with IL-1β (100U/mL), IFN-γ (20U/mL) and TNF-α (500U/mL) alone resulted in no significant decrease in cell viability when assessed by MTT and neutral red assay, or by trypan blue vital dye exclusion for total and viable cells, suggesting singular cytokine treatment has minimal effect on cell viability under these conditions. Whilst parental RINm5F cells have been shown to respond to singular treatment with IL-1β or IFN-γ (Ankarcrona *et al.,* 1994; Holohan *et al.,* 2008), the concentrations used were considerably higher than those in the current study, with effects of IL-1β apparent only at concentrations of 180-540U/mL (Holohan *et al.,* 2008), and others have reported minimal effects of these cytokine treatments alone in BRIN-BD11 cells (Hsu *et al.,* 2012). In agreement with others, treatment of BRIN-BD11 cells with cytokines in combination markedly enhanced the cytotoxic response, with loss in cell viability witnessed over 24-48 hours incubation across all assay formats used, supporting cytokine synergy (Rabinovitch and Suarez-Pinzon, 1998; Chen *et al.,* 2000; Eizirik and Mandrup-Poulsen, 2001; Hsu *et al.,* 2012).

Cytokine synergism was most evident in treatment combinations with either IL-1β or TNF-α plus IFN-γ, or the combination of all three cytokines, with the combination of IL-1β plus TNF-α producing a markedly reduced effect on loss in cell viability in both the MTT and neutral red assays. Minimal synergism with this cytokine combination compared to when either cytokine was combined with IFN-γ is likely due to TNF-α receptor binding activating similar pathways to IL-1β; particularly downstream activation of NF-κB. Saldeen *et al.,* (2001) showed that in rat insulinoma cells TNF-α signalling preferentially leads to phosphorylation and activation of JNK and p38 MAPK, similar to IL-1β signalling, whereas in contrast, IFN-γ receptor binding leads to the activation of STAT-1. Concomitant activation of STAT-1 and NF-κB then coordinate changes in gene expression associated with orchestrated beta cell death in part mediated via an enhanced cellular stress response, associated with increased oxidative and nitrosative stress (Cnop *et al.,* 2005). Maximum iNOS expression and nitrite production are achieved under these conditions, as shown by the highest nitrite levels recorded with combined cytokine treatments, with the exception of IL-1β plus TNF-α, in the current model. Additionally a reduction in beta cell defence capacity is also thought to contribute to cytokine toxicity, with IFN-γ shown to synergise with IL-1β in the induction of ER stress via downregulation of the ER chaperone BiP (Pirot *et al.,* 2006). Synergistic action of TNF-α plus IFN-γ in the absence of IL-1β, as observed in the current study, have also been reported by others (Chang *et al.,* 2004), effects suggested to be mediated by activation of IRF-1 downstream of IFN-γ/STAT-1 sensitising MIN6 and islet beta cells to TNF-α (Suk *et al.,* 2001).

In the current model, nitrite levels and increased iNOS expression correlated with the degree of cytokine-induced loss in cell viability, with highest nitrite levels observed when cytokines were used in combination. Although cytokine-induced iNOS expression and

production of the NO radical are considered a classical feature of cytokine action in pancreatic beta cells, with exogenous NO donors (in part) mimicking cytokine toxicity (Eizirik *et al.,* 1996; Oyadomari *et al.,* 2001; Cardozo *et al.,* 2005), inhibition of iNOS only partially protects against cytokine-induced beta cell death *in vitro* and may only delay onset of DM in *in vivo* models (Lindsay *et al.,* 1995). Establishing the NO-dependency of cytokine toxicity was not a focus of the data presented here however, Hsu *et al.,* (2012) have shown that the iNOS inhibitor L-NAME failed to attenuate cytokine toxicity in BRIN-BD11, in agreement with unpublished data in our group (Cunningham and Watson, unpublished observations) and others on the lack of a protective effect of iNOS inhibition against cytokine-induced loss in insulin secretion in these cells (Michalska *et al.,* 2010).

The current data also highlights important differences in sensitivity between assays used to measure the cytotoxic response of the cells, as observed in the comparison between the MTT and neutral red assay. The use of the MTT assay solely to determine cell viability, like other assays, is limited by its mode of action; MTT data direct correlate with cell viability by assessing the cells' ability to reduce the tetrazolium salt into a blue formazan product (Mossman, 1983) and although non-mitochondrial MTT reduction has also been reported (Bernas and Dobrucki, 2002), the assay is largely considered a measure of cellular metabolic activity. In contrast, the neutral red assay measures cellular ability to incorporate the cationic neutral red dye into the lysosomal matrix in viable cells with retained membrane integrity, which is considered proportional to cell viability (Griffon *et al.,* 1995), therefore it was considered as an appropriate comparator to the MTT assay in the current study.

Previous studies observed an increase in the sensitivity of neutral red over the MTT assay (Fotakis and Timbrell, 2006) which was also evident in the current study when

comparing the extent of loss in cell viability in BRIN-BD11 cells in response to combined cytokine treatments, with a significant reduction in cell viability over 24 hours observed in the neutral red assay in contrast to the MTT assay, where effects were not noted until after 48 hours. This apparent higher sensitivity of the neutral red assay was also confirmed by trypan blue vital dye exclusion assay, again demonstrating a significant reduction in cell viability with cytokine combinations over 24 hours. Given that these assays both reflect cell membrane integrity, this agreement is not surprising but considering that cytokine toxicity is largely considered to occur by apoptosis, an ATP-dependent process, retained mitochondrial respiratory capacity (as evidenced by the MTT assay) suggests loss in membrane integrity as an early event in cell death in this model. However, given the closer agreement between the MTT and neutral red assays when cells were treated with palmitate (which was also associated with increased apoptosis markers), this may suggest differences in assay sensitivity are dependent on the nature of the apoptotic stimuli applied. Additionally, this may be reflective of differential sensitivity between cell types, since Kiely *et al.,* (2007) also reported no loss in cell viability in BRIN-BD11 cells exposed to cytokines in combination, when assessed using the MTT assay with concentrations broadly consistent with those in the current study, concluding that mitochondrial capacity is relatively resistant to cytokine-induced effects in these cells (though apoptosis levels were increased).

Data from treatment of BRIN-BD11 cells with the saturated fatty acid palmitate produced a typical dose-dependent decrease in cell viability when assessed by MTT, neutral red, trypan blue vital dye exclusion and total apoptosis. Results obtained are broadly consistent with other observations in BRIN-BD11 cells (Welters *et al.,* 2004; Dhayal and Morgan 2008), as well the INS-1 and RINm5F rat beta cell lines (Cuhna *et al.,* 2008; Elsner *et*

al., 2011), with a concentration of 250µM palmitate reducing cell viability to ≤ 50%. Mechanistically, palmitate toxicity is associated with induction of an ER stress response following lipid overload and increased oxidative stress (Laybutt *et al.,* 2007; Cuhna *et al.,* 2008; Diakogiannaki *et al.,* 2008; Elsner *et al.,* 2011). Although a contribution of palmitate-induced NO production and nitrosative stress remains unclear, in the current study the Griess assay failed to detect any increase in nitrite levels in BRIN-BD11 cells at all palmitate concentrations used (data not shown); discrepancy between other studies in this regard may be related to methods in which palmitate treatment was carried out (Welters *et al.,* 2004; Keane *et al.,* 2011).

Owing to inherent difficulties in the aqueous solubility of long-chain fatty acids when applied to these *in vitro* studies, palmitate was first complexed to BSA at a molar ratio of 3.3:1, which also mimics *in vivo* transport of fatty acids where, under physiological conditions an average of two fatty acid modules are bound to BSA (Oliveria et al., 2015). Under pathophysiological conditions this ratio can exceed 5:1 (with six fatty acid binding sites located in BSA), however culture models approaching these higher ratios should be avoided to minimise detergent-like effects on cell membranes from higher unbound fatty acid levels. Whilst it was not feasible to determine the total unbound fatty acid concentrations in the current model, Oliveria *et al.,* (2015) showed that treatment of INS-1 cells with a palmitate:BSA complex (3.3:1) at a final palmitate concentration of 500µM resulted in unbound palmitate concentrations of 27nM. However, Cistola and Small (1991) suggested unbound FFAs could be greater than 400nM under similar conditions, though others report that at a 6:1 molar ratio, the estimated unbound FFA is in the region of 300nM (Chu *et al.,*

2010); levels which induced apoptosis when applied to MIN6 cells, not resulting from non-specific detergent effects as previously described (Jeffrey *et al.,* 2008; Gwiazda *et al.,* 2009).

A further consideration in these models is the contribution of BSA present in FBS in supplemented cell culture media, in the region of 0.25% (Oliveria *et al.,* 2015; Alsabeeh *et al.,* 2018), therefore direct application of palmitate:BSA complexes to cells under these conditions would alter the molar ratio, increasing variability between data sets. Whilst some studies therefore conduct palmitate treatments under serum-free conditions, this was poorly tolerated in the current model and so media was supplemented with 1% FBS; a level providing a low endogenous BSA content, whilst supporting cell health under control conditions (El-Assaad *et al.,* 2003 Alsabeeh *et al.,* 2018). The effect of low serum conditions was explored in the current data, showing a modest increase in the basal apoptosis rate of control cultures; though this may reflect the higher sensitivity of the flow cytometry method used for apoptosis assessment, as trypan blue vital dye exclusion and MTT assays suggested no significant difference in total or viable cells under these conditions (data not shown). Additionally, the apoptosis profiles also confirmed that palmitate-induced loss in cell viability in BRIN-BD11 cells is associated with a significant increase in the percentage of cells scored as apoptotic.

The focus of this thesis is on the cytoprotective effects of AA-derived eicosanoids (EETs; subsequent chapters) and therefore the protective effect of AA against palmitate and cytokine toxicity was first established. BRIN-BD11 cells treated with 250µM palmitate co-incubated with AA, ameliorated palmitate toxicity with all treatments from 62.5-1000µM in preliminary MTT dose responses and trypan blue vital dye exclusion assays, confirming previous studies by Keane *et al.,* (2011) who showed co-treatment with 10µM AA reduced cell death from 70% (250µM palmitate alone) to ~15% after 24 hours in BRIN-BD11 cells. These

effects are also consistent with the cytoprotective actions of AA in other beta cell models including INS-1, MIN6 and HIT-T15 cell lines, as well as mouse islets (Papadimitriou *et al.,* 2007; Dhayal and Morgan, 2008; Cho *et al.,* 2012). Effects of AA were also established in the current model at a higher (500µM) palmitate dose which, as with 250µM palmitate, demonstrated a dose-dependent effect of AA, with concentrations greater that 5µM significantly protecting BRIN-BD11 cells against palmitate toxicity This data also indicated that a 2-fold increase in palmitate concentrations required a similar 2-fold increase in the concentration of AA required to achieve a comparable increase in cell viability.

Further confirmatory assays with trypan blue vital dye exclusion showed that at a concentration of 5µM AA there was no significant difference compared to control for total and viable cell numbers, which was not evident from the MTT assays where, regardless of AA concentration, co-incubation with palmitate did not result in viability exceeding 70-80%. This again may reflect variability between methods of assessing cell viability, in this case possibly attributed to changes in mitochondrial activity as a result of altered intracellular lipid handling. Therefore, this emphasises the importance of additional assays to more clearly establish the extent of cytoprotection, as witnessed by the reduction in palmitate-induced apoptosis levels below control in the current data. This also additionally supports that AA may protect against the effects of serum withdrawal (though necessary under these treatment conditions), and is in agreement with similar data reporting this effect of mono-unsaturated species in BRIN-BD11 cells (Welters *et al.,* 2004). Similarly, the observation that 80µM AA treatment alone markedly increased total and viable cell numbers over control also highlights this protective effect and is agreement with others that 100µM (but not 50µM) may increase proliferation in

BRIN-BD11 cells (Keane *et al.,* 2011); though this study assessed these effects using a WST-1 assay (comparable to the MTT assay) rather than absolute cell number.

3.6 Conclusion

The data collected in this chapter reports preliminary investigations into the cytotoxic effects of cytokines and palmitate in *in vitro* models of type 1 and 2 DM, establishing these model systems in BRIN-BD11 cells for further investigations. Reflecting the most pathophysiologically relevant cytokine profile, treatment of BRIN-BD11 cells with IL-1β (100U/mL), IFN-γ (20U/mL) and TNF-α (500U/mL) in combination for 24 and 48 hours was selected for use in subsequent chapters. Alongside this, the data confirms appropriate cytotoxicity profiles, assessed using several methods and showing that loss in cell viability coincides with cytokine-induced nitrite accumulation and iNOS expression, as a marker for cytokine action. Lipotoxicity profiles confirmed previous studies in this cell line, with concentrations of 250-500μM producing appropriate responses for use in further studies. Prior to commencing studies into the cytoprotective action of AA-derived EETs in these models, this chapter also corroborates earlier work demonstrating that this polyunsaturated fatty acid can attenuate palmitate toxicity.

Chapter Four

4 Cytoprotective effects of epoxyeicosatrienoic acids and their derivatives in *in vitro* models of type 2 DM

4.1 Introduction

Prolonged exposure to elevated fatty acids are well-known to cause a reduction in beta cell mass, associated with inhibition of GSIS. In rat islets, incubation with 1mM palmitate resulted in hallmark events of apoptosis; increase in expression of apoptotic genes, ceramide formation, increase in caspase activity and DNA fragmentation (Shimabukuro *et al.,* 1998), with pro-apoptotic action well-established in a number of beta cell line models (Karaskov *et al.,* 2006; Lai *et al.,* 2008; Dhayal and Morgan, 2011). Hyperglycaemia may also promote the cytotoxic effects of palmitate, consequential to dyslipidaemia, in a process of glucolipotoxicity (El-Assaad *et al.,* 2003; Maedler *et al.,* 2003; Maris *et al.,* 2012; Sargsyan and Bergsten, 2011). In contrast, (poly)-unsaturated species are well-tolerated and attenuate the cytotoxicity of saturated FFAs, therefore understanding the mechanisms of these differential responses in models of type 2 DM continues to be a major aim of diabetes research and in this thesis, gives rise to investigations into the actions of the hitherto largely unexplored EETs and DHETs in this context.

Polyunsaturated fatty acids in models of type 2 DM have been extensively studied, with species such as AA showing protective characteristics in many *in vitro* beta cell lines (Papadimitriou *et al.,* 2007; Dhayal and Morgan, 2011; Keane et al., 2011). Metabolism of AA can occur by three major routes: the cyclooxygenase (COX), lipoxygenase (LOX) pathways, which have been extensively studied, and to a lesser extent, CYP450 enzymes. The latter route

results in the production of epoxyeicosatrienoic acids (EETs) comprising of four main isomers: 5(6)-EET, 8(9)-EET, 11(12)-EET and 14(15)-EET, with two enantiomers of each (R,S), which have been shown to exert protective actions in several models, including in maintaining vascular tone and the attenuation of inflammation. The conversion of EETs to their less active vicinal diols (DHETs) represents the major route of EET metabolism however, due to earlier reports on their lack of activity, a view which has been challenged by some (Lu *et al.,* 2001; Suzuki *et al.,* 2008), investigations into their actions in several models is lacking. In particular, little attention has focused on the role(s) of CYP450-derived EETs/DHETs in DM models, in contrast to the more well-studied contributions of COX and LOX metabolites (Xu *et al.,* 2016).

Studies in the 1970s into the regulation of GSIS by AA were conducted with a primary focus on one of the three major routes of AA metabolism: the COX pathway (Robertson, 2017). AA is esterified at the sn-2 position of the glycerol backbone of membrane phospholipids and is released via hydrolysis by the action of PLA_2 (Imig, 2000), which is known to be expressed in human and rodent islets, as well as beta cell lines (Loweth *et al.,* 1995). The released AA can be metabolised by COX-1 and -2 to produce prostaglandins (PGs) and thromboxane (TX) (Hao and Breyer, 2007), with COX-2 predominately expressed in islets (Sorli *et al.,* 1998). Prostaglandins have several biological roles including in inflammation and the regulation of insulin release from pancreatic beta cells. The production of a number of COX metabolites, including PGD_2, PGE_2, $PGF_2\alpha$, PGI_2 and TXA_2 act as signalling molecules and exert their action on cells though GPCRs, with 50-60% of current drug targets used in treatment of type 2 DM known to be associated with GPCR signalling (Lundstrom, 2009). Radiolabelled AA has been reported to predominately produce PGD_2, PGE_2, $PGF_2\alpha$, PGI_2 in rat islets (Carboneau *et al.,* 2017) and some have suggested that PGE_2 may protect against STZ-induced DM in mice

(Vennemann *et al.,* 2012) and PGI_2 has been shown to enhance GSIS in rat islets (Gurgul-Convey *et al.,* 2012). In contrast, in BRIN-BD11 cells, AA metabolism by COX-2 has been suggested to directly impair insulin secretion following co-incubation with a COX-2 inhibitor and exogenously administered AA. Although this data suggests a negative impact of COX-2 metabolites on insulin release in beta cells, studies in human islets have shown conflicting results (Persaud *et al.,* 2007) and others have similarly reported that PGE_2 inhibits GSIS in rodent islets and beta cell lines, compared to human islets (Heitmeier *et al.,* 2004). These observations were similarly confirmed by Sandberg and Jansson (2014), showing that 2 hour incubation with several COX-2 inhibitors produced no deleterious effects on insulin secretion in islets however, 2 day incubation in the presence of indomethacin did result in a slight increase in GSIS and in basal insulin secretion in co-incubation with the COX-1 inhibitors, SC 560 and FR122047. Differences between these *in vivo, ex vivo* and *in vitro* models may arise due to differences in expression levels of PLA_2 (Loweth *et al.,* 1995) or COX isoforms and/or sensitivity in terms of downstream PG signalling.

Further to the metabolism of AA by the COX pathway, AA can also be metabolised by LOX to produce hydroxyeicosatetranoic acids (HETEs) and leukotrienes (LTs), with 12-LOX shown to be specifically expressed in pancreatic cells and Zucker fatty rat islets, predominately producing 12-HETE (Haeggström *et al.,* 2011). 12-LOX expression and the contribution of subsequent lipid-derived signalling species have been reported in several models including neurodegenerative disease, stroke, cardiovascular disease and insulin resistance (Hernadez-Perez *et al.,* 2017). Implications of the contribution of 12-LOX have been studied in context of whole body metabolism and the impact in respect to high-fat-diets and obesity in knockout mice, with evidence that 12-LOX knockout reduced insulin resistance, enhanced beta cell

function and improved glucose tolerance (Sears *et al.,* 2009). The production of 12-HETE has been proposed to regulate mitochondrial dysfunction and an increase in oxidative stress, including in models of cytokine-induced beta cell death, with inhibition of 12-LOX protecting against beta cell apoptosis (Bleich *et al.,* 1997).

With much attention focused on AA metabolism by the COX pathway in DM models and, to a lesser extent, the LOX pathway, evidence for the contribution of CYP450 metabolites remains lacking, especially in beta cell lines in cytotoxicity studies relevant to type 1 and 2 DM. Cytochrome P450s are classified according to their sequence homology and ability to metabolise a variety of endogenous ligands, including AA; primarily 2C and 2J isoforms are expressed in humans and are known AA-directed epoxygenases, producing EETs, with pro-inflammatory cytokines reported to decrease 2C activity in human hepatocytes (Abdel-Razzack *et al.,* 1999). The second class of AA-directed CYPs hydroxylate substrates at or near the ω-terminus, with prominent isoforms 4A and 4F expressed in humans and are known as CYP ω-oxidases producing 20-hydroxyeicosatetreaneoic acid (20-HETE) (Capdevila and Falck, 2001). CYP isoforms 2C and 2J metabolise AA in the presence of oxygen and NADPH to yield four EET isomers and high levels of CYP 2J have been reported in both human and rat islets (Zeldin *et al.,* 1997), as well as high levels of 2C11 (the rat homolog of human CYP2C8) also found in rat islets (Chen *et al.,* 2013). Comparison between expression levels of the two major AA-directed CYP epoxygenases in rat tissues observed high levels of 2C11 in islets compared to kidney, in contrast to 2J where higher levels of this isoform and the EET-metabolising sEH were observed in the kidney as determined by Western blotting (Chen *et al.,* 2013). This observation is important and suggests that EET production in islets *in vivo* may exert important

biological activity and that manipulation of EET production/metabolism could be an attractive strategy in controlling beta cell (dys)function.

The production of EETs has been shown to induce potent anti-inflammatory effects and repress ER stress in *in vivo* models of heart failure (Wang *et al.,* 2014), as well as important roles in regulating vasodilation, functioning as endothelial-derived hyperpolarizing factors, inhibiting sodium transport in nephrons and the inhibition of vasodilation in renal arterioles (Zhao and Imig, 2003). EETs are further metabolised by several pathways including β-oxidation, entry into phospholipids by acyl transferases, binding to intracellular fatty acid-binding proteins (FABP), conversion into less active diols (DHETs) by sEH, proposed to be the main metabolic fate, glutathione conjugation of EETs by glutathione S-transferases, subsequent oxidation by prostaglandin endoperoxide H synthase (PGHS) and chain elongation (Zeldin, 2001). Since sEH-directed metabolism to DHET represents the major route of EET metabolism, producing products with reduced activity and that can be rapidly conjugated and excreted (Deng *et al.,* 2010), the use of sEH inhibitors in cardiovascular models have been well studied, showing protective actions of sEH inhibition in decreasing EET hydration making them attractive for the development of novel therapeutics in cardiovascular disease (Imig, 2006). Of relevance to DM models, sEH knockout or inhibition augmented GSIS in mouse islets and reduced STZ-induced apoptosis (Luo *et al.,* 2010), with similar observations reported by others (Chen *et al.,* 2013), though direct activity of EETs in these models is yet to be properly established (Xu *et al.,* 2016).

Of the EETs produced, 14(15)-EET has been reported to represent the major product of CYP450 action, comprising 44% of the total EETs detected in samples from human kidney cortex, followed by 11(12)-EET at 33% and 8(9)-EET at 23%, with the group reporting difficulty

in obtaining levels of 5(6)-EET owing to its reactivity due to the proximity of the epoxide to the carboxylic acid group, facilitating rapid hydration to DHET (Karara *et al.,* 1990). Esterification of EETs at the *sn*-2 position into membrane phospholipids, with 90% of EETs sequestered in this way, likely represents an important mechanisms of controlling available free-EETs mediating biological activity, with concentrations in the region of 1nM available (Karara *et al.,* 1991; Bernstrom *et al.,* 1992). Of note, this has also been suggested as mechanism of regulating EET levels with effects on the control of insulin secretion and whilst some have suggested that free-EETs negatively regulate GSIS (Klett *et al.,* 2013), others have reported stimulatory actions (Flack *et al.,* 1993) though further direct evidence is limited.

Mechanisms of EET action are still not fully defined, though as FFA derivatives, much of their biological activity is associated with binding interactions and/or metabolic processes that are known to be involved in lipid homeostasis/signalling, including processes relevant to lipotoxicity in beta cells, though evidence for EET action in this context is lacking. FFAR1 or GPR40 has been identified as a medium- and long-chain fatty acid receptor and more recently EETs have been shown in GPR40-over-expressing HEK293 cells to bind GPR40, significantly enhancing proliferation associated with increased EGFR expression and phosphorylation of ERK (Ma *et al.,* 2015), though this is inconsistent with a more recent study which failed to identify potent EET binding at a single high-affinity GPCR target (Lui *et al.,* 2017). Nonetheless, GPR40 could represent an important site for EET action in beta cells, with known activities of this receptor in mediating beta cell responses to FFAs. Previous studies using NIT-1 beta cells have shown that GPR40 siRNA transfected cells observed an increase in apoptosis compared to mock transfections when treated with 500µM oleate co-incubated with 500µM palmitate (Zhang *et al.,* 2007). As with previous studies, ERK 1/2 phosphorylation was associated with

oleate treatment and GPR40 knockdown showed reduced levels of ERK 1/2 phosphorylation, furthermore, oleate activation of the ERK-MAPK pathway was associated with GPR40 activation and termed GPR40-dependent, although treatment with palmitate alone was GPR40-independent, the protective actions of oleate were markedly diminished following GPR40 knockdown (Zhang *et al.,* 2007; Alquier *et al.,* 2009). In support of this, studies in mice models have shown that oleate acts through GPR40-dependent mechanisms in the activation of protein kinase D (PKD), with rottlerin, a PKD inhibitor, completely blocking GSIS, which was further confirmed using islets from $Prkd1^{flox/flox}$ mice bearing PKD1 allele flanked by Lox-P sites, with Ad-Cre used to delete segments of DNA flanked by LoxP sites, showing a 75% reduction in PKD1 expression at the protein level and reducing potentiation of oleate on GSIS (Ferdaoussi *et al.,* 2012).

Further to potential activation of GPR40 by EETs, FFAR4 (GPR120) has also been shown to have a high affinity for long-chain saturated fatty acids (14-18 carbons) and unsaturated fatty acids (16-22 carbons), as well as potentially binding EETs (Park *et al.,* 2018). GPR120 signals through $G\alpha_{q/11}$, activating phospholipase C (PLC), increasing IP_3, which is associated with an increase in intracellular calcium levels, increasing DAG and subsequent activation of PKC (Wellendorph *et al.,* 2009; Vangaveti *et al.,* 2010). GPR120 expression has been identified in monocytes and adipocytes, though is mainly expressed in the gastrointestinal tract, where it may serve to potentiate the incretin effect (Hirasawa *et al.,* 2005) and in pancreatic beta cells, GPR120 expression has been identified at the mRNA level in INS-1 and BRIN-BD11 cells and human islets (unpublished studies by Dhayal and Morgan; Dhayal and Morgan, 2009). In STC-1 intestinal cells, several long-chain fatty acids have been reported to increase cell viability and reduce caspase 3-activity, with linoleic acid shown to preferentially bind GPR120 over

GPR40, whereby knockdown of GPR120 showed a decrease in inhibition of caspase-3 activity, which was also associated with changes in ERK, c-Jun, JNK, p38 MAPK and Akt activation (Katsuma *et al.,* 2005).

Whilst extracellular (GPCR) binding by EETs may mediate some of their biological roles, a single high-affinity receptor site is yet to be identified (Lui *et al.,* 2017), including establishing whether or not this could be mediated via activation of GPCRs with known expression/biological activity in beta cells, one of the well-established roles of EETs is their activity as endogenous ligands to PPARγ, protecting against LPS-induced cytotoxicity in cardiomyocytes (Spector *et al.,* 2004; Liu *et al.,* 2005; Samokhalov *et al.,* 2014). Furthermore, treatment with 10μM 14(15)-EEZE, a reported EET antagonist, blocked the protective effects of 14(15)-EET, which was accompanied by a decrease in PPARγ binding (Samokhalov *et al.,* 2014). In human umbilical vein ECs (HUVEC) transfected with a GAL-mPPARγ-LBD construct, measurement of PPARγ activity, assessed by luciferase activity, showed all four EETs, in the presence of the sEH inhibitor AUDA, increased relative luciferase activity, though to a lower level than with the synthetic PPARγ ligand rosiglitazone (Liu *et al.,* 2005). Moreover, DHETs failed to increase luciferase activity and in co-incubation with rosiglitazone resulted in a 50% decrease in luciferase activity compared to rosiglitazone treatment alone, confirming lack of activity of DHETs and suggesting possible competitive antagonistic activity at PPARγ (Liu *et al.,* 2005).

EETs have also been reported to bind PPARα and in COS-7 cells luciferase activity following transfection with a PPARα reporter construct showed that at 10μM each EET significantly increased PPARα activation compared to control (Fang *et al.,* 2006). In support of this, similar findings were observed in HEK293 cells with 8(9)-EET and 11(12)-EET up to 1μM,

showing significant increases in PPARα activation (Wray *et al.,* 2009). Interestingly, Fang *et al.,* (2006) also showed that 14(15)-DHET produced a significant increase in PPARα-luciferase activity compared to 14(15)-EET, comparable to the PPARα activator Wy-14643, suggesting differential activity of distinct EET/DHET species at different targets. Of note, in HepG2 cells these effects were associated with an increase in mRNA levels of CPT1A (Fang *et al.,* 2006) which, in the context of regulating lipid homeostasis, may increase FFA oxidation, with CPT1 over-expression shown to protect against palmitate toxicity in beta cell models (Sol *et al.,* 2008). Further to activating PPARα and γ, EETs have been reported to activate PPARβ/δ, however, less attention has focused on this as a target for EETs. PPARβ/δ has been shown to be highly expressed in ES cell-derived INS^+ cells (Li *et al.,* 2015) and has also been detected in mouse islets in both alpha and beta cells, as well as human islets, with its activation shown to increase fatty acid oxidation in INS-1 cells (Lglesias *et al.,* 2012; Ravnskjaer *et al.,* 2009). PPARβ/δ activation was also reported in INS-1 cells by using a luciferase PPRE reporter construct, and treatment with unsaturated fatty acids showed similar activation to the use of PPARβ/δ agonists. Furthermore, PPARβ/δ activation synergised with RXR in the increased expression of a fatty acid translocase (CD36) and CPT1, promoting fatty acid oxidation capacity and potentiating GSIS (Ravnskjaer *et al.,* 2009).

As with other FFAs, EETs are activated for further metabolic processing by esterification to CoA, necessary for their incorporation into the phospholipid pool, with acyl-CoA-synthetase-4 shown (ACS4) to be important in controlling the ratio of esterified/free-EETs (Klett *et al.,* 2013), additionally the synthesis of 2-EG, with endocannabinoid-like activity, may also support that EETs can be incorporated into glycerol-lipids (Chen *et al.,* 2008). With TAG and sterol esters making up the main lipids found in lipid droplets, and knockout of DGAT (the

enzyme responsible for the terminal, rate limiting step in TAG synthesis) in mice resulting in reduced TAG formation, several fatty acids have been studied for their contribution to TAG accumulation (Chen *et al.,* 2002). Treatment with palmitate in rat hepatoma cells resulted in a significant increase in cell death, which was rescued by co-incubation with oleate, furthermore knockdown of DGAT1 and 2 reduced palmitate incorporation into TAG, alone or in combination with oleate, and decreased intracellular lipid accumulation (Leamy *et al.,* 2016), as supported by similar studies in CHO cells (Listernberger *et al.,* 2003). Similarly, in several beta cell models, TAG formation is reportedly enhanced in co-incubation with palmitate and with unsaturated species, with one study reporting that DGAT inhibition reduced the protective effect of AA against palmitate in HIT-T15 cells (Cho *et al.,* 2012); though whether or not this represents an important cytoprotective mechanism, sequestering FAs into neutral lipids, has been questioned (Plotz *et al.,* 2006; Cnop *et al.,* 2001; Diakogiannaki et al., 2007; Borg *et al.,* 2009). It is, though, tempting to speculate that EETs may play a role in the formation of TAG in beta cells, since these species are substrates for esterification to CoA. However, in HepG2 cells over-expression of CYP 2J2 or exogenous treatment with 14(15)-EET has been shown to reduce TAG accumulation and instead, lipid homeostasis appears to be achieved via a PPARα- and AMPK- dependent increase in FFA β-oxidation (Zhang *et al.,* 2015). Enhancement of β-oxidation of FFAs in response to EETs may also infer potential mechanistic action of these species against palmitate-induced lipotoxicity in beta cells. Over-expression of CPT1 has been shown to protect against palmitate toxicity in INS-1 cells (Sol *et al.,* 2008), with the CPT1 inhibitor Etomoxir augmenting palmitate toxicity in other studies (Choi *et al.,* 2011; Sargsyan and Bergsten, 2011; Baldwin *et al.,* 2012). In contrast, at low concentrations 2-Bromopalmitate, a poorly metabolisable palmitate analogue known to inhibit CPT1, protected RINm5F cells against palmitate toxicity, however this was suggested to occur by mechanisms

independent to β-oxidation (Baldwin *et al.,* 2012), although higher concentrations (>250μM) of this species alone are also toxic to beta cells (Cnop *et al.,* 2001). In addition to stimulating FFA β-oxidation (Zhang *et al.,* 2015), EETs are also substrates for oxidation, with several shortened-chain EET (and DHET) derivatives reported to possess potent biological activity (Fang et al., 1996; Fang et al., 2001; Fang et al., 2004).

4.2 Aims

Growing evidence supports an important biological role for EETs as AA-derived eicosanoids produced by CYP450 epoxygenases. Whilst much attention has focused on their activity in a variety of model systems, comparatively little is known about their roles in beta cell models of cytotoxicity. Evidence supports biological modes of action in context to mediating changes in lipid homeostasis, which may be attractive for the amelioration of lipotoxicity in type 2 DM, including PPAR-dependent activity and alterations in cellular FFA metabolism. Indeed, CYP 2J2 over-expression has been observed to restore glucose tolerance and improve hepatic insulin resistance in db/db mice (Li *et al.,* 2015) and EETs have been suggested to protect liver cells against high fat diet-induced ER stress (Battaieb *et al.,* 2013), yet no studies have directly assessed a role of EETs in beta cell models of palmitate toxicity. Therefore, the aim of this chapter is to establish the cytoprotective actions of the epoxyeicosatrienoic acids: 8(9)-EET, 11(12)-EET and 14(15)-EET and their corresponding DHETs in BRIN-BD11 cells exposed to palmitate, as well as potential mechanisms of EET action in this context. Specifically, the aims are to:

- characterise the cytoprotective actions of EETs and DHETs in response to palmitate-induced loss in cell viability and apoptosis induction in BRIN-BD11 cells.
- investigate whether EETs mediate these effects through activation of known extracellular and intracellular fatty acid receptors using appropriate receptor antagonists.
- investigate whether EETs alter FFA utilisation in BRIN-BD11 cells by comparing gene expression of relevant FFA-metabolising enzymes by RT-PCR and using pharmacological inhibitors.

- further explore potential mechanisms of EET action utilising the poorly metabolisable palmitate and EET analogues; 2-Bromohexadecanoic acid and 14(15)-EET-SI, respectively.

4.3 Methods

Cell viability was determined using MTT and trypan blue vital dye exclusion assays and apoptosis induction quantified by flow cytometry using MUSE® MutliCaspase assay. Although previous data for apoptosis quantification (Chapter 3) used an Annexin V & Dead Cell assay, the MUSE™ MultiCaspase assay was used for further studies, owing to better discrimination between live and early apoptotic cell populations. Similarly, given the comparable results obtained between the MTT and neutral uptake assays in response to palmitate treatment (Chapter 3) and the difficulties encountered in carrying out the final steps of the assay, this method was not considered further here. For all EET studies, BRIN-BD11 cells were treated with a fixed concentration of a 250µM palmitate:BSA complex, as established (Chapter 3), with EETs and their derivatives (DHETs and 14(15)-EET-SI) firstly prepared in BSA to a molar ratio of 3.3:1 and used at the concentrations indicated in relevant figure legends in media supplemented with 1% FBS. Of the four EETs produced by CYP450 epoxidation of AA: 8(9)-, 11(12)-, and 14(15)-EET were used in this study since, during preparation of 5(6)-EET in BSA it was noted that, unlike the other EET isomers, 5(6)-EET failed to complex effectively, resulting in precipitation. Initial trials treating cells with 5(6)-EET in combination with 250µM palmitate failed to produce reliable results and examination of the cells under a light microscope revealed crystal-like structures, suggesting poor solubility and/or high reactivity facilitating rapid modification to and aggregation of the FFA, as reported by others. Due to these difficulties, no further investigations into the actions of 5(6)-EET were carried out. A range of pharmacological antagonists/inhibitors were also used in this study in co-treatment of cells with palmitate and EETs, using the concentrations indicated in table 2.1 (Chapter 2), having determined appropriate concentrations found to be non-toxic under control conditions, or

with minimal potentiate of palmitate toxicity, by MTT assay screening (data not shown). During these studies, co-treatment with palmitate/EETs was preceded by a 1 hour pre-incubation in the presence of the antagonists/inhibitors at the indicated concentrations. RT-PCR analysis for quantification of changes in gene expression was performed and analysed as described (Chapter 2.9).

4.4 Results

This chapter reports novel observations on the treatment of BRIN-BD11 cells with EETs and their actions against palmitate-induced cytotoxicity. Initially, dose-dependent protective effects of 8(9)-EET, 11(12)-EET and 14(15)-EETs and their corresponding DHETs were determined using the MTT assay against a fixed concentration of 250µM palmitate (figure 4.1).

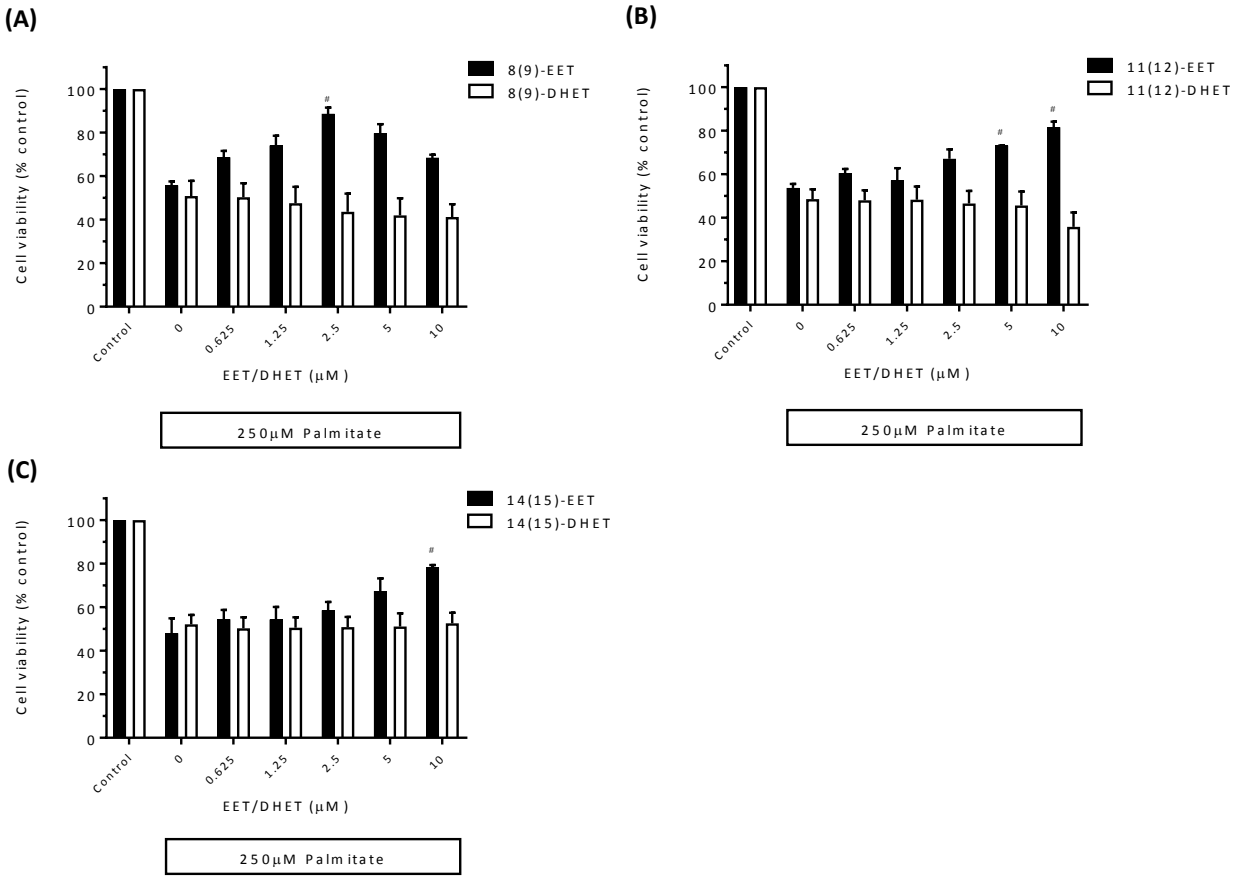

Figure 4.1. Protective effects of EETs but not DHETS against palmitate-induced BRIN-BD11 cell death. Cells were treated with a fixed concentration of 250µM palmitate co-incubated with increasing concentrations (0.625µM–10µM) of each EET or DHET, as indicated for 24 hours before cell viability was assessed using the MTT assay. Values are represented as mean (+/- SEM), n=3. #P<0.05 relative to palmitate treatment alone as determined by one-way ANOVA and Tukey's post-test.

Consistent with preliminary observations (Chapter 3), 250µM palmitate decreased cell viability to ~50% of control, an effect attenuated in co-incubation with increasing concentrations of each EET. With 8(9)-EET at 2.5µM, cell viability was increased to 88.6% (+/-

2.8), indicating near complete-protection against palmitate toxicity (P<0.05), to a level comparable to that previously seen with AA. There is an apparent decline in cell viability at concentrations from 2.5-10µM 8(9)-EET, decreasing to 68.5% (+/-1.3); an effect not observed with the other EETs used. However, as previously observed this may be an artefact of using the MTT assay in these models since visual inspection under light microscopy of the culture plates following treatment revealed an intact, healthy cellular morphology, comparable to control cultures (this was later confirmed with additional viability/apoptosis assays, figure 5.2). Similarly, 11(12)-EET attenuated the palmitate-induced loss in cell viability, with 5µM and 10µM showing a significant increase in cell viability compared to palmitate treatment alone, increasing from 53.6% (+/-1.9) to 73.1% (+/-0.1) and 81.5% (+/-2.6) (P<0.05), respectively. Interestingly, the concentration of 11(12)-EET required to achieve significant protection against palmitate was double that required with 8(9)-EET and there was no apparent decline in viability at higher concentrations, although even at 10µM 11(12)-EET cell viability was lower than that observed with 2.5µM 8(9)-EET. A similar difference is also evident with 14(15)-EET, with only 10µM significantly increasing cell viability to 78.3% (+/- 1.0) compared to palmitate alone (P<0.05).

In contrast, incubation with DHETs failed to ameliorate the cytotoxic effects of palmitate-induced beta cell death regardless of the isomer used. Collectively, this initial data therefore supports that EETs, but not DHETs, are cytoprotective against lipotoxicity in BRIN-BD11 cells treated with palmitate and with some subtle differences in the extent of the protective effect between distinct EET isomers, it is tempting to speculate that the difference in epoxide position in relation to the carboxylic acid group may be important. These effects

were further confirmed for each EET/DHET using the trypan blue vital dye exclusion assay and flow cytometry for apoptosis induction using the MUSE™ MultiCaspase assay (figure 4.2-4.4).

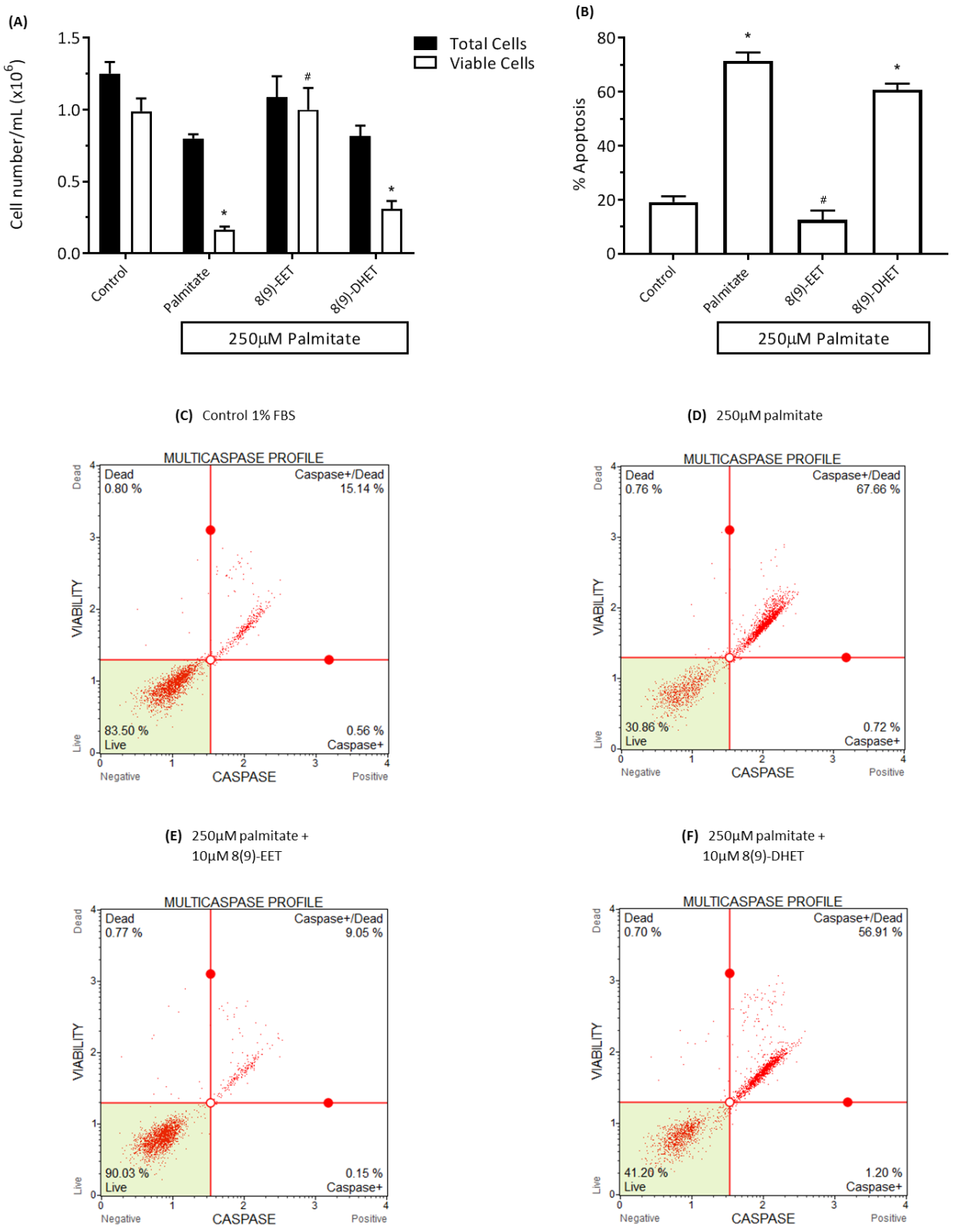

Figure 4.2 Comparative analysis of 8(9)-EET and 8(9)-DHET on palmitate-induced cell death and apoptosis. Cells were treated for 24 hours with 250µM palmitate in combination with 10µM 8(9)-EET or 8(9)-DHET and the total and viable cell numbers were determined using trypan blue vital dye exclusion (A) and apoptosis profile (B) was assessed by flow cytometry using the Muse™ MultiCaspase. Panels (C) to (F) show representative apoptosis profiles of cells under each treatment condition. Values represented as mean (+/- SEM), n=3. *P<0.05 relative to corresponding control. #P<0.05 relative to palmitate alone as determined by two-way ANOVA and Bonferroni's post-test (A) and by one-way ANOVA and Tukey's post-test (B).

Treatment with 250µM palmitate for 24 hours resulted a significant reduction in viable cell number compared to control from 0.99 x10^6 cells/mL (+/-0.09) to 0.16 x10^6 cells/mL (+/-0.2) (*P*<0.05), as suggested from previous data. When treated with the addition of 10µM 8(9)-EET, there was a significant increase in viable cell number compared to palmitate treatment alone from 0.16 x10^6 cells/mL (+/-0.2) to 1.00 x10^6 cells/mL (+/-0.15) (*P*<0.05), an increase of ~6-fold, to a level not significant to control (*P*>0.05). Of note, this in contrast to the apparent reduction in cell viability with 10µM 8(9)-EET observed in the MTT assay and supports potential limitations of the MTT assay in these models. Similar to the initial screening, 8(9)-DHET failed to protect against the reduction in viable cell number when incubated with 250µM palmitate (*P*>0.05).

Confirmation of protective effects is evident from the apoptosis profile, with 250µM palmitate significantly increasing apoptosis compared to control from 19.2% (+/-2.1) to 71.5% (+/-3.1) (*P*<0.05). In co-incubation, 8(9)-EET significantly reduced the percentage of cells displaying caspase activation to 12.7% (+/-3.4) (*P*<0.05), in comparison to 8(9)-DHET (*P*>0.05); effects which are evident in the representative profiles. Additionally, there is also some suggestion that 8(9)-EET may compensate for an increase in basal apoptosis exerted by using media supplemented with 1% FBS, as was observed in the preliminary Annexin V & Dead Cell assays with AA. Compared to the apoptosis profiling gathered from the preliminary results (Chapter 3, figure 3.13), where apoptosis was assessed by flow cytometry with an Annexin V & Dead Cell assay, palmitate increased the apoptotic population to 22.8% (+/-1.9) compared to 71.5% (+/-3.1) when assessed by MUSE™ MultiCaspase. The almost 5-fold difference suggests that MultiCaspase assay has a greater sensitivity compared to Annexin V & Dead Cell assay in this model, likely reflecting that caspase activation represents an early step in the initiation/execution of apoptosis.

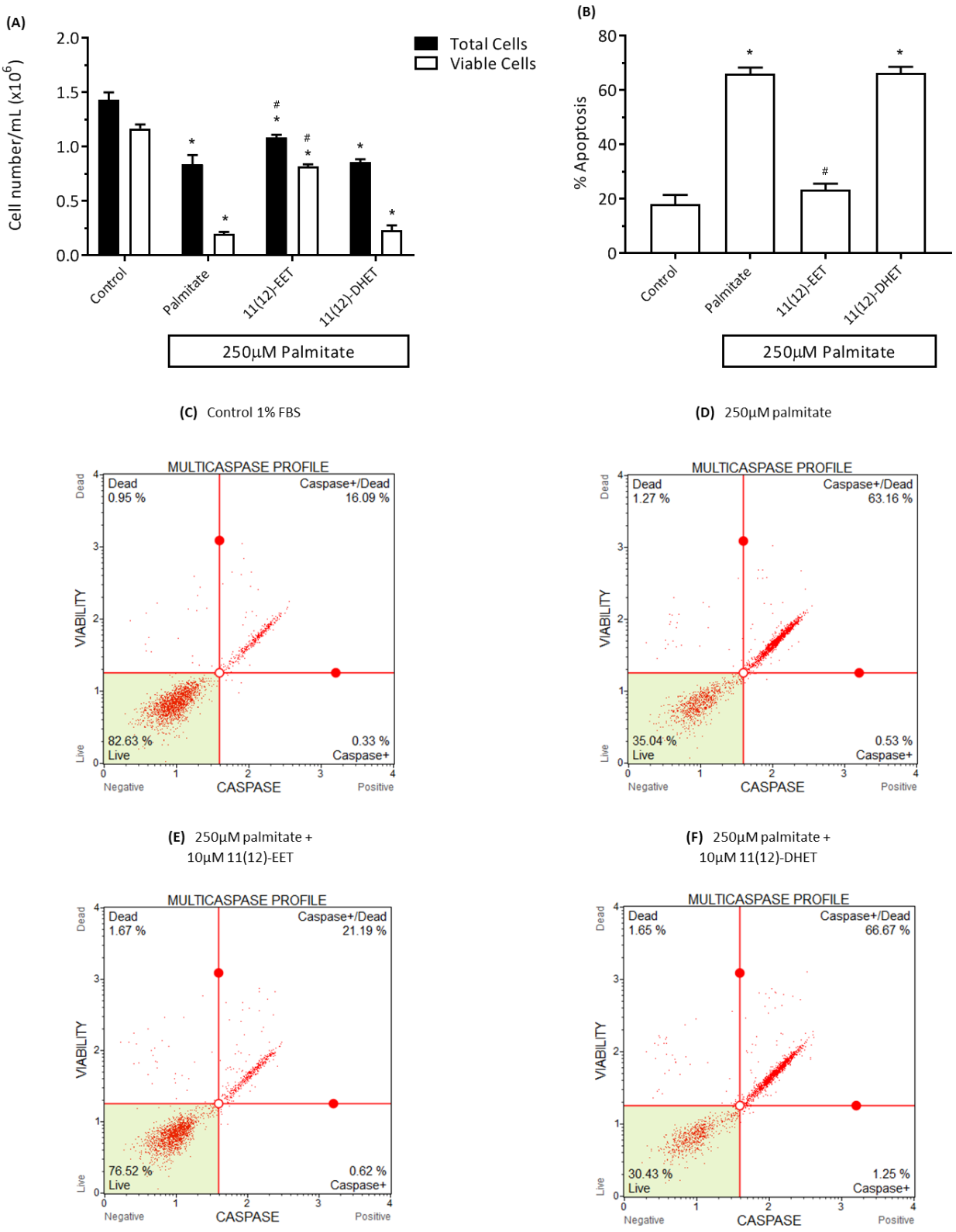

Figure 4.3 Comparative analysis of 11(12)-EET and 11(12)-DHET on palmitate-induced cell death and apoptosis. Cells were treated for 24 hours with 250µM palmitate in combination with 10µM 11(12)-EET or 11(12)-DHET and the total and viable cell numbers were determined using trypan blue vital dye exclusion (A) and apoptosis profile (B) was assessed by flow cytometry using the Muse™ MultiCaspase. Panels (C) to (F) show representative apoptosis profiles of cells under each treatment condition. Values represented as mean (+/- SEM), n=3. *P<0.05 relative to corresponding control. #P<0.05 relative to palmitate alone as determined by two-way ANOVA and Bonferroni's post-test (A) and by one-way ANOVA and Tukey's post-test (B).

Similarly, the protective effects of 11(12)-EET were also confirmed, with 11(12)-EET significantly increasing total and viable cell numbers compared to palmitate alone from 0.84 $x10^6$ cells/mL (+/-0.09) to 1.08 $x10^6$ cells/mL (+/-0.03) and 0.200 $x10^6$ cells/mL (+/-0.02) to 0.82 $x10^6$ cells/mL (+/-0.02) (P<0.05), respectively. The increase in viable cell number corresponds to previous data showing that 10µM 11(12)-EET is protective against palmitate toxicity, with 11(12)-DHET failing to significantly increase viable cell number (P>0.05). As with 8(9)-EET, 10µM 11(12)-EET reduced the percentage of cells displaying caspase activation from 66.1 (+/-2.3) to 23.4% (+/-2.2) (P<0.05), a decrease to levels not significantly different to control (P>0.05), unlike data obtained with the MTT and trypan blue vital dye exclusion assays. In contrast, apoptosis levels in co-incubation with 11(12)-DHET, were comparable and insignificant to that seen in response to palmitate alone (P>0.05), again clearly visible in the representative apoptosis profiles.

Data obtained with 14(15)-EET also demonstrate that co-incubation with 14(15)-EET significantly increased viable cell number from 0.21 $x10^6$ cells/mL (+/-0.01) with palmitate alone to 0.72 $x10^6$ cells/mL (+/-0.08) (P<0.05), to a level not significant to control (P>0.05). As seen with other DHET isomers, 14(15)-DHET failed to protect BRIN-BD11 cells against palmitate toxicity (P>0.05). Analysis of the apoptosis profiles also confirms that 14(15)-EET protects against palmitate-induced caspase activation, significantly decreasing apoptosis from 75.9% (+/-1.6) to 34.1% (+/-2.5) (P<0.05), respectively. However, unlike 8(9)-EET and 11(12)-EET, the effects of 14(15)-EET were not complete, with apoptosis remaining significantly higher than the 18.4% (+/-2.0) under control conditions. As with previous DHETs, 14(15)-DHET failed to protect BRIN-BD11 cells from palmitate toxicity, with no decrease in apoptosis observed (P>0.05).

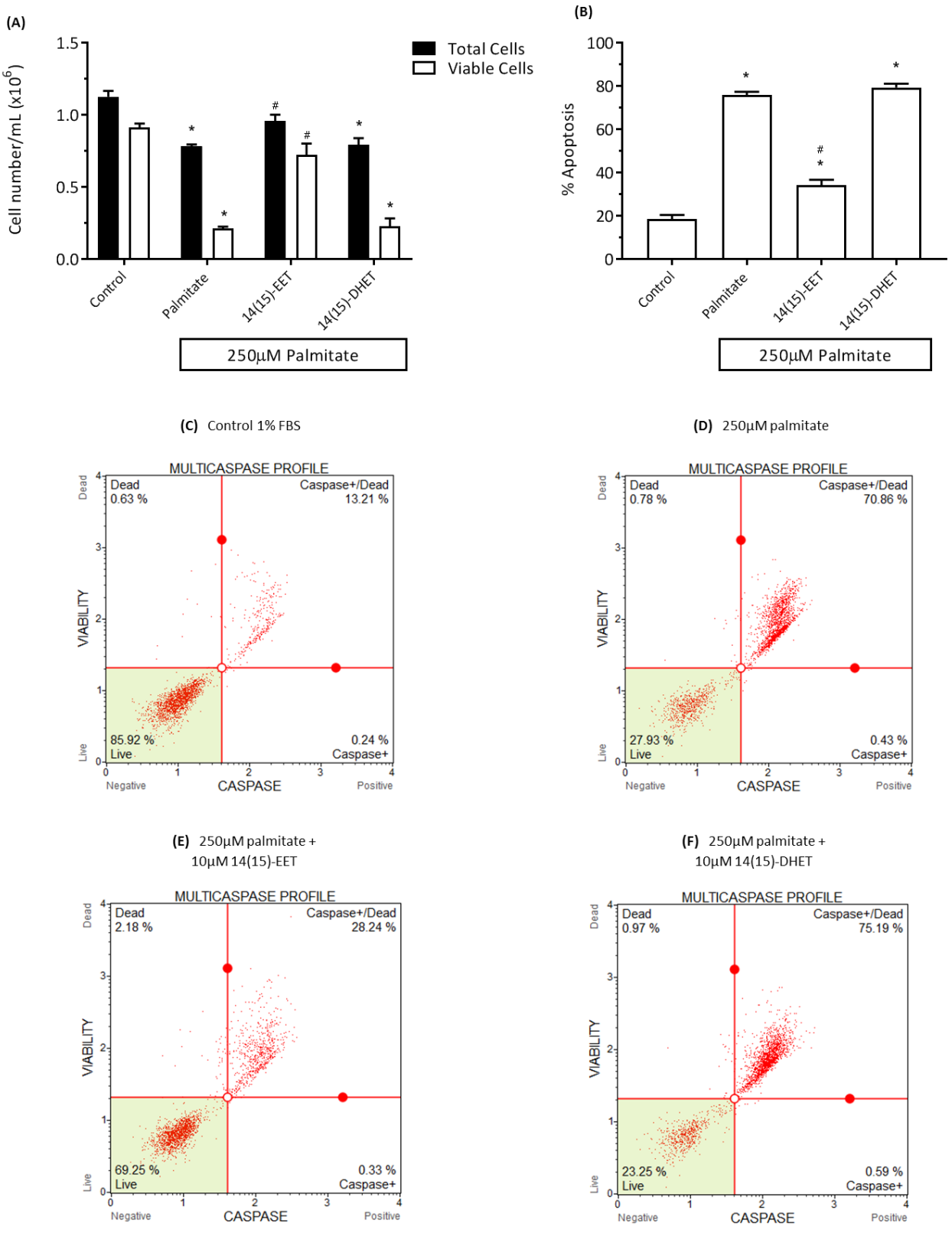

Figure 4.4 Comparative analysis of 14(15)-EET and 14(15)-DHET on palmitate-induced cell death and apoptosis. Cells were treated for 24 hours with 250µM palmitate in combination with 10µM 14(15)-EET or 14(15)-DHET and the total and viable cell numbers were determined using trypan blue vital dye exclusion (A) and apoptosis profile (B) was assessed by flow cytometry using the Muse™ MultiCaspase. Panels (C) to (F) show representative apoptosis profiles of cells under each treatment condition. Values represented as mean (+/- SEM), n=3. *P<0.05 relative to corresponding control. #P<0.05 relative to palmitate alone as determined by two-way ANOVA and Bonferroni's post-test (A) and by one-way ANOVA and Tukey's post-test (B).

Collectively, 8(9)-EET, 11(12)-EET and 14(15)-EET protect against palmitate-induced loss in cell viability and increased apoptosis in BRIN-BD11 cells. Interestingly, from the data collected, 8(9)-EET consistently displays a higher level of protection, followed by 11(12)-EET and then 14(15)-EET. Although significant variation was not always obtained, this is a consistent observation and it is tempting to speculate that, depending on the position of the epoxide group in relation to the carboxylic acid, this may influence its protective actions.

Several GPCRs have been identified as targets for EETs and FFAs including GPR40 and GPR120 and whilst high-affinity binding of EETs to a well-defined GPCR is yet to be fully established, there is evidence supporting a role for these two GPCRs in beta cell (dys)function. Therefore, whether or not the protective actions of EETs against palmitate toxicity were, in part, mediated by their binding to GPR40 or GPR120 was investigated using the selective antagonists DC260126 (GPR40) and AH7614 (GPR120). Initial MTT screening across varying concentrations of DC260126 and AH7614 were investigated (data not shown), showing low toxicity in BRIN-BD11 cells under control conditions. Furthermore, DC260126 and AH7614 were screened against 250µM palmitate, showing low additional toxicity; from this data concentrations of 1.25µM and 2.5µM DC260126 or AH7614 were selected. Cells were pre-incubated with either antagonist for 1 hour before treatment with 250µM palmitate alone or co-incubated with EETs; DHETs were not investigated further here, as the current data suggests no protective actions against palmitate toxicity. Since initial inhibitor screens were carried out using the MTT assay, 8(9)-EET was used at a concentration of 2.5µM, based on earlier observations (figure 4.1); the other EETs were used at 10µM (figure 4.5 A-F).

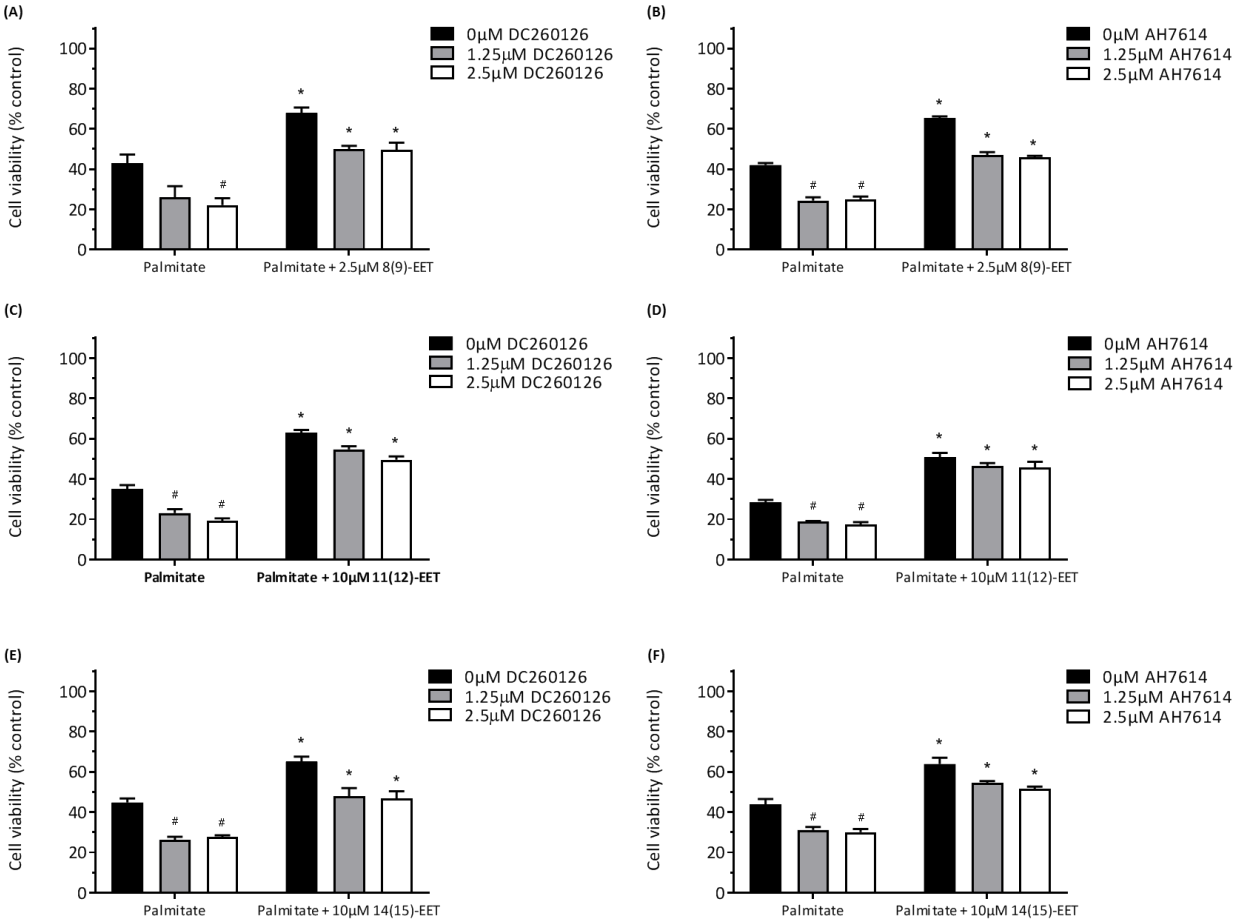

Figure 4.5. Effects of the GPR40 (DC260126) or GPR120 (AH7614) antagonists on the cytoprotective actions of EETs against palmitate toxicity. Cells were pre-incubated with the antagonists at the indicated concentrations for 1 hour followed by treatment with palmitate, alone or in combination, with 2.5µM 8(9)-EET (panels A-B), 10µM 11(12)-EET (panels C-D) or 10µM 14(15)-EET (panels) for 24 hours before cell viability was assessed using the MTT assay. Values are represented as mean (+/- SEM), n=3. *P<0.05 relative to corresponding palmitate treatment (without EET) #P<0.05 relative to palmitate alone as determined by two-way ANOVA and Bonferroni's post-test.

Treatment with 250µM palmitate decreased cell viability, compared to untreated control for all treatments and, as previously observed (figure 4.1), co-incubation with 2.5µM 8(9)-EET, 10µM 11(12)-EET or 10µM 14(15)-EET significantly increased cell viability compared to palmitate alone (*P*<0.05). Similarly, in the presence of 1.25µM or 2.5µM DC260126 and AH7614, all EETs showed a significant increase in cell viability compared to the corresponding treatments with palmitate in the presence of the antagonists, showing that DC260126 and AH7614 failed to antagonise the protective effects of each EET isomer. Although in some treatment conditions, cell viability was lower with EETs in the presence of the antagonists, this

was mirrored by a comparable small decrease in viability in the palmitate-alone groups, supporting that GPR40 and GPR120 do no contribute to the action of EETs in this model in BRIN-BD11 cells.

Further to this, since EETs have been reported to act, in part, as PPAR agonists, investigations into the effects of PPAR antagonists; PPARα (GW6471), PPARβ/δ (GSK3787) and PPARγ (T0070907) were carried out in the presence of each EET isomer in combination with 250µM palmitate (figure 4.6-4.8). BRIN-BD11 cells were pre-treated with either GW6471, GSK3787 or T0070907 for 1 hour prior to treatment in the presence of 250µM palmitate alone or in co-incubation with either 10µM AA, 2.5µM 8(9)-EET, 10µM 11(12)-EET or 10µM 14(15)-EET. Cell viability was screened with all EETs and AA using the MTT assay, with the trypan blue vital dye exclusion and MUSE™ MultiCaspase flow cytometry assays used as confirmatory tests with 8(9)-EET.

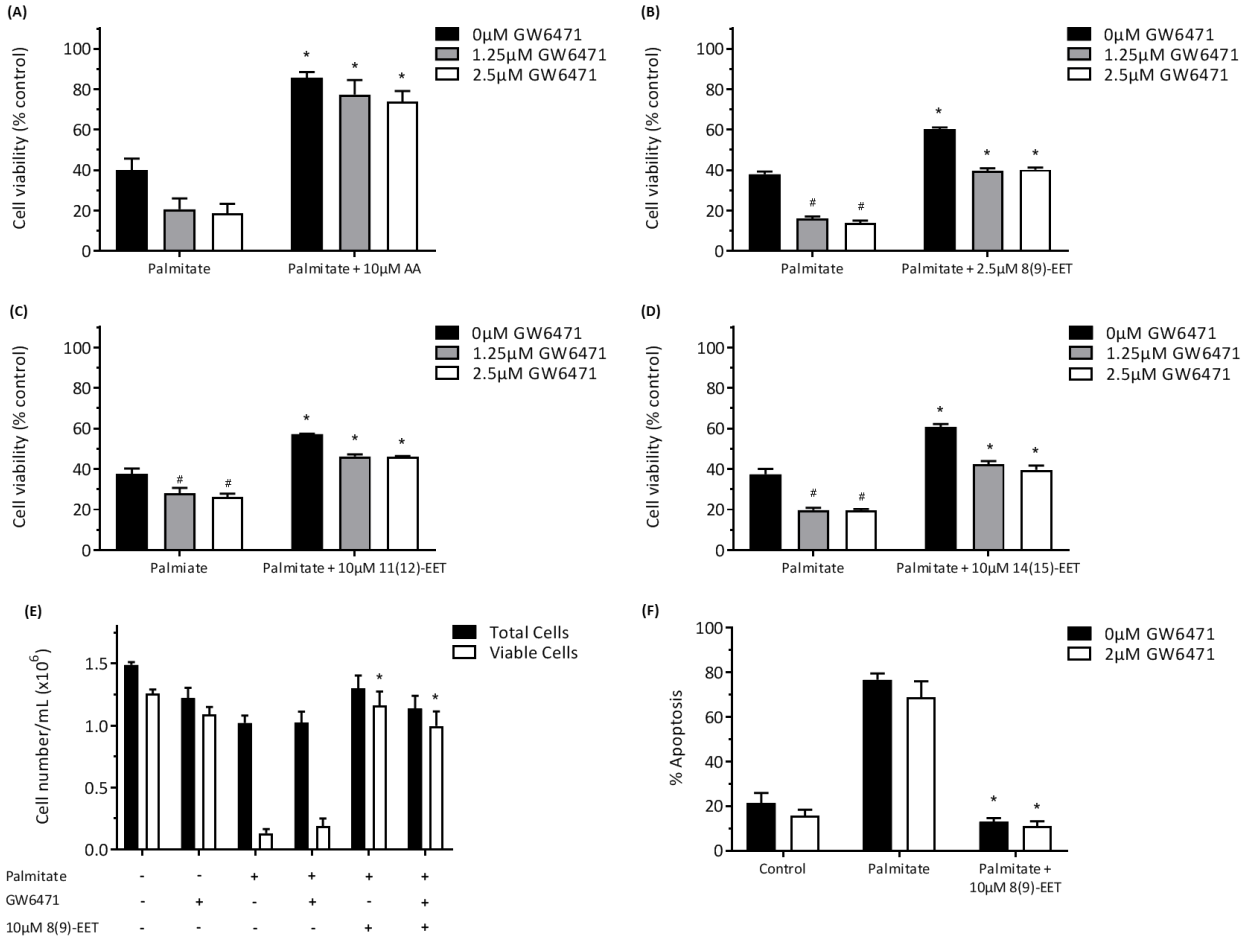

Figure 4.6. Effects of the PPARα (GW6471) antagonist on the cytoprotective actions of EETs against palmitate toxicity. Cells were pre-incubated with GW6471 at the indicated concentrations for 1 hour followed by co-treatment with palmitate, alone or in combination, with 10μM AA, 2.5μM 8(9)-EET, 10μM 11(12)-EET or 10μM 14(15)-EET in the presence of the antagonist for 24 hours before cell viability was assessed using the MTT assay (panels A-D). Cell viability was further assessed in the presence of 10μM 8(9)-EET and the antagonist using the trypan blue vital dye exclusion assay and flow cytometry using the MUSE™ MultiCaspase (panels E-F). Values are represented as mean (+/- SEM), n=3. *P<0.05 relative to corresponding palmitate treatment (without EET) #P<0.05 relative to palmitate alone as determined by two-way ANOVA and Bonferroni's post-test.

In the presence of the antagonist GW6471, AA and all EET isomers resulted in a significant increase in cell viability compared to corresponding palmitate only treatment when assessed by the MTT assay (*P*<0.05), showing that GW6471 failed to decrease their protective actions, indicating effects are PPARα-independent. As with previous data using the GPR antagonists, decrease in viability in the presence of EETs/palmitate was mirrored with a comparable decrease in response to palmitate alone, indicating no difference in the relative

increase in viability in combination with EETs (similar observations apply to the data with PPARβ/δ and PPARγ antagonists, figures 4.7-4.8). To confirm a lack of inhibitory activity of PPARα antagonism on the effects of EET protection against palmitate toxicity, cell viability was also assessed by trypan blue vital dye exclusion. No significant effect of GW6471 on the reduction in viable cell number from 1.26 $x10^6$ cells/mL (+/- 0.03) at control to 0.13 $x10^6$ cells/mL (+/-0.03) with palmitate was observed (P<0.05). Both 8(9)-EET alone and in combination with 2μM GW6471 significantly increased viable cell number compared to the corresponding palmitate-only treatment (P<0.05), with no significant difference between these two group. Similarly, the increase in palmitate-induced caspase activation was unaffected by the presence of the antagonist and was significantly attenuated by 10μM 8(9)-EET, reducing apoptosis to levels comparable to control, indicating complete protection. This effect was equally unaltered in the presence of GW6471, with no significant difference in apoptosis compared to 10μM 8(9)-EET alone, confirming that GW6471 fails to reduce the protective effects of EETs against palmitate toxicity and supporting PPARα-independent effects. The PPARβ/δ antagonists GSK3787 was then used under the same treatment conditions.

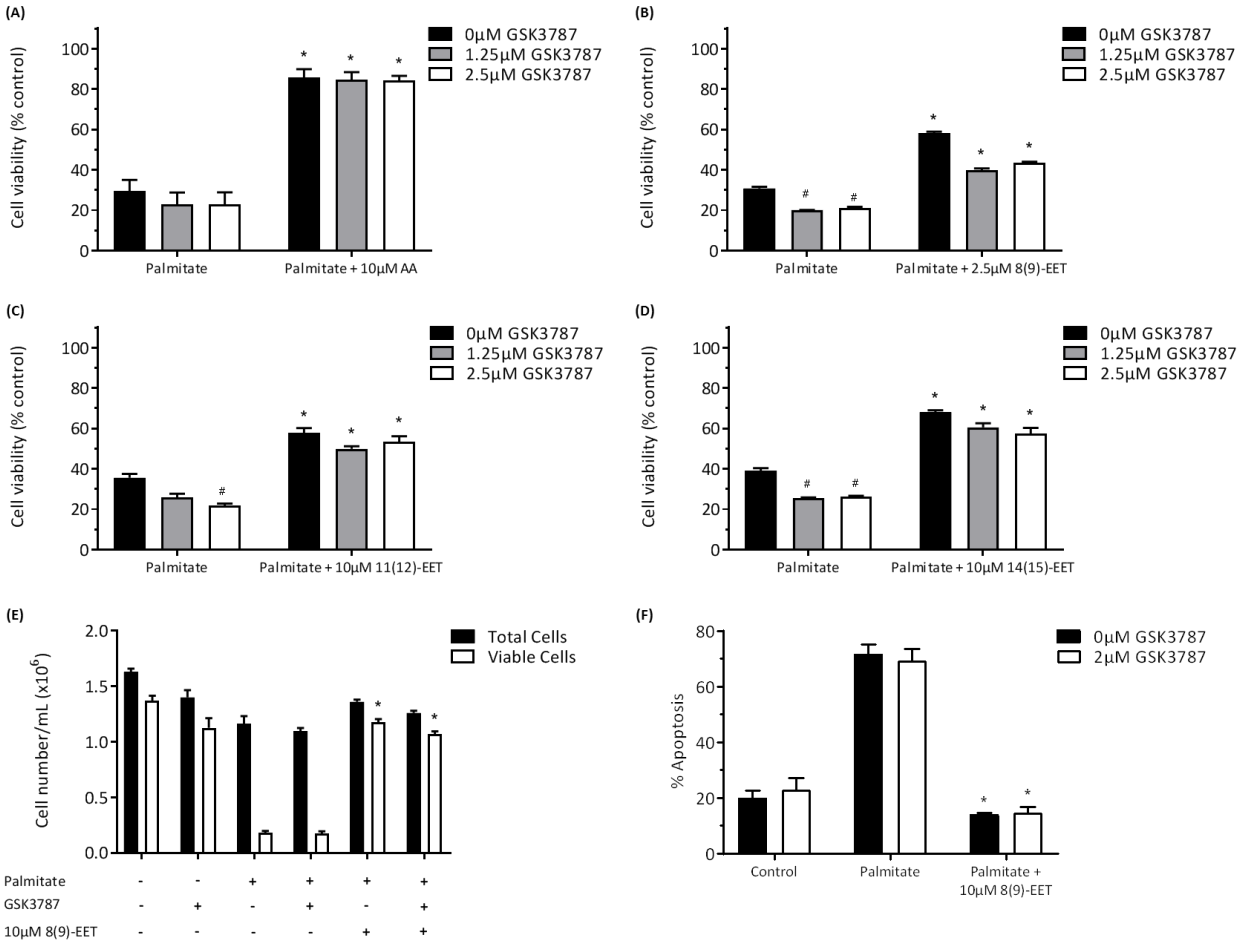

Figure 4.7. Effects of the PPARβ/δ (GSK3787) antagonist on the cytoprotective actions of EETs against palmitate toxicity. Cells were pre-incubated with GSK3787 at the indicated concentrations for 1 hour followed by co-treatment with palmitate, alone or in combination, with 10μM AA, 2.5μM 8(9)-EET, 10μM 11(12)-EET or 10μM 14(15)-EET in the presence of the antagonist for 24 hours before cell viability was assessed using the MTT assay (panels A-D). Cell viability was further assessed in the presence of 10μM 8(9)-EET and the antagonist using the trypan blue vital dye exclusion assay and flow cytometry using the MUSE™ MultiCaspase (panels E-F). Values are represented as mean (+/- SEM), n=3. *P<0.05 relative to corresponding palmitate treatment (without EET) #P<0.05 relative to palmitate alone as determined by two-way ANOVA and Bonferroni's post-test.

Comparable results to that seen in the presence of GW6471 were observed, with AA and EETs significantly attenuating the palmitate-induced loss in cell viability irrespective of the presence of increasing concentrations of GSK3787 when assessed by MTT assay (*P*<0.05 compared to corresponding treatment with palmitate alone). When assessed by trypan blue vital dye exclusion and MUSE™ MultiCaspase assay, 8(9)-EET significantly increased viable cell number compared to palmitate alone from 0.18 x10^6 cells/mL (+/-0.02) to 1.18 x10^6 cells/mL

(+/-0.03) and reduced apoptosis from 69.5% (+/-4.1) to 14.9% (+/-1.8) (P<0.05). With the addition of 2µM GSK3787, no significant difference with corresponding treatment groups was observed, with 8(9)-EET co-incubated with 2µM GSK3787 producing comparable protection against palmitate toxicity. Therefore, similar to GW36471, GSK3787 failed to inhibit the protective actions of all EET isomers suggesting that EET effects are independent to the activation of PPARβ/δ.

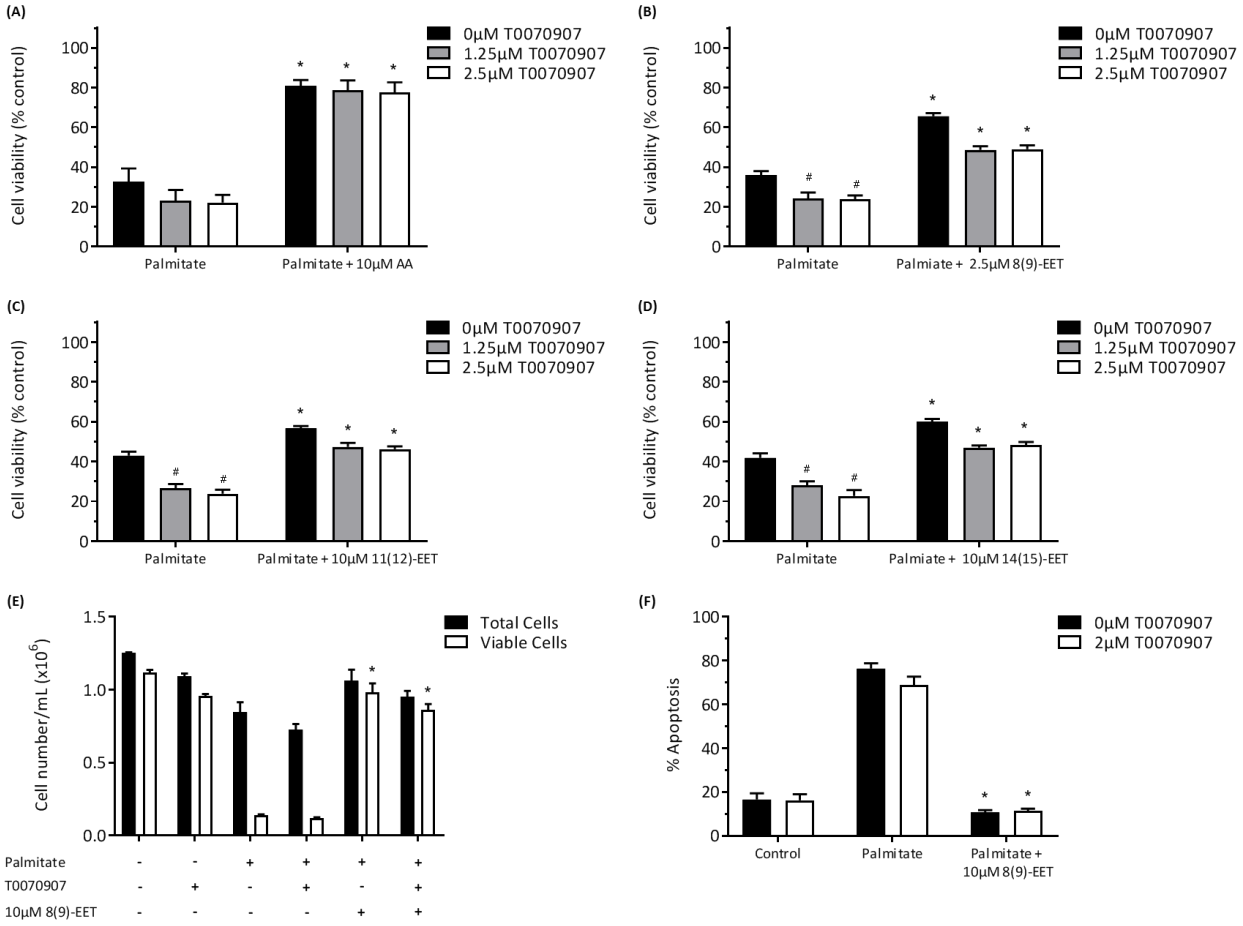

Figure 4.8. Effects of PPARγ (T0070907) antagonist on the cytoprotective actions of EETs against palmitate toxicity. Cells were pre-incubated with T0070907 at the indicated concentrations for 1 hour followed by co-treatment with palmitate, alone or in combination, with 10µM AA, 2.5µM 8(9)-EET, 10µM 11(12)-EET or 10µM 14(15)-EET in the presence of the antagonist for 24 hours before cell viability was assessed using the MTT assay (panels A-D). Cell viability was further assessed in the presence of 10µM 8(9)-EET and the antagonist using the trypan blue vital dye exclusion assay and flow cytometry using the MUSE™ MultiCaspase (panels E-F). Values are represented as mean (+/- SEM), n=3. *P<0.05 relative to corresponding palmitate treatment (without EET) #P<0.05 relative to palmitate alone as determined by two-way ANOVA and Bonferroni's post-test.

As with GW6471 and GSK3787, the PPARγ antagonists T0070907 failed to alter the protective effects of all EET isomers or AA against palmitate, with all EETs showing a significant increase in cell viability compared to palmitate alone when co-incubated with either 1.25μM or 2.5μM T0070907 (P<0.05). Similar results were obtained when cell viability was assessed by trypan blue vital dye staining, with 10μM 8(9)-EET significantly increasing viable cells compared to palmitate alone (P<0.05) and the addition of 2μM T0070907 resulting in no significant difference between treatment groups, showing that T0070907 fails to antagonise the protective effects of 8(9)-EET. Compared to corresponding treatment with palmitate in the presence of T0070907, viable cell number increased from 0.12 $x10^6$ cells/mL (+/-0.01) to 0.86 $x10^6$ cells/mL (+/-0.04) with 8(9)-EET (P<0.05). In agreement with this, 8(9)-EET significantly reduced the palmitate-induced increase in apoptosis from 76.4% (+/-2.3) to 10.7% (+/-1.0), a response unaffected with the addition of 2μM T0070907 (P>0.05). Collectively, the addition of each PPAR antagonists resulted in no significant changes in the extent of cytoprotection afforded by each EET isomer against palmitate toxicity, with confirmatory vital dye exclusion and apoptosis assays overall supporting the initial MTT data and together suggest that EETs exert these effects in a PPAR-independent manner.

Upon activation, PPARs form heterodimers with RXR, therefore further to the effect of PPAR antagonists alone, co-stimulatory action of EETs in this context was also explored under similar experimental conditions as with the previous PPAR antagonist data. Firstly, the protective effects of 8(9)-EET and AA against palmitate-induced loss of cell viability were investigated in the presence of the RXR antagonist, HX531, alone and then in combination with each of the PPAR antagonists in the presence of each EET isomer (figure 4.9).

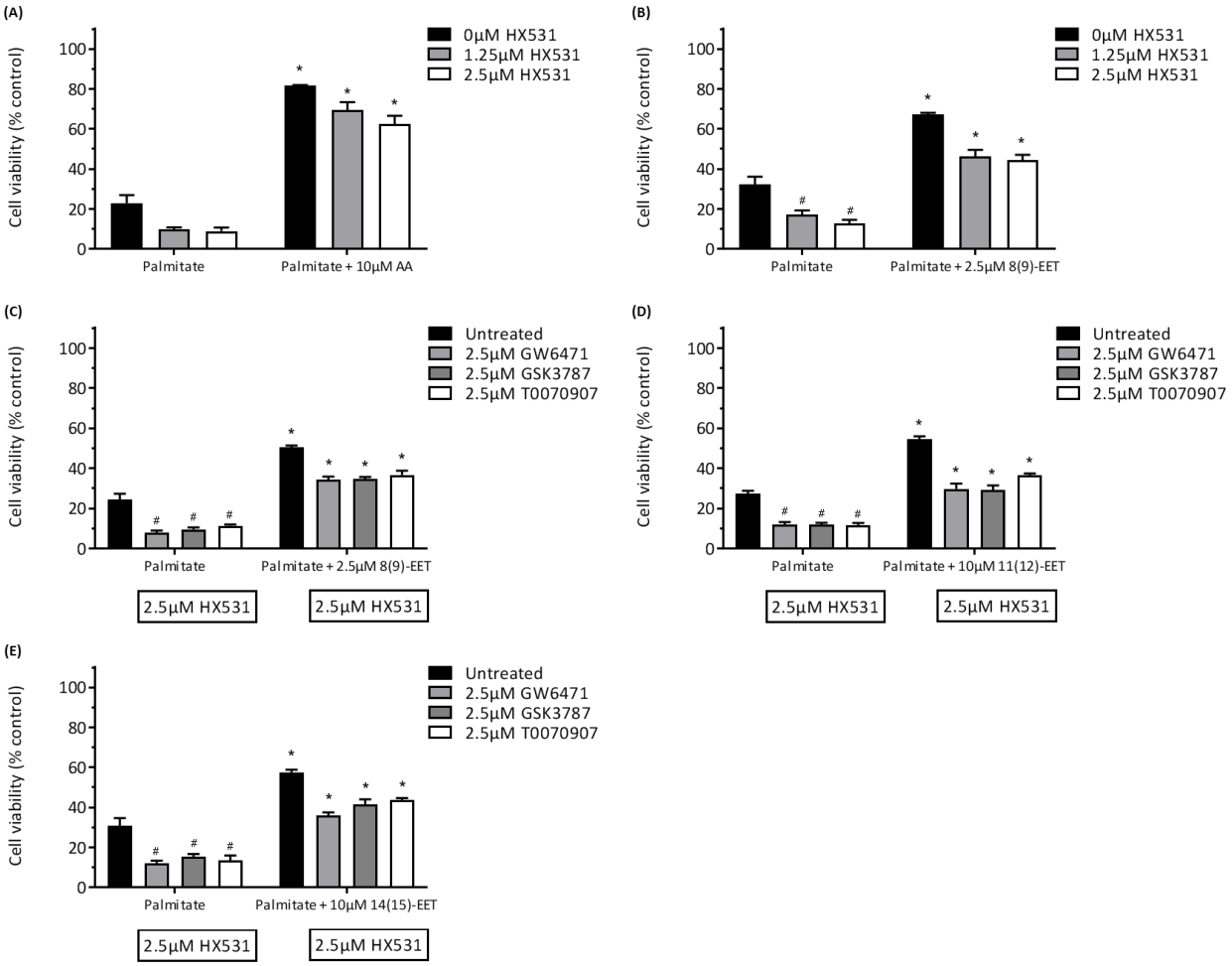

Figure 4.9. Effects of the RXR (HX531) antagonist alone and in combination with PPAR antagonists on the cytoprotective actions of EETs against palmitate toxicity. Cells were pre-incubated with HX531, GW6471, GSK3787, T0070907 alone or in combination at the indicated concentrations for 1 hour followed by co-treatment with palmitate alone or in combination with 10µM AA, 2.5µM 8(9)-EET, 10µM 11(12)-EET or 10µM 14(15)-EET in the presence of the antagonists for 24 hours before cell viability was assessed using the MTT assay. Values are represented as mean (+/- SEM), n=3. *P<0.05 relative to corresponding palmitate treatment (without EET) #P<0.05 relative to palmitate alone as determined by two-way ANOVA and Bonferroni's post-test.

Treatment of BRIN-BD11 cells with palmitate co-incubated with 10µM AA or 2.5µM 8(9)-EET observed a significant increase in cell viability compared to palmitate treatment alone (*P*<0.05). The addition of HX531 resulted in a slight decrease in viability in the palmitate-only treatment, as observed in previous data, under these conditions, the relative effect of AA or 8(9)-EET was comparable regardless of the presence of HX561 (figure 4.9, panels: A-B), indicating effects on increased cell viability were independent to RXR activation. Similar

effects were observed with the inclusion of the PPAR antagonists, though overall this data demonstrates a more consistent reduction in cell viability in the palmitate treatment alone. With all EETs, a significant reduction in viability was observed in the presence of the combined inhibitors, though this remained significantly higher than the corresponding palmitate-only controls. Again, the relative increase in cell viability between this group and the data from the presence of the EETs is comparable to that in the absence of the antagonists, with ~30% increase in viability with each EET. Collectively, this data suggests PPAR/RXR-independent actions of EETs in this model of lipotoxicity in BRIN-BD11 cells.

Following from this, other potential mechanisms of EET action were explored, extending the approach with pharmacological receptor antagonists to other intracellular targets, with potential activity in the metabolism of EETs and other FFAs. Firstly, since release of AA from cellular phospholipids is controlled by the activity of PLA_2 and that EETs can also be incorporated into membrane phospholipids, as a mechanism controlling total free-EET levels (Klett *et al.,* 2013), the PLA_2 inhibitor OBBA was investigated to explore whether cellular levels of exogenously applied EETs may be regulated in a similar way (figure 4.10).

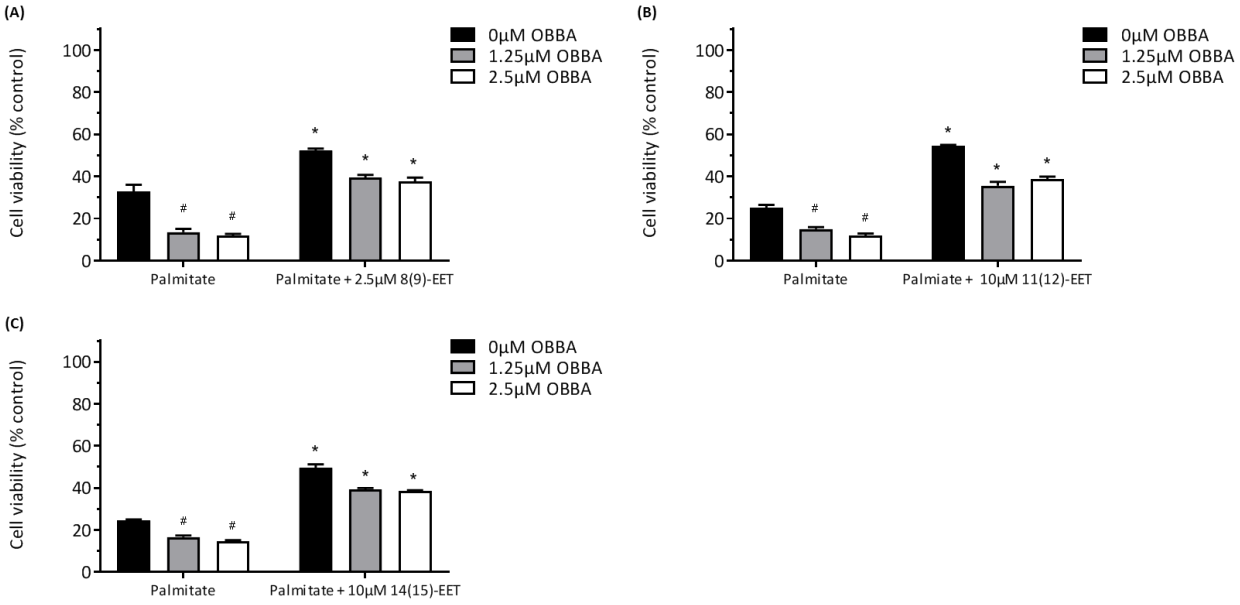

Figure 4.10. Effects of the PLA_2 (OBBA) inhibitor on the cytoprotective actions of EETs against palmitate toxicity. Cells were pre-incubated with OBBA at the indicated concentrations for 1 hour followed by treatment with palmitate alone or in combination with 10µM of each EET in the presence of the inhibitor for 24 hours before cell viability was assessed using the MTT assay. Values are represented as mean (+/- SEM), n=3. *P<0.05 relative to corresponding palmitate treatment (without EET) #P<0.05 relative to palmitate alone as determined by two-way ANOVA and Bonferroni's post-test.

A similar modest enhancement of palmitate toxicity (alone) was observed following treatment with either 1.25µM or 2.5µM OBBA. As with data obtained with the previous antagonists, treatment with each EET in combination with either 1.25µM or 2.5µM OBBA resulted in a significant increase in cell viability compared to their corresponding treatments comparable to the increase observed in the absence of the inhibitor (*P*<0.05).

Changes in lipid homeostasis in response to FFA treatment may, in part, be mediated by alterations in TAG synthesis, thereby sequestering toxic FFA species into neutral lipids, or by increasing β-oxidation, decreasing cytosolic levels of acyl-CoAs. Alternatively the SCD enzyme family are involved in the conversion of saturated FFAs to unsaturated species, which may facilitate their incorporation into TAG. Processing of FFAs by these routes were then investigated in cells treated with 250µM palmitate co-incubated with 8(9)-EET in the presence

of 2µM of the SCD inhibitor A939572, or with 50µM of the CPT1 inhibitor, Etomoxir, and 5µM of the DGAT inhibitor, Xanthohumol, alone and in combination with cell viability assessed using the MTT and MUSE MultiCaspase assays (figure 4.11).

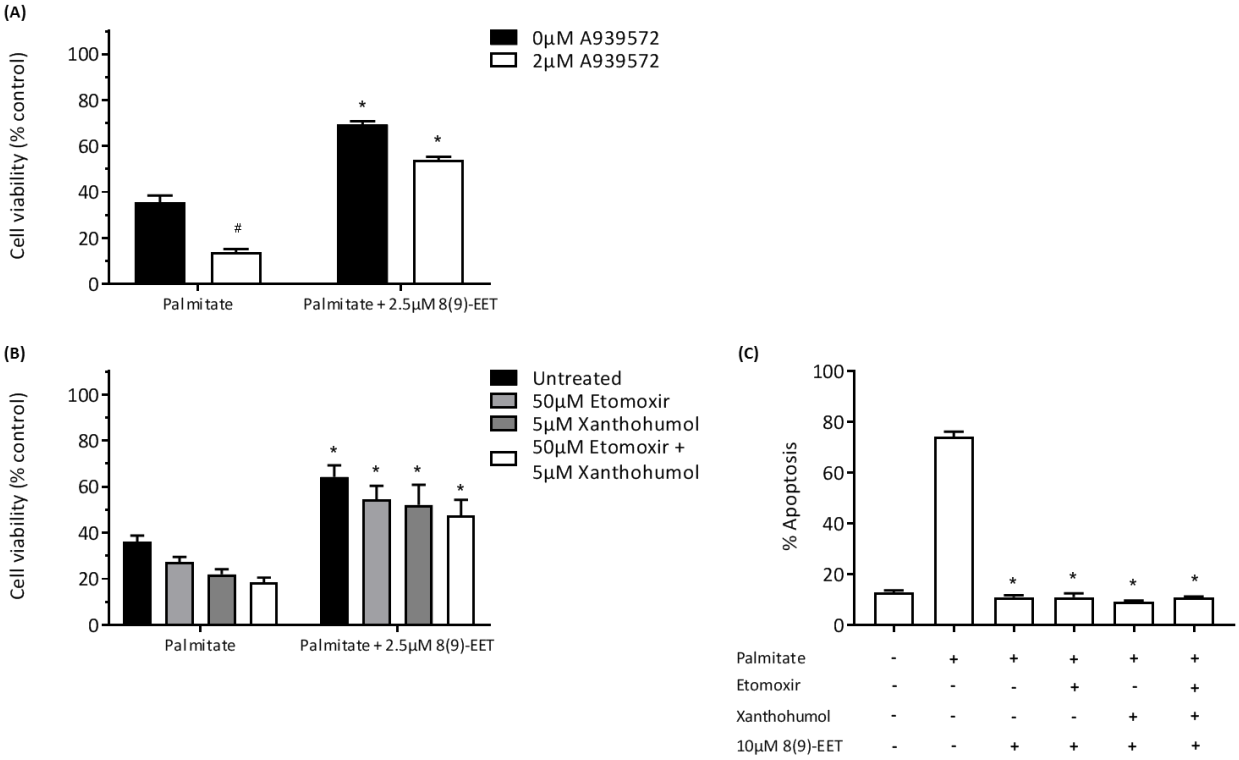

Figure 4.11. Effects of SCD (A939572), CPT1 (Etomoxir) and/or DGAT-1 (Xanthohumol) inhibition on the cytoprotective actions of EETs. Cells were pre-incubated with A939572, Etomoxir or Xanthohumol alone or in combination at the indicated concentrations for 1 hour followed by treatment with palmitate alone or in combination with 2.5µM (A-B) or 10µM (C) 8(9)-EET in the presence of the inhibitors for 24 hours before cell viability was assessed using the MTT assay (A-B) or by flow cytometry with the MUSE™ MultiCaspase assay (C). Values are represented as mean (+/- SEM), n=3. *P<0.05 relative to corresponding palmitate controls and #P<0.05 compared to treatment without the inhibitor as determined by two-way ANOVA and Bonferroni's post-test (A-B) or one-way ANOVA and Tukey's post-test (C).

The SCD inhibitor A939572 enhanced palmitate toxicity (effects which were also evident when used at lower concentrations, data not shown), significantly reducing cell viability (P<0.05). As with previous antagonist/inhibitor data, the effect of 8(9)-EET was not significantly altered in the presence of the inhibitor, with a comparable increase in cell viability in the two EET treatment groups as compared to palmitate alone groups (P<0.05). Similarly, neither inhibition of CPT1 or DGAT diminished the protective effect of 8(9)-EET against

palmitate toxicity, with all inhibitor treatment groups producing a comparable increase in cell viability compared to their corresponding palmitate controls. Similarly, combined inhibition of these pathways had no effect on the reduction in caspase activity in response to 8(9)-EET ($P>0.05$), though the apparent trend on a reduction in cell viability in the combined inhibitor group is not evident here. This may indicate collectively that EETs regulate a distal step downstream in the apoptotic pathway/caspase activation, though given the nature of the MTT assay this is likely to continue to be an artefact of this assay format, particularly in data obtained using inhibitors that will likely alter mitochondrial substrate availability/reducing capacity.

Although a range of complementary pharmacological inhibitors/receptor antagonists have so far been used to explore potential mechanisms of EET action in the current lipotoxicity model, problems may occur from poor cellular uptake (though a 1 hour pre-incubation was included) and/or potential off-target effects. Additionally, the minor enhancement of palmitate toxicity in some of the data obtained may limit the conclusions that can be drawn, though this may reflect a higher sensitivity to toxicity in palmitate/EET challenged cells and whilst collectively the data support that EETs may act downstream of a pro-apoptotic signal in controlling cell death, this does not preclude the possibility that other EET actions are contributing to changes in lipid handling in these cells, effects which are not directly apparent in inhibitor studies. Therefore, RT-PCR was used to determine the relative expression of select genes associated FFA metabolism in BRIN-BD11 cells treated with palmitate alone, or in the presence of each EET (figure 4.12).

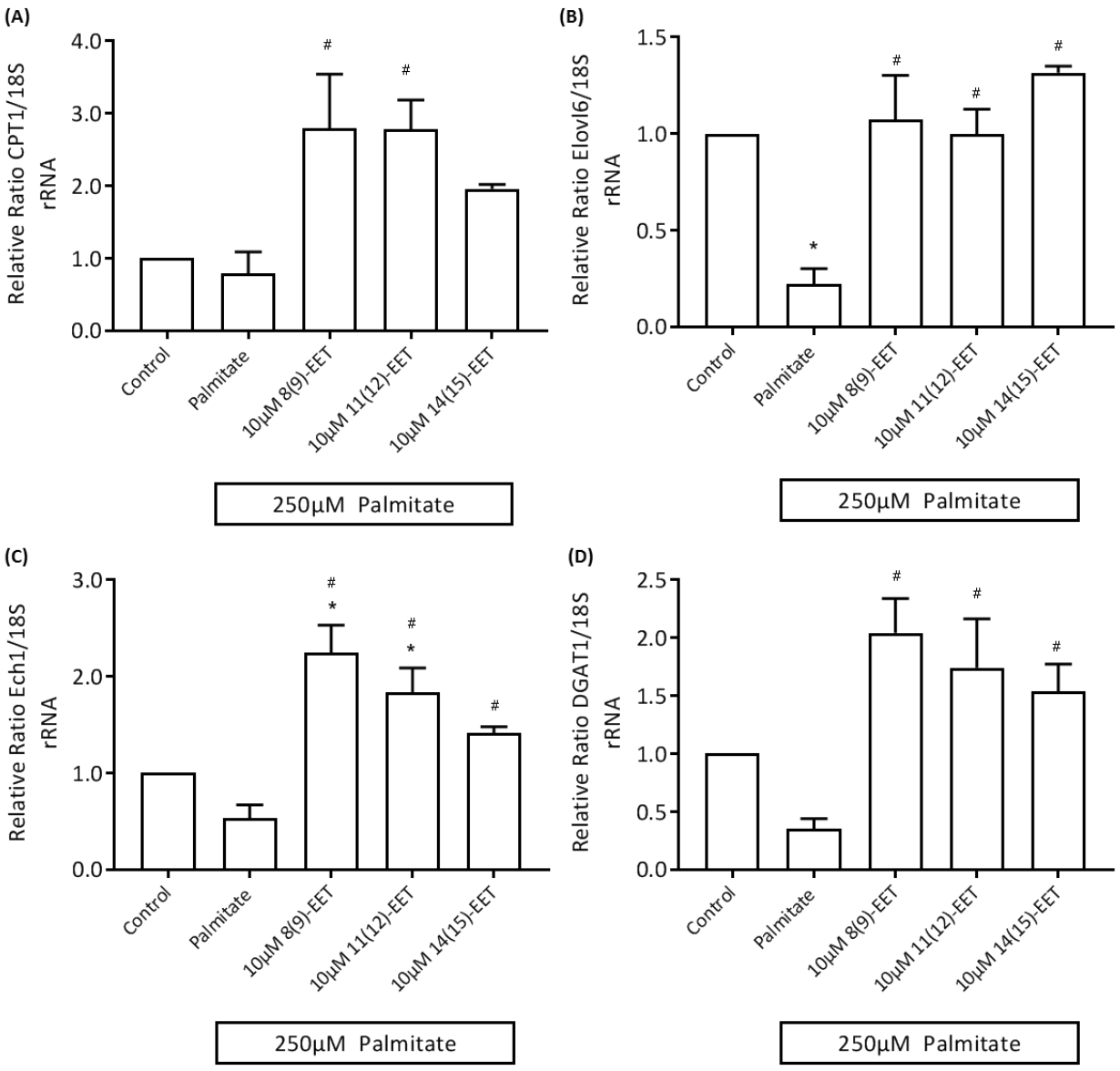

Figure 4.12. Effects of palmitate and EETs on relative gene expression. Cells were treated with a fixed concentration of 250μM palmitate co-incubated with 10μM 8(9)-EET, 10μM 11(12)-EET or 10μM 14(15)-EET for 24 hours before samples were processed for RNA extraction, cDNA synthesis with relative gene expression determined by real-time PCR using SYBR green for CPT1 (A), Elovl6 (B), Ech1 (C) and DGAT1 (D). Expression levels were determined relative to 18S rRNA using the $\Delta\Delta C_t$ method and values represented as mean fold change in relative expression (+/- SEM), n=3. *P<0.05 relative to control. #P<0.05 relative to palmitate. Statistically analysed by one-way ANOVA and Tukey's post-test.

A significant increase in the relative expression of CPT1, Ech1 and DGAT1 compared to palmitate control of ~2-fold, ~1.7-fold and ~1.6-fold (*P*<0.05), respectively, was observed in co-incubation with 8(9)-EET. Similarly, an increase in expression of these genes was also observed in co-incubation with 11(12)-EET and, to a lesser extent, 14(15)-EET, with the

exception of CPT1. Although Elovl6 showed a significant increase compared to palmitate treatment alone, its relative expression was minimally different to the control level when compared to the increase over control with CPT1, Ech1 and DGAT1. This is likely due to EETs protecting against palmitate-induced cell death and so the relative change in expression of ELovl6 compared to palmitate alone may reflect cell/mRNA loss over the culture period used. Collectively, 8(9)-EET treatment resulted in the highest increase in gene expression for the majority of targets, followed by 11(12)-EET and 14(15)-EET; a consistent albeit not always significant trend seen throughout this chapter following treatments of cells with EETs co-incubated with palmitate. Of note here is the observations that genes associated with increased β-oxidation (CPT1 and Ech1) and TAG synthesis (DGAT) are upregulated consistently across EET treatments and may support alterations in lipid handling in these cells under these conditions, though not necessarily reflective in the effects on cell viability, as reported by others (Diakogiannaki et al., 2007; Keane *et al.,* 2011). Upregualtion of DGAT, as observed with all EETs (increasing 1.5-2 fold over control and a marked increase compared to palmitate treatment) may suggest an increase in TAG synthesis under these conditions and although DGAT inhibition suggested EET effects were independent to this, any increase in cellular lipid droplet accumulation was assessed by flow cytometry using Nile Red staining (figure 4.13).

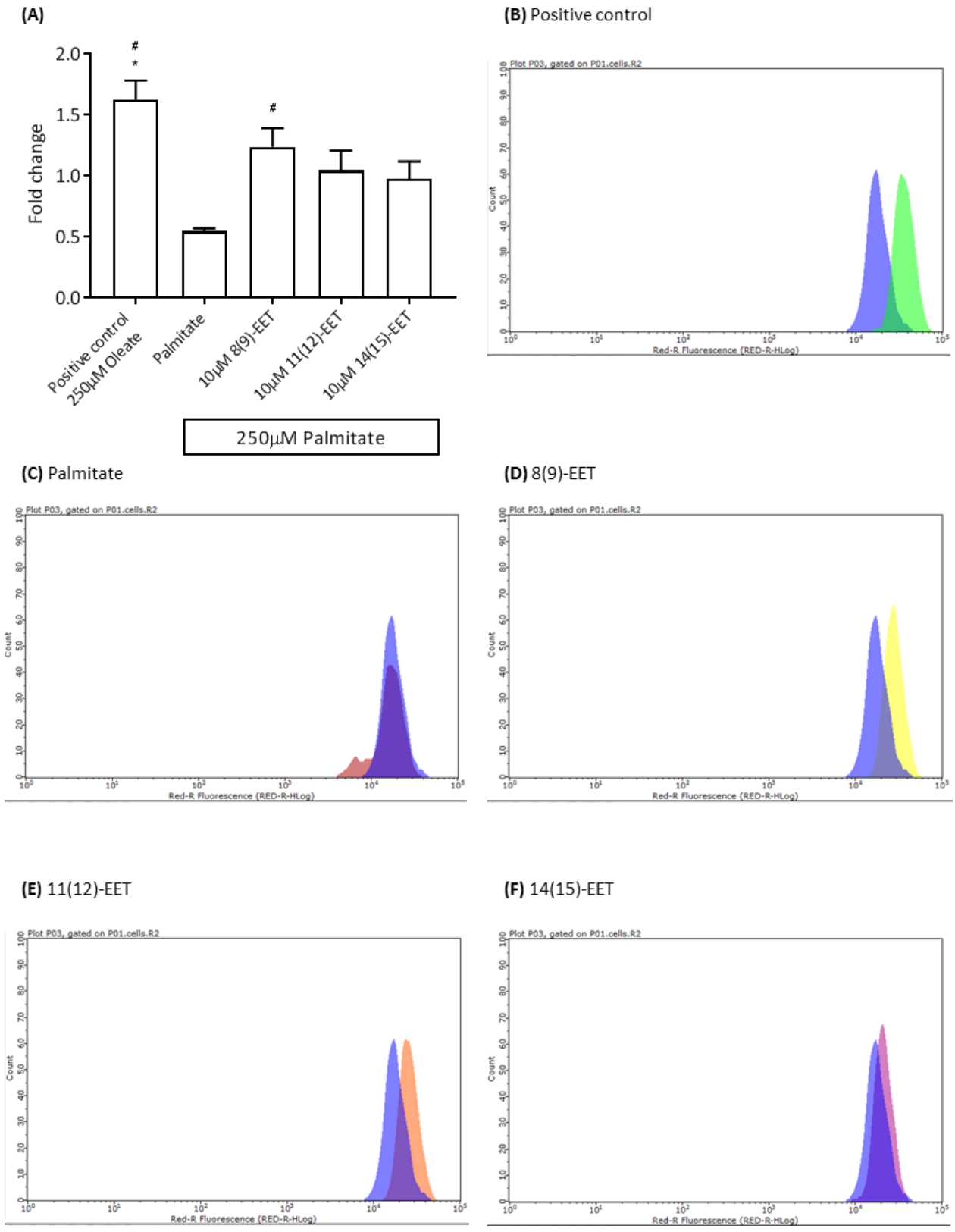

Figure 4.13. Effects of EETs on lipid droplet accumulation in palmitate-treated BRIN-BD11 cells. Cells were treated with 250µM palmitate +/- 10µM 8(9)-EET, 10µM 11(12)-EET, 10µM 14(15)-EET or 250µM oleate as a positive control for 24 hours before lipid droplet accumulation was assessed by Nile Red staining and flow cytometry. Data in panel A is expressed as relative fold change of mean fluorescence compared to control. n=3, with representative prolife plots shown in panels B-F (in all panels the control population is indicated in blue, with a right shift in response to treatment indicating an increase in lipid droplet accumulation). *P<0.05 relative to control. #P<0.05 relative to palmitate as determined by one-way ANOVA and Tukey's post-test.

As would be expected, treatment with the monounsaturated fatty acid oleate significantly increased the accumulation of intracellular lipid droplets ($P<0.05$ compared to control) and in contrast, the saturated fatty acid palmitate did not. Representative profiles show a right shift in mean fluorescence with all EETs indicating an increase in intracellular lipid droplets in co-incubation with palmitate; however, the relative fold change was only significant in the presence of 8(9)-EET, with a modest increase in 11(12)-EET and to a lesser extent 14(15)-EET. Collectively, this supports the DGAT inhibitor data suggesting that intracellular lipid droplet accumulation is not required for EET action. To further explore the protective effects of EETs in context to whether changes in TAG formation and/or β-oxidation in response to palmitate are necessary, the palmitate analogue, 2-Bromopalmitate acid was investigated in co-incubation with each EET (figure 4.14). This palmitate derivative, as well as inhibiting palmitoylation and fatty acid oxidation, is a species capable of being esterified to CoA but is a poor substrate for further metabolic processing, including β-oxidation and is has not been observed to be incorporated into TAG (Cnop *et al.,* 2001).

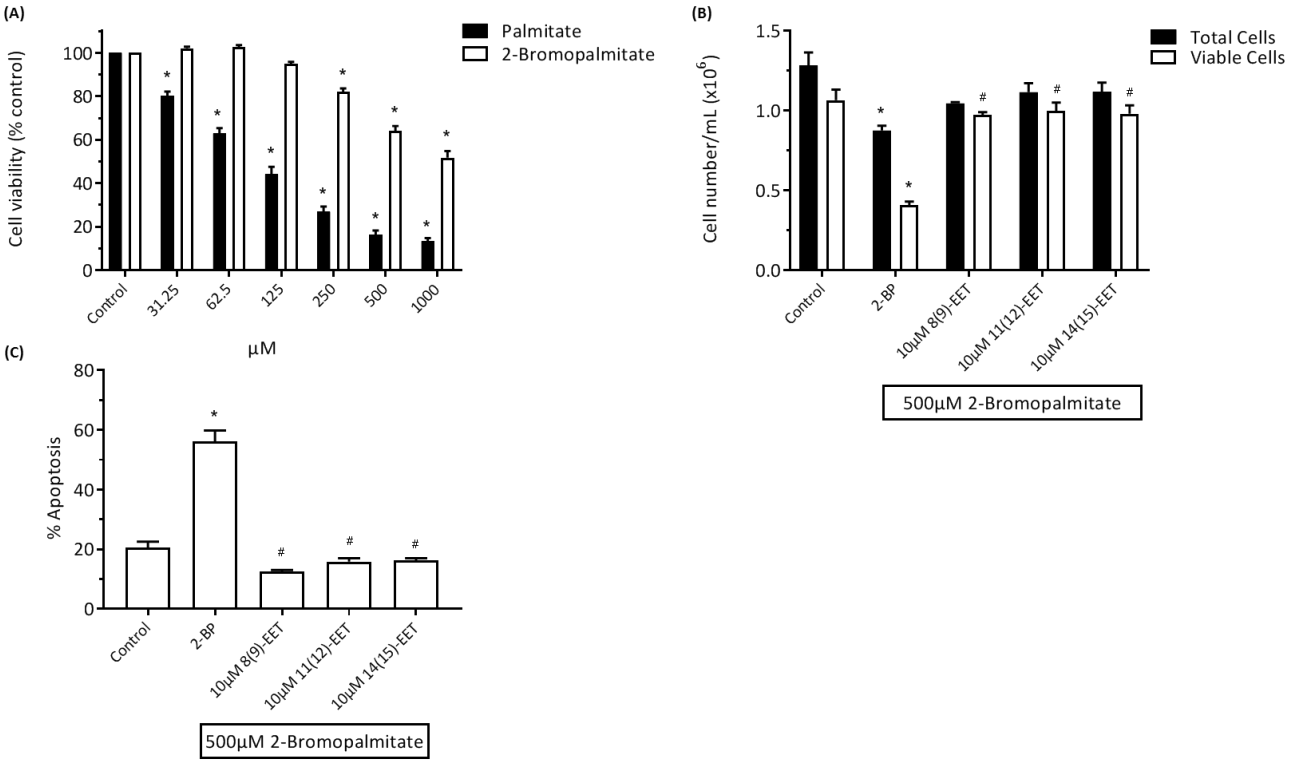

Figure 4.14. Effects of 2-Bromopalmitate on loss in cell viability in BRIN-BD11 and its attenuation by EETs. Cells were treated with increasing concentrations of palmitate and 2-Bromopalmitate (2-BP) for 24 hours before cell viability was assessed using MTT assay (A). 500µM 2-Bromopalmitate was used alone or in co-incubation with 10µM 8(9)-EET, 10µM 11(12)-EET or 10µM 14(15)-EET for 24 hours before total and viable cell numbers were assessed by trypan blue vital dye exclusion (B) or apoptosis levels quantified by flow cytometry using the MUSE™ MultiCaspase assay (C). Values are represented as mean (+/- SEM), n=3. *P<0.05 relative to corresponding control. #P<0.05 relative to corresponding 2-Bromopalmitate treatment as determine by two-way ANOVA and Bonferroni's post-test (A-B) or one-way ANOVA and Tukey's post-test (C).

Comparison of the dose-dependent loss in cell viability as assessed by the MTT assay showed that all concentrations of palmitate resulted in a significant decrease in cell viability compared to control (*P*<0.05). In contrast, 2-Bromopalmitate displayed reduced toxicity and was well-tolerated up to 125µM, with a significant decrease in cell viability observed at a concentration of 250µM, decreasing to 82.2% (+/-1.5) in comparison to 26.9% (+/-2.4) with the same concentration of palmitate; ~3-fold difference in toxicity. Increasing concentrations of 2-Bromopalmitate to 500µM and 1000µM dose-dependently reduced cell viability to 64.1% (+/-2.3) and 51.7% (+/-3.0) (*P*<0.05 vs. control), respectively. Subsequent treatment of BRIN-BD11 cells with 500µM 2-Bromopalmitate resulted in a significant decrease in viable cell number compared to control from 1.07 x10^6 cells/mL (+/-0.07) to 0.41 x10^6 cells/mL (+/-0.02)

(*P*<0.05). Although the MTT assay shows a ~3-fold difference in cell viability between palmitate and 2-Bromopalmitate, data from the trypan blue vital dye exclusion assay shows similar findings to previous data collected with 250µM palmitate with this method, again suggesting difference in assay sensitivity. Co-incubation with either 10µM 8(9)-EET, 10µM 11(12)-EET or 10µM 14(15)-EET attenuated the loss in viable cell number with 500µM 2-Bromopalmitate, resulting in a significant increase from 0.41 $x10^6$ cells/mL (+/-0.02) to 0.97 $x10^6$ cells/mL (+/-0.02), 1.00 $x10^6$ cells/mL (+/-0.05) and 0.98 $x10^6$ cells/mL (+/-0.05) (*P*<0.05), respectively. The protective effects of all EET isomers against 500µM 2-Bromopalmitate was further confirmed when apoptosis was assessed, showing a significant increase in apoptosis in response to 2-Bromopalmitate alone compared to control from 20.5% (+/-2.0) to 56.2% (+/-3.6) (*P*<0.05), an almost 3-fold increase, similar to the data with palmitate. The addition of 10µM of each EET isomer, resulted in a significant decrease in apoptosis compared to 2-Bromopalmitate alone from 56.2% (+/-3.6) to 12.6% (+/-0.4) for 8(9)-EET, 15.9% (+/-1.1) for 11(12)-EET and 16.3% (+/-0.7) for 14(15)-EET (*P*<0.05), to levels not significantly different to the control (*P*>0.05), showing that EETs can protect against cell death and apoptosis in response to the poorly metabolisable palmitate analogue, supporting data from some of the inhibitor studies.

Poorly metabolisable unsaturated FFA analogues, such as methyl-palmitoleate, have also been extensively studied to explore potential mechanisms of cytoprotection. One such analogue of EETs, a methylsulphonamide derivative which cannot be esterified to CoA and so is not a substrate for TAG formation or β-oxidation, was employed in the current study. As a 14(15)-EET-SI derivative was used, its effects against palmitate toxicity were compared against 14(15)-EET at equal concentrations (figure 4.15).

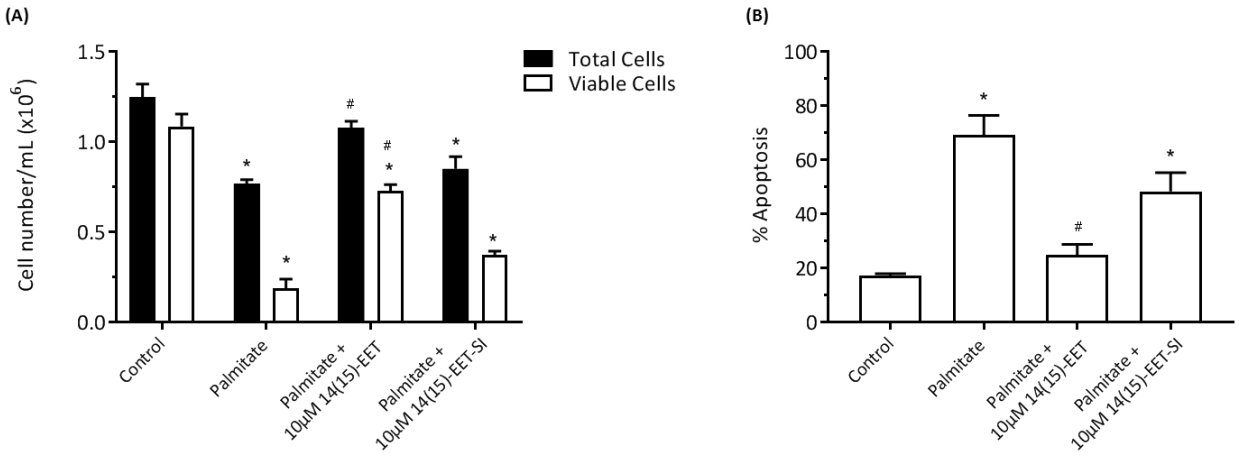

Figure 4.15. Effects of 14(15)-EET-SI and 14(15)-EET against palmitate-induced loss in cell viability and apoptosis induction. Cells were treated with 250μM palmitate alone or in co-incubation with 10μM 14(15)-EET or 10μM 14(15)-EET-SI for 24 hours before total and viable cell numbers were determined by trypan blue vital dye exclusion assay (A) and apoptosis assessed by flow cytometry using the MUSE™ MultiCaspase assay (B). Values are represented as mean (+/- SEM), n=3. *P<0.05 relative to corresponding control and #P<0.05 relative to corresponding palmitate alone as determined two-way ANOVA and Bonferroni's post-test (A) or one-way ANOVA and Tukey's test (B).

In support of all previous data, 14(15)-EET exerted protective effects against palmitate toxicity, significantly increasing viable cell number from 0.19 x10^6 cells/mL (+/-0.05) to 0.73 x10^6 cells/mL (+/-0.04) (*P*<0.05). In comparison, co-incubation with 14(15)-EET-SI resulted in a significant decrease of ~50% in viable cell number compared to 14(15)-EET, with no significant increase compared to palmitate alone (*P*>0.05). To confirm this result, apoptosis profiling was carried out by assessment of caspase activation which showed that 14(15)-EET significantly attenuated the increase in apoptosis induced by palmitate from 69.2% (+/-7.3) to 25% (+/-3.8) (*P*<0.05). Although 14(15)-EET-SI failed to significantly protect against palmitate-induced apoptosis, the analysis shows no significant difference in apoptosis compared to 14(15)-EET (*P*>0.05). Analysis of the data from using 14(15)-EET-SI collectively suggests that this EET derivative does not protect against palmitate toxicity, although both viable cell number and apoptosis were favourably altered, albeit not significantly. This may directly reflect that the mode of action of EETs require esterification to CoA, or the trend towards a protective effect may indicate that a higher concentration of 14(15)-EET-SI would significantly

protect against palmitate toxicity, though this was not feasible in the current study. Nonetheless, comparison of the extent of the cytoprotective effects with equivalent concentrations of EET and EET-SI, comparable to the concentrations used throughout this chapter for all EETs, demonstrates a less potent effect of the SI derivative against palmitate toxicity. Collectively, the data presented in this chapter demonstrates that EETs protect against palmitate toxicity in BRIN-BD11 cells and that whilst increased expression of genes associated with altered cellular lipid handling and a modest increase in lipid droplet accumulation was observed, data from pharmacological inhibition of some of these pathways and use of the poorly metabolisable palmitate analogues, suggest that EET action is distinct from direct changes in palmitate metabolism.

4.5 Discussion

The aims of this chapter were to investigate the potential actions of epoxyeicosatrienoic acids (EETs) and their corresponding diols, dihydroxyeicosatrienoic acids (DHETs), in an *in vitro* model of lipotoxicity associated with the pathogenesis of type 2 DM, in BRIN-BD11 cells. AA can be metabolised by COX, LOX and cytochrome P450 enzymes which, in addition to various prostaglandins and leukotrienes, produce three classes of NADPH-dependent oxidative reaction products; i) epoxidation leading to the production of 5(6)-EET, 8(9)-EET, 11(12)-EET and 14(15)-EET, ii) allylic oxidation producing 5,8,9,11,12 and 15 HETEs and iii) hydroxylation forming 19 and 20-HETE (Capdevila *et al.,* 1992). Although the roles of the COX and LOX pathways of AA metabolism have been well-studied in beta cell models, with the contribution of their reaction products when applied exogenously reported (Bleich *et al.,* 1997; Carboneau *et al.,* 2017; Robertson, 2017), comparatively little is known about the contribution of CYP450-derived EETs in these models (Xu *et al.,* 2016). Therefore the current data provides the entirely novel observations that EETs, but not DHETs, protect against palmitate-induced loss in cell viability and apoptosis induction in BRIN-BD11 cells. Whilst the anti-inflammatory activity of EETs is well-established in a number of models and others have shown that modulation of endogenous EET levels through over-expression of CYP 2J2, knockout of sEH or its inhibition can attenuate diet-induced hepatic dysfunction and improve insulin resistance in *db/db* mice (Battaieb *et al.,* 2013; Li *et al.,* 2015), little is known about the contribution of EETs to beta cell dysfunction. Earlier observations that EETs may positively influence insulin secretion (Falck *et al.,* 1983) have been challenged more recently (Klett *et al.,* 2013), although others have shown that sEH inhibition or knockout can improve glucose tolerance and increase beta cell mass in STZ-induced DM in mice (Luo *et al.,* 2010; Chen *et al.,*

2013). Therefore the current data provides the first direct evidence of a role for EETs in a cellular model of lipotoxicity in response to a physiologically relevant inducer of beta cell death.

The current study investigated the roles of three distinct EET isomers, 8(9)-EET, 11(12)-EET and 14(15)-EET, reported to be produced by CYP450 isoforms 2J and 2C from the epoxidation of AA. Human CYP2C9, which displays high sequence homology to rat CYP2C11, with the rat isoforms shown to be present in rat islets (Chen *et al.,* 2013), produces these three EETs at a relative ratio of 2.3:1.0:0.5 and so the 14(15)-EET is the predominant species (Zeldin, 2001). Whilst these enzymes are capable of producing all four EET isomers, the 5(6)-EET species is highly reactive due to the proximity of the epoxide group to the carboxylic acid group, facilitating rapid hydration to the DHET and/or other products, hence why a comparison between any effects of 5(6)-EET and 5(6)-DHET was not included in the current study. Initial investigations into the protective effects of 5(6)-EET were explored however, inherent difficulties in preparation with BSA and subsequent cell treatment, resulted in an increase in cell death, likely due to poor solubility and formation of aggregate species, visible under a light microscope at all 5(6)-EET concentrations trialled.

Cytoprotective actions of EETs against cell death and apoptosis induction in response to 250µM palmitate was assessed by the MTT assay, trypan blue vital dye exclusion assays and the MUSE™ MultiCaspase assay for apoptosis assessment by flow cytometry. Establishing protective effects with several complementary viability assay was necessary, since limitations with the nature of some assays was highlighted in the current data. With the MTT assay largely reflective of mitochondrial activity, it is likely that treatment with fatty acids may alter the respiratory capacity of mitochondria, resulting in an artefact of this assay being that cell

viability appeared limited to ~80-90% regardless of EET concentration (also observed with AA treatment in Chapter 3). This was particularly evident with 8(9)-EET, where concentrations above 2.5µM showed an apparent decrease in cell viability, which was not observed when viable cell numbers were determined, or from apoptosis profiling. Indeed a consistent observation in the current data is that the relative decrease in palmitate toxicity in response to EET treatment was greatest with 8(9)-EET, with this and 11(12)-EET showing complete protection, in comparison to 14(15)-EET, when assessed with the MultiCaspase assay. Reasons for this are not known but it may be that the position of the epoxide groups relates to a differential binding affinity to extra- or intra- cellular targets, or that the mode of action differs between distinct EET species, though there is no evidence to support the latter in the current data. Equally, these differences may also relate to the ability of EET species to readily undergo further metabolic processing, with EETs known to be substrates for COX and LOX pathways producing hydroxy-EETs (Rand *et al.,* 2017). Similarly, EETs are thought to also under β-oxidation producing several shortened-chain epoxide and hydroxy species with reported biological activity (Fang *et al.,* 2004). Therefore it is interesting that of the EET species considered in the current data, 8(9)-EET displayed a higher degree of cytoprotection than the more predominant 11(12)-EET and, to a greater degree, 14(15)-EET isomers. Given this, fewer studies have directly assessed the biological role of 8(9)-EET/DHET in cellular models, with most reporting on the action of 11(12)- and 14(15)-EETs and similarly, studies on the endogenous production of EETs through over-expression of relevant CYP450- epoxygenases have largely attributed observed effects to production of these two EETs, therefore the current data also emphasises an important biological role, with an overall greater potency, of 8(9)-EET compared to other isomers.

In contrast to EETs, all DHETs failed to attenuate palmitate toxicity in the current data. The conversion of EETs to DHETs represents the major route of EET metabolism and the diol products are widely reported to display considerably reduced activity compared to EETs, supported in studies exploring the beneficial effects of sEH inhibition (Xu *et al.,* 2016). sEH inhibitors, limiting EET conversion to DHETs, have been shown to partially enhance the mitogenic activity of 8(9)-EET in endothelial cells (Pozzi *et al.,* 2005) and sEH inhibitors enhanced beta cell mass in STZ-induced DM (Luo *et al.,* 2010), though this study did not address the relative ratios of different EET/DHET species, nor mechanisms of EET action. Activity of 11(12)- and 14(15)-DHETs in Ca^{2+}-activated K^{+} channels has been reported in isolated rat coronary arterial myocytes (Lu *et al.,* 2001) and the hypoxic response of human hepatoma cells and umbilical artery endothelial cells (Suzuki *et al.,* 2008), and whilst others have shown that 14(15)-DHET has weak binding affinity to a putative EET membrane receptor (Yang *et al.,* 2010), this was attributed to antagonistic activity with a radiolabelled 14(15)-EET analogue. Nonetheless, the current data supports a low activity of DHETs in context to the attenuation of lipotoxicity in BRIN-BD11 cells and that sEH inhibitors may be attractive in improving functional beta cell mass, as shown in limited *in vivo* data (Luo *et al.,* 2010; Chen *et al.,* 2013).

Mechanisms of EET action remain to be fully elucidated, though data have suggested activity at an, as yet unidentified, extracellular receptor (Yang *et al.,* 2008; Lui *et al.,* 2017). GPR40 is reported to be highly expressed in islets (Itoh *et al.,* 2003), predominately in beta cells and its expression has also been shown in several beta cell lines, with MIN6 cells showing the highest expression at the mRNA level, followed by β-TC-3, HIT-T15 and RINm5F. Although expression in BRIN-BD11 cells is uncertain, with low levels of GPR40 expression in RINm5f (the

parental cell line to BRIN-BD11) it is possible that BRIN-BD11 cells retain a low level of this (Itoh and Hinuma, 2005). GPR40 has been suggested to mediate, in part, the cytoprotective effects of oleate against palmitate toxicity, with reduction in effects observed with GPR40 knockdown by siRNA. Previous studies have also shown that 8(9)-EET and 14(15)-EET stimulate GPR40 activity at concentrations of 6.1µM and 1.4µM, respectively (Itoh *et al.,* 2003), broadly comparable to the EET concentrations used in the current study. Introduction of the epoxide group into AA and alteration in position of the epoxide group in different EET isomers has been shown to preferentially alter binding ability of EETs to GPR40, as seen in a study comparing 14(15)-EET GPR40 activation with AA in HEK293 cells, which required a 6.7-fold increase in the concentration of AA to produce comparable activity (Park *et al.,* 2018). Co-incubation with 5(6)-, 8(9)-, 11(12)- and 14(15)-EET stimulated an increase in Ca^{2+}, downstream of GPR40 activation, with concentration-dependent agonistic activity and 11(12)-EET and 14(15)-EET observing increased potency compared to 5(6)-EET and 8(9)-EET (Park *et al.,* 2018), though this would not support the observations in the current data that 8(9)-EET appeared more potent in terms of attenuating palmitate toxicity. Of note though, Park *et al.,* (2018) also showed that 11(12)-DHET and 14(15)-DHET had comparably lower affinity in activating GPR40 than EETs (Park *et al.,* 2018). However in the current data, treatment with the GPR40 antagonist in combination with 250µM palmitate co-incubated either 2.5µM 8(9)-EET, 10µM 11(12)-EET or 10µM 14(15)-EET, failed to attenuate EET action suggesting that although EETs may be reported to bind GPR40, effects in this model are GPR40-independent. Equally, whether or not EETs display potent activity at GPR40 waits to be confirmed in further studies, especially since other recent data screening EET activity at 105 GPCRs failed to identify a single high-affinity receptor site (Lui *et al.,* 2017). Similarly, although GPR120 has been shown to be involved in insulin secretion and its activation may be protective against

palmitate toxicity through regulation of Pdx-1 activity (Wang *et al.,* 2019), effects of EET action in BRIN-BD11 cells were unaffected by the presence of a GPR120 antagonist.

Whether EETs signal through an extracellular receptor site remains to be determined and cannot be entirely excluded based on the current data. However, the recent observations that EETs may act through several low affinity prostaglandin (PG) receptors (including $PTGER_2$, $PTGER_4$, PTGFR, PTGDR and $PTGER_3$IV), conclude that EETs may signal through multiple GPCRs (Lui *et al.,* 2017). Of note, this may be important in a beta cell context since the roles of prostaglandins in regulating beta cell function have been well-studied (reviewed recently by Carboneau *et al.,* 2017) and whilst the role of PGE_2 in insulin secretion (which signals through $PTGER_2$, $PTGER_4$ and $PTGER_3$IV) remains unclear, activation of these receptors (and PTGDR by PGD) leads to increased cAMP, supporting a possible role in EET-Gαs signalling, as reported by others; an effect that can be blocked with the EET antagonist 14(15)-EEZE (Wong *et al.,* 2000; Yang *et al.,* 2008). The concentrations of EETs used in this study (10µM), whilst comparable to some other studies (Davies *et al.,* 2002; Gross *et al.,* 2013), precluded use of the 14(15)-EEZE antagonist, since the requirement for a molar excess of the antagonist would have resulted in a higher residual ethanol concentration yielding artefactual effects in vehicle controls. However, although EETs are reported to bind to extracellular sites and indeed may display important autocrine and paracrine signalling activity (Spector and Norris 2006), extracellular activity of EETs in the current model is inconsistent with the observation that the non-metabolisable analogue 14(15)-EET-SI failed to confer a similar level of protection against palmitate as the free-EET, which may support intracellular activity and the requirement for EET esterification to CoA.

Other more well-established mechanisms of EET action are their roles as endogenous PPAR agonists, particularly PPARγ and, to a lesser extent, PPARα (Liu *et al.,* 2005; Fang *et al.,* 2006). However, in the current data investigations into the actions of each EET isomers co-incubated with 250μM palmitate in the presence of PPARα, β/δ, γ antagonists did not attenuate EET action. Although a modest reduction in cell viability when assessed by the MTT assay was observed in response to palmitate treatment alone and with EETs, the relative increase in cell viability between this group and in co-incubation was comparable regardless of the presence of the PPAR antagonists. Confirmatory analysis with trypan blue vital dye exclusion and MultiCaspase assay with 8(9)-EET supported these observations and although it was not feasible to carry out additional confirmatory tests in this way with all EET isomers, comparable data in the MTT assay support this observation. With RXR known to be a PPAR heterodimer binding partner, HX531 (RXR antagonist), was also used alone and in combination with all PPAR antagonists under the same experimental conditions. As with PPAR antagonists alone, HX531 did not attenuate EET action, including in combination with the PPAR antagonists, further supporting these observations. All PPAR isoforms have been reported to be expressed in BRIN-BD11 cells (Welters *et al.,* 2004c), so a lack of PPAR-dependency cannot be attributed to lack of expression in the current model. Additionally, the activation of PPARγ by TZDs in this cell line has only been observed using supraphysiological concentrations of rosiglitazone, at concentrations which failed to attenuate palmitate-induced cell death (Welters *et al.,* 2004c). Similarly, conflicting observations in MIN6 mouse beta cells have reported differential effects of TZDs in models of lipotoxicity (Nakamichi *et al.,* 2003; Saitoh *et al.,* 2008; Hong *et al.,* 2018); such differences may be reflective of differential expression levels of PPARs and/or co-activator proteins between different beta cell line models (Welters

et al., 2004c). Additional studies should determine through use of PPRE luciferase constructs whether or not EETs lead to an increase in PPAR activation in BRIN-BD11 cells.

Others have reported a differential expression of genes associated with FFA metabolism in BRIN-BD11 cells in response to AA treatment (Keane *et al.,* 2011). Although there is conflicting data in beta cell models on whether changes in lipid handling can alter the extent of lipotoxicity (Cnop *et al.,* 2001; Busch *et al.,* 2005; Borg *et al.,* 2009; Sol *et al.,* 2008; Sargsyan and Bergsten*,* 2011) and if this contributes to the cytoprotective effects of mono- and poly-unsaturated FFAs (Moffitt *et al.,* 2005; Diakogiannaki et al., 2007; Plotz *et al.,* 2016), whether or not similar changes were associated with EET effects were explored in the current model. RT-PCR analysis showed that CPT1, Ech1 and DGAT were over-expressed in cells treated with palmitate in the presence of each EET, with effects more pronounced with 8(9)-EET. Collectively, this may indicate increased entry of fatty acids into β-oxidation pathways and/or TAG formation, with current data also suporting a modest increase in intracellular lipid droplets in response to EET treatment. However, pharamcological inhibition of DGAT or CPT1, alone and in combination, did not block the protective effects of EETs against palmitate toxicity. A previous study in HIT-T15 beta cells did show that the DGAT inhibitor, Xanthohumol, markedly reduced the protective effects of AA against palmitate toxicty at concentrations up to 10µM of the inhibitor (Cho *et al.,* 2012). However, this data was only reported from an MTT assay, which may be limited in application to studies focused on FFA treatment/metabolic dysfucntion, with additional confirmatory analysis required, evident in the current data. Although attenuation of AA effects were observed at 10µM Xanthohumol, concentrations of 20µM were shown to be toxic to the cells, with 1µM producing a measured cell viability approaching 75% (Cho *et al.,* 2012), close to the limit of 80-90% achieved with EETs in the

current data. Overall this data suggests that whilst an increase in DGAT expression and formation of TAG/lipid droplets was observed in BRIN-BD11 cells treated with all EETs in the presence of palmitate, that this is dispensible for their cytoprotetive effects. In support of this, previous studies have shown that although palmitoleate increased TAG formation in BRIN-BD11 cells, this was not observed with the poorly metabolisable methyl-ester; a treatment which still protected against palmitate-induced loss in cell viability (Diakogiannaki *et al.,* 2007). Similarly, previous studies have shown that 200μM Etomoxir failed to block the protective effects of palmitoleate after 48 hours (Welters *et al.,* 2004a), with similar effects observed with EET treatment, suggesting that increased mitochondrial β-oxidation is not a mode of action of EETs against palmitate toxicity. Inhibition of SCD was also explored, this has been previously shown to desaturate palmitate into palmitoleate and protect CHO cells against apoptosis (Listenberger *et al.,* 2003). However, treatment of BRIN-BD11 cells with 2μM of the SCD inhibitor A939572, similar to the CPT1 and DGAT inhibitor did not alter the relative effect of EETs in increasing cell viability in response to palmitate. Collectively, this data with a range of pharmacological inhibitors suggest that EET action is independent to TAG synthesis or enhancement of palmitate β-oxidation.

In HepG2 cells Zhang *et al.,* (2015) reported that EETs increased fatty oxidation in a PPARα and AMPK-dependent manner and although this is in contrast to the current data with Etomoxir, alone and in combination with Xanthohumol, whether EET action against lipotoxicity occurs via an enhancement of β-oxidation was explored using the palmitate derivative, 2-Bromopalmitate. This species has been shown to display toxicity in primary culture models exceeding that of palmitate and although it can be esterified to CoA it is not a substrate for further metabolic processing in context to TAG synthesis or β-oxidation (Cnop *et*

al., 2001). In cell line models, low concentrations of 2-Bromopalmitate appear well-tolerated and may protect against lipotoxicity, likely through sequestration of CoA and inhibition of post-translational protein modification by palmitoylation, as well as reported inhibitory action at CPT1 (Chase and Tubbs, 1972; Bladwin *et al.,* 2012). Higher concentrations of 2-Bromopalmitate are toxic to beta cells (Cnop *et al.,* 2001), as demonstrated in the current data whereby concentrations exceeding 250μM significantly reduced cell viability in BRIN-BD11 cells. Similar to the palmitate data, all EET isomers markedly reduced the loss in cell viability and increased apoptosis induction in response to 2-Bromopalmitate, suggesting that EET action is not via an enhancement of fatty acid oxidation, as suggested by others (Zhang *et al.,* 2015) and supporting the current data with Etomoxir.

The poorly metabolisable 14(15)-EET analogue, 14(15)-EET-SI, which contains a substituted methyl sulphonamide group insensitive to esterification to CoA, β-oxidation or membrane esterification, showed no significant protection against palmitate. In contrast to other studies using methyl-ester derivatives and poorly metabolisable mono- and poly-unsaturated FFAs (Diakogiannaki et al., 2007; Dhayal and Morgan 2011), this data suggests that esterification to CoA and/or further metabolic processing is necessary for EET action. Although EETs are substrates for membrane esterification to phospholipids, represening an important mechanisms controlling cellular levels of free EETs (Klett *et al.,* 2013), EET action in the current model was insentive to PLA_2 inhibition, suggesting against incorporation/release of EETs into phosopholipid pools. EETs are also known to be converted to biologically active shortened-chained epoxides and other derivatives, as well as being metabolites for COX and LOX enzymes, which may indicate an important contribution of EET metabolites in this model. However, whilst 14(15)-EET-SI did not significantly attenuate the palmitate-induced increase

in apoptosis, in contrast to 14(15)-EET, the mean apoptosis was reduced to a level not significant to either palmiate alone or in the presence of 14(15)-EET. This may indicate that higher concentrations of the SI derivative would be required, possibly reflecting a reduction in delivery of the analogue to the cells and/or changes in binding affinity to BSA in which the EETs were first prepared to maintain the 3.3:1 FFA:BSA ratio during culture. Nonetheless, the data demonstrates a limited effect of the EET derivative in the amelioration of palmitate toxicity.

4.6 Conclusion

The data collected in this chapter report novel observations of the protective actions of 8(9)-EET, 11(12)-EET and 14(15)-EETs against palmitate toxicity in BRIN-BD11 cells as an *in vitro* model of lipotoxicity associated with the pathogenesis of type 2 DM. In agreement with others that report reduced activity of the EET vicinal diol products from sEH metabolism; 8(9)-DHET, 11(12)-DHET and 14(15)-DHET did not exert any protective effects against palmitate toxicity. The current data also indicate that EET action appears independent of agonistic activity at the extracellular receptors, GPR40 and 120 or intracellular PPAR receptors. Whilst this does not preclude that EETs are acting via receptor-mediated agonistic effects, further studies are needed to define a specific high-affinity EET putative receptor, or to further confirm that activity may be mediated through multiple low-affinity sites. The current data from RT-PCR, lipid droplet formation and inhibitor studies targeting SCD1, CPT1 and DGAT suggest that although EET actions may modulate intracellular lipid handling, cytoprotective effects appear independent to this, supported with data showing protective effects against 2-Bromopalmitate. Collectively, this suggests that EETs may act at a distal step in the apoptotic pathway, possibly via regulation of the release of cytochrome c from the mitochondria through alterations in the synthesis of cardiolipin, a mitochondrial phospholipid with activity associated with the regulation of apoptosis. It has been suggested that increased levels of monounsaturated fatty acids may promote cardiolipin synthesis in beta cells contributing to mechanisms of cytoprotection (Welters *et al.,* 2004a). Of note Kiebish *et al.,* (2012) observed an increase in cellular EET levels in mice with transgenic over-expression of cardiolipin synthase and Ting *et al.,* (2015) showed that treatment of H9C2 cardiac myoblasts with polyunsaturated FFAs, including AA, increased cellular cardiolipin content. Although no

studies have directly addressed the role of EETs in cardiolipin modelling, this may represent an important control point in the regulation of apoptosis by EETs. The current data therefore observes, for the first time, that the AA-derived eicosanoids EETs are cytoprotective against palmitate toxicity in a beta cell model and supports a rationale for further studies to elucidate their mode of action and indeed whether their cytoprotective effects and reported anti-inflammatory activity can be recapitulated in beta cell models of pro-inflammatory cytokine toxicity.

Chapter Five

5. Cytoprotective effects of epoxyeicosatrienoic acids and their derivatives in *in vitro* models of type 1 DM

5.1 Introduction

In type 1 DM, pro-inflammatory cytokines are well-documented to contribute to a reduction in functional beta cell mass as part of the autoimmune attack during insulitis. The presence of $CD8^+$ T-cells and other APCs form the basis of a regimented attack, specifically targeting beta cells, resulting in beta cell apoptosis and reduced insulin production (Cardozo *et al.,* 2003; Pirot *et al.,* 2008; Willcox *et al.,* 2009). Mechanisms associated with this include FasL/FasR binding and the release of the pro-apoptotic factors perforin/granzyme B, pro-inflammatory cytokines and an increase in NO/ROS (Yoon and Jun, 2005). Treatment of beta cell lines with the cytokines IL-1β, IFN-γ and TNF-α in varying concentrations and combinations increase cell death and apoptosis via synergistic effects resulting in the induction of several known pro-apoptotic pathways. These effects are exerted through activation of NF-κB, IRF-1 and STAT1, leading to alterations in target gene expression, including iNOS expression and subsequent production of NO however, both NO-dependent and NO-independent effects in different beta cell and islet models have been reported (Southern *et al.,* 1990; Eizirik *et al.,* 1996; Cnop *et al.,* 2005). Although limited studies have documented the cytokine response in BRIN-BD11 cells, particularly with regards the contribution of cytokine-derived NO production, collectively, the data reported in comparison to other cell line models suggest that BRIN-BD11 cells are less sensitive to NO (Michalska *et al.,* 2010; Hsu *et al.,* 2012). In context to the effects of unsaturated FFA species in cell line models of pro-inflammatory cytokine toxicity, previous

studies in BRIN-BD11 cells have shown that co-incubation with 500µM palmitoleate ameliorates cytokine-induced cell death by ~50%, a response that was not associated with a reduction in cytokine-induced NO production, suggesting an NO-independency of cytokine toxicity in this model and that unsaturated species may act at a distal step in the apoptotic pathway (Welters *et al.,* 2004).

Whilst EETs have not been studied in the context of pro-inflammatory cytokine toxicity in beta cell models, their anti-inflammatory activity is well-documented in other models, with 8(9)-EET, 11(12)-EET and 14(15)-EET attenuating TNF-α-induced apoptosis in primary rat cardiomyocytes (Zhao *et al.,* 2012). In other cardiovascular models IL-1β and TNF-α negatively impact the production of EETs and reduce expression of cytochrome p450 2C epoxygenases in endothelial cells and 11(12)-EET has been shown to decrease LPS-stimulated PGE_2 production via dose-dependent inhibition of COX-2 (Kessler *et al.,* 1999; Sudhahar *et al.,* 2010). Mechanistically, the anti-inflammatory action of EETs is, in part, attributed to a reduction in NF-κB activation, with studies in endothelial cells observing that treatment with 11(12)-EET in the presence of TNF-α reduced nuclear accumulation of the p65 subunit of activated NF-κB, showing that 11(12)-EET and to a lesser extent 5(6)-EET and 8(9)-EET, but not 14(15)-EET, prevented the rapid degradation of IκB-α by inhibition of IKK (Node *et al.,* 1999). In support of this action, human dermal fibroblasts transfected with NF-κB-responsive IL6 luciferase reporter vector showed TNF-α induced luciferase activity was reduced in co-incubation with EETs (Rompe *et al.,* 2010).

Anti-inflammatory activity of EETs, including their capacity to limit NF-κB activation, have been partly attributed to their role as PPAR antagonists, with PPARγ shown to increase expression of IκBα, which retains NF-κB in an inactivate state in the cytosol (Scirpo *et al.,*

2016). EETs have been shown to dose-dependently antagonise the binding of a radiolabelled rosiglitazone to a recombinant PPARγ-LBD and in endothelial cells the inhibitory action of EETs against TNF-α-induced IκBα degradation was reduced in the presence of the PPARγ antagonist GW9662 (Liu *et al.,* 2005), with similar effects also reported in cardiomyocytes, attenuating LPS-induced caspase-3 activation (Zhang *et al.,* 2012; Samokhvlov *et al.,* 2014). Treatment of H9C2 cardiomyocytes with 11(12)-EET has also been associated with increased Akt phosphorylation and enhanced PI3K expression, effects markedly enhanced with a dual EET mimetic and sEH inhibitor, UA-8, and which were blocked by GW9662, again supporting a PPARγ-dependent mechanism, (Batchu *et al.,* 2011). Further *in vivo* studies observed that the EET antagonist, 14(15)-EEZE, and PI3K inhibitor, PI-103, attenuated the protective actions of EET-mediated improvements in left ventricular functional recovery following ischaemia-reperfusion, supporting a PI3K-dependent activity of EETs (Batchu *et al.,* 2012). Increased activity of the pro-survival PI3K pathway in response to EETs has also been observed to protect against apoptosis induction via upregulation of anti-apoptotic Bcl2 and Bcl_{xL} and down regulation of pro-apoptotic Bax (Dhanasekaran *et al.,* 2008), with overexpression of CYP 2J2 producing comparable EET-dependent results (Zhao *et al.,* 2012). Others have also reported that EETs can protect against apoptosis via attenuating a loss in mitochondrial membrane potential (Katragadda *et al.,* 2009), effects which may be associated with activation of a mitochondrial ATP-sensitive potassium channel (Seubert *et al.,* 2004).

5.2 Aims

Accumulating evidence supports an important anti-inflammatory action of EETs, with activity associated with the modulation of pro-inflammatory signalling pathways, including NF-κB activation, though to date no studies have directly explored such activity in a beta cell model. Therefore, the aim of this chapter is to investigate the actions of EET and DHET isomers in response to pro-inflammatory cytokine toxicity as an *in vitro* model of type 1 DM in BRIN-BD11 cells and to explore potential mechanisms of action. Specifically, the aims are to:

- characterise the actions of EETs and DHETs in response to pro-inflammatory cytokines in BRIN-BD11 cells in terms of effects on cell viability and apoptosis induction.
- investigate whether any effects of EETs and DHETs in response to cytokines are associated with changes in cytokine-induced NF-κB activity and nitrite production as an indirect assessment of cytokine-induced iNOS expression/activity.
- further investigate potential mechanisms of EET action in this model using the poorly metabolisable analogue of 14(15)-EET; 14(15)-EET-SI and an antagonist of PPARγ.

5.3 Method

Cells were treated with IL-1β (100U/mL), IFN-γ (20U/mL) and TNF-α (500U/mL) in combination; the most pathophysiologically relevant combination and having been previously established as appropriate in inducing loss in BRIN-BD11 cell viability (Chapter 3). Cell viability was assessed using the trypan blue vital dye exclusion assay since, during preliminary investigations (Chapter 3), the use of the MTT assay in the context of cytokine treatment in this cell line resulted in low-sensitivity when compared to the neutral red and trypan blue vital day exclusion assays. Equally, treatment of BRIN-BD11 cells with media supplemented with 1% FBS resulted in difficulties in obtaining reproducible results by neutral red assays under these conditions. Therefore this method was not considered further here since, in congruence with the methods used to study EET/DHET action in response to palmitate treatment (Chapter 4), all FFA species, including the EET analogue 14(15)-EET-SI, were prepared in BSA (3.3:1 molar ratio) and diluted to a final assay concentration of 10µM in media supplemented with 1% FBS for cell treatment. Apoptosis induction was determined by flow cytometry using the MUSE™ MultiCaspase assay, as a preferred method in this cell line model compared to the Annexin V & Dead Cell assay. Effects of EETs/DHETs on cytokine-induced NF-κB activation were determined using the pNL3.2.NF-κB-RE[NlucP/NF-κB-RE/Hygro] reporter vector (Promega) transfected into BRIN-BD11 cells using Lipofectamine2000® and activity determined using the Nano-Glo® Luciferase Assay System (Chapter 2.7.2), with data expressed as fold-change in luminescence units. Nitrite levels were determined using Griess reagent, relative to a sodium nitrite standard curve. To determine whether activation of PPARγ was, in part, responsible for mediating EET action against cytokine-induced apoptosis, the PPARγ antagonist T0070907 (2µM) was used in co-incubation studies.

5.4 Results

Having established the cytoprotective actions of EETs against palmitate-induced lipotoxicity in BRIN-BD11 cells, in contrast to their DHET metabolites (Chapter 4), these effects were then explored in models of cytokine toxicity. Firstly, the cytoprotective actions of 8(9)-EET, 11(12)-EET and 14(15)-EET in the presence of IL-1β (100U/mL), IFN-γ (20U/mL) and TNF-α (500U/mL) in combination were assessed by trypan blue vital dye exclusion (figure 5.1).

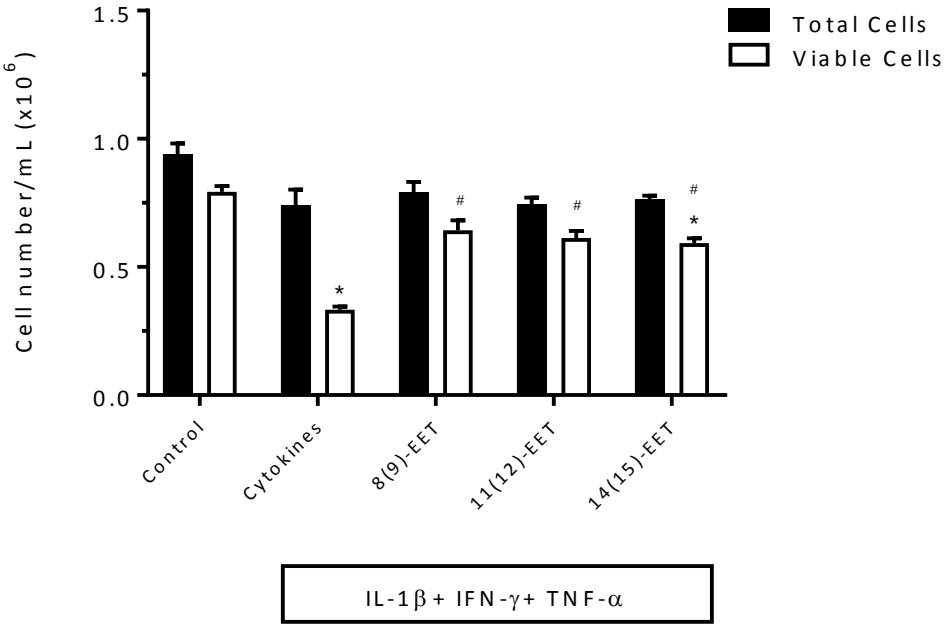

Figure 5.1. Effects of EETs on cytokine-induced BRIN-BD11 cell death. Cells were treated with IL-1β (100U/mL), IFN-γ (20U/mL) and TNF-α (500U/mL) in co-incubation with 10μM 8(9)-EET, 10μM 11(12)-EET or 10μM 14(15)-EET for 24 hours, before total and viable cell numbers were assessed by trypan blue vital dye exclusion. Values are represented as mean (+/- SEM), n=3. *P<0.05 relative to corresponding control and #P<0.05 relative to corresponding cytokine treatment alone as determined by two-way ANOVA and Bonferroni's post-test.

Treatment with cytokines for 24 hours witnessed a significant decrease in BRIN-BD11 viable cell number compared to control from 0.79 x10^6 cells/mL (+/-0.02) to 0.33 x10^6 cells/mL (+/-0.01) (*P*<0.05), confirming earlier work during preliminary investigations (Chapter 3). Co-incubation with each EET isomers and cytokines resulted in a significant increase in viable cell

number from 0.33 x10^6 cells/mL (+/- 0.01) to 0.64 x10^6 cells/mL (+/-0.04) for 10µM 8(9)-EET, 0.61 x10^6 cells/mL (+/-0.03) for 10µM 11(12)-EET and 0.59 x10^6 cells/mL (+/-0.02) for 10µM 14(15)-EET (P<0.05). Treatment with 8(9)-EET and 11(12)-EET in combination with cytokines resulted in no significant decrease in viable cells compared to control (P>0.05), suggesting complete protection from cytokine toxicity in the presence of these two EETs however, in the presence of 14(15)-EET viable cell number remained significantly lower than control (P<0.05). To further establish the protective effects of EETs in this models, BRIN-BD11 cells were assessed for apoptosis induction when treated with cytokines co-incubated with 10µM 8(9)-EET, 11(12)-EET, or 14(15)-EET, assessed by MUSE™ MultiCaspase (figure 5.2).

Cytokines in combination resulted in a significant increase in apoptosis compared to control from 14.1% (+/-2.2) to 35.4% (+/-5.7) (P<0.05). Furthermore, co-incubation with 10µM of each EET resulted in a significant decrease in total apoptosis from 35.4% (+/-5.7) to 18.5% (+/-1.9) for 8(9)-EET, 19.1% (+/-2.0) for 11(12)-EET and 19.3% (+/-1.9) for 14(15)-EET (P<0.05). Broadly in agreement with effects of EETs on cell viability, there was no significant increase in apoptosis above control in all co-incubation groups, suggesting complete protection from cytokine-induced beta cell toxicity (P>0.05).

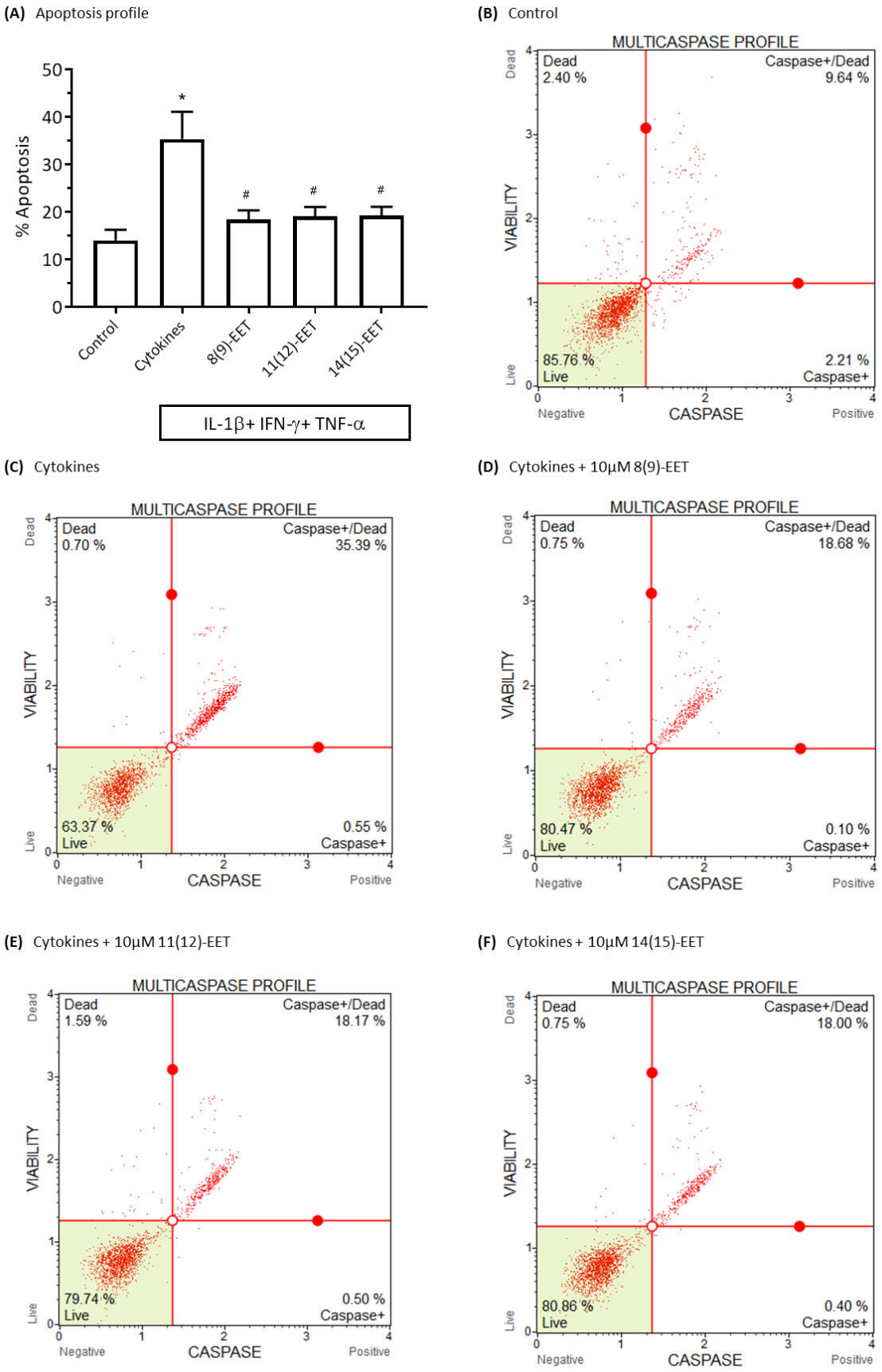

Figure 5.2. Effects of EETs on cytokine-induced apoptosis in BRIN-BD11 cells. Cells were treated with IL-1β (100U/mL), IFN-γ (20U/mL) and TNF-α (500U/mL) in combination co-incubation with either 10µM 8(9)-EET, 10µM 11(12)-EET or 10µM 14(15)-EET for 24 hours before total apoptosis profile (A) was assessed by flow cytometry with the MUSE™ MultiCaspase assay. Panels B-F show representative apoptosis profiles of cells under each treatment condition. Values in panel (A) are mean (+/- SEM), n=3. *P<0.05 relative to control and #P<0.05 relative to cytokines alone as determined by one-way ANOVA and Tukey's post-test.

With all EET isomers showing protective actions against cytokines toxicity, trypan blue vital dye exclusion and MUSE™ MultiCaspase assays were then used to assess any effects of their corresponding DHETs; 10μM 8(9)-DHET, 11(12)-DHET, or 14(15)-DHET (figures 5.3 and 5.4).

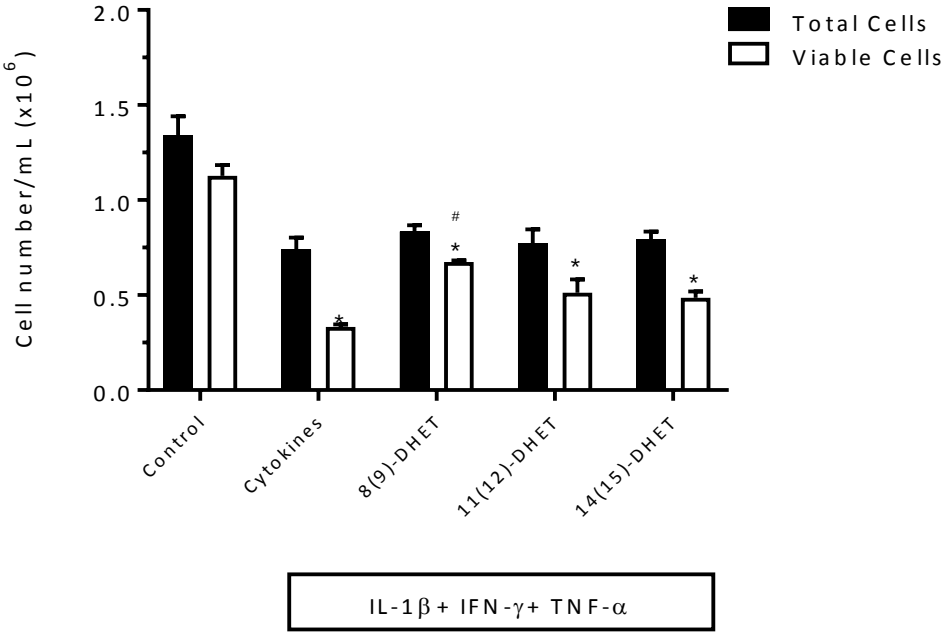

Figure 5.3. Effects of DHETs on cytokine-induced BRIN-BD11 cell death. Cells were treated with IL-1β (100U/mL), IFN-γ (20U/mL) and TNF-α (500U/mL) in co-incubation with 10μM 8(9)-DHET, 10μM 11(12)-DHET or 10μM 14(15)-DHET for 24 hours before total and viable cell numbers were assessed by trypan blue vital dye exclusion. Values are represented as mean (+/- SEM), n=3. *P<0.05 relative to corresponding control and #P<0.05 relative to corresponding cytokines alone as determined by two-way ANOVA and Bonferroni's post-test.

Remarkably, 8(9)-DHET significantly increased viable cell numbers compared to corresponding cytokine treatment alone from 0.33 x10^6 cells/mL (+/-0.01) to 0.67 x10^6 cells/mL (+/-0.01), an over 2-fold increase. As with the lipotoxicity model (Chapter 4), 11(12)-DHET and 14(15)-DHET failed to ameliorate cytokine-induced loss in cell viability. Furthermore, co-incubation with 10μM of each DHET resulted in a significant decrease in total apoptosis only with 8(9)-DHET from 41.33% (+/-4.5) to 21.71% (+/-2.4) (P<0.05), with 11(12)-DHET and 14(15)-DHET showing no significant decrease in total apoptosis (P>0.05).

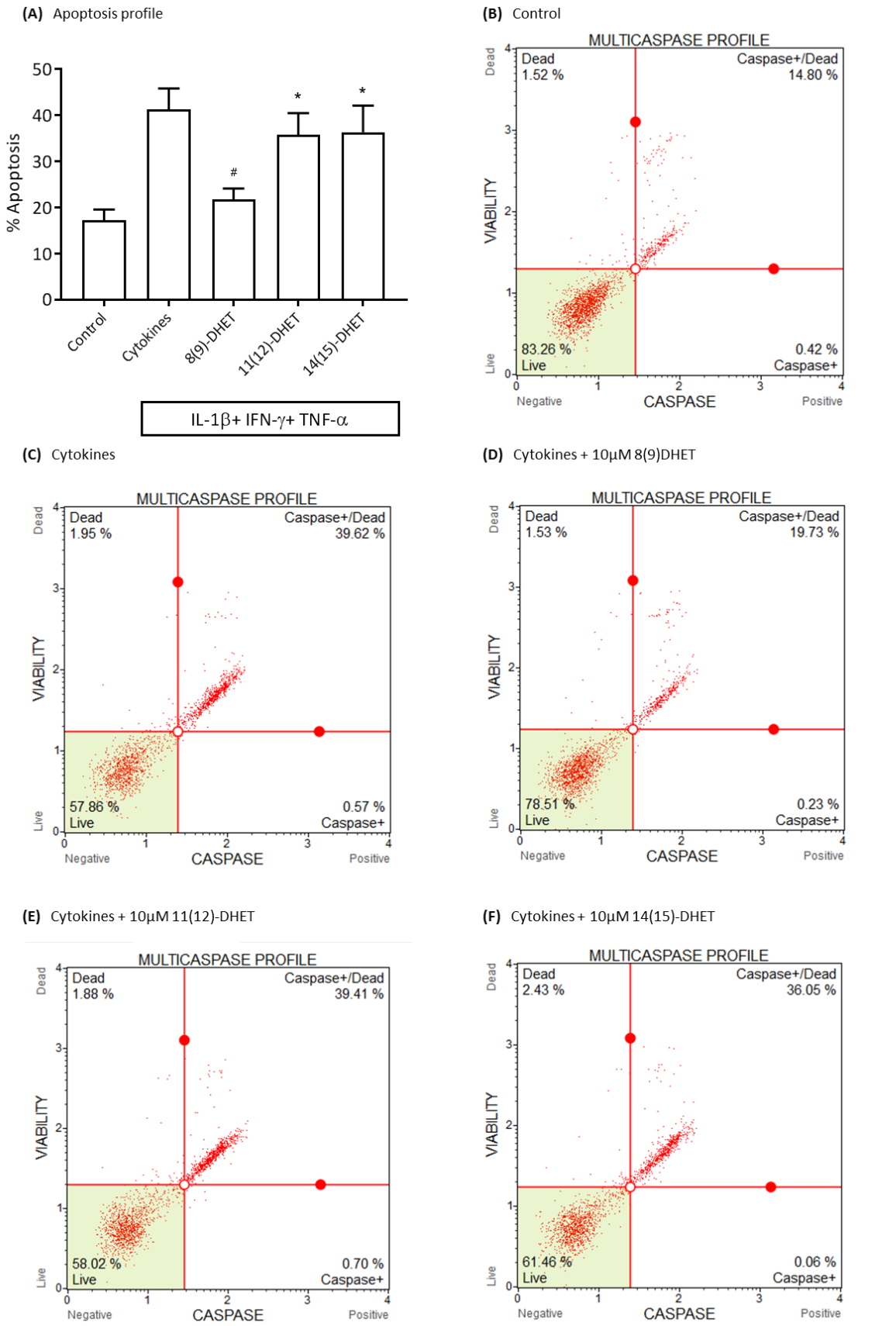

Figure 5.4 Effects of DHETs on cytokine-induced apoptosis in BRIN-BD11 cells. Cells were treated with IL-1β (100U/mL), IFN-γ (20U/mL) and TNF-α (500U/mL) in combination co-incubation with either 10µM 8(9)-DHET, 10µM 11(12)-DHET or 10µM 14(15)-DHET for 24 hours before total apoptosis profile (A) was assessed by flow cytometry with the MUSE™ MultiCaspase assay. Panels B-F show representative apoptosis profiles of cells under each treatment condition. Values in panel (A) are mean (+/- SEM), n=3. *P<0.05 relative to control and #P<0.05 relative to cytokines alone as determined by one-way ANOVA and Tukey's post-test.

With 8(9)-DHET unexpectedly showing similar protective effects to EETs, apoptosis induction was re-assessed to confirm this observation and provide a direct comparison between EETs and 8(9)-DHET (figure 5.5).

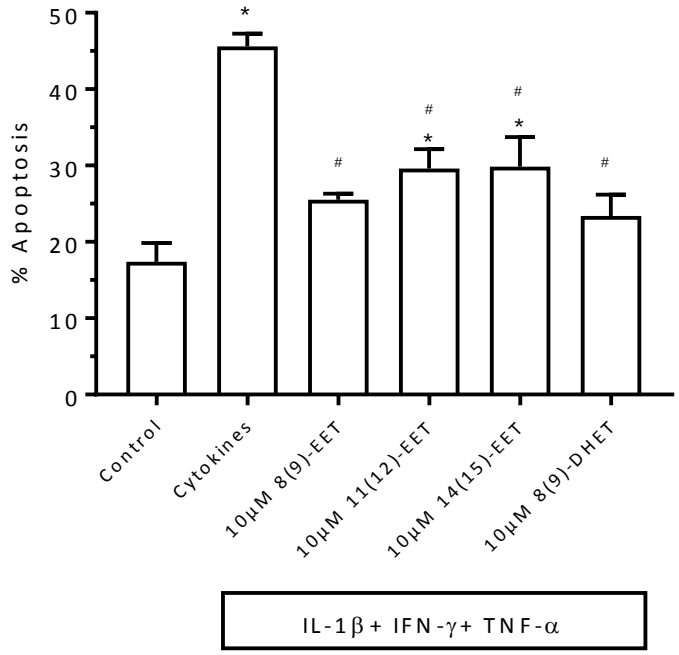

Figure 5.5. Effects of EETs and 8(9)-DHET on cytokine-induced apoptosis. Cells were treated with IL-1β (100U/mL), IFN-γ (20U/mL) and TNF-α (500U/mL) in combination co-incubated with either 10μM 8(9)-EET, 10μM 11(12)-EET, 10μM 14(15)-EET or 10μM 8(9)-DHET for 24 hours before apoptosis induction was assessed by flow cytometry with the MUSE™ MultiCaspase assay. Values are represented as mean (+/- SEM), n=3. *P<0.05 relative to control and #P<0.05 relative to cytokines alone as determined by one-way ANOVA and Tukey's post-test.

Treatment with cytokines in combination with 10μM 8(9)-EET, 10μM 11(12)-EET, 10μM 14(15)-EET and 10μM 8(9)-DHET resulted in a significant decrease in apoptosis from 45.6% (+/-1.6) to 25.5% (+/-0.8), 29.6% (+/-2.6), 29.8% (+/-3.9) and 23.4% (+/-2.8) (P<0.05), respectively, confirming the previous data on their protective effects (figure 5.2). Interestingly, 8(9)-DHET produced the largest decrease in apoptosis compared to all EETs, however there was no significance between EET and DHET treatments (P>0.05), confirming the surprising protective effects of 8(9)-DHET against cytokine toxicity.

With EETs reported to reduce NF-κB activity in other models, NF-κB activation was assessed using a NF-kB luciferase reporter assay in BRIN-BD11 cells treated with cytokines in combination, co-incubated with 10μM 8(9)-EET, 10μM 11(12)-EET and 10μM 14(15)-EET for 24 hours (figure 5.6).

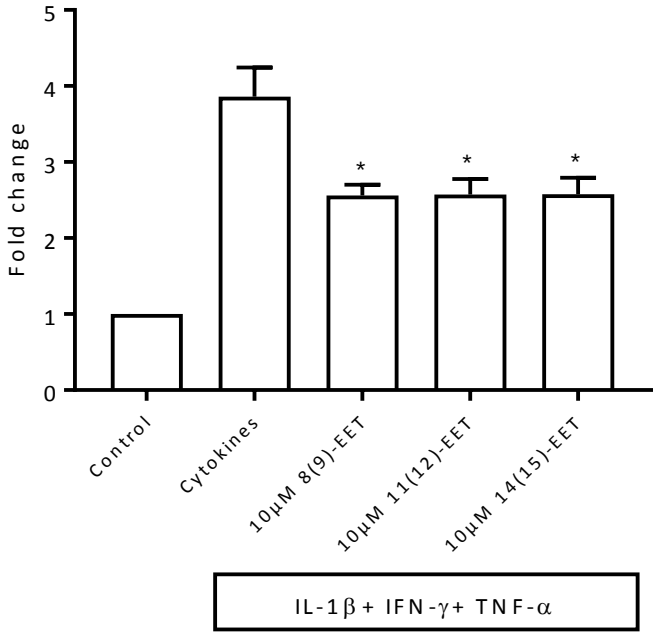

Figure 5.6. Effects of EETs on cytokine-induced NFκB activity in BRIN-BD11 cells. Cells were treated with IL-1β (100U/mL), IFN-γ (20U/mL) and TNF-α (500U/mL) in combination co-incubation with either 10μM 8(9)-EET, 10μM 11(12)-EET or 10μM 14(15)-EET for 24 hours before NF-κB activity was assessed using a NF-κB Luciferase Reporter assay. Values are represented as mean fold change in luminescence units relative to control (+/- SEM), n=5. *P<0.05 compared to cytokines as determined by one-way ANOVA and Tukey's post-test.

Treatment with cytokines alone resulted in a significant increase in NF-κB activity 3.9-fold compared to control (P<0.05) which was significantly reduced by ~34% in co-incubation with each EET isomer (P<0.05), though this remained elevated over 2-fold above control. With all EETs showing a significant decrease in NF-κB activity, investigations into whether this was also associated with a decrease in nitrite production, likely by a reduction in iNOS expression,

nirite levels were assessed by Griess assay over 24 and 48 hours (figure 5.7); this data was additionally collected in cells treated with different cytokine combinations.

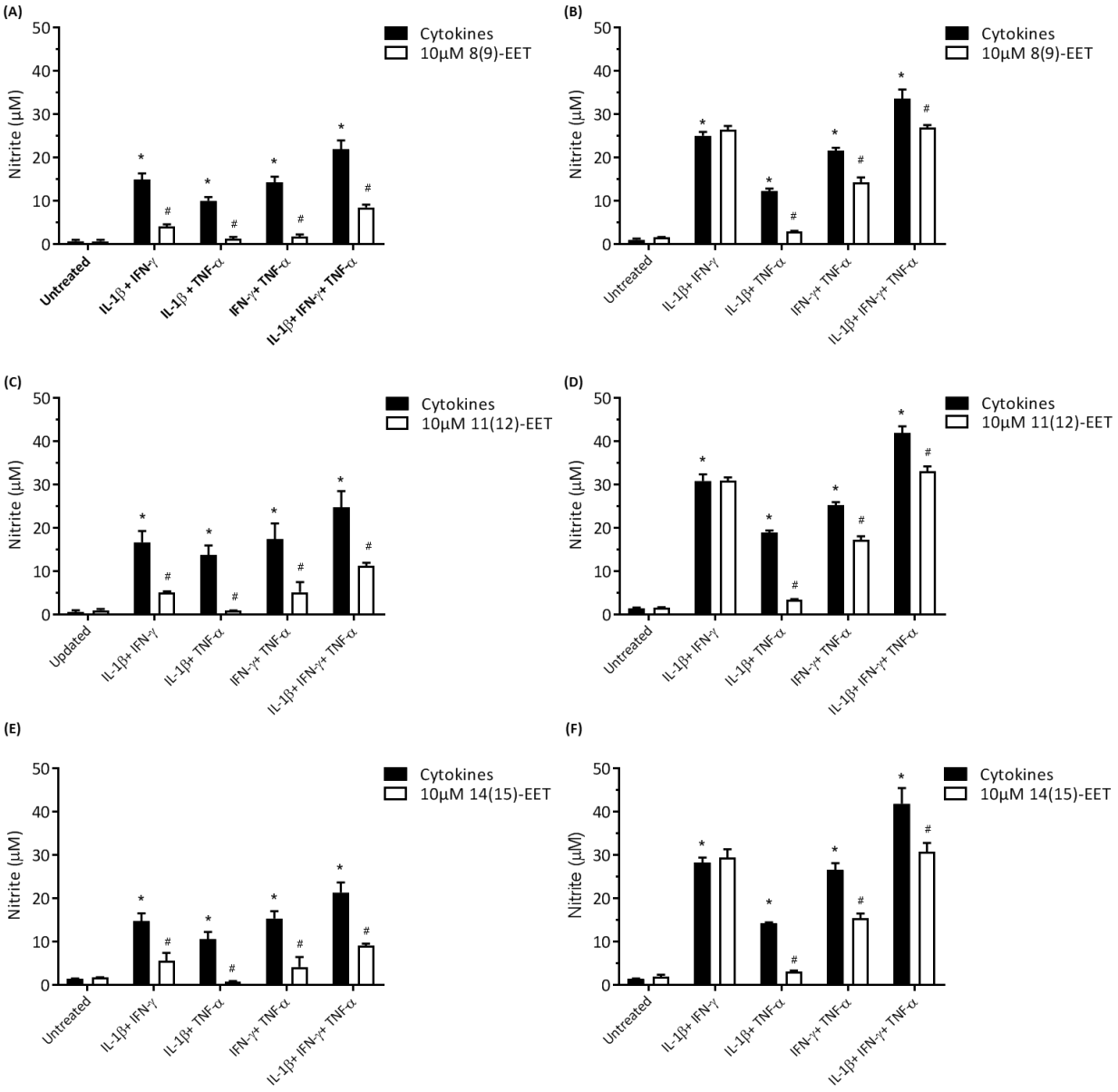

Figure 5.7. Nitrite production in BRIN BD11 cells exposed to cytokines co-incubated with EETs. Cells were treated with IL-1β (100U/mL), IFN-γ (20U/mL) and TNF-α (500U/mL) in different combination with or without 10μM of each EET for 24 (panels A, C, E) or 48 (panels B, D, F) hours before nitrite production was assessed by Griess reagent. Values are represented as mean (+/- SEM), n=3. *P<0.05 relative to corresponding control and #P<0.05 relative to corresponding cytokine treatment alone as determined by two-way ANOVA and Bonferroni's post-test.

As with preliminary investigations, treatment of BRIN-BD11 cells with varying combinations of cytokines resulted in a significant increase in nitrite production compared to untreated cells over both 24 and 48 hours (P<0.05), with the combination of all three cytokines

producing the largest increase. The addition of 10μM of all EETs resulted in a significant decrease in nitrite production compared to their corresponding cytokine treatments after both 24 and 48 hours ($P<0.05$), with the exception of the combination of IL-1β plus IFN-γ after 48 hours ($P>0.05$). This is a surprising, yet consistent observation that all EETs failed to reduce nitrite production in treatment with IL-1β plus IFN-γ in combination for 48 hours, despite attenuating the higher level of nitrite production on the addition of TNF-α with all three cytokines. This may indicate a maximum level of iNOS activity in the presence of EETs, regardless of the presence of TNF-α, given the similar nitrite levels in these groups. Nonetheless, the data suggests that, likely as a result of a decrease in NF-κB activity, iNOS expression/activity is also reduced under these conditions, which is most evident after 24 hours. A diminishing effect in prolonged culture up to 48 hours may reflect a reduction in available EETs, or that higher concentrations may be required, though it was not feasible to explore this in the current study.

With each EET isomer reducing NF-κB activity and nitrite production, and 8(9)-DHET showing protective actions against cytokine-induced toxicity, BRIN-BD11 cells were then assessed for NF-κB activity in co-incubation with cytokines and all DHET isomers (figure 5.8).

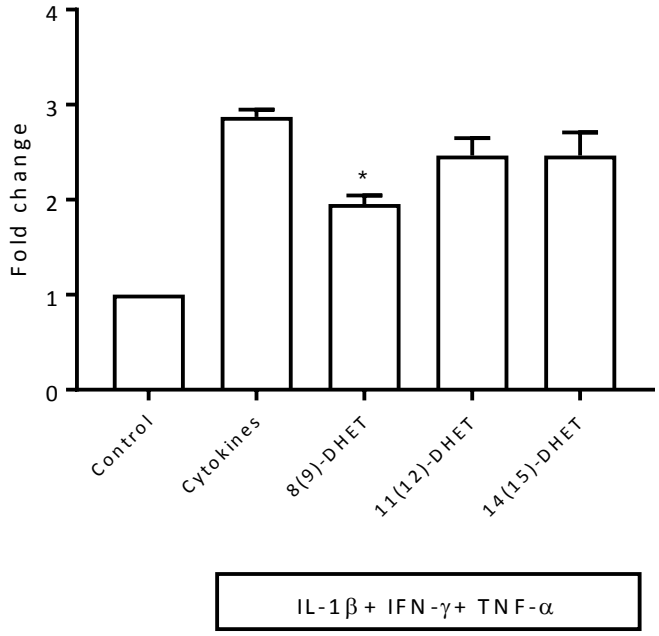

Figure 5.8. Effects of DHETs on cytokine-induced NF-κB activity in BRIN-BD11 cells. Cells were treated with IL-1β (100U/mL), IFN-γ (20U/mL) and TNF-α (500U/mL) in combination co-incubation with either 10μM 8(9)-DHET, 10μM 11(12)-DHET or 10μM 14(15)-DHET for 24 hours before NF-κB activity was assessed using a NF-κB Luciferase Reporter assay. Values are represented as mean fold change in luminescence units relative to control (+/- SEM), n=3. *P<0.05 compared to cytokines as determined by one-way ANOVA and Tukey's post-test.

The addition of 10μM 8(9)-DHET reduced the ~3-fold increase in NF-κB activity induced by cytokines by ~32% (P<0.05), similar to the 34% reduction in activity observed in co-incubation with 8(9)-EET (figure 5.5), confirming the positive effect of 8(9)-DHET against cytokine toxicity. However, the addition of 11(12)-DHET or 14(15)-DHET failed to significantly reduce NF-κB activity (P>0.05). As with EETs, DHET actions were further explored through assessment of their effects on cytokine-induced nitrite production over 24 hours (figure 5.9).

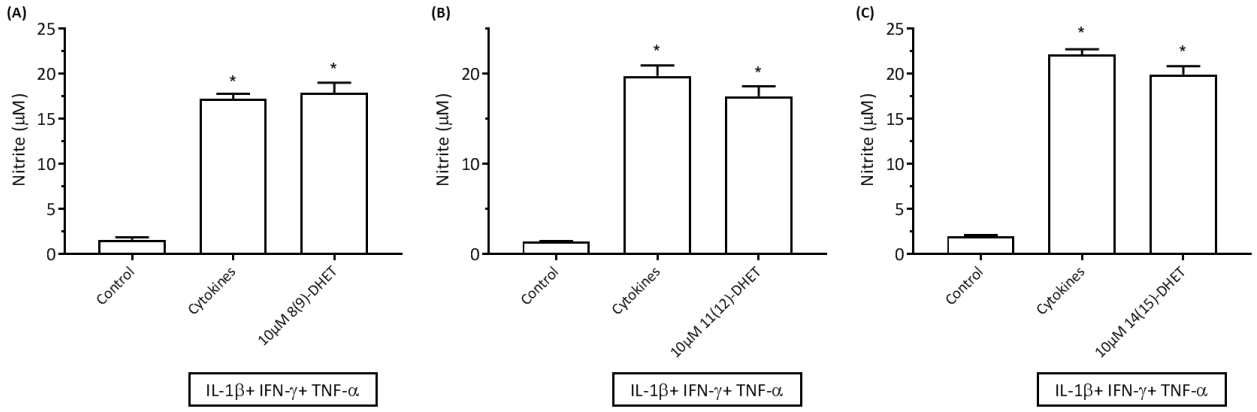

Figure 5.9 Nitrite production in BRIN-BD11 cells exposed to cytokines co-incubated with DHETs. Cells were treated with IL-1β (100U/mL), IFN-γ (20U/mL) and TNF-α (500U/mL) in combination co-incubation with 10µM of each DHET for 24 hours before nitrite production was assessed by Griess reagent. Values are represented as mean (+/- SEM), n=3. *P<0.05 relative to control as determined by one-way ANOVA and Tukey's post-test.

Treatment of BRIN-BD11 cells with IL-1β, IFN-γ and TNF-α in combination resulted in a significant increase in nitrite levels compared to control (*P*<0.05) however, unlike their EET counterparts, all DHETs failed to reduce nitrite production (*P*>0.05 vs. cytokine treatment alone). Although 8(9)-DHET reduced NF-κB activity by 32% compared to cytokines alone, this was not associated with changes in iNOS activity, and may suggest a differential mode of action of distinct EET/DHET species.

The effects of EETs on NF-κB activity have been (partly) attributed to their action as PPARγ agonists in other models, therefore the selective antagonist of PPARγ, T0070907 was used in co-incubation with cytokines and all EETs or 8(9)-DHET to determine whether this would reduce their effects against cytokine-induced apoptosis (figure 5.10).

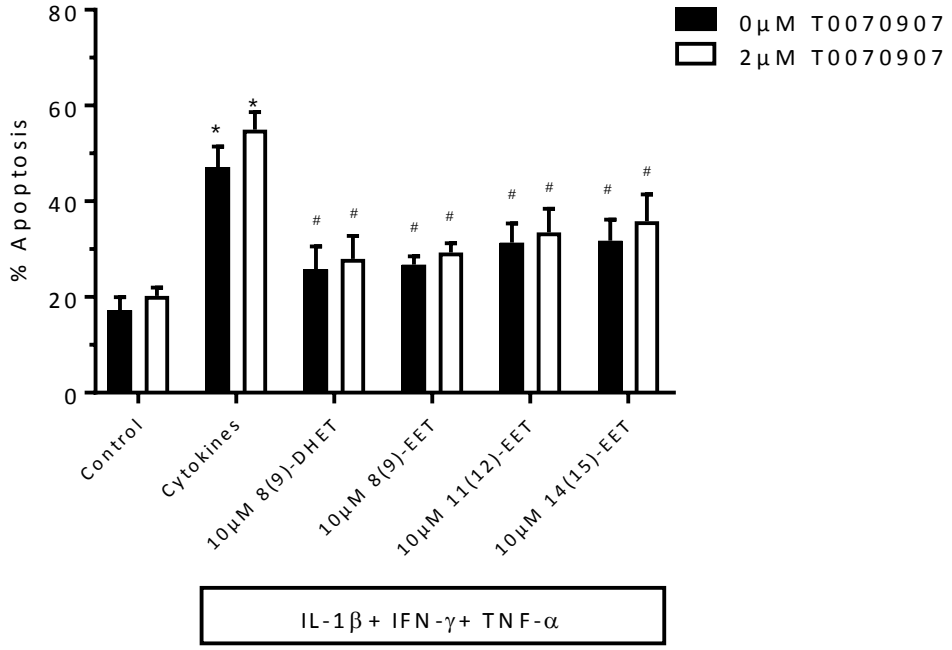

Figure 5.10. Effects of the PPARγ (T0070907) antagonist on the protective actions of EETs and 8(9)-DHET against cytokine-induced apoptosis. Cells were treated with IL-1β (100U/mL), IFN-γ (20U/mL) and TNF-α (500U/mL) in combination co-incubated with 10µM of each EET or 8(9)-DHET in the presence or absence of 2µM T0070907 for 24 hours before total apoptosis was assessed by flow cytometry using the MUSE™ MultiCaspase assay. Values are represented as mean (+/- SEM), n=3. *P<0.05 relative to control and #P<0.05 relative to corresponding cytokine treatment as determined by two-way ANOVA and Bonferroni's post-test

As with previous data, a significant increase in apoptosis was observed in response to cytokine treatment alone as compared to control (*P*<0.05). Similarly, co-incubation with cytokines and either 8(9)-DHET or each EET isomer resulted in a significant decrease in apoptosis compared to cytokine treatment alone (*P*<0.05). However, the addition of 2µM T0070907 failed to alter the ability of EETs or 8(9)-DHET to protect against cytokine-induce apoptosis, similar to data obtained with investigations into the role of PPARγ in this context in the lipotoxicity model (Chapter 4).

Previous data with the use of the poorly metabolisable EET analogue, 14(15)-EET-SI, showed no significant protection against palmitate toxicity, suggesting, in part, that cytoprotective effects of EETs in BRIN-BD11 cells may arise from EETs being able to undergo additional metabolic processing. With clear differences in mechanisms of cytotoxicity in terms of the nature of the apoptotic stimuli between cellular models of type 1 and 2 DM, investigations into the actions of 14(15)-EET-SI against cytokine toxicity were also explored by apoptosis assessment and trypan blue vital dye exclusion (figure 5.11).

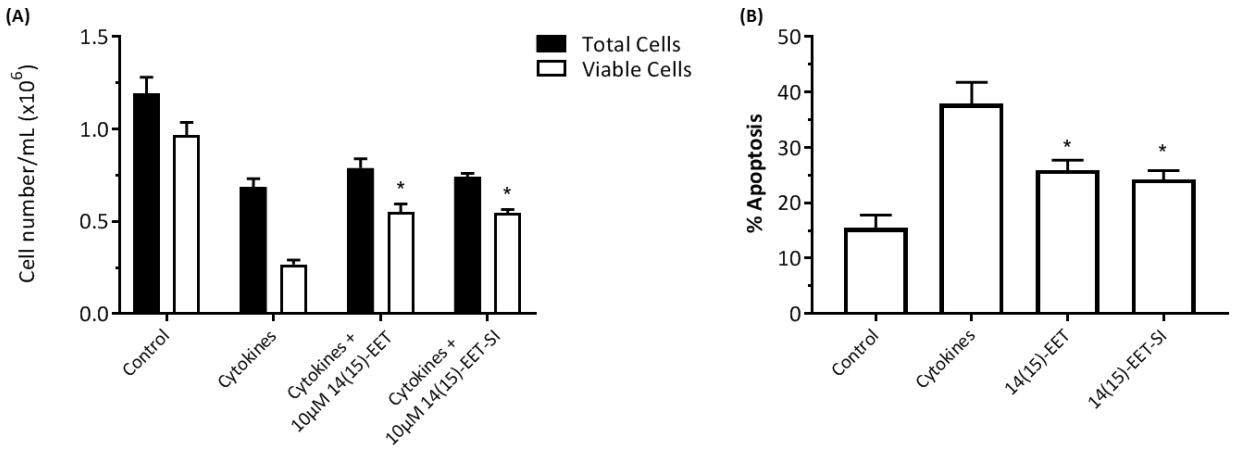

Figure 5.11 Effects of 14(15)-EET or 10μM 14(15)-EET-SI against cytokine-induced loss in viability and apoptosis induction. Cells were treated with IL-1β (100U/mL), IFN-γ (20U/mL) and TNF-α (500U/mL) in combination co-incubated with 10μM 14(15)-EET or 10μM 14(15)-EET-SI for 24 hours. Total and Viable cell numbers was assessed by trypan blue exclusion dye (A) and apoptosis profiling assessed by MUSE™ MultiCaspase (B). Values are represented as mean (+/- SEM), n=3. *P<0.05 relative to cytokines as determined by two-way ANOVA and Bonferroni's post-test (A) or one-way ANOVA and Tukey's post-test (B).

Treatment of BRIN-BD11 cells with IL-1β, IFN-γ and TNF-α in combination resulted in a significant decrease in viable cell numbers and a significant increase in apoptosis compared to control (P<0.05), as expected. Similarly, co-incubation with 10μM 14(15)-EET significantly increased viable cell number compared to cytokine treatment alone and significantly decreased apoptosis levels (P<0.05). Furthermore, co-incubation with 14(15)-EET-SI produced a comparable effect to the free-EET, attenuating both the decrease in viable cell number and increased apoptosis levels (P<0.05 vs. cytokines alone), with no significant difference between

the two EET treatments (P>0.05). Treatment with 14(15)-EET-SI in models of palmitate toxicity showed no protective effect, however the result in this model of cytokine toxicity, suggests that EETs may act differently depending on the type of *in vitro* investigations and nature of the apoptotic stimuli.

5.5 Discussion

The aims of this chapter were to characterise the response of BRIN-BD11 cells to pro-inflammatory cytokines in co-incubation with EETs and their corresponding diols, DHETs, to reflect potential anti-inflammatory actions in an *in vitro* model of type 1 DM. Additionally, this chapter also aimed to investigate whether effects of EETs and DHETs were associated with changes in NF-κB activity and subsequent NO production/nitrite accumulation, as well as establishing any PPARγ-dependency.

With EETs shown to protect BRIN-BD11 cells against palmitate-induced lipotoxicity (Chapter 4), similar investigations into the protective effects of EETs and DHETs were assessed. Since preliminary studies (Chapter 3) highlighted lack of sensitivity of the MTT assay in context to cytokine toxicity and the neutral red assay in models of fatty acid (and EET) treatment, these were not considered here. With all EET isomers observed to significantly attenuate a cytokine-induced loss in cell viability and apoptosis induction in BRIN-BD11 cells, the current data provides the first direct assessment of the cytoprotective effects of EETs in a beta cell context, in agreement with anti-inflammatory activity reported in other models (Liu *et al.,* 2005; Rompe et al., 2010; Zhao et al., 2012) and in contrast in the lack of effect of AA against cytokine toxicity in BRIN-BD11 cells (Chapter 3).

Whilst others have shown that potential manipulation of endogenous EET levels through inhibition or knockdown of sEH can improve glucose tolerance and functional beta cell mass in STZ-induced DM in mice (Luo *et al.,* 2010; Chen *et al.,* 2013), the current data directly links EET action to the inhibition of pro-inflammatory cytokine toxicity; pathophysiologically relevant inducers of beta cell death and dysfunction. Both of these

previous studies used a multiple-low-dose regime to induce DM with STZ, a process which is thought to initiate an inflammatory response in islets leading to beta cell loss via cell-mediated autoimmune processes, broadly comparable to the pathophysiology of type 1 DM and attributed, in part, to the presence of pro-inflammatory cytokines (Graham *et al.,* 2011). However, whilst Luo *et al.,* (2010) observed a marked reduction in apoptotic cells of sEH knockout mice with STZ-induced DM, no direct assessment of any islet infiltrate (or lack of) was measured, nor were *ex vivo* islet beta cells studied for their response to EETs in context to cytokine toxicity. Additionally, although a complementary approach to sEH inhibition and/or sEH knockout was used, pancreatic levels of EETs were not measured, which would have allowed direct inference of improved beta cell mass consequential to increased endogenous EET levels; though an enhancement of plasma EET:DHET ratios has been reported by others in sEH knockout models (Seubert *et al.,* 2006). Similar data was reported by Chen *et al.,* (2013), demonstrating a reduction in apoptotic cells in islets of STZ models with sEH inhibition, though this study failed to detect differences in pancreatic EET:DHET ratios, questioning whether the effects were reflective of EET action, further supporting that the current data represents a novel observation for the cytoprotective effects of EETs against cytokine toxicity in a beta cell model.

The previous data in the lipotoxicity model (Chapter 4) supported observations by others that DHETs displayed reduced activity to their respective EETs (Imig and Hammock, 2009), with no effect against palmitate-induced cytotoxicity. However, in the current model of pro-inflammatory cytokine toxicity, 8(9)-DHET exerted comparable effects against cytokine-induced beta cell death and apoptosis compared to the effect of 8(9)-EET. In contrast, whilst 11(12)-DHET and 14(15)-DHET showed a modest increase in viable cell number, they failed to

significantly attenuate cytokine toxicity. Although it is widely reported that DHET products of sEH action on EETs are considerably less active, Fang et al., (2006) showed that 14(15)-DHET was as potent as a the full agonist, Wy-14643, in the activation of PPARα. Others have also reported that 14(15)-DHET displays weak binding to a putative EET receptor (Yang *et al.,* 2008) and that this and 11(12)-DHET may also display activity in the regulation of Ca^{2+}-activated K^{+} channels (Lu *et al.,* 2001), though no reports have assessed 8(9)-DHET in this context. This may therefore indicate differential actions of EETs/DHETs in a cell-specific manner, possibly attributed to variation in expression of membrane receptors capable of binding, albeit with low affinity, to EETs/DHETs, or intracellular targets including PPAR isoforms. Whether these receptors display differential affinity across all EET and DHET isomers is yet to be clearly established but could account for the surprising observation in this study that 8(9)-DHET conferred similar protection against cytokine-induced cell death as 8(9)-EET, unlike other DHET isomers. Such an observation warrants further investigation, since this suggests differential activity of distinct EET/DHET species, which may also be reflective of the specific apoptotic stimuli, given the lack of DHET activity against palmitate toxicity.

Further to the protective effects of EETs and 8(9)-DHET against pro-inflammatory cytokine-induced cell death and apoptosis, the current data supports observations in other models that EETs can inhibit a cytokine-induced increase in NF-κB activity (Node *et al*., 1999; Liu *et al.,* 2005; Rompe *et al.,* 2010; Zhao *et al.,* 2012). All EETs reduced NF-κB activation by ~34% in response to cytokine treatment, with a comparable ~32% reduction in activity with 8(9)-DHET, supporting the surprising action of this species, but not 11(12)-DHET or 14(15)-DHET, in the attenuation of cytokine toxicity. Protective effects of EETs were also mirrored in the reduction of cytokine-stimulated increases in nitrite levels, reflective of iNOS activity.

These effects were more evident after 24 hours, with the nitrite levels in treatment with IL-1β plus IFN-γ in combination after 48 hours not being significantly altered by EET treatment, whereas despite the addition of TNF-α increasing nitrite further, levels were significantly reduced, albeit to a level similar to that with the IL-1β plus IFN-γ treatment. Collectively, this may suggest that the reduction in NF-κB activity contributes to a decrease in iNOS expression, reducing nitrite levels, with the overall relative decrease in effect compared to cytokine treatment alone at 48 hours compared to 24 hours suggesting the EET concentration may become limiting in prolonged culture. The observations that nitrite levels in the presence of EETs appeared to reach a maximum level after 48 hours, regardless of co-stimulatory cytokine activity on NF-κB and STAT may support [EETs] as a limiting factor for the regulation of iNOS expression, though NF-κB activity was not measured at 48 hours it may be expected that the relative decrease in activity by EETs would be smaller than the ~34% reduction after 24 hours. However, whether the EET effects on nitrite levels can be directly attributed to the inhibition of NF-κB activity is questionable given that with 8(9)-DHET treatment nitrite levels were unchanged, despite a comparable reduction in NF-κB activity. Together, this would suggest that changes in NF-κB activation are a likely contributing factor in the attenuation of cytokine toxicity by EET and 8(9)-DHET but that these effects are independent of iNOS expression and NO production. Similarly, Welters *et al.,* (2004a) showed that palmitoleate could protect BRIN-BD11 cells against cytokine toxicity but that this was independent of a reduction in nitrite levels, which supports data from others suggesting that cytokine toxicity does not require NO generation in these cells (Hsu *et al.,* 2012). Given the variation in effect of EETs or 8(9)-DHET on nitrite levels, this may indicate additional differential modes of action of these species, possibly in terms of potential receptor binding activity, though little is known about the mechanisms of 8(9)-DHET action.

Since EET activity is, in part, attributed to agonistic activity at PPARγ (Liu *et al.,* 2005), investigations into the contribution to protective actions against cytokines in the current model were explored using the PPARγ antagonist (T0070907). However, similar to the actions of EETs in the previous lipotoxicity model, the application of T0070907 failed to antagonise the protective actions of EETs and 8(9)-DHET, suggesting PPARγ-independent activity. This may indicate that effects in this model are either attributed to the regulation of a distal step in the apoptotic pathway via undefined EET activity, which could be in relation to effects on cardiolipin modelling and the regulation of the release of apoptotic factors from the mitochondria. However, this is inconsistent with the observation that 14(15)-EET-SI similarly protected against cytokine-induced apoptosis, in contrast to the data from palmitate treatment (Chapter 4), suggesting that EET-CoA esterification is not a requirement for cytoprotection in the current model. This, and the observations that effects of EETs appear PPARγ-independent may suggest that mechanisms of action are via extracellular receptor activation, thought to be associated with Gαs signalling, increasing cellular cAMP levels (Yang *et al.,* 2008). In support of this hypothesis, cAMP levels have also been linked to an inhibitory effect on NF-κB activity, mediated via PKA activation (Minguet *et al.,* 2005) and the GPCR kinase 5 has been shown to inhibit NF-κB activation in endothelial cells, attributed to nuclear retention of IκBα and impaired transcriptional activity of NF-κB (Sorriento *et al.,* 2008). Potential activity of EETs at multiple low affinity GPCR sites known to mediate prostaglandin signalling, via cAMP levels (Lui *et al.,* 2017) may similarly support this as a mode of EET action in the current model of cytokine toxicity, though if such a spectrum of receptor sites is mediating the effect, then it will be difficult to fully dissect the pathways involved.

5.6 Conclusion

The data collected in this chapter report the novel observations that 8(9)-EET, 11(12)-EET, 14(15)-EET and, surprisingly, 8(9)-DHET protect BRIN-BD11 cells from pro-inflammatory cytokine-induced beta cell death as a model of type 1 DM. Furthermore, this is associated with a down regulation of NF-κB activity by >30% and appears to be mediated by a PPARγ-independent mechanism. The effect of 8(9)-DHET in this context is particularly interesting, since activity of DHETs are less well documented and comparatively few studies have directly assessed a role of 8(9)-EET and 8(9)-DHET, in contrast to other isomers (Pozzi *et al.,* 2005). The current data therefore suggests that although the 8(9)- species may represent a minor product of the endogenous EET (and DHET) pool produced by CYP450 epoxygenases, these possess comparable biological activity to the more well-studied 11(12)- and 14(15)- species. Further work is needed to define the modes of action of distinct EET/DHET species, since some have shown that, independent to PPARγ, these may also signal through PPARα, which may display greater activity than 14(15)-DHET than EETs, though this species was inactive in the current model. Additionally, others have noted that anti-inflammatory actions of EETs in terms of iNOS activity in smooth muscle cells appears to be independent to the activation of all thee PPAR isoforms (Thompson and Bishop-Bailey, unpublished observations, cited in Thompson *et al.,* 2015) and so a better understanding of their mechanisms of action is needed. Whether activity at a single high-affinity or multiple low-affinity receptor site(s) is responsible is yet to be fully established, a wider range of EET analogues may be used to study this further. Of note, the current data with the more stable, poorly metabolisable EET analogue, 14(15)-EET-SI, suggest that EET-esterification to CoA, EET β-oxidation or esterification into the phospholipid pool is not a requirement for cytoprotection, in contrast to the result observed in the previous

lipotoxicity model (Chapter 4), this may therefore indicate a differential mode of action dependent on the nature of the apoptotic stimuli. In the current model of cytokine toxicity, EETs may be regulating PI3K/Akt activity and/or downstream apoptosis regulators, Bcl-2, Bcl-xL and Bax, as suggested by others (Dhanasekaran et al., 2008; Katragadda et al., 2009; Batchu et al., 2012), though further investigations would be needed to confirm this. The current data therefore observes, for the first time, that EETs and 8(9)-DHET protect against cytokine-induced cell death in a beta cell line, effects partly associated with an inhibition of NF-κB activity, providing a rationale for further study in their mechanisms of action in this context. Additionally, it is also yet to be determined whether manipulation of endogenous EET levels can confer similar activity; given the uncertainty regarding a direct EET action in *in vivo* DM models with sEH inhibition (Luo *et al.,* 2010; Chen *et al.,* 2013), studies focussing on the over-expression of CYP450 epoxygenases in beta cell models of cytotoxicity are warranted.

Chapter Six

6 Overexpression of CYP 2C11 in *in vitro* models of type 1 and 2 DM

6.1 Introduction

With exogenous application of 8(9)-EET, 11(12)-EET and 14(15)-EET showing protective actions against palmitate and cytokine-induced beta cell death and apoptosis, and 8(9)-DHET showing comparable effects in the cytokine model in BRIN-BD11 cells, investigations into modulation of endogenous levels of EETs were explored by over-expression of CYP 2C11. Several CYP isoforms have been reported to produce EETs through selective epoxidation of AA, with CYP 2J and CYP 2C isoforms reported to be expressed in islets (Imig and Hammock, 2009), particularly CYP 2C11 where higher expression than 2J3 in comparison to kidney was report in one study (Chen *et al.,* 2013). CYPs are known for their contribution to oxidative metabolism of many drugs and carcinogenic chemicals, as well as endogenous roles in steroid and prostaglandin synthesis, and are usually expressed in the ER. CYPs are predominantly expressed in the liver, though several isoforms show wider tissue-distribution and catalyse monoxygenase biotransformation reactions, requiring molecular oxygen and reducing one oxygen atom to water whilst incorporating the other atom into an organic product (Huang *et al.,* 2016). The reaction mechanism of CYPs require a four part component system: the CYP enzyme; consisting of a haem prosthetic group, NADPH CYP450 reductase, cytochrome b_5 and phosphatidylcholine (White, 1991; Huang *et al.,* 2016). Substrate molecules bind to the active heme with the iron in a 3^+ (ferric) oxidation state, this binding changes the redox potential facilitating single electron transfer from the reductase domain, requiring FAD and FMN as electron donors, reducing the iron to a 2^+ (ferrous) oxidation state. Molecular oxygen then

binds, abstracting an electron from the higher spin heme iron, followed by the transfer of a second electron from the reductase domain, activating the oxygen for scission.

A role for EETs in beta cell and islet function was first reported by Falck *et al.,* (1983), whereby 1µM 5(6)-EET, but not 8(9)-EET, 11(12)-EET or 14(15)-EET, induced insulin secretion from beta cells, though all EETs were able to induce glucagon release by alpha cells. Though later studies (Klett *et al.,* 2013) observed an inhibitory action of EETs on insulin, which was not explored in the current study, this thesis has reported on the novel cytoprotective effects of EETs in BRIN-BD11 cells. Others have reported on the *in vivo* manipulation of endogenous EET levels in positively regulating dysglycaemia and dyslipidaemia in context to insulin action, with over-expression of CYP 2J3 in mice models increasing 14(15)-EET levels and potentiating insulin receptor signalling in kidney, heart, muscle and liver, resulting in improved insulin sensitivity (Zeldin *et al.,* 1997; Xu *et al.,* 2010). Whilst there is limited direct evidence for functional roles of EETs and DHETs *in vitro* and *in vivo* models reflecting the pathophysiology of beta cell dysfunction in type 1 and 2 DM, the first *in vivo* investigations by Luo *et al.,* (2010) showed sEH knockout in STZ-mice increased insulin secretion and prevented hyperglycaemia, associated with increased beta cell mass, with application of the sEH inhibitor t-AUCB producing similar findings. Similar results were also reported in a later study (Chen *et al.,* 2013) and together suggest that strategies aimed at altering the EET to DHET ratio may produce beneficial effects on beta cell function as observed with exogenous EET application in the current data. Moreover, whilst in other model systems over-expression of relevant CYP-epoxygenases increase EET levels and produce comparable functional activity to exogenous EET application, such a role, including with rat CYP 2C11, has not been investigated in a beta cell context.

6.2 Aims

Having established protective effects of exogenous EET treatment in BRIN-BD11 cells against palmitate and pro-inflammatory cytokines, the aim of this chapter is to establish whether these effects can also be achieved through manipulation of endogenous EET levels by over-expression of rat CYP 2C11. Specifically, the aims are to:

- generate a BRIN-BD11 cell line with stable over-expression of CYP 2C11 and appropriate vector-controls.
- characterise the response of the stable 2C11 expressing cells to lipotoxicity and pro-inflammatory cytokine exposure, including in the presence of the endogenous 2C11 substrate, AA.
- explore the effects of sEH inhibition in increasing endogenous EET levels in 2C11 expressing cells.

6.3 Methods

Initially, transient transfection of a pCMV6-2C11 vector was trialled however, the requirement to maintain cultures for up to 48 hours post-transfection prior to re-plating for 24 hours prior to treatment with test agents may result in significant loss of transgene expression, particularly approaching 96-hours post-transfection, further hampered by the short doubling time of ~20 hours of BRIN-BD11 cells. Therefore, stable cell lines were generated as described in Chapter 2 (section 2.7.3), stable lines transfected with the pCMV6 empty vector were also produced, with cells maintained in Geneticin (G481) (1µg/mL)-supplemented complete media. Successful stable expression of CYP 2C11 was confirmed by Western blotting using a mouse mono-clonal mouse anti-rat 2C11 antibody (1:1000) following separation of proteins on 12% resolving gels, all other processing steps were as described (Chapter 2.8). The response of the cells to the cytotoxic action of palmitate (dose response (15.625µM-1000µM) or a fixed 250µM) or cytokines (100U/mL IL-1β, 20U/mL IFN-γ and 500U/mL TNFα) were determined using the MTT assay and by flow cytometry with the MUSE™ MultiCaspase assay. In the palmitate model, effects of 2C11 over-expression on cell viability were also explored in the presence of increasing concentrations of AA (0.156-20µM) or 10µM of the sEH inhibitors t-AUCB or TPPU.

6.4 Results

Following transfection of BRIN-BD11 cells with relevant vectors and isolation of colonies by G418 selection, four cell lines from CYP 2C11 (arbitrarily designated 2C11-1 – 2C11-4) and two cell lines from vector-only transfections were generated. Before proceeding with cytotoxicity studies, these were evaluated for the expression of CYP 2C11 by Western blotting (figure 6.1).

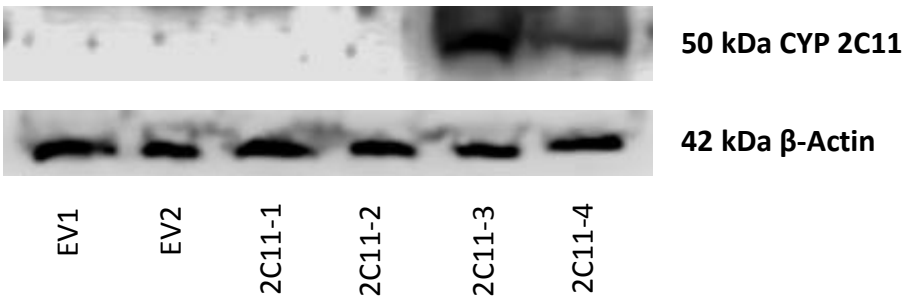

Figure 6.1 Expression of rat CYP 2C11 in stable-transfected BRIN-BD11 cells. Cells were transfected with either pCMV6-rat-CYP2 C11, or corresponding empty vector (EV) and single cell lines selected and expanded by G418 selection. Cell lysates were separated on 12% resolving gels followed by transfer to PVDF membranes and probed with primary antibodies for rat 2C11 (1:1000) or β-actin (1:1000), followed by detection using an HRP-conjugated secondary antibody (1:1000) and ECL blot imaging. A representative blot image is shown where n=3.

Analysis of the expression level of CYP 2C11 in EV1 and 2 BRIN-BD11 cell lines showed no CYP 2C11 expression, suggesting lack of expression of this epoxygenase in these cells. Of the four stable CYP 2C11- transfected cell lines established 2C11-1 and -2 showed no successful transfection/over-expression of CYP 2C11 enzyme at the protein level, which may indicate lack of successful integration and/or low expression of the construct. In contrast, the 2C11-3 and -4 cell lines both demonstrated successful generation of two stable cells, consistently showing a differential level of 2C11 expression, with clone line -3 having a higher expression than clone line -4. To establish whether stable over-expression in either of these

two lines could attenuate palmitate cytotoxicity, cells were incubated in the presence of a palmitate dose response for 24 hours and viability assessed with the MTT assay and MUSE™ MulitCaspase assay using a fixed 250µM palmitate (figure 6.2).

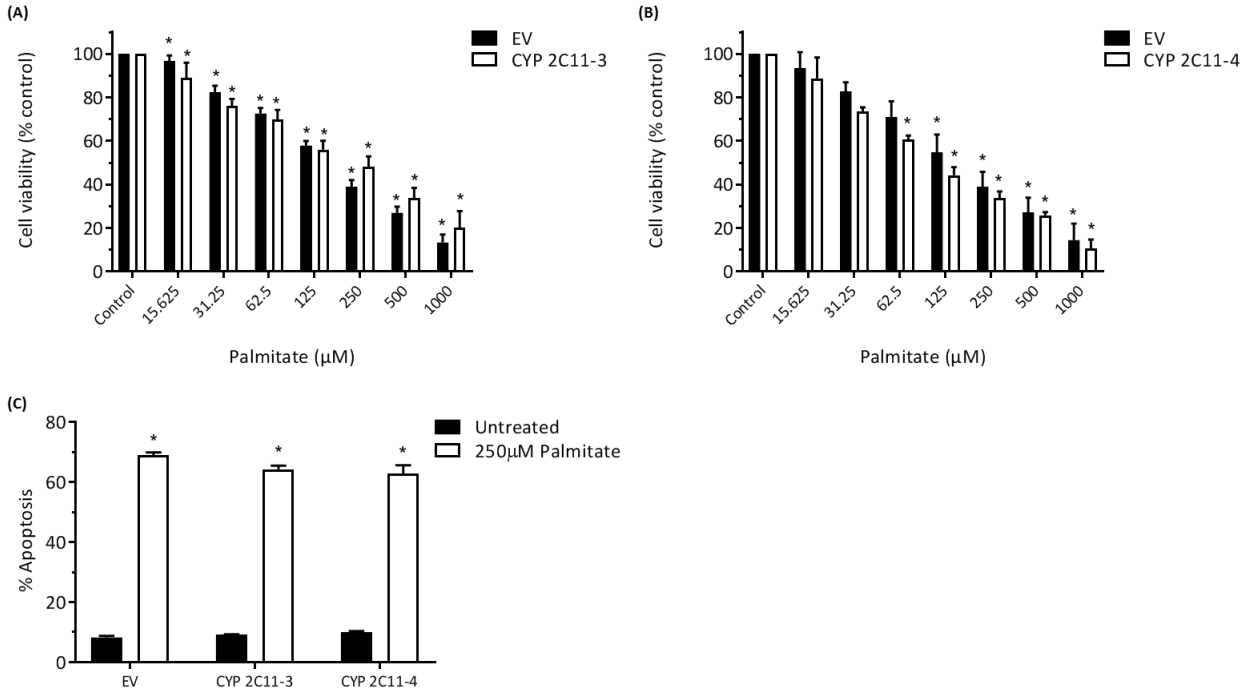

Figure 6.2. Effects of CYP 2C11 over-expression against palmitate toxicity. A stable EV cell line and both lines with stable expression of 2C11 were treated with increasing concentrations of palmitate (15.625µM-1000µM) for 24 hours before cell viability was assessed with the MTT assay (panels A-B), or with a fixed 250µM palmitate for 24 hours and apoptosis assessed by flow cytometry using the MUSE™ MultiCaspase assay (C). Values are represented as mean (+/- SEM), n=3. *P<0.05 relative to corresponding control as determined by two-way ANOVA and Bonferroni's post-test

Increasing concentrations of palmitate resulted in a dose-dependent reduction in cell viability in EV transfected cells and palmitate toxicity was not attenuated in either of the 2C11 over-expressing cell lines (*P*>0.05 vs. corresponding palmitate concentrations in EV cells). Similar results were obtained by apoptosis profiling showing that over-expression of CYP 2C11 failed to ameliorate the cytotoxic effects of palmitate, with no reduction in apoptosis witnessed for both stable lines (*P*>0.05). This may indicate that although 2C11 is over-expressed, the enzyme is non-functional, or that availability of the endogenous substrate AA is rate-limiting. This may be reflective of low expression of PLA_2, necessary for the release of

AA from membrane phospholipids as a precursor for many metabolic pathways, including EET production. To explore this further, these cells were treated with exogenous AA to investigate whether over-expression of 2C11 would alter the dose-dependent attenuation of palmitate toxicity as a consequence of increased substrate availability for EET synthesis, screened using the MTT assay (figure 6.3).

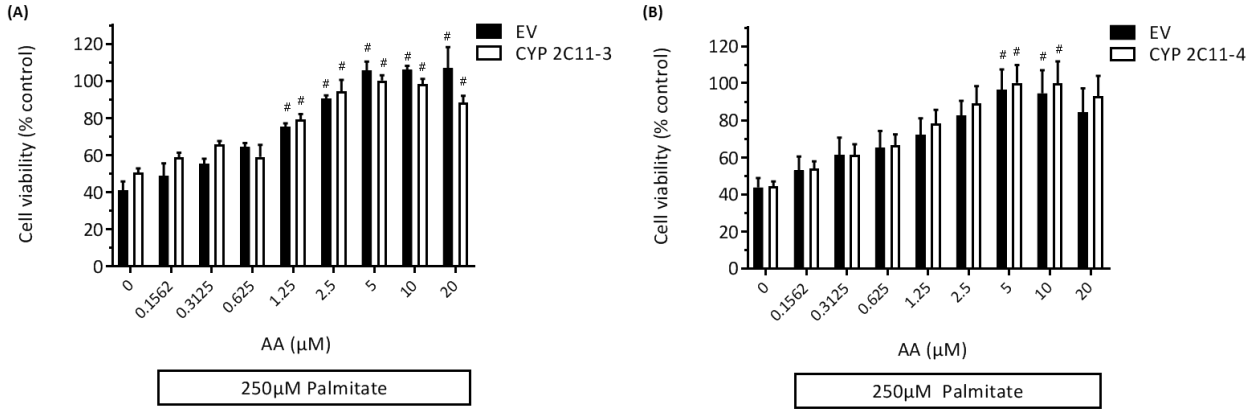

Figure 6.3 Effects of CYP 2C11 over-expression on the dose-dependent effects of AA against palmitate toxicity. EV and 2C11 over-expressing BRIN-BD11 cell lines were treated with increasing concentrations AA from 0.1562μM-20μM in co-incubation with 250μM palmitate for 24 hours before cell viability was assessed by the MTT assay. Values are represented as mean (+/- SEM), n=3. #P<0.05 relative to palmitate treatment alone as determined by two-way ANOVA and Bonferroni's post-test.

Increasing concentrations of AA resulted in a significant dose-dependent increase in cell viability both in BRIN-BD11 cells transfected with EV and in 2C11 stable cell lines compared to palmitate treatment alone (P<0.05). At all concentrations of AA there was no significant difference between the increase in cell viability between 2C11 lines and corresponding EV controls (P>0.05), suggesting that increasing substrate availability by exogenous AA treatment does not increase the production of EETs supporting an increase in cell viability in BRIN-BD11 cells overexpressing CYP 2C11; though in the current study it was not possible to directly measure whether or not EETs were being produced in these cells.

Since EETs are converted to DHETs by the action of sEH, with these products previously shown not to attenuate palmitate toxicity in BRIN-BD11 cells, and this being the predominant

route for EET metabolism, whether significant sEH activity in these cells was responsible for rapid clearance of any EETs being produced by these cells was explored. Initially, five sEH inhibitors were screened under control conditions for 24 hours (data not shown) to determine suitable concentrations that were non-toxic to BRIN-BD11 cells; AUDA, CUDA, t-AUCB, TPPU and CAY10640. From these screens, t-AUCB and TPPU were selected for further study, with lower solubility of some of the other inhibitors, particularly AUDA and CUDA, limiting their application in the current model. Both BRIN-BD11 2C11 stable lines and the EV control were pre-treated with either 10µM t-AUCB or TPPU followed by co-incubation against a palmitate dose response for 24 hours and viability assessed with the MTT assay and MUSE™ MultiCaspase assay (figure 6.4).

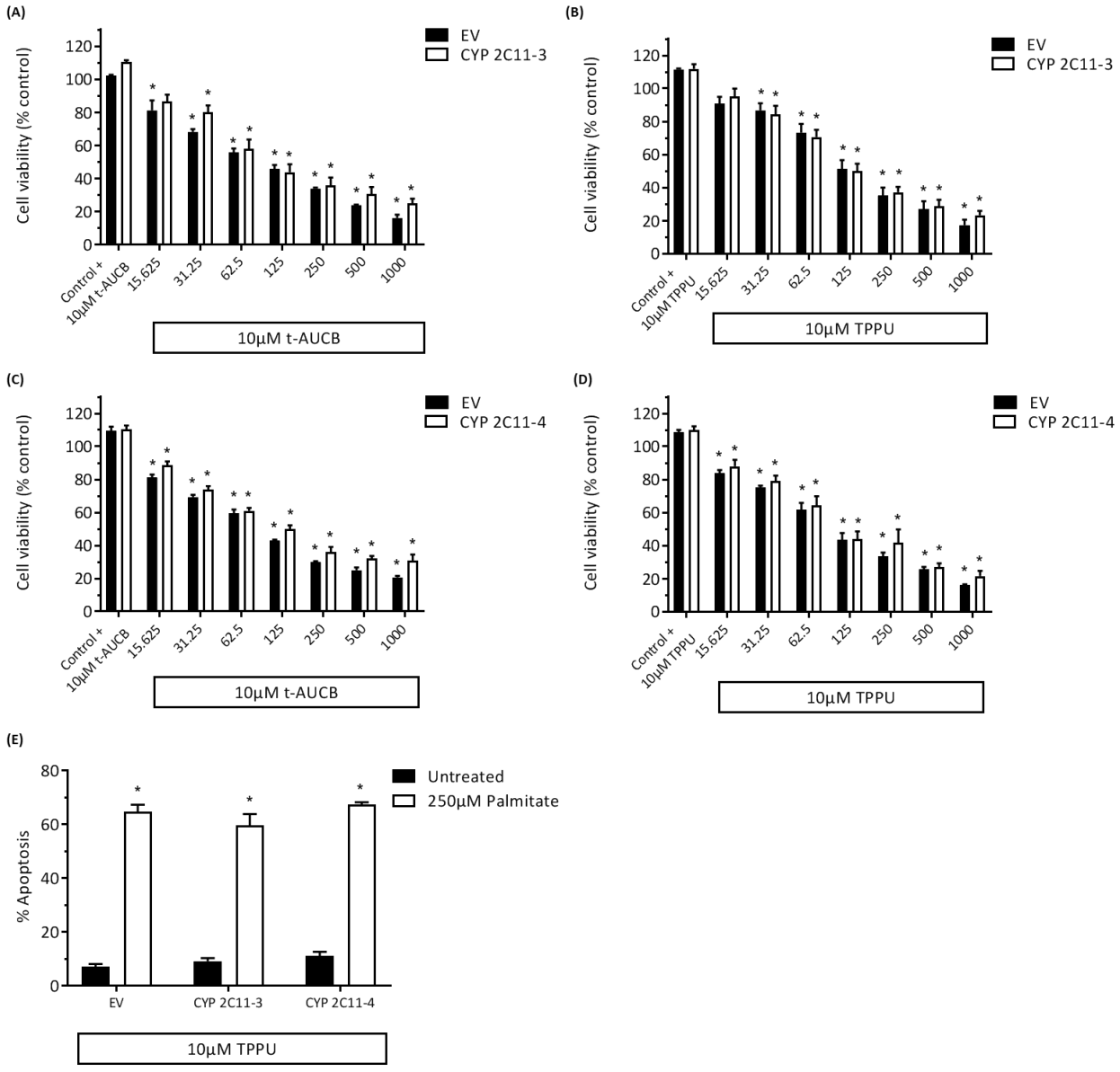

Figure 6.4. Effects of sEH inhibition on palmitate toxicity in CYP 2C11 stable cells. Cells were pre-treated with 10μM of either t-AUBC or TPPU for 1 hour followed by co-treatment with increasing concentrations of palmitate (15.62μM-1000μM) (panels A-D) or a fixed 250μM palmitate with 10μM TPPU (panel E) in co-incubation for 24 hours before cell viability was assessed by the MTT assay (A-D) or flow cytometry with the MUSE™ MultiCaspase assay. Values are represented as mean (+/- SEM), n=3. *P<0.05 relative to corresponding control (sEH inhibitor alone) as determined by two-way ANOVA and Bonferroni's post-test.

In all cases, treatment with increasing concentrations of palmitate dose-dependently reduced cell viability in both EV controls and 2C11 expressing cell lines. The addition of either 10μM t-AUCB or 10μM TPPU failed to increase cell viability compared to corresponding treatments in both stable lines (*P*>0.05), suggesting that inhibition of sEH in all models does

not increase cell viability against all concentrations of palmitate, with neither cell lines over-expressing CYP 2C11 exerting protective actions. These effects were also confirmed by assessment of apoptosis, which again showed that overexpression of CYP 2C11 in BRIN-BD11 cells did not attenuate palmitate toxicity in the presence of the sEH inhibitor TPPU. Since exogenous EET treatment at levels exceeding 5μM was observed to exert significant cytoprotective against palmitate toxicity (Chapter 4), the data presented here would suggest that the over-expressed 2C11 was non-functional, or that spatio-temporal differences between endogenous EET production and exogenous application may impact on the extent of their activity, though further work is needed to confirm this. Since this was beyond the scope of this thesis and since the data demonstrating EET cytoprotective effects against cytokines (Chapter 5) suggested potential mechanistic differences in their mode of action between these models, the cytotoxic response of the 2C11 over-expressing cell lines to cytokines was assessed by the MUSE™ MulitCaspase assay (figure 6.5).

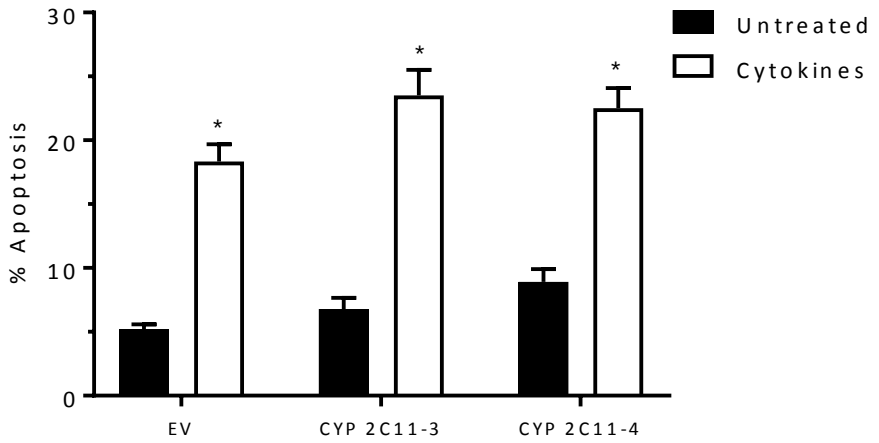

Figure 6.5. Effects of CYP 2C11 over-expression against cytokine-induced apoptosis. EV and 2C11 over-expressing cell lines were treated with or without IL-1β (100U/mL), IFN-γ (20U/mL) and TNF-α (500U/mL) in for 24 hours before apoptosis induction was assessed by flow cytometry using the MUSE™ MultiCaspase assay. Values are represented as mean (+/- SEM), n=3. *P<0.05 relative to corresponding control treatment (without cytokines) as determined by two-way ANOVA and Bonferroni's post-test.

As with the palmitate model, pro-inflammatory cytokines increased apoptosis in BRIN-BD11 cells, effects not attenuated in either CYP 2C11 over-expressing cell lines (P<0.05). Since previous data (Chapter 5) showed that 8(9)-DHET protects against cytokine toxicity and that sEH inhibitors did not alter the response of the 2C11 over-expressing cells to palmitate, investigations into sEH inhibition in the cytokine model were not considered. Collectively this data suggests that over-expression of CYP 2C11 in BRIN-BD11 cells cannot emulate the cytoprotective effects observed with exogenous EET treatment, although overall the data may suggest that 2C11 was non-functional.

6.5 Discussion

The aims of this chapter were to investigate the response of BRIN-BD11 cells following selection of stable cell lines over-expressing CYP 2C11 to palmitate and pro-inflammatory cytokines to see whether increasing production of endogenous EETs could mimic the effects of exogenous EET treatments in these models (Chapter 4 and 5). Of the CYP 450 epoxygenases in rat, CYP 2C11 accounts for 50% of total P450 enzymes expressed in rat male livers, with roles including the epoxidation of AA producing EETs (Morgan *et al.,* 1985; Zeldin *et al.,* 1996; Imig and Hammock, 2009). Additionally, whilst other CYP450 isoforms, particularly 2J, are also known to produce EETs, limited previous data has reported higher expression of 2C11 in rat islets compared to 2J isoforms (Chen *et al.,* 2013), hence the initial focus on 2C11 in the current model.

In this study, two BRIN-BD11 cell lines over-expressing CYP 2C11 were produced for further characterisation following stable transfection and G418-selective culture. Of the two cell lines produced, a differential expression level of 2C11 was observed, with a 'high' and 'low' expression model produced. However, the current data has shown that increased expression in both models was unable to attenuate the cytotoxicity of either palmitate or pro-inflammatory cytokines in contrast to EV transfections, as determined by MTT assay and flow cytometry for apoptosis profiling, confirming lack of cytoprotection. Similarly, modulation of endogenous substrate available with application of AA, or inhibition of sEH, limiting EET conversion to DHETs, also failed to emulate the effect of exogenous treatment.

To explore whether sEH could enhance the production of EETs in the current model, a range of inhibitors were initially screened, with t-AUCB and TPPU selected for further study. Although previous studies have shown that administration of the sEH inhibitor AUDA in the drinking water in *in vivo* animal models at 25mg/L can decrease mean arterial blood pressure, associated with an increase in urinary epoxide-to-diol ratios (Imig *et al.,* 2005), in the current model, AUDA presented with poor solubility, contributing to cytotoxicity and so was not continued in these investigations. Similarly, although CUDA has been reported to block the conversion of 1μM 14(15)-EET to 14(15)-DHET by 94% in COS-7 cells (Fang *et al.,* 2005), similar poor solubility and lack of effect of this inhibitor against palmitate toxicity alone in preliminary screening (data not shown) limited its application in this study. Unlike AUDA and CUDA, t-AUCB displays a more favourable solubility profile and did not exert similar toxicity at equivalent concentrations. t-AUCB has been shown to promote dose-dependent angiogenesis when treated in co-incubation with EETs in endothelial progenitor cells in a myocardial infarction model (Xu et al., 2013), effects which were attributed to the EET-PPARγ pathway, suggesting that there is a potential utility of sEHi in the therapy of ischemic heart disease. As with t-AUCB, TPPU and CAY10640 (phenyl-urea classes of sEH inhibitors) were well tolerated by BRIN-BD11 cells, with no concentrations displaying significant loss of cell viability. TPPU has previously been shown to be a potent inhibitor of both human and mouse sEH (Rose *et al.,* 2010) however, a study by Ostermann *et al.,* (2015) concluded that whilst TPPU showed high metabolic stability *in vivo* it showed no significant effect on epoxide/diol ratio in plasma, though favourable effects were observed in tissue samples suggesting inhibition *ex vivo*. Similarly, CAY10640 has been shown to be a potent inhibitor of both human and mouse sEH and has demonstrated a 1,000-fold increase in potency compared to morphine in reducing hyperalgesia in an *in vivo* carrageenan-induced inflammatory pain model (Rose *et al.,* 2010),

though there are comparatively few studies reporting its use. Collectively, the use of t-AUCB and TPPU in BRIN-BD11 cells over-expressing CYP 2C11 failed to attenuate the cytotoxic effects exerted by palmitate, suggesting that in the current model, over-expression of CYP 2C11 was ineffective, possibly attributable to lack of function.

Lack of function of the expressed 2C11 is unlikely to be due to improper vector sequence or random point mutations, since purified vectors were sequenced prior to transfection into BRIN-BD11 cells, with results showing 100% homology to the ncbi database entry for 2C11. Similarly the methods used for amplification and purification of the vector are robust, producing a high-yield of transfection-ready plasmids. Non-functional expression of 2C11 may instead be attributed to the association of CYP450 enzymes with oxidoreductase domains in cells, necessary for their catalytic activity. In support of this Yang *et al.,* (2007) used an adenoviral vector containing rat NADPH-cytochrome P450 oxidoreductase fused with CYP 2C11: rAAV-CYP2C11-CYPOR, which was used to infect endothelial cells and observed to synthesise a biologically active regioisomeric mixture of 5(6)-EET, 8(9)-EET, 11(12)-EET and 14(15)-EETs. In contrast, others have shown that over-expression of CYP 2J isoforms alone in a pcDNA vector produced EETs and inhibited NF-κB activation in HEK293T cells in a PPARα-dependent manner (Wray *et al.,* 2009) and a similar pcDNA3.1-CYP 2J2 construct reduced oxidative stress markers and increased antioxidant enzyme expression in lung endothelial cells (Chen *et al.,* 2014). Further work is therefore necessary in the current model to directly compare the effect of over-expression of CYP 2C11 alone to that of a similar CYPOR fusion construct. Although it was not possible to explore this in the current study, others have shown that the addition of a molar excess of a mammalian NADPH oxidoreducatse to purified CYP 2C11 markedly enhanced catalytic efficiency and production of AA-derived eicosanoids (Helvig

and Capdevila, 2000), therefore one initial approach could be to transiently transfect the BRIN-BD11-2C11 stable cell lines with a vector encoding the oxidoreductase enzyme, though expression of the fusion construct is likely to be more favourable given the necessary P450-OR interactions required. NADPH substrate availability for oxidoreductase activity is unlikely to have been a limiting factor in the current data, since beta cells are reported to have a high turnover of cellular NADPH/NADP+, as well as expressing several NADPH oxidase isoforms, which contribute to oxidative stress (Koulajian *et al.,* 2013). Further characterisation of BRIN-BD11 cells under these conditions, and in the 2C11 stable lines generated in the current study with an EET/DHET ELISA format would be necessary to establish whether the effect (or lack of) in cytotoxicity studies is directly associated with changes in cellular EET levels.

6.6 Conclusion

The data presented in this chapter successfully met the aim of producing two BRIN-BD11 cell lines with stable over-expression of CYP 2C11. However, in contrast to the application of exogenous EETs, these cells displayed no resistance to palmitate or pro-inflammatory cytokines, effects which were insensitive to the application of AA or sEH inhibition. This is possibly suggestive of low functionality of the expressed enzyme and so provides a rationale for further studies into the use of a CYP450-OR fusion construct and/or other CYP450-epoxyganses for manipulating endogenous EET levels.

Chapter Seven

General Discussion & Future Work

7 General Discussion

Diabetes mellitus is primarily classified as type 1 and type 2 DM, with type 1 resulting from an autoimmune attack, specifically targeting pancreatic beta cells in the islets of Langerhans, leading to a reduction beta cell mass of ~80%, associated with a progressive decline in insulin production. The condition manifests as a consequence of, as yet poorly defined, environmental trigger(s) in genetically predisposed individuals and necessitates life-long exogenous insulin replacement; though establishing normoglycaemia comparable to a non-diabetic state can be difficult. Type 2 DM, as a continuum of a DM 'spectrum', represents an extreme of metabolic dysfunction, typically associated with sedentary lifestyles and obesity, leading to elevated circulating glucose and fatty acids. Dyslipidaemia and chronic hyperglycaemia directly contribute to the development of insulin resistance in peripheral tissues, worsening a dysregulation in metabolic control and increasing secretory demands on beta cells. The capacity of the beta cells to maintain insulin output may become overwhelmed, in part, as a consequence of increased demands on the ER for protein translation and export, but also as a direct consequence of the presence of high a glucose load and increased circulating FFAs, which in a process of glucolipotoxicity, directly contribute to a decline in functional beta cell mass and increased beta cell apoptosis. Whilst current therapeutic strategies aimed at restoring appropriate insulin responses either through exogenous treatment (type 1 and in some cases type 2) or by promoting endogenous secretion, together with countering peripheral insulin resistance and metabolic dysregulation (type 2), improves glycaemic control and metabolic homoeostasis, long-term co-morbidities as a result of the secondary complications of sub-optimal control and associated mortalities continue to place a large burden on global healthcare. Therefore, one of the major aims of diabetes research

continues to be to increase our understanding of the intracellular mechanisms contributing to beta cell death and dysfunction, to identify novel areas for potential therapeutic intervention to preserve functional cell mass. To this end, pancreatic beta cell lines as *in vitro* models of type 1 and 2 DM have been extensively utilised, alongside *ex vivo* islet models and *in vivo* animal studies. Whilst there may be important differences between model systems, not least how well the data can be translated to human beta cell biology, the lack of well-established human beta cell lines and limited primary human islet tissue available means rodent beta cell lines have prevailed in much of the initial basic science research in DM.

In *in vitro* cellular models reflecting pro-inflammatory cytokine toxicity, application of cytokines IL-1β, IFN-γ and TNF-α alone or in combinations replicates pro-apoptotic autoimmune activity against beta cells with pathophysiological relevance. Similarly, in cellular models reflective of type 2 DM, application of saturated fatty acids, such as palmitate, have been used to induce beta cell death and study processes of glucolipotoxicity, as well as the now well-established cytoprotective actions of mono- and poly- unsaturated fatty acids such as palmitoleate, oleate and arachidonic acid. Therefore the initial aim of this thesis was to establish models of pro-inflammatory cytokine- and lipo- toxicity in the rat pancreatic beta cell line BRIN-BD11 (Chapter 3), in preparation for future investigations. In agreement with others (Cnop *et al.,* 2005), the data (Chapter 3 and 5) observed that the cytokines IL-1β (100U/mL), IFN-γ (20U/mL) and TNF-α (500U/mL) alone and in combination significantly reduced cell viability and increased total apoptosis as determined by a variety of complementary methods for the assessment of cell death and apoptosis, supporting the synergistic activity of cytokines in this context. As seen in RINm5F cells, cytokine-induced beta cell death was observed with IL-1β and IFN-γ treatment, but not with TNF-α (Holohan *et al.,*

2007), which corresponds to previous studies showing similar effects in isolated primary rat beta cells and human beta cells (Rabinovitch and Suarez-Pinzon, 1998; Eizirik and Mandrup-Poulsen, 2001). Nonetheless, synergistic activity of TNF-α has been observed, including in the current data, and the combination of these three main pro-inflammatory cytokines in the islets milieu *in vivo* represents the most pathophysiologically relevant treatment. Cytokine signalling is associated with the activation of the transcription factors NF-κB and STAT1, leading to changes in expression of target genes, promoting an increase in cellular nitrosative and oxidative stress (in part via increased expression of iNOS), a reduction in beta cell function, increased ER stress and mitochondrial dysfunction, and further recruitment of mononuclear immune cells associated with the augmentation of insulitis *in vivo* (Cnop *et al.,* 2005). The contribution of cytokine-induced iNOS expression and NO production are well-established mediators of beta cell death in a number of model systems (Cnop *et al.,* 2005), with a sub-set of genes differentially expressed in response to cytokines shown to be NO-dependent over 8-24 hours treatment (Kutlu *et al.,* 2003). Whilst iNOS expression is largely dependent on NF-κB activation (Flodstrom *et al.,* 1996; Kutlu *et al.,* 2003), with co-stimulatory activity of STAT1 and IRF-1 in combined treatment, the contribution of NO production and its impact on beta cell death may largely be species dependent, as although exogenous treatment with chemical NO donors has replicated cytokine-induced beta cell death in several models (Eizirik *et al.,* 1996; Oyadomari *et al.,* 2001; Cardozo *et al.,* 2005), the impact of iNOS silencing on mitigating beta cell death *in vivo* and sensitivity of human islets to NO toxicity have questioned the overall significance of this species. Though effects of cytokines on cellular oxidative and nitrosative are likely to extend beyond a single dependency on the NO radical directly, instead associated with a complex interplay between distinct pools of ROS and RNS produced under these conditions. Even so, iNOS expression and assessment of nitrite accumulation are commonly

used in the assessment of cytokine action in beta cells, evident in the current model with the effect of cytokine treatment combinations on loss in cell viability largely reflected in data from the Griess assay.

Further to establishing a model of cytokine toxicity in BRIN-BD11 cells, palmitate treatment (Chapter 3 and 4) observed a significant dose-dependent decrease in cell viability and an increase in total apoptosis, supporting observations in a number of other *in vitro* beta cell lines, as well as toxicity in islet cultures and *in vivo* studies using high-fat diet-induced DM and spontaneous obesity-induced DM models such as the *ob/ob* mouse and Zucker-fatty rat. Excessive intracellular palmitate levels result in an accumulation of acyl-CoA from cellular lipid overload and increased rates of production of ceramide and extra-mitochondrial metabolism, including peroxisomal β-oxidation, which leads to an increase in H_2O_2 suggesting a strong link between ROS accumulation and lipotoxicity (Tiedge *et al.,* 1997; Elsner *et al.,* 2011). Further mechanisms of palmitate toxicity as a result of dysregulated lipid homeostasis include the activation of ER stress, with a marked increase in expression and/or activation of the three main branches of the UPR observed under these conditions in a variety of models (Cnop *et al.,* 2008; Diakogiannaki *et al.,* 2008; Cuhna *et al.,* 2008), though the dependence of palmitate-induced cell death on these pathways has been questioned (Lai *et al.,* 2008).

Much interest has also focused on strategies aimed at the attenuation of beta cell cytotoxicity, including in the context of mono- and poly- unsaturated fatty acids and whilst these studies have focused more in lipotoxicity models, cytoprotective effects in models of cytokine toxicity have also been reported (Welters *et al.,* 2004a). Current data for preliminary investigations also support that the polyunsaturated FFA, AA, can protect against both palmitate and, to a limited extent, cytokine-induced beta cell death. Mechanisms for how this

is achieved are still poorly understood and although effects of exogenous treatment with AA (and indeed other unsaturated species) have been suggested to be independent to their metabolism, established from using methyl ester derivatives and other analogues (Dhayal and Morgan, 2011), endogenous pathways of AA metabolism and the products produced from some of these have also been explored. However, much attention has focused on COX and LOX metabolites in this context, with comparatively few studies concerned with the action of CYP450-derived eicosanoids in these models. Consequently, the primary aim of this thesis was to investigate the cytoprotective actions of CYP450 epoxygenase-derived products of AA metabolism, epoxyeicosatrienoic acids (EETs) and their corresponding diols, dihydroxyeicosatrienoic acids (DHETs), produced by the action of soluble epoxide hydrolase (sEH) against pro-inflammatory cytokines and palmitate-induced lipotoxicity in BRIN-BD11 cells. Since protective effects of EETs and, to a lesser extent, DHETs are reported in a number of other disease models and the reported activity of precursor polyunsaturated FFAs in beta cells (Keane *et al.,* 2011), there is a clear rationale for the investigation into EET action in these models (Xu *et al.,* 2016). Therefore this thesis reports, for the first time, that 8(9)-EET, 11(12)-EET and 14(15)-EET are cytoprotective against cytokine- and palmitate- induced beta cell death and apoptosis in BRIN-BD11 cells and furthermore reports the novel observation that 8(9)-DHET similarly protects against cytokine-induced beta cell death, with comparable activity to that of all EETs. Although earlier studies have yielded conflicting observations on the effect of EETs on insulin secretion (Falck *et al.,* 1983; Klett *et al.,* 2013) and that diminished activity of sEH protected against STZ-induced DM in mice (Luo *et al.,* 2010), effects which could not be attributed to changes in endogenous EET/DHET ratios (Chen *et al.,* 2013), the current data reports the first observations of a direct cytoprotective action against pathophysiologically-relevant inducers of beta cell death.

The differential effect of EETs and 8(9)-DHET on the attenuation of cytokine-induced nitrite accumulation, despite a comparable reduction in NF-κB activity, as determined using an NF-κB luciferase reporter vector, and observations that 8(9)-DHET failed to protect against lipotoxicity, suggest that the mode of action may differ between distinct EET/DHET species, which may depend on the nature of the apoptotic stimuli. This is further supported by observations that the poorly metabolisable EET analogue, 14(15)-EET-SI failed to attenuate palmitate toxicity, in contrast to comparable effects to 14(15)-EET observed in response to cytokine treatment. As a result, receptor-mediated activity of EETs (and 8(9)-DHET) in the latter model is supported, effects associated with a reduction in NF-κB activity, whereas with palmitate treatment, EET action may be associated with the generation of further EET metabolites, or from esterification into other cellular lipids, such as cardiolipin, though further work is needed to confirm this. Collectively, in context to the effects of EETs in response to cytokines, reflecting a model of type 1 DM, the data suggests that EETs act, in part, by reducing NF-κB activity, through a PPARγ-independent mechanism. Since whilst EETs are reported to act as endogenous PPARγ ligands (Liu *et al.,* 2005), a PPARγ antagonist failed to block to the protective effect of EETs against cytokine-induced apoptosis. This further supports that EET action may be mediated through an extracellular receptor site in this model, as also suggested in the data with 14(15)-EET-SI, though additional intracellular receptor activity cannot be excluded based on the current data. With recent studies suggesting that EETs display activity at multiple low-affinity extracellular receptor sites (Lui *et al.,* 2017; Park *et al.,* 2018), dissecting the contribution of distinct receptor-mediated signalling pathways may well be difficult to achieve, further hampered by a potential differential affinity between EET and DHET isomers.

In contrast, in the current model of lipotoxoicity, all DHETs failed to attenuate palmitate toxicity and a general trend in the extent of cytoprotective effects of EETs was also noted, with 8(9)-EET exerting the highest level of protection, followed by 11(12)-EET and then 14(15)-EET and the apoptosis level in this latter treatment remained significant elevated compared to control. This may suggest that position of the epoxide group is important in the extent of cytoprotection, which may directly contribute to the reactivity of EETs towards esterification to CoA and/or further metabolic processing, or that these structural features reflect binding affinity at receptor site(s). A requirement for EET esterification to CoA, β-oxidation or incorporation into the phospholipid membrane/other cellular lipids, is supported by the observation that 14(15)-EET-SI, which is resistant to esterification to CoA failed to protect BRIN-BD11 cells from palmitate-induced toxicity and others have shown that 90% of EETs are sequestered by this route (Bernstrom *et al.,* 1992). Additional extra- or intra-cellular receptor activity of EETs in this model cannot be entirely excluded from the current data, although neither pharamacological antagonism of GPR40 and GPR120 nor PPAR isoforms (including co-antagonism with the heterodimer partner RXR) blocked EET effects. Whether action was dependent on EET-mediated changes in lipid handling were also explored in a number of complementary methods and although a modest increase in lipid droplets was observed, inhibition of DGAT, the terminal committed enzyme in the pathway of TAG synthesis, did not alter EET action in terms of attenuating palmitate toxicity. Similar effects were observed with CPT1 inhibition, including when combined with DGAT inhibition, suggesting that EETs do not stimulate an increase in palmitate oxidation in the mitochondria. Although CPT1 over-expression has been shown to protect INS-1 cells from palmitate toxicity (Sol *et al.,* 2008) and the current data showed an increased in CPT1 at the mRNA level following EET treatment, with the relative fold increase in the expression of this and DGAT

broadly reflecting the extent of apoptosis suppression by each EET, that EETs protected against loss in viability and apoptosis in response to the poorly metabolisable 2-Bromopalmitate, further supports that EET action is independent to increased β-oxidation. Although EETs are also reported to undergo β-oxidation themselves, producing shortened-chain epoxides, with biological activity (Fang *et al.,* 2001; Fang *et al.,* 2004), this is also unlikely to solely reflect EET action in this model, since this would also be limited in the presence of the CPT1 inhibitor, etomoxir, or 2-Bromopalmitate. Collectively, these data suggest EETs may act at a distal step in apoptosis, possibly by release of cytochrome c through alterations in synthesis of cardiolipin, as an increase in EET levels has been associated with over-expression of cardiolipin synthase, similar to that seen with treatment of AA in H9C2 cells (Kiebish *et al.,* 2012; Ting *et al.,* 2015).

7.1 Future Work

Having now established that EETs are cytoprotective in BRIN-BD11 cells in response to both cytokines and palmitate, future work should include replicating these studies across a range of beta cell lines, including the other commonly used beta cell lines INS-1 and MIN6, as well as determining whether this can be reproduced in primary beta cells and islet cultures. The validity of this to human beta cell biology should also be explored in human islets, though the more recent human pancreatic beta cell line EndoC-βH1 or 1.1B4 could initially explore this. However, as with earlier attempts to produce an established clonal human cell line the validity of these more recent models has been questioned (Oleson *et al.,* 2015), though recent evidence has shown that EndoC-βH1 cells do resemble human islet physiology in context of

GSIS and the incretin effect (Tsonkova *et al.,* 2018). Having established, for the first time, that EETs are cytoprotective in a beta cell model, the limited studies in this field (save two reports on the effect of sEH activity on STZ-induced DM) and the inherent differences between beta cell models provides a further clear rationale for additional work on EET action. In context to the type 2 DM lipotoxicity model, the current data suggest that EET effects may be independent of changes in lipid handling, though there is some evidence that increased lipid droplet accumulation may be occurring; subtle differences between beta cell line models in terms of lipid homeostasis should allow further analysis of the relative contribution of these process to EET action. Not least since a differential effect of glucose on the enhancement, or lack thereof, on palmitate toxicity has been reported in INS-1 and MIN6 beta cell lines, respectively, possibly attributed to a higher acetyl-CoA carboxylase activity in INS-1 cells, increasing sensitivity to glucose-derived malonyl-CoA (Sargsyan and Bergsten, 2011). Moreover, human islets and MIN6 cells express higher levels of SCD1 in comparison to INS-1 cells, suggesting a higher tolerance of these model to saturated fatty acids. Collectively, the use of these additional cell lines and model systems will further our understanding of the functional roles of EETs in beta cells and exploration of their mode of action. Though this was not feasible in the current study, further work should also explore the contribution of EETs to insulin secretion and importantly whether secretory capacity is retained in cells where the pro-apoptotic actions of palmitate and/or cytokines are attenuated by EETs, given the limited and conflicting data in this area (Falck *et al.,* 1983; Klett *et al.,* 2013).

Further to the investigations carried out in the current study to define potential mechanisms of EET action, a wider range of antagonists/inhibitors could be implemented in both of the models established in the current BRIN-BD11 cell line and other model beta cell

systems. In particular, the current data does not support a PPAR-dependent activity of EETs in either of the BRIN-BD11 cytotoxicity models, in contrast to reported activity in other models (Liu *et al.,* 2005; Wray *et al.,* 2009) and whilst agonistic activity of EETs at PPARs, particularly PPARγ, are not the sole mechanisms of EET action, a further understanding of any potential activity at these targets is important, given their roles in regulating lipid homoeostasis and that PPARγ is the target of the glitazone class of oral antidiabetic agents. In particular, whether EETs activate PPARγ directly could be explored using a PPRE-luciferase reporter construct, as reported in other models using EETs and DHETs (Fang *et al.,* 2006; Wray *et al.,* 2009). It will be interesting to see if a differential activity and/or dependence of EETs on PPARγ can be observed in different beta cell models, since though BRIN-BD11 cells express PPARγ (and other PPAR isoforms), its activation required supra-physiological concentrations of rosiglitazone, at concentrations which failed to attenuate palmitate-induced cell death in a model of lipotoxicity (Welters *et al.,* 2004b). Of note, pioglitazone has been shown to attenuate palmitate-induced lipotoxicity in MIN6 cells (Hong *et al.,* 2018) and in response to cytokines in NIT-15 cells (Wang *et al.,* 2013), though others failed to detect PPARγ expression in MIN6 cells and showed that its over-expression in the presence of pioglitazone diminished GSIS (Nakamich *et al.,* 2003). Although these studies disagree on whether PPARγ is expressed in beta cell lines, a dual and conflicting action of both PPARγ-dependent cytoprotection against palmitate toxicity and PPARγ-dependent inhibition of insulin secretion with pioglitazone are reported in these studies. This may rationalise why EETs were shown to confer cytoprotective effects in BRIN-BD11 cells in the current data, whilst one previous study reported that EETs partially reduced insulin secretion in INS-1 cells (Klett *et al.,* 2013). However, this study did not determine whether PPARγ was required for this and the current data supports PPARγ-independent mechanisms of cytoprotection by EETs in BRIN-BD11 cells, therefore further

studies exploring both of these factors in a more PPARγ responsive model would be useful. Furthering the data on EET action and exploring PPARγ dependency is also of relevance to pro-inflammatory cytokine toxicity since studies have reported the effects of EETs on NF-κB activation as PPARγ-dependent (Spector *et al.,* 2004; Liu *et al.,* 2005). Although the current data would suggest that the cytoprotective effects of EETs in context to cytokine-induced apoptosis are PPARγ-independent, whether this was necessary for inhibitory action against NF-κB was not determined. Overall though the dependency of any of these responses on PPARγ should be explored by its down-regulation with siRNA, an approach complementary to and, perhaps, more selective than the pharmacological antagonist approach used in the current model.

Additional studies should also further consider the relative roles of pathways responsible for EET metabolism, particularly given the differential action of the EET-SI derivative used in the two models in this thesis. Whether receptor-mediated activity is directly responsible for their mode of action can be explored using the purported EET antagonist 14(15)-EEZE and additional methyl-ester EET derivatives, which similarly are not substrates for esterification to CoA, can be used to support the current data with 14(15)-EET-SI. With membrane esterification to phospholipids important in controlling free cellular EET levels, a contribution of both the acyl-CoA-synthetase enzymes necessary for EET activation for esterification and the phospholipase enzymes responsible for their release from the phospholipid pool, should allow a further insight into the regulation of endogenous EET levels in these models and the fate of EETs when exogenously applied, given that as much as 90% of total cellular EETs may be sequestered in this way (Bernstrom *et al.,* 1992). Furthermore, the scarcity of data on the functional roles of β-oxidation products of both EET and DHET

metabolites warrants further study. However, the major route for EET metabolism, once liberated from phospholipids, is the conversion to DHETs from the action of sEH and the current data largely support that this is a mechanisms which would inhibit cytoprotective actions, save for that of the largely unexplored 8(9)-DHET in context to cytokine toxicity. Whilst the current study could not determine an attenuation of palmitate toxicity in the presence of a range of sEH inhibitors, including when CYP 2C11 was over-expressed, the use of siRNA to down-regulate sEH expression could again be a more selective approach, particularly given the poor solubility of some of the current sEH inhibitors available. An approach to manipulating EET levels through a combination of CYP450 epoxygenase over-expression or exogenous application in combination with sEH inhibition is supported by observations in endothelial cells showing that PPARγ transcriptional activity was enhanced following EET treatment but only in the presence of the sEH inhibitor, AUDA (Liu *et al.,* 2005). Further to this, the use of the EET mimetic and sEH inhibitor, UA-8, could be utilised in context to these models, since treatment with UA-8 in H9C2 cardiomyocytes protected against mitochondrial injury following anoxia, and *in vivo*, protected against ischaemia reperfusion; effects which were blocked by the PPARγ antagonist, GW9662 (Batchu *et al.,* 2011).

Evidently EET action is not solely mediated through the activation of PPARγ and whilst evidence supports an extracellular binding site, which may signal through Gαs-associated GPCR activation (Yang *et al.,* 2008; Lui *et al.,* 2017), the identification of the receptor(s) involved is yet to be determined. If the more recent data suggesting binding activity at multiple low-affinity sites is substantiated, then defining the contribution of these will be difficult. Recent reports of EET activity at GPR40 (Park *et al.,* 2018) are not supported by the current data and so future work could further explore a wider range of potential targets.

However, this may be a laborious process and it is difficult to envisage a meaningful outcome, since the requirement to target multiple sites will increase the likelihood of additional cytotoxicity, though the potential activity of EETs at prostaglandin receptors (Lui *et al.,* 2017), with characterised activity in beta cell models (Carboneau *et al.,* 2017) should provide an initial starting point. Furthermore, development of additional EET analogues may help further define the relative contribution of receptor sites, given that 14(15)-EEZE can antagonise EET action and competitively block binding of a radiolabelled 14(15)-EET to the plasma membrane in U937 cells (Yang *et al.,* 2008). However, this species is cell permeable and has been shown to block EET-induced activation of PPARγ (Samokhalov *et al.,* 2014) and so its application in the current model would be theorised to anatagonise a range of potential EET binding sites, limiting its applicability to differentiating between extra- and intra-cellular effects, though the requirement for a molar excess of 14(15)-EEZE precluded its application in the current data. Therefore further work is necessary to identify relevant binding sites and their contribution to EET action.

Having now established that EETs are cytoprotective in a beta cell model when exogenously applied, this provides a further rationale to expand the current data on the over-expression of relevant CYP450 epoxygenases responsible for their production. Although this thesis successfully generated stable BRIN-BD11 cell lines with over-expression of CYP 2C11, a CYP epoxygenase previously reported to be expressed at high levels in rat islets (Chen *et al.,* 2013), the data indicates that the construct may be non-functional. So additional studies are necessary to characterise this further, including a direct assessment of EET/DHET levels in these cells and, more importantly, the use of CYP2C11-CYPOR fusion construct, as reported by others (Helvig and Capdevila, 2000). It is important to note however, other studies using

the isoform CYP 2J have shown protective actions with transiently transfecting a CYP 2J pcDNA3 vector alone, arising to the rationale in overexpressing CYP 2C11 without the CYPOR attachment in this study. This therefore provides a preliminary foundation on which to further explore a range of CYP450 enzymes known to produce EETs and importantly, these studies should be replicated in a range of other beta cell models. In human pancreatic tissues samples the CYP 2C8 and 2C9 isoforms have been detected, with expression associated with islets (Standop *et al.,* 2002), supporting expression of the 2C11 rat homology reported by Chen *et al.,* (2013) in rat islets, though the current data could not detect a baseline expression of 2C11 in the empty-vector stable transfection BRIN-BD11 lines. Therefore, further work should aim to establish, by RT-PCR and Western blotting, the expression level of a range of CYP450-epoxygenases and sEH in a number of beta cell lines and islets models, followed by exploration of their roles in controlling endogenous EET levels and potential cytoprotective activity.

7.2 Concluding Remarks

Overall this thesis reports, for the first time, the novel observations that EETs are cytoprotective against palmitate and cytokine toxicity in the rat pancreatic beta cell line BRIN-BD11 and also the surprising observation that 8(9)-DHET conferred similar protection against cytokines. Since no studies have previously reported EET (and DHET) activity in these models, these data now provide a foundation for further studies to explore mechanisms of EET action, including in terms of other beta cell functions, as well as the roles of CYP450 epoxygenases and other pathways responsible for controlling endogenous EET levels in this context. The parity in the extent of cytoprotection mediated by EETs observed in both of the models utilised in this thesis and data on EETs reported in other model systems, with synergy to some of the processes associated with beta cell dysfunction and DM development, suggests that strategies targeting EET production and/or metabolism may possess future clinical utility in the amelioration of beta cell death in both type 1 and 2 DM. Whilst application of such an approach to controlling beta cell demise in type 1 DM may well be limited to an early pre-diabetic state, non-specific intra-islet inflammatory responses are also associated with the low yield of islets currently used in clinical islet transplantation. This, and a variety of confounding factors in the host system post-transplantation, including portal vein glucolipotoxicity at the transplant site, contributes to a rapid early loss in functional islet mass in the immediate post-transplant period and so pre-transplant culture conditions associated with enhancing intra-islet EET production may promote long-term survival during initial transplant adaptation. With limited previous data on the beneficial action of EETs in a beta cell context, the current data provides a rationale for further studies to build on our knowledge of the functional roles of these hitherto largely unexplored eicosanoids in beta cell biology.

References

References

Abdel-Razzak Z, Loyer P, Fautrel A, Gautier JC, Corcos L, Turlin B, Beaune P, Guillouzo A. (1993). Cytokines down-regulate expression of major cytochrome P-450 enzymes in adult human hepatocytes in primary culture. Molecular pharmacology. 44(4), 707-715.

Alam U, Asghar O, Azmi S, Malik R. (2014). General aspects of diabetes mellitus. Handbook of clinical neurology. 126(9), 211-222.

Alquier T, Peyot ML, Latour MG, Kebede M, Sorensen CM, Gesta S, Ronald Kahn C, Smith RD, Jetton TL, Metz TO, Prentki M, Poitout V. (2009). Deletion of GPR40 impairs glucose-induced insulin secretion in vivo in mice without affecting intracellular fuel metabolism in islets. Diabetes. 58(11), 2607-2615.

American Diabetes Association. (2008). Diagnosis and Classification of Diabetes Mellitus. Diabetes Care. 31(Supplement 1), S55-S60.

Ankarcrona M,Dypbukt JM, Bernhard B, Nicotera P, (1994). Interleukin-1β-Induced Nitric Oxide Production Activates Apoptosis in Pancreatic RINm5F Cells. Experimental Cell Research. 213(4), 172-177.

Arakawa T, Laneuville O, Miller CA, Lakkides KM, Wingerd BA, DeWitt DL, Smith WL. (1996). Prostanoid receptors of murine NIH 3T3 and RAW 264.7 cells. Structure and expression of the murine prostaglandin EP4 receptor gene. The Journal of biological chemistry. 271(47), 29569-29575.

Augstein P, Bahr J, Wachlin G, Heinke P. (2004). Cytokines activate caspase-3 in insulinoma cells of diabetes-prone NOD mice directly and via upregulation of Fas. Journal of Autoimmunity. 23(4), 301-309.

Azevedo-Martins AK, Lortz S, Lenzen S, Curi R, Eizirik DL, Tiedge M. (2003). Improvement of the mitochondrial antioxidant defense status prevents cytokine-induced nuclear factor-kappaB activation in insulin-producing cells. Diabetes. 52(1), 93-101.

Baldwin AC, Green CD, Olson LK, Moxley MA, Corbett JA. (2012). A role for aberrant protein palmitoylation in FFA-induced ER stress and β-cell death. American journal of physiology. Endocrinology and metabolism. 302(11), E1390-1398.

Bano, G. (2013). Glucose homeostasis, obesity and diabetes. Best practice & research. Clinical obstetrics & gynaecology. 27(5), 715-726.

Bao S, Bohrer A, Ramanadham S, Jin W, Zhang S, Turk J..(2006). Effects of stable suppression of Group VIA phospholipase A2 expression on phospholipid content and composition, insulin secretion, and proliferation of INS-1 insulinoma cells. The Journal of biological chemistry. 281(1), 187-198.

Barry M, Heibein JA, Pinkoski MJ, Lee SF, Moyer RW, Green DR, Bleackley RC. (2000). Granzyme B short-circuits the need for caspase 8 activity during granule-mediated cytotoxic T-lymphocyte killing by directly cleaving Bid. Molecular and cellular biology. 20(11), 3781-3794.

Batchu SN, Chaudhary KR, El-Sikhry H, Yang W, Light PE, Oudit GY, Seubert JM. (2012). Role of PI3Kα and sarcolemmal ATP-sensitive potassium channels in epoxyeicosatrienoic acid mediated cardioprotection. Journal of molecular and cellular cardiology. 53(1), 43-52.

Batchu SN, Lee SB, Qadhi RS, Chaudhary KR, El-Sikhry H, Kodela R, Falck JR, Seubert JM. (2011). Cardioprotective effect of a dual acting epoxyeicosatrienoic acid analogue towards ischaemia reperfusion injury. British journal of pharmacology. 162(4), 897-907.

Battle TE, Frank DA. (2002). The role of STATs in apoptosis. Current Molecular Medicine. 2(22), 381-392.

Bernas T, Dobrucki J. (2002). Mitochondrial and nonmitochondrial reduction of MTT: interaction of MTT with TMRE, JC-1, and NAO mitochondrial fluorescent probes. Cytometry. 47(4), 236-242.

Bernstrom K, Kayganich K, Murphy RC, Fitzpatrick FA. (1992). Incorporation and distribution of epoxyeicosatrienoic acids into cellular phospholipids. The Journal of biological chemistry. 267(6), 3686-3690.

Berridge MJ. (2002). The endoplasmic reticulum: a multifunctional signaling organelle. Cell calcium. 32(5-6), 235-249.

Berridge MV, Tan AS. (1993). Characterization of the cellular reduction of 3-(4,5-dimethylthiazol-2-yl)-2,5-diphenyltetrazolium bromide (MTT): subcellular localization, substrate dependence, and involvement of mitochondrial elect. Archives of biochemistry and biophysics. 303(2), 474-482.

Bertolotti A, Zhang Y, Hendershot LM, Harding HP, Ron D. (2000). Dynamic interaction of BiP and ER stress transducers in the unfolded-protein response. Nature cell biology. 2(6), 326-332.

Bikman BT, Summers SA. (2011). Ceramides as modulators of cellular and whole-body metabolism. The Journal of clinical investigations. 121(11), 4222-4230.

Bleich D, Chen S, Gu JL, Nadler JL. (1998). The role of 12-lipoxygenase in pancreatic -cells (Review). International journal of molecular medicine. 1(1), 265-272.

Bleich D, Chen S, Gu JL, Thomas L, Scott S, Gonzales N, Natarajan R, Nadler JL. (1995). Interleukin-1 beta regulates the expression of a leukocyte type of 12-lipoxygenase in rat islets and RIN m5F cells. Endocrinology. 136(12), 5736-5744.

Bleich D, Chen S, Wen Y, Nadler JL. (1997). The stress-activated c-Jun protein kinase (JNK) is stimulated by lipoxygenase pathway product 12-HETE in RIN m5F cells. Biochemical and biophysical research communications. 230(2), 448-451.

Bleich D, Chen S, Zipser B, Sun D, Funk CD, Nadler JL. (1999). Resistance to type 1 diabetes induction in 12-lipoxygenase knockout mice. The Journal of clinical investigations. 103(10), 1431-1436.

Borg J, Klint C, Wierup N, Ström K, Larsson S, Sundler F, Lupi R, Marchetti P, Xu G, Kimmel A, Londos C, Holm C. (2009). Perilipin is present in islets of Langerhans and protects against lipotoxicity when overexpressed in the beta-cell line INS-1. Endocrinology. 150(7), 3049-3057.

Bottazzo B, Dean BM, McNally JM, MacKay EH, Swift PGF, Gamble, DR. (1985). In situ characterization of autoimmune phenomena and expression of HLA molecules in the pancreas in diabetic insulitis. *New England Journal of Medicine.* 313, 353-360.

Boslem E, MacIntosh G, Preston AM, Bartley C, Busch AK, Fuller M, Laybutt DR, Meikle PJ, Biden TJ. (2011). A lipidomic screen of palmitate-treated MIN6 β-cells links sphingolipid metabolites with endoplasmic reticulum (ER) stress and impaired protein trafficking. The Biochemical journal. 435(1), 267-276.

Boyce M1, Bryant KF, Jousse C, Long K, Harding HP, Scheuner D, Kaufman RJ, Ma D, Coen DM, Ron D, Yuan J. (2005). A selective inhibitor of eIF2alpha dephosphorylation protects cells from ER stress. Science. 307(5711), 935-939.

Briant LJB, Dodd MS, Chibalina MV, Rorsman NJG, Johnson PRV, Carmeliet P, Rorsman P, Knudsen JG. (2018). CPT1a-Dependent Long-Chain Fatty Acid Oxidation Contributes to Maintaining Glucagon Secretion from Pancreatic Islets. Cell reports. 23(11), 3300-3311.

Briaud I, Harmon JS, Kelpe CL, Segu VB, Poitout V. (2001). Lipotoxicity of the pancreatic beta-cell is associated with glucose-dependent esterification of fatty acids into neutral lipids. Diabetes. 50(2), 315-321.

Briscoe CP, Tadayyon M, Andrews JL, Benson WG, Chambers JK, Eilert MM, Ellis C, Elshourbagy NA, Goetz AS, Minnick DT, Murdock PR, Sauls HR Jr, Shabon U, Spinage LD, Strum JC, Szekeres PG, Tan KB, Way JM, Ignar DM, Wilson S, Muir Al. (2003). The orphan G protein-coupled receptor GPR40 is activated by medium and long chain fatty acids. The Journal of biological chemistry. 278(13), 11303-11311.

Broniowska KA, Mathews CE, Corbett JA. (2013). Do β-cells generate peroxynitrite in response to cytokine treatment? Jorunal of Biological Chemistry. 288(13), 36567-36578.

Brovkovych V, Zhang Y, Brovkovych S, Minshall RD, Skidgel RA. (2011). A novel pathway for receptor-mediated post-translational activation of inducible nitric oxide synthase. Journal of Cellular and Moleculare Medicine. 15(11), 258-269.

Brown AJ, Goldsworthy SM, Barnes AA, Eilert MM, Tcheang L, Daniels D, Muir AI, Wigglesworth MJ, Kinghorn I, Fraser NJ, Pike NB, Strum JC, Steplewski KM, Murdock PR, Holder JC, Marshall FH, Szekeres P, Wilson S, Ignar DM, Foord SM, Wise A, Dowell SJ. (2003). The

Orphan G protein-coupled receptors GPR41 and GPR43 are activated by propionate and other short chain carboxylic acids. The Journal of biological chemistry. 278(13), 11312-11319.

Brozzi F, Gerlo S, Arturo Grieco F, Romanna Nardelli T, Lievens S, Gysemans C, Marselli L, Marchetti P, Mathieu C, Tavernier J, Eizirik, D. (2014). A Combined "Omics" Approach Identifies N-Myc Interactor as a Novel Cytokine-induced Regulator of IRE1α Protein and c-Jun N-terminal Kinase in Pancreatic Beta Cells. The Journal of biological chemistry. 289(30), 20677-20693.

Brozzi F, Nardelli TR, Lopes M, Millard I, Barthson J, Igoillo-Esteve M, Grieco FA, Villate O, Oliveira JM, Casimir M, Bugliani M, Engin F, Hotamisligil GS, Marchetti P, Eizirik DL. (2015). Cytokines induce endoplasmic reticulum stress in human, rat and mouse beta cells via different mechanisms. Diabetologia. 58(10), 2307-2316.

Busch AK, Gurisik E, Cordery DV, Sudlow M, Denyer GS, Laybutt DR, Hughes WE, Biden TJ. (2005). Increased fatty acid desaturation and enhanced expression of stearoyl coenzyme A desaturase protects pancreatic beta-cells from lipoapoptosis. Diabetes. 54(10), 2917-2924.

Cameron MJ, Arreaza GA, Grattan M, Meagher C, Sharif S, Burdick MD. (2000). Differential expression of CC chemokines and the CCR5 receptor in the pancreas is associated with progression of type 1 diabetes. Journal of Immunology. 165(2), 1102-1110.

Capdevila JH, Falck JR. (2001). The CYP P450 arachidonic acid monooxygenases: from cell signaling to blood pressure regulation. Biochemical and biophysical research communications. 285(3), 571-576.

Capdevila JH, Falck JR, Harris RC. (2000). Cytochrome P450 and arachidonic acid bioactivation. Molecular and functional properties of the arachidonate monooxygenase. Journal of lipid research. 41(2), 163-181.

Cardozo AK, Proost P, Gysemans C, Chen MC, Mathieu C, Eizirik DL. (2003). IL-1beta and IFN-gamma induce the expression of diverse chemokines and IL-15 in human and rat pancreatic islet cells, and in islets from pre-diabetic NOD mice. Diabetologia. 46(3), 255-266.

Cardozo AK, Ortis F, Storling J, Feng YM, Rasschaert J, Tonnesen M, Van Eylen F, Mandrup-Poulsen T, Herchuelz A, Eizirik DL. (2005). Cytokines downregulate the sarcoendoplasmic reticulum pump Ca2+ ATPase 2b and deplete endoplasmic reticulum Ca2+, leading to induction of endoplasmic reticulum stress in pancreatic beta-cells. Diabetes. 54(2), 452-461.

Carpenter L, Cordery D, Biden TJ. (2001). Protein kinase Cdelta activation by interleukin-1beta stabilizes inducible nitric-oxide synthase mRNA in pancreatic beta-cells. The Journal of biological chemistry. 276(7), 5368-5374.

Carpenter L, Cordery D, Biden TJ. (2002). Inhibition of protein kinase C delta protects rat INS-1 cells against interleukin-1beta and streptozotocin-induced apoptosis. Diabetes. 51(2), 317-324.

Carta G, Murru E, Lisai S, Sirigu A, Piras A, Collu M, Batetta B, Gambelli L, Banni S. (2015). Dietary triacylglycerols with palmitic acid in the sn-2 position modulate levels of N-acylethanolamides in rat tissues. PloS One. 10(3), e0120424.

Cazanave SC, Elmi NA, Akazawa Y, Bronk SF, Mott JL, Gores GJ. (2010). CHOP and AP-1 cooperatively mediate PUMA expression during lipoapoptosis. Am. Journal Physiology-Gastr. L. 299(2), 236-243.

Cetkovic-Cvrlje M, Eizirik DL. (1994). TNF-alpha and IFN-gamma potentiate the deleterious effects of IL-1 beta on mouse pancreatic islets mainly via generation of nitric oxide. Cytokine. 6(4), 399-406.

Chen L, Fan C, Zhang Y, Bakri M, Dong H, Morisseau C, Maddipati KR, Luo P, Wang CY, Hammock BD, Wang MH. (2013). Beneficial effects of inhibition of soluble epoxide hydrolase on glucose homeostasis and islet damage in a streptozotocin-induced diabetic mouse model. Prostaglandins & other lipid mediators. 104-105(2), 42-48.

Chase JF, Tubbs PK. (1972). Specific inhibition of mitochondrial fatty acid oxidation by 2-bromopalmitate and its coenzyme A and carnitine esters. The Biochemical journal. 129(1), 55-65.

Chen HC, Smith SJ, Ladha Z, Jensen DR, Ferreira LD, Pulawa LK, McGuire JG, Pitas RE, Eckel RH, Farese RV Jr. (2002). Increased insulin and leptin sensitivity in mice lacking acyl CoA:diacylglycerol acyltransferase 1. The Journal of clinical investigations. 109(8), 1049-1055.

Chen J, Chen JK, Falck JR, Guthi JS, Anjaiah S, Capdevila JH, Harris RC. (2007). Mitogenic activity and signaling mechanism of 2-(14,15- epoxyeicosatrienoyl)glycerol, a novel cytochrome p450 arachidonate metabolite. Molecular and cellular biology. 27(8), 3023-3034.

Chen JK, Capdevila J, Harris RC. (2001). Cytochrome p450 epoxygenase metabolism of arachidonic acid inhibits apoptosis. Molecular and cellular biology. 21(18), 6322-6331.

Chen JK, Chen J, Imig JD, Wei S, Hachey DL, Guthi JS, Falck JR, Capdevila JH, Harris RC. (2008). Identification of novel endogenous cytochrome p450 arachidonate metabolites with high affinity for cannabinoid receptors. The Journal of biological chemistry. 283(36), 24514-24524.

Chen N, Ma Wy, Huang C, Dong Z. (1999). Translocation of protein kinase Cepsilon and protein kinase Cdelta to membrane is required for ultraviolet B-induced activation of mitogen-activated protein kinases and apoptosis. The Journal of biological chemistry. 274(22), 15389-15394.

Chen M, Yang ZD, Smith KM, Carter JD, Nadler JL. (2005). Activation of 12-lipoxygenase in proinflammatory cytokine-mediated beta cell toxicity. *Diabetologia*. 48(3), 486-495.

Chen W, Zheng G, Yang S, Ping W, Fu X, Zhang N, Wang DW, Wang J. (2014). CYP2J2 and EETs Protect against Oxidative Stress and Apoptosis in Vivo and in Vitro Following Lung Ischemia/Reperfusion. Cellular physiology and biochemistry: international journal of experimental cellular physiology, biochemistry, and pharmacology. 33(6), 1663-1680.

Choi SE, Lee SM, Lee YJ, Li LJ. (2008). Protective role of autophagy in palmitate-induced INS-1 beta-cell death. Endocrinology. 150(8), 126-134.

Choi SE, Jung IR, Lee YJ, Lee SJ, Lee JH, Kim Y, Jun HS, Lee KW, Park CB, Kang Y. (2011). Stimulation of lipogenesis as well as fatty acid oxidation protects against palmitate-induced INS-1 beta-cell death. Endocrinology. 152(3), 816-827.

Cho YS, Kim CH, Kim KY, Cheon HG. (2012). Protective effects of arachidonic acid against palmitic acid-mediated lipotoxicity in HIT-T15 cells. Molecular and cellular biochemistry. 364(1-2), 19-28.

Chu ZL, Carroll C, Alfonso J, Gutierrez V, He H, Lucman A, Pedraza M, Mondala H, Gao H, Bagnol D, Chen R, Jones RM, Behan DP, Leonard J. (2008). A role for intestinal endocrine cell-expressed g protein-coupled receptor 119 in glycemic control by enhancing glucagon-like

Peptide-1 and glucose-dependent insulinotropic Peptide release. Endocrinology. 149(5), 2038-2047.

Cnop M, Foufelle F, Velloso LA. (2012). Endoplasmic reticulum stress, obesity and diabetes. Trends in molecular medicine. 18(1), 59-68.

Cnop M, Hannaert JC, Hoorens A, Eizirik DL, Pipeleers DG. (2001). Inverse relationship between cytotoxicity of free fatty acids in pancreatic islet cells and cellular triglyceride accumulation. Diabetes. 50(8), 1771-1777.

Cnop M, Hannaert JC, Pipeleers DG. (2002). Troglitazone does not protect rat pancreatic beta cells against free fatty acid-induced cytotoxicity. Biochemical pharmacology. 63(7), 1281-1285.

Cnop M, Igoillo-Esteve M, Cunha DA, Ladrière L, Eizirik DL. (2008). An update on lipotoxic endoplasmic reticulum stress in pancreatic beta-cells. Biochemical Society transactions. 36(Part 5), 909-915.

Cnop M, Ladriere L, Hekerman P, Ortis F, Cardozo AK, Dogusan Z, Flamez D, Boyce M, Yuan J, Eizirik DL. (2007). Selective inhibition of eukaryotic translation initiation factor 2 alpha dephosphorylation potentiates fatty acid-induced endoplasmic reticulum stress and causes pancreatic beta-cell dysfunction and apoptosis. The Journal of biological chemistry. 282(6), 3989-3997.

Cnop M, Toivonen S, Igoillo-Esteve M, Salpea P. (2017). Endoplasmic reticulum stress and eIF2α phosphorylation: The Achilles heel of pancreatic β cells. Molecular metabolism. 6(9), 1024-1039.

Cnop M, Welsh N, Jonas JC, Jorns A, Lenzen S, Eizirik D. (2005) Mechanisms of Pancreatic Beta-Cell Death in Type 1 and Type 2 Diabetes. Diabetes. 54,(no. 2), 97-107.

Cunha D, Hekerman P, Ladriere L,Bazarra-Castro A, Ortis F, Wakeham MC, Eizirik DL, Cnop M. (2008). Initiation and execution of lipotoxic ER stress in pancreatic Beta-cells. Journal of Cell Science 121(2), 2308-2318.

Cunningham GA, McClenaghan NH, Flatt PR, Newsholme P. (2005). L-Alanine induces changes in metabolic and signal transduction gene expression in a clonal rat pancreatic beta-cell line and protects from pro-inflammatory cytokine-induced apoptosis. Clinical Science. 109(5), 447-455.

Darville MI, Eizirik DL. (2001). Cytokine induction of Fas gene expression in insulin-producing cells requires the transcription factors NF-kappaB and C/EBP. Diabetes. 50(8), 1741-1748.

De Jersey J, Snelgrove SL, Palmer SE, Teteris SA, Mullbacher A, Miller JF, Slattery RM. (2007). Beta cells cannot directly prime diabetogenic CD8 T cells in nonobese diabetic mice. Proceedings of the National Academy of Sciences of the United States of America. 104(4), 1295-1300.

DeLaney CA, Cunningham JM, Green MH, Green IC. (1997) Nitric oxide rather than superoxide or peroxynitrite inhibits insulin secretion and causes DNA damage in HIT-T15 cells. Advances in experimental medicine and biology. 426(17), 335-339.

Deng Y, Theken KN, Lee CR. (2010). Cytochrome P450 epoxygenases, soluble epoxide hydrolase, and the regulation of cardiovascular inflammation. Journal of molecular and cellular cardiology. 48(2), 331-341.

Dhanasekaran A, Gruenloh SK, Buonaccorsi JN, Zhang R, Gross GJ, Falck JR, Patel PK, Jacobs ER, Medhora M. (2008). Multiple antiapoptotic targets of the PI3K/Akt survival pathway are activated by epoxyeicosatrienoic acids to protect cardiomyocytes from hypoxia/anoxia. American journal of physiology. Heart and circulatory physiology. 294(2), H724-735.

Dhayal S, Morgan NG. (2011). Pharmacological characterization of the cytoprotective effects of polyunsaturated fatty acids in insulin-secreting BRIN-BD11 cells. British journal of pharmacology. 162(6), 1340-1350.

Dhayal S, Morgan NG. (2011). Structure-activity relationships influencing lipid-induced changes in eIF2α phosphorylation and cell viability in BRIN-BD11 cells. FEBS letters. 585(14), 2243-2248.

Diakogiannaki E, Dhayal S, Childs CE, Calder PC, Welters HJ, Morgan NG.(2007). Mechanisms involved in the cytotoxic and cytoprotective actions of saturated versus monounsaturated long-chain fatty acids in pancreatic Beta-cells. Journal Endocrinology. 194(7), 283-291.

Diakogiannaki E, Morgan NG. (2008). Differential regulation of the ER stress response by long-chain fatty acids in the pancreatic Beta-cell. Viochemical Society Transactions. 36(8), 959-962.

Dixit VD. (2013). Nlrp3 Inflammasome Activation in Type 2 Diabetes: Is It Clinically Relevant? Diabetes. 62(2), 22-24.

Dobrian AD, Morris MA, Taylor-Fishwick DA, Holman TR, Imai Y, Mirmira RG, Nadler JL. (2019). Role of the 12-lipoxygenase pathway in diabetes pathogenesis and complications. Pharmacology & therapeutics. 195, 100-110.

Donath MY, Dalmas E, Sauter NS, Boni-Schnetzler M. (2013). Inflammation in Obesity and Diabetes: Islet Dysfunction and Therapeutic Opportunity. Cell Metabolism. 17(13), 860-872.

Dyntar D, Eppenberger-Eberhardt M, Maedler K, Pruschy M, Eppenberger HM, Spinas GA, Donath MY. (2001). Glucose and palmitic acid induce degeneration of myofibrils and modulate apoptosis in rat adult cardiomyocytes. Diabetes. 50(9), 2105-2113.

Eitel K, Staiger H, Rieger J, Mischak H, Brandhorst H, Brendel MD, Bretzel RG, Häring HU, Kellerer M. (2003). Protein kinase C delta activation and translocation to the nucleus are required for fatty acid-induced apoptosis of insulin-secreting cells. Diabetes. 52(4), 991-997.

Eizirik DL, Cardozo AK, Cnop M. (2008). he role for endoplasmic reticulum stress in diabetes mellitus. Endocrine reviews. 29(1), 42-61.

Eizirik DL, Cnop M. (2010). ER stress in pancreatic beta cells: the thin red line between adaptation and failure. Science signalling. 23;3(110), pe7.

Eizirik DL, Flodström M, Karlsen AE, Welsh N. (1996). The harmony of the spheres: inducible nitric oxide synthase and related genes in pancreatic beta cells. Diabetologia. 39(8), 875-890.

Eizirik DL, Mandrup-Poulsen T. (2001). A choice of death--the signal-transduction of immune-mediated beta-cell apoptosis. Diabetologia. 44(12), 2115-2133.

Eguchi K, Manabe I, Oishi-Tanaka Y, Ohsugi M, Kono N, Ogata F, Yagi N, Ohto U, Kimoto M, Miyake K, Tobe K, Arai H, Kadowaki T, Nagai R. (2012). Saturated fatty acid and TLR signaling link β cell dysfunction and islet inflammation. Cell metabolism. 15(4), 518-533.

El-Assaad W, Buteau J, Peyot ML, Nolan C, Roduit R, Hardy S, Joly E, Dbaibo G, Rosenberg L, Prentki M. (2003). Saturated fatty acids synergize with elevated glucose to cause pancreatic beta-cell death. Endocrinology. 144(9), 4154-4163.

Lai E, Bikopoulos G, Wheeler MB, Rozakis-Adcock M, Volchuk A. (2008). Differential activation of ER stress and apoptosis in response to chronically elevated free fatty acids in pancreatic -cells. American journal physiology. Endocrinology and metabolism. 294(2), E540-E550.

Ellgaard L, Helenius A. (2003). Quality control in the endoplasmic reticulum. Nature reviews. Molecular cell biology. 4(3), 181-191.

Elsner M, Gehrmann W, Lenzen S. (2011). Peroxisome-generated hydrogen peroxide as important mediator of lipotoxicity in insulin-producing cells. Diabetes. 60(1), 200-208.

Estella E, McKenzie MD, Catterall T, Sutton VR, Bird PI, Trapani JA, Kay TW, Thomas HE. (2006). Granzyme B-mediated death of pancreatic beta-cells requires the proapoptotic BH3-only molecule bid. Diabetes. 55(8), 2212-2219.

Falck JR, Manna S, Moltz J, Chacos N, Capdevila J. (1983). Epoxyeicosatrienoic acids stimulate glucagon and insulin release from isolated rat pancreatic islets. Biochemical and biophysical research communications. 114(2), 743-749.

Fang X, Hu S, Xu B, Snyder GD, Harmon S, Yao J, Liu Y, Sangras B, Falck JR, Weintraub NL, Spector AA. (2006). 14,15-Dihydroxyeicosatrienoic acid activates peroxisome proliferator-activated receptor-alpha. American journal of physiology. Heart and circulatory physiology. 290(1), H55-63.

Fang X, Kaduce TL, Weintraub NL, Harmon S, Teesch LM, Morisseau C, Thompson DA, Hammock BD, Spector AA.. (2001). Pathways of epoxyeicosatrienoic acid metabolism in endothelial cells. Implications for the vascular effects of soluble epoxide hydrolase inhibition. The Journal of biological chemistry. 27618), 14867-14874.

Fang X, Kaduce TL, Weintraub NL, VanRollins M, Spector AA. (1996). Functional implications of a newly characterized pathway of 11,12-epoxyeicosatrienoic acid metabolism in arterial smooth muscle. Circulation research. 79(4), 784-793.

Fang X, Weintraub NL, McCaw RB, Hu S, Harmon SD, Rice JB, Hammock BD, Spector AA. (2004). Effect of soluble epoxide hydrolase inhibition on epoxyeicosatrienoic acid metabolism in human blood vessels. American journal of physiology. Heart and circulatory physiology. 287(6), H2412-2420.

Fang X, Weintraub NL, Oltman CL, Stoll LL, Kaduce TL, Harmon S, Dellsperger KC, Morisseau C, Hammock BD, Spector AA. (2002). Human coronary endothelial cells convert 14,15-EET to a biologically active chain-shortened epoxide. American journal of physiology. Heart and circulatory physiology. 283(6), H2306-2314.

Ferdaoussi M, Bergeron V, Zarrouki B, Kolic J, Cantley J, Fielitz J, Olson EN, Prentki M, Biden T, MacDonald PE, Poitout V. (2012). G protein-coupled receptor (GPR)40-dependent potentiation of insulin secretion in mouse islets is mediated by protein kinase D1. Diabetologia. 55(10), 2682-2692.

Flodstrom M, Eizirik DL. (1997). Interferon-gamma-induced interferon regulatory factor-1 (IRF-1) expression in rodent and human islet cells precedes nitric oxide production. *Endocrinology* 138(7), 2747-2753.

Fotakis G, Timbrell JA. (2006). In vitro cytotoxicity assays: comparison of LDH, neutral red, MTT and protein assay in hepatoma cell lines following exposure to cadmium chloride. Toxicology letters. 160(2), 171-177.

Foulis AK, Liddle CN, Farquharson MA, Richmond JA, Weir RS. (1986). The histopathology of the pancreas in type 1 (insulin-dependent) diabetes mellitus: a 25-year review of deaths in patients under 20 years of age in the United Kingdom. *Diabetelogia.* 29(3), 267-274

Fujiwara K, Maekawa F, Yada T. (2005). Oleic acid interacts with GPR40 to induce Ca2+ signaling in rat islet beta-cells: mediation by PLC and L-type Ca2+ channel and link to insulin release. American journal physiology. Endocrinology and metabolism. 289(4), E670-677.

Gan MJ, O'Meill A, Haller MJ. (2012). Type 1 Diabetes: Current concepts in Epidemiology, Pathophysiology, Clincal Care and Research. *Curr Probl Pediatr Adolsc Heath Care* 1. 4(2), 269-291.

Gao H, Mourtada M, Morgan NG. (2003). Effects of the imidazoline binding site ligands, idazoxan and efaroxan, on the viability of insulin-secreting BRIN-BD11 cells. Journal of the pancreas. 4(3), 117-124.

Gao J, Morrison DC, Parmely TJ, Russell SW, Murphy WJ. (1997). An interferon-gamma-activated site (GAS) is necessary for full expression of the mouse iNOS gene in response to interferon-gamma and lipopolysaccharide. The Journal of biological chemistry. 272(2), 1226-1230.

Gepts W. (1965). Pathologic anatomy of the pancreas in juvenile diabetes mellitus. Diabetes. 14(5), 619-633.

Gerin I, Dolinsky VW, Shackman JG, Kennedy RT, Chiang SH, Burant CF, Steffensen KR, Gustafsson JA, MacDougald OA. (2005). LXRbeta is required for adipocyte growth, glucose homeostasis, and beta cell function. The Journal of biological chemistry. 280(24), 23024-23031.

Gosmanov AR, Gosmanova EO, Kitabchi AE. (2000). Hyperglycemic Crises: Diabetic Ketoacidosis (DKA), And Hyperglycemic Hyperosmolar State (HHS). Endotext.

Graham ML, Janecek JL, Kittredge JA, Hering BJ, Schuurman HJ. (2011). The streptozotocin-induced diabetic nude mouse model: differences between animals from different sources. Comparative medicine. 61(4), 356-360.

Green CD, Olson LK. (2011). Modulation of palmitate-induced endoplasmic reticulum stress and apoptosis in pancreatic β-cells by stearoyl-CoA desaturase and Elovl6.. American journal physiology. Endocrinology and metabolism. 300(4), E640-649.

Groop L, Poicot F. (2014). Genetics of Diabetes - are we missing the genes or the disease. Molecular and Cellular Endocrinology. 382(8), 726-739.

Gu X, Li K, Laybutt DR, He ML, Zhao HL, Chan JC, Xu G. (2010). Bip overexpression, but not CHOP inhibition, attenuates fatty-acid-induced endoplasmic reticulum stress and apoptosis in HepG2 liver cells. Life Sciences. 87(23-26), 724-732.

Gurgul-Convey E, Hanzelka K, Lenzen S. (2012). Mechanism of prostacyclin-induced potentiation of glucose-induced insulin secretion. Endocrinology. 153(6), 2612-2622.

Gurgul-Convey E, Lortz S, Tiedge M, Jörns A, Lenzen S. (2004). Mitochondrial catalase overexpression protects insulin-producing cells against toxicity of reactive oxygen species and proinflammatory cytokines. Diabetes. 53(9), 2271-2280.

Gysemans C, Stoffels K, Giulietti A, Overbergh L, Mathieu C. (2003). Prevention of primary non-function of islet xenografts in autoimmune diabetic NOD mice by anti-inflammatory agents. Diabetologia. 46, 1115-1123.

Haeggström JZ, Funk CD. (2011). Lipoxygenase and leukotriene pathways: biochemistry, biology, and roles in disease. Chemical reviews. 111(10), 5866-5898.

Hassan RH, Pacheco de Sousa AC, Mahfouz R, Hainault I, Blachnio-Zabielska A, Bourron O, Koskas F, Górski J, Ferré P, Foufelle F, Hajduch E. (2016). Sustained Action of Ceramide on the Insulin Signaling Pathway in Muscle Cells: IMPLICATION OF THE DOUBLE-STRANDED RNA-ACTIVATED PROTEIN KINASE. The Journal of biological chemistry. 291(6), 3019-3029.

Hao CM, Breyer MD. (2007). Roles of lipid mediators in kidney injury. Seminars in nephrology. 27(3), 338-351.

Hara T, Hirasawa A, Sun Q, Sadakane K, Itsubo C, Iga T, Adachi T, Koshimizu TA, Hashimoto T, Asakawa Y, Tsujimoto G. (2009). Novel selective ligands for free fatty acid receptors GPR120 and GPR40. Naunyn-Schmiedeberg's archives of pharmacology. 380(3), 247-255.

Harding HP, Zhang Y, Zeng H, Novoa I, Lu PD, Calfon M, Sadri N, Yun C, Popko B, Paules R, Stojdl DF, Bell JC, Hettmann T, Leiden JM, Ron D. (2003). An integrated stress response regulates amino acid metabolism and resistance to oxidative stress. Molecular cell. 11 (3), 619-633.

Hartman MG, Lu D, Kim ML, Kociba GJ, Shukri T, Buteau J, Wang X, Frankel WL, Guttridge D, Prentki M, Grey ST, Ron D, Hai T. (2004). Role for Activating Transcription Factor 3 in Stress-Induced β-Cell Apoptosis. Molecular and cellular biology. 24(13), 5721-5732.

Heimberg H, Heremans Y, Jobin C, Leemans R, Cardozo AK, Darville M, Eizirik DL. (2001). Inhibition of cytokine-induced NF-kappaB activation by adenovirus-mediated expression of a NF-kappaB super-repressor prevents beta-cell apoptosis. Diabetes. 50 (5), 2219-2224.

Heitmeier MR, Kelly CB, Ensor NJ, Gibson KA, Mullis KG, Corbett JA, Maziasz TJ. (2004). Role of cyclooxygenase-2 in cytokine-induced beta-cell dysfunction and damage by isolated rat and human islets. The Journal of biological chemistry. 279(51), 53145-53151.

Hellemans K, Kerckhofs K, Hannaert JC, Martens G, Van Veldhoven P, Pipeleers D. (2007). Peroxisome proliferator-activated receptor alpha-retinoid X receptor agonists induce beta-cell protection against palmitate toxicity. FEBS letters. 274(23), 6094-6105.

Hennige AM, Ranta F, Heinzelmann I, Düfer M, Michael D, Braumüller H, Lutz SZ, Lammers R, Drews G, Bosch F, Häring HU, Ullrich S. (2010). Overexpression of kinase-negative protein kinase Cdelta in pancreatic beta-cells protects mice from diet-induced glucose intolerance and beta-cell dysfunction. Diabetes. 59(1), 119-127.

Hernandez-Perez M, Chopra G, Fine J, Conteh AM, Anderson RM, Linnemann AK, Benjamin C, Nelson JB, Benninger KS, Nadler JL, Maloney DJ, Tersey SA, Mirmira RG. (2017). Inhibition of 12/15-Lipoxygenase Protects Against β-Cell Oxidative Stress and Glycemic Deterioration in Mouse Models of Type 1 Diabetes. Diabetes. 66(11), 2875-2887.

Hohmeier HE, Thigpen A, Tran VV, Davis R, Newgard CB. (1998). Stable expression of manganese superoxide dismutase (MnSOD) in insulinoma cells prevents IL-1beta- induced cytotoxicity and reduces nitric oxide production. The Journal of clinical investigations. 101(9), 1811-1820.

Holohan C, Szegezdi E, Ritter T, O'Brien T, Samali A. (2008). Cytokine-induced beta-cell apoptosis is NO-dependent, mitochondria-mediated and inhibited by BCL-XL. Journal of cellular and molecular medicine. 12(2), 591-606.

Hong M, Luo S, Baumeister P, Huang JM, Gogia RK, Li M, Lee AS. (2004). Underglycosylation of ATF6 as a novel sensing mechanism for activation of the unfolded protein response. The Journal of biological chemistry. 27(12), 11354-11363.

Hong SW, Lee J, Cho JH, Kwon H, Park SE, Rhee EJ, Park CY, Oh KW, Park SW, Lee WY. (2018). Pioglitazone Attenuates Palmitate-Induced Inflammation and Endoplasmic Reticulum Stress in Pancreatic β-Cells. Endocrinology and metabolism. 33(1), 105-113.

Hsieh CH, Frink M, Hsieh YC, Kan WH, Hsu JT, Schwacha MG, Choudhry MA, Chaudry IH. (2008). The role of MIP-1 alpha in the development of systemic inflammatory response and organ injury following trauma hemorrhage. Journal of immunology. 181(4), 2806-2812.

Huang CJ, Lin CY, Haataja L, Gurlo T, Butler AE, Rizza RA, Butler PC. (2007). High expression rates of human islet amyloid polypeptide induce endoplasmic reticulum stress mediated beta-cell apoptosis, a characteristic of humans with type 2 but not type 1 diabetes. Diabetes. 56(8), 2016-2027.

Huang H, Weng J, Wang MH. (2016). EETs/sEH in diabetes and obesity-induced cardiovascular diseases. Prostaglandins & other lipid mediators. 125, 80-89.

Ichimura A, Hirasawa A, Poulain-Godefroy O, Bonnefond A, Hara T, Yengo L, Kimura I, Leloire A, Liu N, Iida K, Choquet H, Besnard P, Lecoeur C, Vivequin S, Ayukawa K, Takeuchi M, Ozawa K, Tauber M, Maffeis C, Morandi A, Buzzetti R, Elliott P, Pouta A, Jarvelin MR, Körner A, Kiess W, Pigeyre M, Caiazzo R, Van Hul W, Van Gaal L, Horber F, Balkau B, Lévy-Marchal C, Rouskas K, Kouvatsi A, Hebebrand J, Hinney A, Scherag A, Pattou F, Meyre D, Koshimizu TA, Wolowczuk I, Tsujimoto G, Froguel P. (2012). Dysfunction of lipid sensor GPR120 leads to obesity in both mouse and human. Nature. 483 7389), 350-354.

Iglesias J, Barg S, Vallois D, Lahiri S, Roger C, Yessoufou A, Pradevand S, McDonald A, Bonal C, Reimann F, Gribble F, Debril MB, Metzger D, Chambon P, Herrera P, Rutter GA, Prentki M, Thorens B, Wahli W. (2012). PPARβ/δ affects pancreatic β cell mass and insulin secretion in mice. The Journal of clinical investigations. 122(11), 4105-4117.

Ikei KN, Yeung J, Apopa PL, Ceja J, Vesci J, Holman TR, Holinstat M. (2012). Investigations of human platelet-type 12-lipoxygenase: role of lipoxygenase products in platelet activation. Journal of lipid research. 53(12), 2546-2559.

Imig JD. (2000). Eicosanoid regulation of the renal vasculature. American journal of physiology. Renal physiology. 279(6), F965-981.

Imig JD. (2006). Cardiovascular therapeutic aspects of soluble epoxide hydrolase inhibitors. Cardiovascular drug reviews. 24(2), 169-188.

Imig, J.D. Hammock, B.D. 2009. "Soluble epoxide hydrolase as a therapeutic target for cardiovascular diseases." Nat Rev Drug Discov 8: 794-805.

In't Veld P. (2011). Insulitis in human type 1 diabetes The quest for an elusive lesion. *Landes Bioscience.* 3, 131-138.

In't Veld P, Lievens D, De Grijse J, Ling Z, Van der Auwera B. (2007). Screening for insulitis in adult autoantibody-positive organ donors. *Diabetes.* 56(2), 2400-2004.

Itoh Y, Hinuma S. (2005). GPR40, a free fatty acid receptor on pancreatic beta cells, regulates insulin secretion. Hepatology research: the official journal of the Japan Society of Hepatology. 33(2), 171-173.

Itoh Y, Kawamata Y, Harada M, Kobayashi M, Fujii R, Fukusumi S, Ogi K, Hosoya M, Tanaka Y, Uejima H, Tanaka H, Maruyama M, Satoh R, Okubo S, Kizawa H, Komatsu H, Matsumura F, Noguchi Y, Shinohara T, Hinumas S, Fujino M. (2003). Free fatty acids regulate insulin secretion from pancreatic beta cells through GPR40. Nature. 422(6928), 173-176.

Jahromi MM, Eisenbarth GS. (2008). Cellular na dmolecular pathogenesis of type 1A diabetes.*Cell. Mol. Life Science.* 64(3), 865-872.

Jakobsson A, Westerberg R, Jacobsson A. (2006). Fatty acid elongases in mammals: their regulation and roles in metabolism. Progress in lipid research. 45(3), 237-249.

Juhl K, Høy M, Olsen HL, Bokvist K, Efanov AM, Hoffmann EK, Gromada J. (2003). cPLA2alpha-evoked formation of arachidonic acid and lysophospholipids is required for exocytosis in mouse pancreatic beta-cells. American journal physiology. Endocrinology and metabolism. 285(1), E73-81.

Kadowaki M, Karim MR, Carpi A, Miotto G,. (2006). Nutrient control of macroautophagy in mammalian cells. Mol Aspects Med. 27(6), 426-443.

Kägi D, Odermatt B, Seiler P, Zinkernagel RM, Mak TW, Hengartner H. (1997). Reduced incidence and delayed onset of diabetes in perforin-deficient nonobese diabetic mice. The Journal of experimental medicine. 186(7), 989-997.

Kamijo R, Harada H, Matsuyama T, Bosland M, Gerecitano J, Shapiro D, Le J, Koh SI, Kimura T, Green SJ. (1994). Requirement for transcription factor IRF-1 in NO synthase induction in macrophages. Science. 263(5153), 1612-1615.

Karara A, Dishman E, Falck JR, Capdevila JH. (1991). Endogenous epoxyeicosatrienoyl-phospholipids. A novel class of cellular glycerolipids containing epoxidized arachidonate moieties. The Journal of biological chemistry. 266(12), 7561-7569.

Karara A, Dishman E, Jacobson H, Falck JR, Capdevila JH. (1990). Arachidonic acid epoxygenase. Stereochemical analysis of the endogenous epoxyeicosatrienoic acids of human kidney cortex. FEBS letters. 268(1), 227-230.

Karaskov E, Scott C, Zhang L, Teodoro T, Ravazzola M, Volchuk A. (2006). Chronic palmitate but not oleate exposure induces endoplasmic reticulum stress, which may contribute to INS-1 pancreatic beta-cell apoptosis. Endocrinology. 147(7), 3398-3407.

Katragadda D, Batchu SN, Cho WJ, Chaudhary KR, Falck JR, Seubert JM. (2009). Epoxyeicosatrienoic acids limit damage to mitochondrial function following stress in cardiac cells. Journal of molecular and cellular cardiology. 46(6), 867-875.

Katsuma S, Hatae N, Yano T, Ruike Y, Kimura M, Hirasawa A, Tsujimoto G. (2005). Free fatty acids inhibit serum deprivation-induced apoptosis through GPR120 in a murine enteroendocrine cell line STC-1. The Journal of biological chemistry. 280(20), 19507-19515.

Kaushik S, Singh R, Cuervo AM. (2010) Autophagic pathways and metabolic stress. Diabetes Obes Metab. 12(2), 4-14.

Kawajiri H, Zhuang D, Qiao N, Yoshimoto T, Yamamoto M, Iseki S, Hamaguchi K. (2000). Expression of arachidonate 12-lipoxygenase in rat tissues: a possible role in glucagon secretion. The journal of histochemistry and cytochemistry : official journal of the Histochemistry Society. 48(10), 1411-1419.

Kawasaki E, Abiru N, Eguchi K. (2004). Prevention of type 1 diabetes: from the view point of beta-cell damage. Diabetes Research Clinical Practice. 66(2), 27-32.

Keane DC, Takahashi HK, Dharyal S, Morgan N, Curi R, Newsholme P. (2011). Arachidonic acid actions on functional integrity and attenuation of the negative effects of palmitic acid in a clonal pancreatic β-cell line. Clincal Science. 120(1), 195-206.

Keller H, Dreyer C, Medin J, Mahfoudi A, Ozato K, Wahli W. (1993). Fatty acids and retinoids control lipid metabolism through activation of peroxisome proliferator-activated receptor-retinoid X receptor heterodimers. Proceedings of the National Academy of Sciences of the United States of America. 90(6), 2160-2164.

Kelpe CL, Johnson LM, Poitout V. (2002). Increasing triglyceride synthesis inhibits glucose-induced insulin secretion in isolated rat islets of langerhans: a study using adenoviral expression of diacylglycerol acyltransferase. Endocrinology. 143(9), 3326-3332.

Kessler P, Popp R, Busse R, Schini-Kerth VB. (1999). Proinflammatory mediators chronically downregulate the formation of the endothelium-derived hyperpolarizing factor in arteries via a nitric oxide/cyclic GMP-dependent mechanism. Circulation. 99(14), 1878-1884.

Kim MS, Polychronakos C. (2005). Immunogenetics of type 1 diabetes. *Hormone Research.* 64(5), 180-188.

Klett EL, Chen S, Edin ML, Li LO, Ilkayeva O, Zeldin DC, Newgard CB, Coleman RA. (2013). Diminished acyl-CoA synthetase isoform 4 activity in INS 832/13 cells reduces cellular epoxyeicosatrienoic acid levels and results in impaired glucose-stimulated insulin secretion. The Journal of biological chemistry. 288(30), 21618-21629.

Kliewer SA, Lenhard JM, Willson TM, Patel I, Morris DC, Lehmann JM. (1995). A prostaglandin J2 metabolite binds peroxisome proliferator-activated receptor gamma and promotes adipocyte differentiation. Cell. 83(5), 813-819.

Kowalski, GM. Bruce, CR. (2014). The regulation of glucose metabolism: implications and considerations for the assessment of glucose homeostasis in rodents. American journal physiology. Endocrinology and metabolism. 307(10), E859-871.

Kozak W, Aronoff DM, Boutaud O, Kozak A. (2003). 11,12-epoxyeicosatrienoic acid attenuates synthesis of prostaglandin E2 in rat monocytes stimulated with lipopolysaccharide. Experimental biology and medicine. 228(7), 786-794.

Kreuwel HTC, Morgan DJ, Krahl T, Ko A, Sarvetnick N, Sherman LA. (1999). Comparing the relative tole of perforin/granzyme versus Fas/Fas ligand cytotoxic pathways in CD8+ T-cell mediated Insulin-dependent Diabetes Mellitus. The Journal of Immunology. 163(9), 4335-4341.

Kruse KB, Brodsky JL, McCracken AA. (2006). Autophagy: an ER protein quality control process. Autophagy. 2(2), 135-137.

Kutlu B, Cardozo AK, Darville MI, Kruhøffer M, Magnusson N, Ørntoft T, Eizirik DL. (2003). Discovery of gene networks regulating cytokine-induced dysfunction and apoptosis in insulin-producing INS-1 cells. Diabetes. 52(11), 2701-2719.

Kwon G, Corbett JA, Rodi CP, Sullivan P, McDaniel ML. (1995). Interleukin-1 beta-induced nitric oxide synthase expression by rat pancreatic beta-cells: evidence for the involvement of nuclear factor kappa B in the signaling mechanism. Endocrinology. 136(11), 4790-4795.

Lallena MJ, Diaz-Meco MT, Bren G, Payá CV, Moscat J. (1999). Activation of IkappaB kinase beta by protein kinase C isoforms. Molecular and cellular biology. 19(3), 2180-2188.

Lang F, Ullrich S, Gulbins E. (2011). Ceramide formation as a target in beta-cell survival and function. Expert opinion on therapeutic targets. 15(9), 1061-1071.

Laybutt DR, Preston AM, Akerfeldt MC, Kench JG, Busch AK, Biankin AV, Biden TJ. (2007). Endoplasmic reticulum stress contributes to beta cell apoptosis in type 2 diabetes. Diabetologia. 50(4), 752-763.

Leamy AK, Hasenour CM, Egnatchik RA, Trenary IA, Yao CH, Patti GJ, Shiota M, Young JD. (2016). Knockdown of triglyceride synthesis does not enhance palmitate lipotoxicity or prevent oleate-mediated rescue in rat hepatocytes. Biochimica et biophysica acta. 1861(9 Part A), 1005-1014.

LeCompte P. (1958). Insulitis in early juvenile diabetes. *Achives of Pathology.* 66(8), 450-457.

Lee K, Tirasophon W, Shen X, Michalak M, Prywes R, Okada T, Yoshida H, Mori K, Kaufman RJ. (2002). IRE1-mediated unconventional mRNA splicing and S2P-mediated ATF6 cleavage merge

to regulate XBP1 in signaling the unfolded protein response. Genes & development. 16(4), 452-466.

Lenzen S, Drinkgern J, Tiedge M. (1996). Low antioxidant enzyme gene expression in pancreatic islets compared with various other mouse tissues. Free radical biology & medicine. 20(3), 463-466.

Lenzen S, Tiedge M, Elsner M, Lortz S, Weiss H, Jorns A. (2001). The LEW.1AR1/Ztm-iddm rat: a new model of spontaneous insulin-dependent diabetes mellitus. *Diabetologia.* 44(21), 1189-1196.

Lerner AG, Upton JP, Praveen PV, Ghosh R, Nakagawa Y, Igbaria A, Shen S, Nguyen V, Backes BJ, Heiman M. (2012). IRE1alpha induces thioredoxin-interacting protein to activate the NLRP3 Inflammasome and promote programmed cell death under irremediable ER stress. Cellular Metabolism. 16(4), 250-264.

Li F, Mahato R. (2008). iNOS gene silencing prevents inflammatory cytokine-induced beta-cell apoptosis. Molecular pharmaceutics. 5(3), 407-417.

Li L, Li T, Zhang Y, Pan Z, Wu B, Huang X, Zhang Y, Mei Y, Ge L, Shen G, Ge RS, Zhu D, Lou Y. (2015). Peroxisome proliferator-activated receptorβ/δ activation is essential for modulating p-Foxo1/Foxo1 status in functional insulin-positive cell differentiation. Cell death & disease. 6, e1715.

Li P, Nijhawan D, Budihardjo I, Srinivasula SM, Ahmad M. (1997). Cytochrome c and dATP-dependent formation of Apaf-1/caspase-9 complex initiates an apoptotic protease cascade. Cell. 91(7), 479-489.

Listenberger LL, Han X, Lewis SE, Cases S, Farese RV Jr, Ory DS, Schaffer JE. (2003). Triglyceride accumulation protects against fatty acid-induced lipotoxicity. Proceedings of the National Academy of Sciences of the United States of America. 100(6), 3077-3082.

Listenberger LL, Ory DS, Schaffer JE. (2001). Palmitate-induced apoptosis can occur through a ceramide-independent pathway. The Journal of biological chemistry. 276(18), 14890-5.

Liu D, Pavlovic D, Chen MC, Flodström M, Sandler S, Eizirik DL. (2000). Cytokines induce apoptosis in beta-cells isolated from mice lacking the inducible isoform of nitric oxide synthase (iNOS-/-). Diabetes. 49(7), 1116-1122.

Liu X, Qian ZY, Xie F, Fan W, Nelson JW, Xiao X, Kaul S, Barnes AP, Alkayed NJ. (2017). Functional screening for G protein-coupled receptor targets of 14,15-epoxyeicosatrienoic acid. Prostaglandins & other lipid mediators. 132(1), 31-40.

Liu Y, Zhang Y, Schmelzer K, Lee TS, Fang X, Zhu Y, Spector AA, Gill S, Morisseau C, Hammock BD, Shyy JY. (2005). The antiinflammatory effect of laminar flow: the role of PPARgamma, epoxyeicosatrienoic acids, and soluble epoxide hydrolase. Proceedings of the National Academy of Sciences of the United States of America. 102(46), 16747-16752.

Long Q, Wang L, Zhou M, Wu Y, Chen T. (2018). A novel peptide Phylloseptin-PBu from Phyllomedusa burmeisteri possesses insulinotropic activity via potassium channel and GLP-1 receptor signalling. Journal of cellular and molecular medicine. 22(5), 2804-2814.

Lortz S, Tiedge M. (2003). Sequential inactivation of reactive oxygen species by combined overexpression of SOD isoforms and catalase in insulin-producing cells. Free radical biology & medicine. 34(6), 683-388.

Loweth AC, Scarpello JH, Morgan NG. (1995). Phospholipase A2 expression in human and rodent insulin-secreting cells. Molecular and cellular endocrinology. 112(2), 177-183.

Luo P, Wang MH. (2011). Eicosanoids, Beta-cell function, and diabetes. Prostaglandins and other Lipid Mediators 95, 1-10.

Lundstrom K. (2009). An overview on GPCRs and drug discovery: structure-based drug design and structural biology on GPCRs. Methods in molecular biology. 552, 51-66.

Lupi R, Dotta F, Marselli L, Del Guerra S, Masini M, Santangelo C, Patané G, Boggi U, Piro S, Anello M, Bergamini E, Mosca F, Di Mario U, Del Prato S, Marchetti P. (2002). Prolonged exposure to free fatty acids has cytostatic and pro-apoptotic effects on human pancreatic islets: evidence that beta-cell death is caspase mediated, partially dependent on ceramide pathway, and Bcl-2 regulated. Diabetes. 51(5), 1437-1442.

Luo P, Chang H, Zhou Y, Zhang S, Hwang S, Wang M, (2010). Inhibition or Deletion of Soluble Epoxide Hydrolase Prevents Hyperglycemia, Promotes Insulin Secretion, and Reduces Islet Apoptosis. Journal of Pharmacology and Experimental Therapeutics. 334, 430-438.

Ly LD, Xu S, Choi SK, Ha CM, Thoudam T, Cha SK, Wiederkehr A, Wollheim CB, Lee IK, Park KS. (2017). Oxidative stress and calcium dysregulation by palmitate in type 2 diabetes. Experimental & molecular medicine. 49(2), e291.

Ma K, Nunemaker CS, Wu R, Chakrabarti SK, Taylor-Fishwick DA, Nadler JL. (2010). 12-Lipoxygenase Products Reduce Insulin Secretion and {beta}-Cell Viability in Human Islets. The Journal of clinical endocrinology and metabolism. 95(2), 887-893.

Ma Z, Ramanadham S, Corbett JA, Bohrer A, Gross RW, McDaniel ML, Turk J. (1996). Interleukin-1 enhances pancreatic islet arachidonic acid 12-lipoxygenase product generation by increasing substrate availability through a nitric oxide-dependent mechanism. The Journal of biological chemistry. 271(2), 1029-1042.

Maedler K, Oberholzer J, Bucher P, Spinas GA, Donath MY. (2003). Monounsaturated fatty acids prevent the deleterious effects of palmitate and high glucose on human pancreatic beta-cell turnover and function. Diabetes. 52(3), 726-733.

Man SM, Karki R, Kanneganti TD. (2017). Molecular mechanisms and functions of pyroptosis, inflammatory caspases and inflammasomes in infectious diseases. Immunological reviews. 277(1), 61-75.

Marhfour I, Lopez XM, Lefkaditis D, Salmon I, Allagnat F, Richardson SJ, Morgan NG, Eizirik DL. (2012). Expression of endoplasmic reticulum stress markers in the islets of patients with type 1 diabetes. *Diabetologia*. 55(9), 2417-2420.

Maris M, Robert S, Waelkens E, Derua R, Hernangomez MH, D'Hertog W, Cnop M, Mathieu C, Overbergh L. (2013). Role of the saturated nonesterified fatty acid palmitate in beta cell dysfunction. Journal of proteome research. 12(1), 347-362.

Mathias S, Peña LA, Kolesnick RN. (1998). Signal transduction of stress via ceramide. The Biochemical journal. 335(Part 3), 465-480.

Martino L,Masini M, Novelli M, Beffy P, Bugliani M, Marselli L, Masiello P, Marchetti P, De Tata, V. (2012). Palmitate Activates Autophagy in INS-1E beta cells and in Isolated Rat and Human Pancreatic Islets. Plos One. 7(2), e36188.

McCabe C, Samali A, O'brien T. (2006). beta cell cytoprotective strategies: establishing the relative roles for iNOS and ROS. Biochemical and biophysical research communications. 342(4), 1240-1248.

McClenaghan NH, Barnett CR, Ah-Sing E, Abdel-Wahab YH, O'Harte FP, Yoon TW, Swanston-Flatt SK, Flatt PR. (1996). Characterization of a novel glucose-responsive insulin-secreting cell line, BRIN-BD11, produced by electrofusion. Diabetes. 45(8), 1132-1140.

McClenaghan NH, Flatt PR. (1999). Engineering cultured insulin-secreting pancreatic B-cell lines. Journal of molecular medicine. 77(1), 235-243.

McCullough KD, Martindale JL, Klotz LO, Aw TY, Holbrook N. (2001). Gadd153 sensitizes cells to endoplasmic reticulum stress by down-regulating Bcl2 and perturbing the cellular redox state. Molecular and cellular biology. 21(4), 1249-1259.

McDaniel ML, Kwon G, Hill JR, Marshall CA, Corbett JA. (1996). Cytokines and nitric oxide in islet inflammation and diabetes. Proceedings of the Society for Experimental Biology and Medicine. 211(1), 24-32.

McKenzie MD, Carrington EM, Kaufmann T, Strasser A, Huang DC, Kay TW, Allison J, Thomas HE. (2008). Proapoptotic BH3-only protein Bid is essential for death receptor-induced apoptosis of pancreatic beta-cells. Diabetes. 57(5), 1284-1292.

McKenzie MD, Jamieson E, Scott CL, Huang DC, Bouillet P, Allison J, Kay TW, Strasser A, Thomas HE. (2010). Glucose induces pancreatic islet cell apoptosis that requires BH3-only proteins bim and puma and multi-BH domain protein Bax. Diabetes. 59(10), 644-652.

Mehnert M, Sommer T, Jarosch E. (2010). ERAD ubiquitin ligases: multifunctional tools for protein quality control and waste disposal in the endoplasmic reticulum. BioEssays: news and reviews in molecular, cellular and developmental biology. 32(10), 905-913.

Michalska M, Wolf G, Walther R, Newsholme P. (2010). Effects of pharmacological inhibition of NADPH oxidase or iNOS on pro-inflammatory cytokine, palmitic acid or H2O2-induced mouse islet or clonal pancreatic β-cell dysfunction. Bioscience reports. 30(6), 445-453.

Mochizuki N, Kwon YG. (2008). 15-lipoxygenase-1 in the vasculature: expanding roles in angiogenesis. Circulation research. 102(2), 143-145.

Moffitt JH, Fielding BA, Evershed R, Berstan R, Currie JM, Clark A. (2005). Adverse physicochemical properties of tripalmitin in beta cells lead to morphological changes and lipotoxicity in vitro. Diabetologia. 48(9), 1819-1829.

Mollah ZU, Wali J, McKenzie MD, Krishnamurthy B, Graham KL, Fynch S, Szanyi J, Santamaria P, Brodnicki T, Allison J, Strasser A, Kay TW, Thomas HE. (2011). The pro-apoptotic BH3-only protein Bid is dispensable for development of insulitis and diabetes in the non-obese diabetic mouse. Apoptosis. 16(8), 822-830.

Montell E, Turini M, Marotta M, Roberts M, Noé V, Ciudad CJ, Macé K, Gómez-Foix AM. (2001). DAG accumulation from saturated fatty acids desensitizes insulin stimulation of glucose uptake in muscle cells. American journal physiology. Endocrinology and metabolism. 280(2), E229-237.

Morgan ET, MacGeoch C, Gustafsson JA. (1985). Hormonal and developmental regulation of expression of the hepatic microsomal steroid 16 alpha-hydroxylase cytochrome P-450 apoprotein in the rat. The Journal of biological chemistry. 260(22), 11895-11898.

Morgan NG, Dhayal S. (2009). G-protein coupled receptors mediating long chain fatty acid signalling in the pancreatic beta-cell. Biochemical pharmacology. 78(12), 1419-1427.

Morgan RO, Laychock SG. (1988). Biosynthesis of peptidyl leukotrienes and other lipoxygenase products by rat pancreatic islets. Comparison with macrophages and neutrophils. Prostaglandins. 35(4), 609-623.

Mossmann, T. (1983). Rapid colorimetric assay for cellular growth and survival: application to proliferation and cytotoxicity assays. Journal of Immunological Methods. 65(1-2), 55-63.

Nagasawa T, Nakamichi H1, Hama Y1, Higashiyama S2, Igarashi Y3, Mitsutake S1. (2018). Phytosphingosine is a novel activator of GPR120. Journal of biochemistry. 164(1), 27-32.

Nakamichi Y, Kikuta T, Ito E, Ohara-Imaizumi M, Nishiwaki C, Ishida H, Nagamatsu S. (2003). PPAR-gamma overexpression suppresses glucose-induced proinsulin biosynthesis and insulin release synergistically with pioglitazone in MIN6 cells. Biochemical and biophysical research communications. 306(4), 832-836.

Natalicchio A, Biondi G, Marrano N, Labarbuta R, Tortosa F, Spagnuolo R, D'Oria R, Carchia E, Leonardini A, Cignarelli A, Perrini S, Laviola L, Giorgino F. (2016). Long-Term Exposure of Pancreatic β-Cells to Palmitate Results in SREBP-1C-Dependent Decreases in GLP-1 Receptor Signaling via CREB and AKT and Insulin Secretory Response. Endocrinology. 157(6), 2243-2258.

Newsholme P, Keane D, Welters HJ, Morgan NG. (2007). Life and death decisions of the pancreatic beta-cell: the role of fatty acids. Clinical Science. 112(1), 27-42.

Node K, Huo Y, Ruan X, Yang B, Spiecker M, Ley K, Zeldin DC, Liao JK. (1999). Anti-inflammatory properties of cytochrome P450 epoxygenase-derived eicosanoids. Science. 285(5431), 1276-1279.

Novoa I, Zeng H, Harding HP, Ron D. (2001). Feedback inhibition of the unfolded protein response by GADD34-mediated dephosphorylation of eIF2alpha. The Journal of cell biology. 153(5), 1011-1022.

O'Harte FP, Ng MT, Lynch AM, Conlon JM, Flatt PR. (2016). Novel dual agonist peptide analogues derived from dogfish glucagon show promising in vitro insulin releasing actions and antihyperglycaemic activity in mice. Molecular and cellular endocrinology. 431, 133-144.

Oh DY, Walenta E, Akiyama TE, Lagakos WS, Lackey D, Pessentheiner AR, Sasik R, Hah N, Chi TJ, Cox JM, Powels MA, Di Salvo J, Sinz C, Watkins SM, Armando AM, Chung H, Evans RM, Quehenberger O, McNelis J, Bogner-Strauss JG, Olefsky JM. (2014). A Gpr120-selective agonist improves insulin resistance and chronic inflammation in obese mice. Nature medicine. 20(8), 942-947.

Oliveira AF, Cunha DA, Ladriere L, Igoillo-Esteve M, Bugliani M, Marchetti P, Cnop M. (2015). In vitro use of free fatty acids bound to albumin: A comparison of protocols. Biotechniques. 58(5), 228-233.

Ortis F, Miani M, Colli ML, Cunha DA, Gurzov EN, Allagnat F, Chariot A, Eizirik DL. (2012). Differential usage of NF-κB activating signals by IL-1β and TNF-α in pancreatic beta cells. FEBS letters. 586(7), 984-999.

Ortis F, Pirot P, Naamane N, Kreins AY, Rasschaert J, Moore F, Théâtre E, Verhaeghe C, Magnusson NE, Chariot A, Orntoft TF, Eizirik DL. (2008). Induction of nuclear factor-kappaB

and its downstream genes by TNF-alpha and IL-1beta has a pro-apoptotic role in pancreatic beta cells. Diabetologia. 51(7), 1213-1225.

Oshima H, Taketo MM, Oshima M. (2006). Destruction of pancreatic beta-cells by transgenic induction of prostaglandin E2 in the islets. The Journal of biological chemistry. 281(39), 29330-29336.

Overton HA, Babbs AJ, Doel SM, Fyfe MC, Gardner LS, Griffin G, Jackson HC, Procter MJ, Rasamison CM, Tang-Christensen M, Widdowson PS, Williams GM, Reynet C. (2006). Deorphanization of a G protein-coupled receptor for oleoylethanolamide and its use in the discovery of small-molecule hypophagic agents. Cell metabolism. 3(3), 167-175.

Oyadomari S, Takeda K, Takiguchi M, Gotoh T, Matsumoto M, Wada I, Akira S, Araki E, Mori M. (2001). Nitric oxide-induced apoptosis in pancreatic beta cells is mediated by the endoplasmic reticulum stress pathway. Proc Natl Acad Sci U S A. 98(2), 10845-10850.

Ozcan U, Cao Q, Yilmaz E, Lee AH, Iwakoshi NN, Ozdelen E, Tuncman G, Görgün C, Glimcher LH, Hotamisligil GS. (2004). Endoplasmic reticulum stress links obesity, insulin action, and type 2 diabetes. Science. 306(5695), 457-461.

Papadimitriou A, King AJ, Jones PM, Persaud SJ. (2007). Anti-apoptotic effects of arachindonic acid and prostaglandin E2 in pancreatic Beta-cells. *Cell Physiology Biochemistry* 20, 607-616.

Panse M, Gerst F, Kaiser G, Teutsch CA, Dölker R, Wagner R, Häring HU, Ullrich S. (2015). Activation of extracellular signal-regulated protein kinases 1 and 2 (ERK1/2) by free fatty acid receptor 1 (FFAR1/GPR40) protects from palmitate-induced beta cell death, but plays no role in insulin. Cellular physiology and biochemistry: international journal of experimental cellular physiology, biochemistry, and pharmacology. 35(4), 1537-1545.

Park SK, Herrnreiter A, Pfister SL, Gauthier KM, Falck BA, Falck JR, Campbell WB. (2018). GPR40 is a low-affinity epoxyeicosatrienoic acid receptor in vascular cells. The Journal of biological chemistry. 293(27), 10675-10691.

Pavlovic D, Chen M, Gysemans CA, Mathieu C, Eizirik DL. (1999). The role of interferon regulatory factor-1 in cytokine induced mRNA expression and cell death in murine pancreatic beta cells. European Cytokine Network. 10(7), 403-412.

Pearly-Yafe M, Kaminitz A, Yolcu ES, Yaniv I, Stein J, Askenasy N. (2007). Pancreatic islets under attack: cellular and molecular effectors. *Curr. Pharm Des.* 13(7), 749-760.

Persaud SJ, Muller D, Belin VD, Kitsou-Mylona I, Asare-Anane H, Papadimitriou A, Burns CJ, Huang GC, Amiel SA, Jones PM. (2007). The role of arachidonic acid and its metabolites in insulin secretion from human islets of langerhans. Diabetes. 56(1), 197-203.

Persaud SJ, Wheeler-Jones CP, Jones PM. (1996). The mitogen-activated protein kinase pathway in rat islets of Langerhans: studies on the regulation of insulin secretion. The Biochemical journal. 313(Part 1), 119-124.

Petrovsky N, Silva D, Socha L, Slattery R, Charlton B. (2002). The role of Fas ligand in beta cell destruction in autoimmune diabetes of NOD mice. Annals of the New York Academy of Sciences. 958(1), 204-208.

Piro S, Anello M, Di Pietro C, Lizzio MN, Patane G, Rabuazzo AM, Vigneri R, Purrello M, Purrello F. (2002). Chronic exposure to free fatty acids or high glucose induces apoptosis in rat pancreatic islets: possible role for oxidative stress. Metabolism. 51(2), 1340-1347.

Pirot P, Cardozo AK, Eizirik DL. (2008). Mediators and Mechanisms of Pancreatic Beta-Cell Death in Type 1 Diabetes. *Arq Bras Endrocrinol Metab* 52,(no. 2), 156-165.

Pirot P, Eizirik DL, Cardozo AK. (2006). Interferon-gamma potentiates endoplasmic reticulum stress-induced death by reducing pancreatic beta cell defence mechanisms. Diabetologia. 49(6), 1229-1236.

Plotz T, Hartmann M, Lenzen S, Elsner M. (2016). The role of lipid droplet formation in the protection of unsaturated fatty acids against palmitic acid induced lipotoxicity to rat insulin-producing cells. Nutrition and Metabolism. 16, 1-11.

Poudyal H, Panchal SK, Ward LC, Brown L. (2013). Effects of ALA, EPA and DHA in high-carbohydrate, high-fat diet-induced metabolic syndrome in rats. The Journal of nutritional biochemistry. 24(6), 1041-1052.

Pozzi A, Macias-Perez I, Abair T, Wei S, Su Y, Zent R, Falck JR, Capdevila JH. (2005). Characterization of 5,6- and 8,9-epoxyeicosatrienoic acids (5,6- and 8,9-EET) as potent in vivo angiogenic lipids. The Journal of biological chemistry. 280(29), 27138-27146.

Prentki M, Joly E, El-Assaad W, Roduit R. (2002). Malonyl-CoA signaling, lipid partitioning, and glucolipotoxicity: role in beta-cell adaptation and failure in the etiology of diabetes. Diabetes. 51(Supplement 3), S405-413.

Rabinovitch A, Baguerizo H, Sumoski W, (1990). Cytotoxic Effects of Cytokines on Islet β-Cells: Evidence for Involvement of Eicosanoids. Endocrinology 126, 67-71.

Rabinovitch A, Suarez-Pinzon WL. (1998). Cytokines and their roles in pancreatic islet beta-cell destruction and insulin-dependent diabetes mellitus. Biochemical pharmacology. 55(8), 1139-1149.

Rabinovitch A, Suarez-Pinzon WL, Strynadka K, Lakey JR, Rajotte RV. (1996). Human pancreatic islet beta-cell destruction by cytokines involves oxygen free radicals and aldehyde production. The Journal of clinical endocrinology and metabolism. 81(9), 3197-3202.

Ramanadham S, Gross RW, Han X, Turk J. (1993). Inhibition of arachidonate release by secretagogue-stimulated pancreatic islets suppresses both insulin secretion and the rise in beta-cell cytosolic calcium ion concentration. Biochemistry. 32(1), 337-346.

Ramanadham S, Song H, Bao S, Hsu FF, Zhang S, Ma Z, Jin C, Turk J. (2004). Islet complex lipids: involvement in the actions of group VIA calcium-independent phospholipase A(2) in beta-cells. Diabetes. 53(Supplement 1), S179-185.

Rand AA, Barnych B, Morisseau C, Cajka T, Lee KSS, Panigrahy D, Hammock BD. (2017). Cyclooxygenase-derived proangiogenic metabolites of epoxyeicosatrienoic acids. Proceedings of the National Academy of Sciences of the United States of America. 114(17), 4370-4375.

Ravnskjaer K, Frigerio F, Boergesen M, Nielsen T, Maechler P, Mandrup S. (2010). PPARdelta is a fatty acid sensor that enhances mitochondrial oxidation in insulin-secreting cells and protects against fatty acid-induced dysfunction. Journal of lipid research. 51(6), 1370-1379.

Reddy MA, Thimmalapura PR, Lanting L, Nadler JL, Fatima S, Natarajan R. (2002). The oxidized lipid and lipoxygenase product 12(S)-hydroxyeicosatetraenoic acid induces hypertrophy and fibronectin transcription in vascular smooth muscle cells via p38 MAPK and cAMP response

element-binding protein activation. Mediation of angiotensin II effects. The Journal of biological chemistry. 277(12), 9920-9928.

Repetto G, del Peso A, Zurita JL. (2008). Neutral red uptake assay for the estimation of cell viability/cytotoxicity. Nature Protocols. 3(7), 1125-1131.

Richardson AJ, Willcox A, Bone AJ, Foulis AK, Morgan NG. (2009). The prevalence of enteroviral capsid protein vp1 immunostaining in pancreatic islets in human type 1 diabetes. Diabetologia. 52(9), 1143-1151.

Robertson RP. (1998). Dominance of cyclooxygenase-2 in the regulation of pancreatic islet prostaglandin synthesis. Diabetes. 47(9), 1379-1383.

Robertson RP. (2017). The COX-2/PGE2/EP3/Gi/o/cAMP/GSIS Pathway in the Islet: The Beat Goes On. Diabetes. 66(6), 1464-1466.

Roduit R, Nolan C, Alarcon C, Moore P, Barbeau A, Delghingaro-Augusto V, Przybykowski E, Morin J, Massé F, Massie B, Ruderman N, Rhodes C, Poitout V, Prentki M. (2004). A role for the malonyl-CoA/long-chain acyl-CoA pathway of lipid signaling in the regulation of insulin secretion in response to both fuel and nonfuel stimuli. Diabetes. 53(4), 1007-1019.

Rompe F1, Artuc M, Hallberg A, Alterman M, Ströder K, Thöne-Reineke C, Reichenbach A, Schacherl J, Dahlöf B, Bader M, Alenina N, Schwaninger M, Zuberbier T, Funke-Kaiser H, Schmidt C, Schunck WH, Unger T, Steckelings UM. (2010). Direct angiotensin II type 2 receptor stimulation acts anti-inflammatory through epoxyeicosatrienoic acid and inhibition of nuclear factor kappaB. Hypertension. 55(4), 924-931.

Ron D, Walter P. (2007). Signal integrattion in the endoplasmic reticulum unfolded protein response. Nat Rev Mol Cell Biol. 8(7), 519-529.

Rouzer CA, Marnett LJ. (2011). Endocannabinoid oxygenation by cyclooxygenases, lipoxygenases, and cytochromes P450: cross-talk between the eicosanoid and endocannabinoid signaling pathways. Chemical reviews. 111(10), 5899-5921.

Saitoh Y, Chun-ping C, Noma K, Ueno H, Mizuta M, Nakazato M. (2008). Pioglitazone attenuates fatty acid-induced oxidative stress and apoptosis in pancreatic beta-cells. Diabetes, obesity & metabolism. 10(7), 564-573.

Saldeen J, Lee LC, Welsh N. (2001). Role of p38 mitogen-activated protein kinase (p38 MAPK) in cytokine-induced rat iselt cell apoptosis. Biochem Pharmacol. 61(21), 1561-1569.

Salvemini D, Misko TP, Masferrer JL, Seibert K, Currie MG, Needleman P. (1993). Nitric oxide activates cyclooxygenase enzymes. Proc. Natl. Acad. Sci. 90, 7240-7244.

Samokhvalov V, Vriend J, Jamieson KL, Akhnokh MK, Manne R, Falck JR, Seubert JM. (2014). PPARγ signaling is required for mediating EETs protective effects in neonatal cardiomyocytes exposed to LPS. Frontiers in pharmacology. 5, 242.

Sandberg M, Jansson L. (2014). Effects of cyclooxygenase inhibition on insulin release and pancreatic islet blood flow in rats. Upsala journal of medical sciences. 119(4), 316-323.

Sargsyan E, Bergsten P. (2011). Lipotoxicity is glucose-dependent in INS-1E cells but not in human islets and MIN6 cells. Lipids in health and disease. 10, 115.

Sears DD, Miles PD, Chapman J, Ofrecio JM, Almazan F, Thapar D, Miller YI. (2009). 12/15-lipoxygenase is required for the early onset of high fat diet-induced adipose tissue inflammation and insulin resistance in mice. PloS One. 4(9), e7250.

Sette S, Le Donne C, Piccinelli R, Arcella D, Turrini A, Leclercq C; INRAN-SCAI 2005-6 Study Group. (2011). The third Italian National Food Consumption Survey, INRAN-SCAI 2005-06--part 1: nutrient intakes in Italy. Nutrition, metabolism, and cardiovascular diseases : NMCD. 21(12), 922-932.

Seubert JM, Sinal CJ, Graves J, DeGraff LM, Bradbury JA, Lee CR, Goralski K, Carey MA, Luria A, Newman JW, Hammock BD, Falck JR, Roberts H, Rockman HA, Murphy E, Zeldin DC. (2006). Role of soluble epoxide hydrolase in postischemic recovery of heart contractile function. Circulation research. 99(4), 442-450.

Seubert JM, Yang B, Bradbury JA, Graves J, Degraff LM, Gabel S, Gooch R, Foley J, Newman J, Mao L, Rockman HA, Hammock BD, Murphy E, Zeldin DC. (2004). Enhanced postischemic functional recovery in CYP2J2 transgenic hearts involves mitochondrial ATP-sensitive K+ channels and p42/p44 MAPK pathway. Circulation research. 95(5), 506-514.

Shanmugam N, Todorov IT, Nair I, Omori K, Reddy MA, Natarajan R. (2006). Increased expression of cyclooxygenase-2 in human pancreatic islets treated with high glucose or ligands of the advanced glycation endproduct-specific receptor (AGER), and in islets from diabetic mice. Diabetologia. 49(1), 100-107.

Shannon VR, Ramanadham S, Turk J, Holtzman MJ. (1992). Selective expression of an arachidonate 12-lipoxygenase by pancreatic islet beta-cells. The American journal of physiology. 263(5 Part 1), E828-836.

Sherry NA, Kushner JA, Glandt M, Kitamura T, Brillantes AM, Herold KC. (2006). Effects of autoimmunity and immune therapy on beta-cell turnover in type 1 diabetes. Diabetes. 55(12), 3238-3245.

Shimabukuro M, Zhou YT, Levi M, Unger RH. (1998). Fatty acid-induced beta cell apoptosis: a link between obesity and diabetes. Proceedings of the National Academy of Sciences of the United States of America. 95(5), 2498-2502.

Shridas P, Noffsinger VP, Trumbauer AC, Webb NR. (2017). The dual role of group V secretory phospholipase A2 in pancreatic β-cells. Endocrine. 58(1), 47-58.

Simmons KM, Gottlieb PA, Michels AW. (2016). Immune Intervention and Preservation of Pancreatic Beta Cell Function in Type 1 Diabetes. Current diabetes reports. 16(10), 97.

Sol EM, Sargsyan E, Akusjärvi G, Bergsten P. (2008). Glucolipotoxicity in INS-1E cells is counteracted by carnitine palmitoyltransferase 1 over-expression. Biochemical and biophysical research communications. 375(4), 517-521.

Song B, Scheuner D, Ron D, Pennathur S, Kaufman RJ. (2008). Chop deletion reduces oxidative stress, improves beta cell function, and promotes cell survival in multiple mouse models of diabetes. The Journal of clinical investigations. 118(10), 3378-3389.

Song K, Zhang X, Zhao C, Ang NT, Ma ZA. (2005). Inhibition of Ca2+-independent phospholipase A2 results in insufficient insulin secretion and impaired glucose tolerance. Molecular endocrinology. 19(2), 504-515.

Sorli CH, Zhang HJ, Armstrong MB, Rajotte RV, Maclouf J, Robertson RP. (1998). Basal expression of cyclooxygenase-2 and nuclear factor-interleukin 6 are dominant and coordinately regulated by interleukin 1 in the pancreatic islet. Proceedings of the National Academy of Sciences of the United States of America. 95(4), 1788-1793.

Spector AA, Fang X, Snyder GD, Weintraub NL. (2004). Epoxyeicosatrienoic acids (EETs): metabolism and biochemical function. Progress in lipid research. 43(1), 55-90.

Spector AA, Norris AW. (2007). Action of epoxyeicosatrienoic acids on cellular function. American journal of physiology. Cell physiology. 292(3), C996-1012.

Spiecker M, Liao JK. (2005). Vascular protective effects of cytochrome p450 epoxygenase-derived eicosanoids. Archives of biochemistry and biophysics. 433(2), 413-420.

Standop J, Ulrich AB, Schneider MB, Büchler MW, Pour PM. (2002). Differences in the expression of xenobiotic-metabolizing enzymes between islets derived from the ventral and dorsal anlage of the pancreas. Pancreatology. 2(6), 510-518.

Stassi G, Todaro M, Richiusa P, Giordano M, Mattina A, Sbriglia MS, Lo Monte A, Buscemi G, Galluzzo A, Giordano C. (1995). Expression of apoptosis-inducing CD95 (Fas/Apo-1) on human beta-cells sorted by flow-cytometry and cultured in vitro. Transplantation proceedings. 27(6), 3271-3275.

Stein DT, Esser V, Stevenson BE, Lane KE, Whiteside JH, Daniels MB, Chen S, McGarry JD. (1996). Essentiality of circulating fatty acids for glucose-stimulated insulin secretion in the fasted rat. The Journal of clinical investigations. 97(12), 2728-2735.

Størling J, Binzer J, Andersson AK, Züllig RA, Tonnesen M, Lehmann R, Spinas GA, Sandler S, Billestrup N, Mandrup-Poulsen T. (2005). Nitric oxide contributes to cytokine-induced apoptosis in pancreatic beta cells via potentiation of JNK activity and inhibition of Akt. Diabetologia. 48(10), 2039-2050.

Stone VM, Dhayal S, Smith DM, Lenaghan C, Brocklehurst KJ, Morgan NG. (2012). The cytoprotective effects of oleoylethanolamide in insulin-secreting cells do not require activation of GPR119. British journal of pharmacology. 165(8), 2758-2770.

Suarez-Pinzon WL, Power RF, Rabinovitch A. (2000). Fas ligand-mediated mechanisms are involved in autoimmune destruction of islet beta cells in non-obese diabetic mice. *Diabetologia*. 43(9 Part A), 1149-1156.

Suckow AT, Polidori D, Yan W, Chon S, Ma JY, Leonard J, Briscoe CP. (2014). Alteration of the glucagon axis in GPR120 (FFAR4) knockout mice: a role for GPR120 in glucagon secretion. The Journal of biological chemistry. 289(22), 15751-15763.

Sudhahar V, Shaw S, Imig JD. (2010). Epoxyeicosatrienoic acid analogs and vascular function. Current medicinal chemistry. 17(12), 1181-1190.

Suk K, Kim S, Kim YH, Kim KA, Chang I, Yagita H, Shong M, Lee MS. (2001). IFN-gamma/TNF-alpha synergism as the final effector in autoimmune diabetes: a key role for STAT1/IFN regulatory factor-1 pathway in pancreatic beta cell death. Journal of immunology. 166(7), 4481-4489.

Su X, Hu Q, Kristan JM, Costa C, Shen Y, Gero D, Matis LA, Wang Y. (2000). Significant role for Fas in the pathogenesis of autoimmune diabetes. Journal of immunology. 164(5), 2523-2532.

Tabatabaie T, Waldon AM, Jacob JM, Floyd RA, Kotake Y. (2000). COX-2 inhibition prevents insulin-dependent diabetes in low-dose streptozotocin-treated mice. Biochemical and biophysical research communications. 273(2), 699-704.

Tanaka T, Katsuma S, Adachi T, Koshimizu TA, Hirasawa A, Tsujimoto G. (2008). Free fatty acids induce cholecystokinin secretion through GPR120. Naunyn-Schmiedeberg's archives of pharmacology. 377(4-6), 523-527.

Tang N, Matsuzaka T, Suzuki M, Nakano Y Zao H1, Ykoo T3, Suzuki-Kemuriyama N, Kuba M Okajima Y1, Takeuchi Y, Kobayashi K, Iwasaki H, Yatoh S, Takahashi A Suzuki H1, Sone H, Shimada M1. (2014). Ablation of Elovl6 protects pancreatic islets from high-fat diet-induced impairment of insulin secretion. Biochemical and biophysical research communications. 450(1), 318-323.

Taylor RC, Cullen SP, Martin SJ. (2008). Apoptosis: controlled demolition at the cellular level. Nature Review of Molecular and Cellular Biology. 9(8, 231-241.

Thomas HE, Biden TJ. (2009). Bad News for β-Cell Apoptosis. Diabetes. 58(8), 1725-1727.

Thomson S, Edin ML, Lih FB, Davies M, Yaqoob MM, Hammock BD, Gilroy D, Zeldin DC, Bishop-Bailey D. (2015). Intimal smooth muscle cells are a source but not a sensor of anti-inflammatory CYP450 derived oxylipins. Biochemical and biophysical research communications. 463(4), 774-780.

Thore S, Dyachok O, Gylfe E, Tengholm A. (2005). Feedback activation of phospholipase C via intracellular mobilization and store-operated influx of Ca2+ in insulin-secreting beta-cells. Journal of cell science. 118(Pt 19), 4463-4471.

Thörn K, Bergsten P. (2010). Fatty acid-induced oxidation and triglyceride formation is higher in insulin-producing MIN6 cells exposed to oleate compared to palmitate. Journal of cellular biochemistry. 111(2), 497-507.

Tiedge M, Lortz S, Drinkgern J, Lenzen S. (1997). Relation between antioxidant enzyme gene expression and antioxidative defense status of insulin-producing cells. Diabetes. 46(11), 1733-1742.

Todd JA, Walker NM, Cooper JD, Clayton DG. (2007). Robust associations of four new chromosome regions from genome-wide analyses of type 1 diabetes. *Nature Genetics.* 39(7), 857-864.

Tomita T1. (2017). Apoptosis of pancreatic β-cells in Type 1 diabetes. Bosnian journal of basic medical sciences. 17(3), 183-193.

Tran PO, Gleason CE, Poitout V, Robertson RP. (1999). Prostaglandin E(2) mediates inhibition of insulin secretion by interleukin-1beta. *The Journal of biological chemistry*. 274(44), 31245-31248.

Tran PO, Gleason CE, Robertson RP. (2002). Inhibition of interleukin-1beta-induced COX-2 and EP3 gene expression by sodium salicylate enhances pancreatic islet beta-cell function. Diabetes. 51(6), 1772-1778.

Tran SL, Puhar A, Ngo-Camus M, Ramarao, N. (2011). Trypan blue dye enters viable cells incubated with the pore-forming toxin HlyII of Bacillus cereus. PloS One. 6(9), e22876.

Tuo Y, Feng DD, Wang DF. 2012. (2012). Long term in vitro treatment of Ins-1 rat pancreatic beta cells against gluco- and lipotoxicities via activation of GPR40 receptors. Clin Exp Pharmacol Physiol. 39, 423-428.

Tsikas, D. (2007). Analysis of nitrite and nitrate in biological fluids by assays based on the Griess reaction: appraisal of the Griess reaction in the L-arginine/nitric oxide area of research. Journal of Chromatography. B, Analytic technologies in the biomedical and life science. 851(1-2), 51-70.

Tsonkova VG, Sand FW, Wolf XA, Grunnet LG, Kirstine Ringgaard A, Ingvorsen C, Winkel L, Kalisz M, Dalgaard K, Bruun C, Fels JJ, Helgstrand C, Hastrup S, Öberg FK, Vernet E, Sandrini MPB, Shaw AC, Jessen C, Grønborg M, Hald J, Willenbrock H, Madsen D, Wernersson R, Hansson L, Jensen JN, Plesner A, Alanentalo T, Petersen MBK, Grapin-Botton A, Honoré C, Ahnfelt-Rønne J, Hecksher-Sørens J, Ravassard P, Madsen OD, Rescan C, Frogne T. (2018). The EndoC-βH1 cell line is a valid model of human beta cells and applicable for screenings to identify novel drug target candidates. Molecular metabolism. 8, 144-157.

Tsuchiya Y, Saito M, Kadokura H, Miyazaki JI, Tashiro F, Imagawa Y, Iwawaki T, Kohno K. (2018). IRE1-XBP1 pathway regulates oxidative proinsulin folding in pancreatic β cells. The Journal of cell biology. 217(4), 1287-1301.

Turpin SM, Nicholls HT, Willmes DM, Mourier A, Brodesser S, Wunderlich CM, Mauer J, Xu E, Hammerschmidt P, Brönneke HS, Trifunovic A, LoSasso G, Wunderlich FT, Kornfeld JW, Blüher M, Krönke M, Brüning JC. (2014). Obesity-induced CerS6-dependent C16:0 ceramide production promotes weight gain and glucose intolerance. Cell metabolism. 20(4), 678-686.

Unger RH, Zhou YT. (2001). Lipotoxicity of beta-cells in obesity and in other causes of fatty acid spillover. Diabetes. 50(Supplement 1), S118-121.

Vangaveti V, Shashidhar V, Jarrod G, Baune BT, Kennedy RL. (2010). Free fatty acid receptors: emerging targets for treatment of diabetes and its complications. Therapeutic advances in endocrinology and metabolism. 1(4), 165-175.

Veluthakal R, Amin R, Kowluru A. (2004). Interleukin-1 beta induces posttranslational carboxymethylation and alterations in subnuclear distribution of lamin B in insulin-secreting RINm5F cells. American journal of physiology. Cell physiology. 287(4), C1152-1162.

Vennemann A, Gerstner A, Kern N, Ferreiros Bouzas N, Narumiya S, Maruyama T, Nüsing RM. (2012). PTGS-2-PTGER2/4 signaling pathway partially protects from diabetogenic toxicity of streptozotocin in mice. Diabetes. 61(7), 1879-1887.

Walchin G, Augstein P, Schroder D, Kuttler B, Kloting I, Heinke P, Schmidt S. (2003). IL-1beta, IFN-gamma and TNF-alpha increase vulnerability of pancreatic beta cells to autoimmune destruction. Journal of Autoimmunity. 20(23), 303-312.

Wali JA, Masters SL, Thomas HE. (2013). Linking Metabolic Abnormalities to Apoptotic Pathways in Beta Cells in Type 2 Diabetes. Cells. 2(3), 266-283.

Wagner R, Kaiser G, Gerst F, Christiansen E, Due-Hansen ME, Grundmann M, Machicao F, Peter A, Kostenis E, Ulven T, Fritsche A, Häring HU, Ullrich S. (2013). Reevaluation of fatty acid receptor 1 as a drug target for the stimulation of insulin secretion in humans. Diabetes. 62(6), 2106-2111.

Wang C, Youle RJ. (2009). The role of Mitochondria in apoptosis. Annual Review of Genetics. 43(9), 95-118.

Wang X, Ni L, Yang L, Duan Q, Chen C, Edin ML, Zeldin DC, Wang DW. (2014). CYP2J2-derived epoxyeicosatrienoic acids suppress endoplasmic reticulum stress in heart failure. Molecular pharmacology. 85, 105-115.

Wang XL, Lu T, Cao S, Shah VH, Lee HC. (2006). Inhibition of ATP binding to the carboxyl terminus of Kir6.2 by epoxyeicosatrienoic acids. Biochimica et biophysica acta. 1761(9), 1041-1049.

Wang Y, Xie T, Zhang D, Leung PS. (2019). GPR120 protects lipotoxicity-induced pancreatic β-cell dysfunction through regulation of PDX1 expression and inhibition of islet inflammation. Clinical Science. 133(1), 101-116.

Watson ML, Macrae K, Marley AE, Hundal HS. (2011). Chronic effects of palmitate overload on nutrient-induced insulin secretion and autocrine signalling in pancreatic MIN6 beta cells. PloS One. 6(10), e25975.

Webler AC, Popp R, Korff T, Michaelis UR, Urbich C, Busse R, Fleming I. (2008). Cytochrome P450 2C9-induced angiogenesis is dependent on EphB4. Arteriosclerosis, thrombosis, and vascular biology. 28(6), 1123-1129.

Wei MC, Zong WX, Cheng EH, Lindsten T, Panoutsakopoulou V, Ross AJ, Roth KA, MacGregor GR, Thompson CB, Korsmeyer SJ. (2001). Proapoptotic BAX and BAK: a requisite gateway to mitochondrial dysfunction and death. Science. 292(5517), 727-730.

Wellendorph P, Johansen LD, Bräuner-Osborne H. (2009). Molecular pharmacology of promiscuous seven transmembrane receptors sensing organic nutrients. Molecular pharmacology. 76(3), 453-465.

Welters HJ, Tadayyon M, Scarpello JH, Smith SA, Morgan NG. (2004a). Mono-unsaturated fatty acids protect Beta-cell apoptosis induced by saturated fatty acids, serum withdrawal or cytokine exposure. Federation of European Biochemical Societies. 103-108.

Welters HJ, Smith SA, Tadayyon M, Scarpello JH, Morgan NG. (2004b). Evidence that protein kinase Cdelta is not required for palmitate-induced cytotoxicity in BRIN-BD11 beta-cells. Journal of molecular endocrinology. 32(1), 227-235.

Welters HJ, McBain SC, Tadayyon M, Scarpello JH, Smith SA, Morgan NG. (2004c). Expression and functional activity of PPARgamma in pancreatic beta cells. British journal of pharmacology. 142 (7), 1162-70.

Wen H, Gris D, Lei Y, Jha S, Zhang L, Huang MT, Brickey WJ, Ting JP. (2011). Fatty acid-induced NLRP3-ASC inflammasome activation interferes with insulin signalling. Nature Immunology. 12(11), 408-415.

Wenzlau JM, Juhl K, Yu L, Moua O, Sarkar SA, Gottlieb P. (2007) The cation efflux transported ZnT8 (Slc30A8) is a major autoantigen in human type 1 diabetes. Proc Natl Acad Science 104(7), 17040-17045.

Widstrom RL, Norris AW, Van Der Veer J, Spector AA. (2003). Fatty acid-binding proteins inhibit hydration of epoxyeicosatrienoic acids by soluble epoxide hydrolase. Biochemistry. 42(40), 11762-11767.

Willcox A, Richardson SJ, Bone AJ, Foulis AK, Morgan NG. (2009). Analysis of islet inflammation in human type 1 diabetes. Clinical and experimental immunology. 155(2), 173-181.

Willcox A, Richardson SJ, Bone AJ, Foulis AK, Morgan NG. (2010). Evidence of increased islet cell proliferation in patients with recent-onset type 1 diabetes. Diabetologia. 53(9), 2020-2028.

Willcox A, Richardson SJ, Bone AJ, Foulis AK, Morgan NG. (2011). Immunohistochemical analysis of the relationship between islet cell proliferation and the production of the enteroviral capsid protein, VP1, in the islets of patients with recent-onset type 1 diabetes. *Diabetologia.* 54(11), 2417-2420.

Wong PY, Lai PS, Falck JR. (2000). Mechanism and signal transduction of 14 (R), 15 (S)-epoxyeicosatrienoic acid (14,15-EET) binding in guinea pig monocytes. Prostaglandins & other lipid mediators. 62(4), 321-333.

Wortham NC, Proud CG2. (2015). eIF2B: recent structural and functional insights into a key regulator of translation. Biochemical Society transactions. 43(6), 1234-1240.

Wray JA, Sugden MC, Zeldin DC, Greenwood GK, Samsuddin S, Miller-Degraff L, Bradbury JA, Holness MJ, Warner TD, Bishop-Bailey D. (2009). The epoxygenases CYP2J2 activates the nuclear receptor PPARalpha in vitro and in vivo. PloS One. 4(10), e7421.

Wu CC, Yen CC, Lee kI, Su CC, Tang FC, Chen KL, Su YC, Chen YW. (2012). Involvement of oxidative stress-induced ERK/JNK activation in the Cu(2+)/pyrrolidine dithiocarbamate complex-triggered mitochondria-regulated apoptosis in pancreatic β-cells. Toxicology letters. 208(3), 275-285.

Wu S, Moomaw CR, Tomer KB, Falck JR, Zeldin DC. (1996). Molecular cloning and expression of CYP2J2, a human cytochrome P450 arachidonic acid epoxygenase highly expressed in heart. The Journal of biological chemistry. 271(7), 3460-3468.

Xie QW, Kashiwabara Y, Nathan C. (1994). Role of transcription factor NF-kappa B/Rel in induction of nitric oxide synthase. The Journal of biological chemistry. 269(7), 4705-4708.

Xu X, Li R, Chen G, Hoopes SL, Zeldin DC, Wang DW. (2016). The Role of Cytochrome P450 Epoxygenases, Soluble Epoxide Hydrolase, and Epoxyeicosatrienoic Acids in Metabolic Diseases. Advances in nutrition. 7(6), 1122-1128.

Xu X, Zhao CX, Wang L, Tu L, Fang X, Zheng C, Edin ML, Zeldin DC, Wang DW. (2010). Increased CYP2J3 expression reduces insulin resistance in fructose-treated rats and db/db mice. Diabetes. 59(4), 997-1005.

Yan G, Chen S, You B, Sun J. (2008). Activation of sphingosine kinase-1 mediates induction of endothelial cell proliferation and angiogenesis by epoxyeicosatrienoic acids. Cardiovascular research. 78(2), 308-314.

Yang S, Lin L, Chen JX, Lee CR, Seubert JM, Wang Y, Wang H, Chao ZR, Tao DD, Gong JP, Lu ZY, Wang DW, Zeldin DC. (2007). Cytochrome P-450 epoxygenases protect endothelial cells from apoptosis induced by tumor necrosis factor-alpha via MAPK and PI3K/Akt signaling pathways. American journal of physiology. Heart and circulatory physiology. 293(1), H142-151.

Yang W, Tuniki VR, Anjaiah S, Falck JR, Hillard CJ, Campbell WB. (2008). Characterization of epoxyeicosatrienoic acid binding site in U937 membranes using a novel radiolabeled agonist, 20-125i-14,15-epoxyeicosa-8(Z)-enoic acid. The Journal of pharmacology and experimental therapeutics. 324(3), 1019-1027.

Yin XM1. (2000). Bid, a critical mediator for apoptosis induced by the activation of Fas/TNF-R1 death receptors in hepatocytes. Journal of molecular medicine. 78(4), 203-211.

Yoon JW, Jun HS. (2005). Autoimmune destruction of pancreatic beta cells. American journal of therapeutics. 12(6), 580-591.

Yuan D, Zou Q, Yu T, Song C, Huang S, Chen S, Ren Z, Xu A. (2014). Ancestral genetic complexity of arachidonic acid metabolism in Metazoa. Biochimica et biophysica acta. 1841(9), 1272-84.

Zeldin DC, (2001). Epoxygenase Pathways of Arachidonic Acid Metabolism. The Journal of Biological Chemistry 276, 36059-36062.

Zeldin DC, Foley J, Boyle JE, Moomaw CR, Tomer KB, Parker C, Steenbergen C, Wu S. (1997). Predominant expression of an arachidonate epoxygenase in islets of Langerhans cells in human and rat pancreas. Endocrinology. 138(3), 1338-1346.

Zeldin D, Kobayashi J, Falck JR, Winder BS, Hammock BD, Snapper JR, Capdevila JH. (1993). Regio-and enantiofacial selectivity of epoxyeicosatrienoic acid hydration by cytosolic exopide hydrolase. Journal Biology Chemistry 9, 6402-6407.

Zhang S, Chen G, Li N, Dai M, Chen C, Wang P, Tang H, Hoopes SL, Zeldin DC, Wang DW, Xu X. (2015). CYP2J2 overexpression ameliorates hyperlipidemia via increased fatty acid oxidation mediated by the AMPK pathway. Obesity. 23(7), 1401-1413.

Zhang Y, Xu M, Zhang S, Yan L, Yang C, Lu W, Li Y, Cheng H. (2007). The role of G protein-coupled receptor 40 in lipoapoptosis in mouse beta-cell line NIT-1. Journal of molecular endocrinology. 38(6), 651-661.

Zhao G, Wang J, Xu X, Jing Y, Tu L, Li X, Chen C, Cianflone K, Wang P, Dackor RT, Zeldin DC, Wang DW. (2012). Epoxyeicosatrienoic acids protect rat hearts against tumor necrosis factor-α-induced injury. Journal of lipid research. 53(3), 456-466.

Zhao X, Imig JD. (2003). Kidney CYP450 enzymes: biological actions beyond drug metabolism. Current drug metabolism. 4(1), 73-84.

Zhou R, Tardivel A, Thorens B, Choi I, Tschopp J. (2010). Thioredoxin-interacting protein links oxidative stress inflammasome activation. Natural Immunology. 11(10), 136-140.

Zhong L, Tran T, Baguley TD, Lee SJ, Henke A, To A, Li S, Yu S, Grieco FA, Roland J, Schultz PG, Eizirik DL, Rogers N, Chartterjee AK, Tremblay MS, Shen W. (2018). A novel inhibitor of inducible NOS dimerization protects against cytokine-induced rat beta cell dysfunction. British journal of pharmacology. 175(17), 3470-3485.

Zummo FP, Cullen KS, Honkanen-Scott M, Shaw JAM, Lovat PE, Arden C. (2017). Glucagon-Like Peptide 1 Protects Pancreatic β-Cells From Death by Increasing Autophagic Flux and Restoring Lysosomal Function. Diabetes. 66(5), 1272-1285.

Zumsteg U, Frigerio S, Hollander GA. (2000). Nitric oxide production and Fas surface expression mediate two independent pathways of cytokine-induced murine beta-cell damage. Diabetes 49(2), 39-47.

Appendices

Appendix A: Supplementary method data

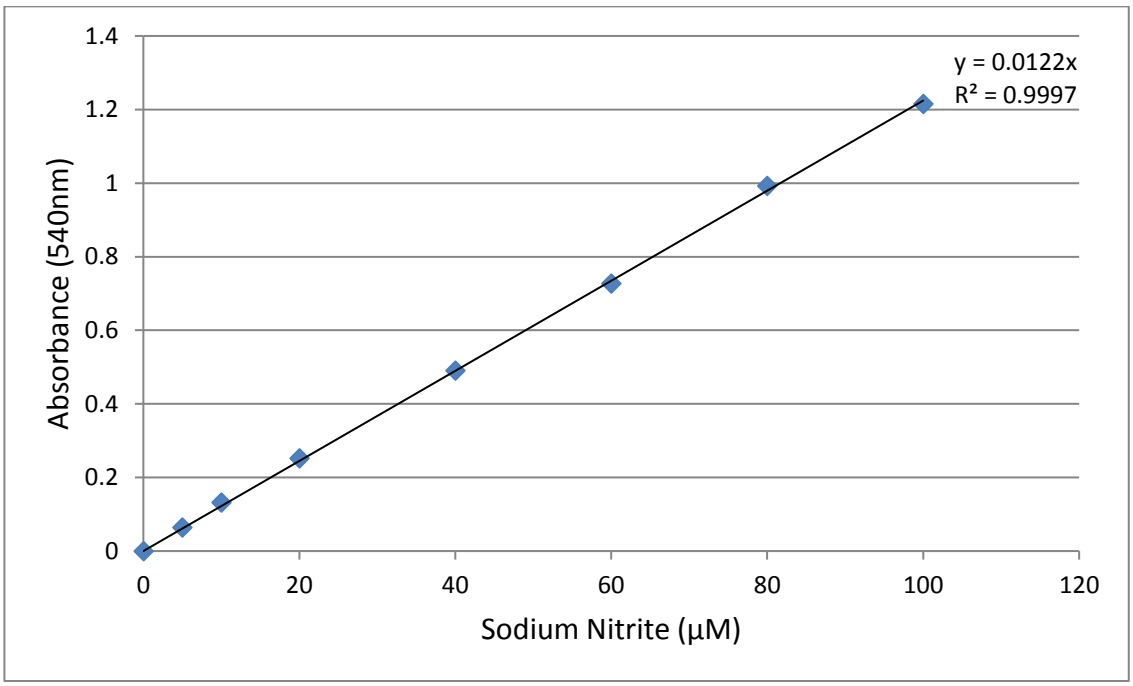

Figure A.1 Representative Sodium Nitrite Calibration Graph: Griess Assay. Sodium nitrite standards (0-100µM) were prepared in distilled water and incubated, in triplicate wells of a 96-well plate, with Griess reagent (1% sulphanilamide in 5% orth-phosphoric acid and 0.1% NEDA) for 10 minutes before absorbance was measured at 540nm, with 0µM sodium nitrite used as a blank. Representative standard is shown, calibration data was collected each time the assay was performed.

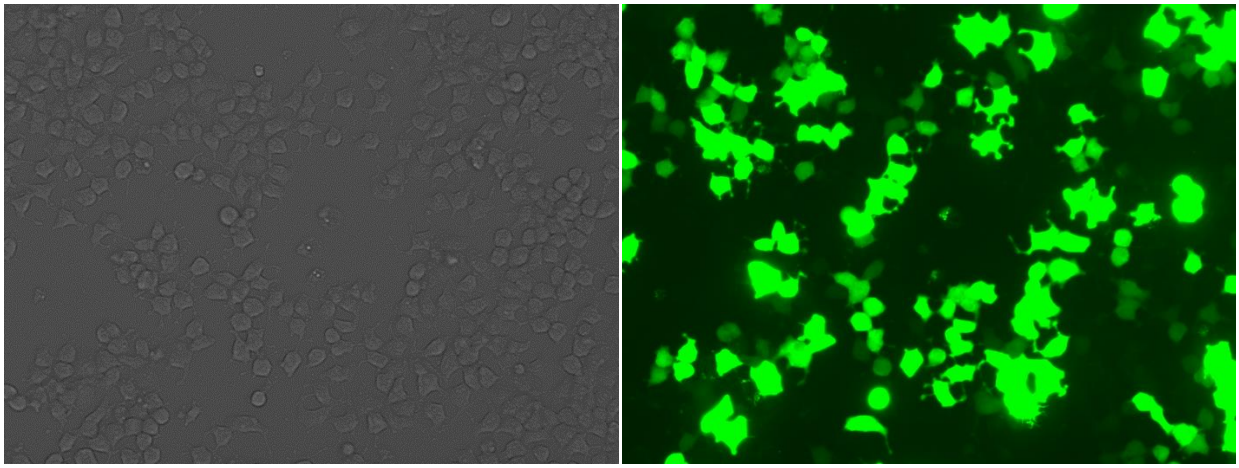

Figure A.2 Optimisation of transfection of BRIN-BD11 cells with a GFP-encoding plasmid. Cells were transfected in 24-well plates with a pmaxGFP expressing plasmid using Lipofectamine® 2000 to a final concentration of 0.5µg DNA:1.5µL Lipofectamine/well. After 24 hours cells were imaged using a EVOS fluorescent microscope. Cells were counted under bright-field illumination with the percentage scored as GFP positive calculated to an average of 56% where n=3.

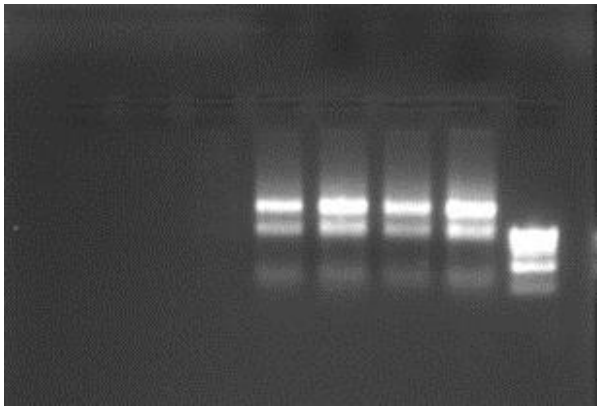

Figure A.3 Representative agarose gel for RNA integrity. Total RNA was extracted in Trizol and processed using a Direct-zol™ RNA MiniPrep kit (Zymo Research) following maufacturers procedures. Eluted RNA was quantified using a ThermoScientific NanoDrop 1000 Spectrophotometer with A260/A280 of 1.8-2.1 indicating a high purity RNA. RNA samples (1µg) were prepared in 1 X loading buffer and separated on a 1% agarose gel containing ethidium bromide in TAE buffer at 100V for 20 minutes and visualised. Representative image shows an approximate 2:1 ratio of the 28S and 18S rRNA bands, the absence of high molecular weight gDNA bands or band smearing. Difuse low molecular weight band indicates the prescence of miRNAs.

Table A.2. RT-PCR primer efficiency and comparative amplification efficiency gradients. cDNA standard (10ng-0.01ng) were amplified using QuantiNova RT-PCR SYBR Green kit (Qiagen). Efficiency values (based on the standard curve gradient between –3.58 and –3.1) were obtained from the Agilent Aria-MX software (column A), comparative amplification efficiency gradients (column B) were determined from a graph of ΔC_t 18SrRNA-GOI against input amount of sample, with gradient <0.1 considered acceptable.

Target	(A) **Primer Efficiency (%) (based on standard curve gradient)**	(B) **Comparative Amplification Efficiency**
18S	108.17	N/A
CPT1	108.09	0.0128
Elovl6	109.38	0.0052
Ech1	104.79	0.0143
DGAT1	109.79	0.0165

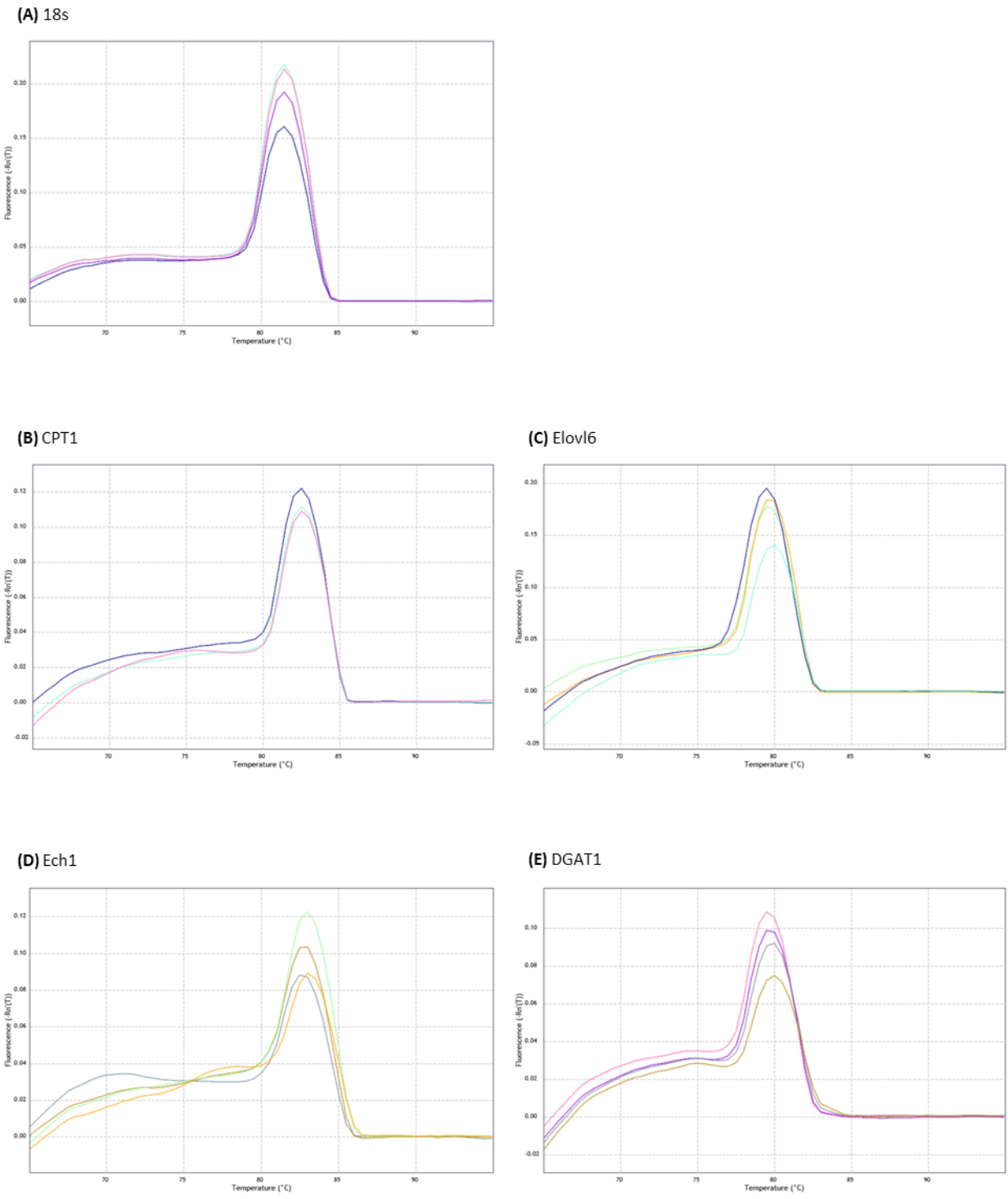

Figure A.4 Melt curve analysis following RT-PCR. Melt curves (XXX temp) generated following RT-PCR amplification, using Agilent-AriaMX programme were generated automatically following amplification for every sample. Representative curves shown are from standard curve amplifications with a single peak above XC at all in-put template amounts indicate amplification specificity and absence of any interference from primer dimers (low temperature peak) or non-specific amplification.

Appendix B: Plasmid Vectors

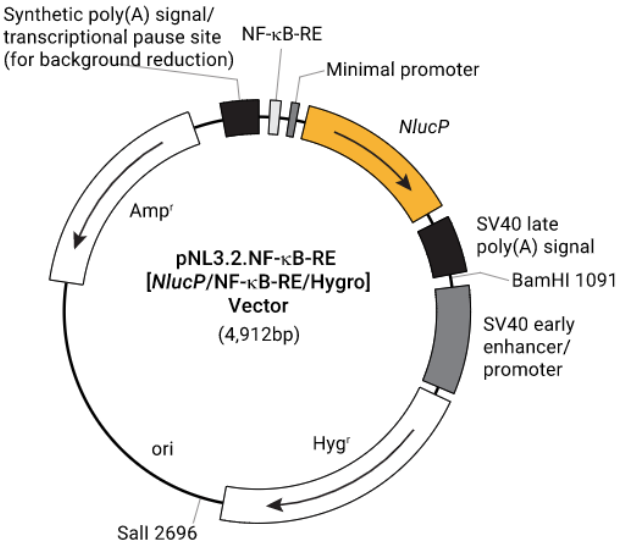

Figure B.1 Vector map of pNL3.2NF-κB-RE plasmid. Vector contains five copies of the NF-κB RE consensus sequence upstream of the NanoLuc® luciferase. The ampicillin resistance gene (Amp^r) was used for selection of bacterial transformation during vector isolation (Promega).

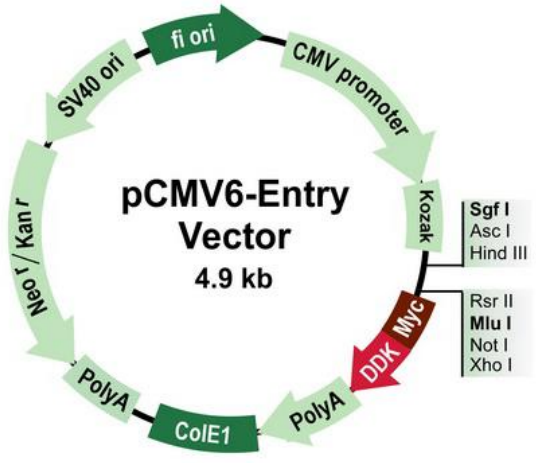

Figure B.2 Vector map of pCMV6-Entry Vector. An untagged vector was used for over-expression of CYP 2C11, inserted between Sgf1 and Mlu1 restriction sites, as supplied by the manufacturer. The kanamycin resistance gene (Kan^r) was used for selection of bacterial transformation during vector isolation and the neomycin resistance gene was used for selection of stable BRIN-BD11 cell lines in G418 selective media (OriGene)

Appendix C: Abstracts arising from this thesis

Grimes, D., Watson, D. (2017). **Structure:activity relationships for the cytoprotective effects of epoxyeicosatrienoic acids (EETs) and their corresponding diols against palmitate-induced lipotoxicity in BRIN-BD11 cells.** *Diabetic Medicine,* vol

Introduction: Palmitate is a well-established contributor to pancreatic beta cell death in type 2 DM, with effects ameliorated by polyunsaturated fatty acids, including arachidonic acid (AA, C20:4). Whilst AA-derived metabolites from COX and LOX enzymes have been extensively studied, little attention has focused on EETs derived from cytochrome-P450 (CYP450) enzymes. This study therefore aimed to investigate the cytoprotective effects of CYP450-derived EET regioisomers and their less-active vicinal diols against palmitate-induced lipotoxicity.

Methods: BRIN-BD11 cells were treated with 250µM palmitate in co-incubation with 8,9; 11,12; 14,15 EETs, or their dihydroxyeicosatrienoic acid derivatives (DHETs) for 24 hours. Cell viability was assessed by vital dye exclusion using Trypan Blue (results expressed as total and viable cells/ml +/-SEM), or multicaspase-activity assay.

Results: Data showed that all EETs protected cells against palmitate-induced cell death, such that palmitate decreased viable cell number from 1.02x106 (+/-0.8) to 0.21x106(+/-XX) and in co-incubation with 8,9EET, 11,12EET and 14,15EET, viable cell number was significantly increased to 1x106, 0.82x106 and 0.72x106, respectively ($P<0.05$). Structural differences for protective activity in relation to position of the epoxide group were also reflected in caspase activity, whereby palmitate alone increased activity to 71%(+/-2.9), decreasing to 13%(+/-), 23%(+/-) and 34%(+/-) in the presence of these EETs, respectively ($P<0.05$). In comparison, corresponding DHETs failed to significantly attenuate palmitate cytotoxicity.

Conclusion: CYP450-derived EETs protect against palmitate-toxicity, with position of epoxide group reflecting structural differences in cytoprotection. Ongoing work is exploring mechanistic actions of EETs in beta cells and the role of CYP450 isoforms in production of endogenous EETs.

Grimes, D., Watson, D. (2018). **Anti-inflammatory effects of epoxyeicosatrienoic acids (EETs) and their corresponding diols against pro-inflammatory cytokine-toxicity in BRIN-BD11 cells.** *Diabetic Medicine,* vol

Introduction: CYP450-derived EETs display anti-inflammatory activity in cardiac models of inflammation, in part through activation of PPARγ and inhibition of NF-κB activation. Therefore we aimed to investigate the cytoprotective effects of EET regioisomers and their corresponding vicinal diols in a beta cell model of pro-inflammatory cytokine-toxicity.

Methods: BRIN-BD11 cells were treated with 100U/mL IL-1β, 20U/mL IFNγ and 500U/mL TNFα in co-incubation with either 10μM 8(9)-EET, 11(12)-EET, 14(15)-EET, or their dihydroxyeicosatrienoic acid derivatives (DHETs) for 24 hours. Cell viability was assessed by vital dye exclusion (Trypan Blue; expressed as viable cells/mL) or multicaspase-activity assay and NF-κB activity was measured using a NanoLuc® luciferase reporter assay.

Results: All EETs protected against cytokine-induced cell death, such that cytokines decreased viable cell number from 0.79x106 to 0.33x106 and in co-incubation with 8(9)-EET, 11(12)-EET and 14(15)-EET, this increased to 0.64x106, 0.61x106 and 0.59x106, respectively ($p<0.05$). Similarly, cytokine treatment increased caspase activity to 35%(+/-5.7), decreasing to 18%(+/-1.9), 19%(+/-2) and 19%(+/-1.9) in the presence of these EETs ($p<0.05$), accompanied by a 32% decrease in NF-κB activation. Of the corresponding diols only 8(9)-DHET attenuated cytokine-toxicity, reducing caspase activity from 41%(+/-4.5) to 21%(+/-2.4) ($p<0.05$).

Conclusion: EETs protected against cytokine-toxicity in BRIN-BD11 cells, in part via reduced activation of NF-κB. We also consider the novel observation that 8(9)-DHET, unlike other EET-derived DHETs, similarly protected against cytokine-induced apoptosis. This data highlights a potential role of EETs in attenuating cytokine-toxicity in type 1 diabetes and our ongoing work is exploring the production of endogenous EETs by CYP450 isoforms and actions of EET analogues.